

**SECONDARY NATURAL GAS RECOVERY: TARGETED APPLICATIONS FOR
INFIELD RESERVE GROWTH IN MIDCONTINENT RESERVOIRS, BOONSVILLE
FIELD, FORT WORTH BASIN, TEXAS**

**VOLUME I: TOPICAL REPORT
(May 1, 1993–June 30, 1995)**

Prepared by

**Bob A. Hardage, David L. Carr, and Robert J. Finley
Bureau of Economic Geology
Noel Tyler, Director
The University of Texas at Austin
Austin, Texas 78713-8924**

**David E. Lancaster
S. A. Holditch & Associates, Inc.**

**Robert Y. Elphick
Scientific Software–Intercomp**

**James R. Ballard
Envirocorp Services & Technology, Inc.**

for

**GAS RESEARCH INSTITUTE
GRI Contract No. 5093-212-2630
Thomas H. Fate, GRI Project Manager**

and

**U.S. DEPARTMENT OF ENERGY
DOE Contract No. DE-FG21-88MC25031
Charles W. Byrer, DOE Project Manager**

October 1995

DISCLAIMER

LEGAL NOTICE This work was prepared by the Bureau of Economic Geology as an account of work sponsored by the Gas Research Institute (GRI). GRI, nor members of GRI, nor any person acting on behalf of either:

- a. Makes any warranty or representation, expressed or implied, with respect to the accuracy, completeness, or usefulness of the information contained in this report, or that the use of any apparatus, method, or process disclosed in this report may not infringe privately owned rights; or
- b. Assumes any liability with respect to the use of, or for damages resulting from the use of, any information, apparatus, method, or process disclosed in this report.

REPORT DOCUMENTATION PAGE	1. REPORT NO. GRI-95/0454.1	2.	3. Recipient's Accession No.
4. Title and Subtitle Secondary Natural Gas Recovery: Targeted Technology Applications for Infield Reserve Growth, Boonsville Field, Fort Worth Basin, Texas			5. Report Date October 1995
7. Author(s) B. A. Hardage, D. L. Carr, R. J. Finley, D. E. Lancaster, R. Y. Elphick, and J. R. Ballard			6.
9. Performing Organization Name and Address Bureau of Economic Geology The University of Texas at Austin University Station, Box X Austin, Texas 78713-8924			8. Performing Organization Rept. No.
12. Sponsoring Organization Name and Address Gas Research Institute 8600 West Bryn Mawr Avenue Chicago, IL 60631 Project Manager: Thomas H. Fate			10. Project/Task/Work Unit No.
Department of Energy Morgantown Energy Technology Center P.O. Box 880, MS E06 Morgantown, West Virginia 26507-0880			11. Contract(C) or Grant(G) No. (C) 5093-212-2630 (G)
15. Supplementary Notes			13. Type of Report & Period Covered Topical Report 5/1/93-6/30/95
16. Abstract (Limit: 200 words) This report documents an assessment of Midcontinent sandstone natural gas reservoirs in Boonsville (Bend Conglomerate Gas) field by integrating four key disciplines: geology, geophysics, reservoir engineering, and petrophysics. Pressure and production data confirm the existence of compartmented or poorly drained gas throughout much of the Bend Conglomerate and suggest that additional gas will be found when well spacing is reduced to 80 acres, although multiple stacked completion opportunities will typically be needed to ensure the economic viability of new infield wells. As part of this analysis, the Lower Atoka Group was divided into 13 third-order genetic sequences, and to our knowledge, this is the first public, comprehensive genetic sequence analysis that relates these Pennsylvanian reservoirs to their seismic response and to gas productivity. A 26-mi ² , 3-D seismic survey was done to test methods for reservoir delineation in thin-bed, hard-rock environments and identified a previously unknown structural component of reservoir compartmentalization in the form of low-displacement faulting commonly associated with karst collapse in deeper carbonate rocks. These karst collapse features extend vertically as much as 2,500 ft and may be a widespread influence on the deposition of younger sediments in the Midcontinent. The ability of the 3-D survey to define stratigraphic entrapments was more variable. Some sequences were imaged quite well, and seismic attribute analyses provided excellent agreement with net reservoir distributions generated from sequence stratigraphic interpretations. In other instances, individual systems tracts and reservoir sandstones that were subsets of genetic sequences proved difficult to trace precisely in the 3-D data, especially when those units were associated with a subtle impedance contrast or were extremely thin.			14.
17. Document Analysis a. Descriptors 3-D seismic, sequence stratigraphy, secondary natural gas recovery, depositional facies, reservoir compartmentalization, Bend Conglomerate Formation, Caddo Formation, Midcontinent, karst collapse			
b. Identifiers/Open-Ended Terms integrated geologic, engineering, petrophysical, and geophysical evaluation of fluvial and fluvio-deltaic reservoirs; identification of secondary natural gas resources			
c. COSATI Field/Group			
18. Availability Statement Release unlimited	19. Security Class (This Report) Unclassified	21. No. of Pages 600	
	20. Security Class (This Page) Unclassified	22. Price	

RESEARCH SUMMARY

Title	Secondary Natural Gas Recovery: Targeted Technology Applications for Infield Reserve Growth in Midcontinent Reservoirs, Boonsville Field, Fort Worth Basin, Texas
Contractor	Bureau of Economic Geology, The University of Texas at Austin GRI Contract No. 5093-212-2630, "Secondary Natural Gas Recovery— Infield Reserve Growth Joint-Venture: Applications in Midcontinent Sandstones."
Principal Investigators	Robert J. Finley and Bob A. Hardage
Report Period	May 1993–June 1995
Objectives	The objectives of this project are to define undrained or incompletely drained reservoir compartments controlled primarily by depositional heterogeneity in a low-accommodation, cratonic Midcontinent depositional setting, and, afterwards, to develop and transfer to producers strategies for infield reserve growth of natural gas. Integrated geologic, geophysical, reservoir engineering, and petrophysical evaluations are described for complex, difficult-to-characterize, fluvial and deltaic reservoirs in Boonsville (Bend Conglomerate Gas) field, a large, mature gas field located in the Fort Worth Basin of North Texas. The purpose of this project is to demonstrate approaches to overcoming the reservoir complexity and target the gas resource, and to do so by using state-of-the-art technologies that can be applied by a large cross section of Midcontinent operators.
Technical Perspective	Reserve growth resources in the Midcontinent region total as much as 41 Tcf. The region contains the second-largest natural gas reserve growth resource after the Texas Gulf Coast and provides an appropriate resource target for secondary gas recovery (SGR) research following the Gulf Coast project. Secondary or incremental gas may be contained in reservoirs (even those that have conventional porosity and permeability) that are untapped or bypassed or that have incompletely drained areas that are a function of depositional facies, diagenetic, and even structural heterogeneity. The Midcontinent reservoirs selected for this project have more deltaic components than do the dominantly fluvial reservoirs that were the focus of the Gulf Coast SGR project. Further, the Midcontinent reservoirs studied were deposited in a cratonic basin that had relatively low accommodation space and a higher frequency of sea-level fluctuation than did depositional patterns in the Tertiary of the Gulf Coast Basin. Pennsylvanian Midcontinent sandstones are complex, but it is this complexity that creates the opportunity for additional infield gas recovery.
Results	Pressure and production data confirm the existence of compartmented or poorly drained gas reserves throughout much of the Bend Conglomerate, suggesting that additional reserves will be found when well spacing is reduced to 80 acres. Three styles of reservoir compartmentalization were identified in Midcontinent clastic gas reservoirs from the Boonsville analysis: structural, stratigraphic, and a combination of these two styles.

Structural compartments are caused by low-displacement faulting that acts as a partial barrier to gas flow and is commonly associated with karst collapse in deeper carbonate rocks; these features extend vertically as much as 2,500 ft in the project area. This previously unknown karst collapse phenomenon, identified by means of the 3-D seismic survey, may be a widespread influence on the deposition of younger sediments in the Midcontinent.

Stratigraphic compartments may be surface bounded, facies bounded, or cement bounded. Combination-style compartments have both structural and stratigraphic elements and are most commonly surface and fault bounded. The best natural gas reservoirs in Boonsville field occur predominantly as lowstand, valley-fill, conglomeratic sandstones overlying erosional surfaces. Isopach mapping indicates a strong relationship between reservoir distribution and structurally low areas on the pre-Atoka seismic time structure surface, suggesting that subtle elevation differences at the pre-Atoka stratigraphic level controlled the geographical location of incised valleys and the fluvial and fluvio-deltaic axes in which high-energy reservoir facies were concentrated.

Interpretation of these complex reservoirs was aided by a 26-mi² 3-D seismic survey. Seismic resolution was maximized by using specialized small (10 oz) directional, explosive-source charges; a high data-sampling rate (1 ms); and staggered source and receiver lines that allowed the data to be stacked into high-fold 110- × 100-ft bins for general interpretation or into lower fold 55- × 55-ft bins when interpretations requiring detailed lateral resolution were needed. Precise calibration of thin-bed depths to seismic traveltime was accomplished by recording detailed vertical seismic profile (VSP) data and explosive-source velocity checkshot data at several locations within the 3-D seismic grid.

Whereas the 3-D seismic survey clearly identified the importance of the karst collapse features to reservoir compartmentalization, the ability of the 3-D survey to identify stratigraphic entrapments was more variable. Some sequences, such as the Upper and Lower Caddo, were imaged quite well, once calibrated to well control, and seismic attribute analyses provided excellent agreement with net reservoir distributions generated from sequence stratigraphic interpretations. In other instances, the 3-D data did not always provide conclusive answers. Individual systems tracts and reservoir sandstones that are subsets of genetic sequences were sometimes difficult to trace in the 3-D data, particularly when the acoustic impedance of these units was approximately the same as the acoustic impedance of the bounding beds or if the units were extremely thin.

Judging from the hydrocarbon distribution in the project area, the gas reserves expected in any particular Bend sequence will be approximately 200 MMscf or less, on average, when well spacing is reduced to 80 acres, whereas gas reserves of at least 400 MMscf will typically be required for new wells to be economically attractive. Although individual Bend completions may still encounter gas reserves in excess of 400 MMscf (some recent wells have), it appears that multiple stacked completion opportunities will be needed in new infield wells. Review of the 3-D seismic data suggests that these stacked trapping geometries often exist throughout the Bend interval. Thus, a reasonable approach to

identifying new well locations may be to focus 3-D seismic evaluation on these apparent stacked trapping geometries in areas having the highest likelihood of encountering multiple completion opportunities. An alternate strategy is to use the 3-D data to identify fault-bounded blocks that have no penetrations in subregional or field-scale areas where the pre-Atoka time structure is low and the total Atoka net reservoir isopachs are thick, again increasing the potential for finding multiple vertically stacked completion opportunities.

Technical Approach

This assessment of Midcontinent sandstone natural gas reservoirs in Boonsville field integrated four key disciplines: geology, geophysics, reservoir engineering, and petrophysics. The entire Atoka Group (Lower and Upper) in the project area was divided into 13 third-order genetic stratigraphic sequences. To our knowledge, this is the first public, comprehensive genetic sequence analysis that relates these prolific Pennsylvanian gas reservoirs to their seismic response and to gas productivity. A 26-mi² 3-D seismic survey was acquired and interpreted to test methods for delineating reservoirs in thin-bed, hard-rock environments. Reservoir facies frameworks, assessed by integrating geological and geophysical approaches, were combined with engineering and petrophysical evaluations of produced gas volumes and reservoir quality.

Project Implications

The compartmentalization of Boonsville field has been demonstrated to have more than one origin. The field, much more complex than originally described, offers a challenge to effective infield drilling. The use of new technologies and the intelligent integration of results of these technologies have shown that fields as complex as Boonsville and their associated problems can be understood and effective production strategies applied. The use of the information gained from this project will have value to other Midcontinent fields and to many basins that have structural and depositional compartmentalization.

CONTENTS—VOLUME I

Executive Summary	0.1
1. Overview	1.1
2. Influence of Paleozoic Carbonate Karst Collapse on Bend Conglomerate Stratigraphy and Reservoir Compartmentalization.....	2.1
3. Correlation between Seismic Attributes and Caddo Reservoir Properties	3.1
4. Complex Bend Conglomerate Stratigraphy Can Lead to Small-Scale Reservoir Compartmentalization	4.1
5. Difficult-to-Image Reservoirs	5.1
6. Siting Boonsville Development Wells—Case Histories.....	6.1
7. References	7.1
8. Glossary	8.1

CONTENTS—VOLUME II

Introduction	A.1
Appendix A. Geologic Evaluation of the Boonsville Project Area	A.2
Appendix B. Reservoir Engineering Analysis of the Boonsville Project Area	B.1
Appendix C. Petrophysical Analysis of the Boonsville Project Area	C.1
Appendix D. Boonsville 3-D Seismic Program—Wavetesting, Design, Acquisition, and Processing	D.1
Appendix E. Seismic Attributes	E.1
Appendix F. Interpreting Thin-Bed Stratigraphy in 3-D Seismic Data Volumes.....	F.1
Appendix G. Glossary	G.1

VOLUME I FIGURES AND TABLES

Figures

1.1.	Location of Boonsville field in Wise and Jack Counties, Texas	1.5
1.2.	History of drilling activity for wells drilled in, and immediately adjacent to, the Boonsville project area.....	1.7
1.3.	Middle Pennsylvanian paleogeographic map showing the Fort Worth Basin and Boonsville project area.....	1.9
1.4.	Time-stratigraphic correlation for Middle Pennsylvanian rocks of the U.S. Midcontinent region.....	1.10
1.5.	Type log from Boonsville project area. Major reservoir zones were defined by genetic sequences, which are upward-coarsening units bounded by impermeable, maximum-flooding shales.....	1.12
1.6.	Composite genetic sequence illustrating key chronostratigraphic surfaces and typical facies successions.....	1.16
1.7.	History of typical completion practices in the Boonsville project area	1.17
1.8.	Detailed map of the Boonsville project area, located just to the west of Lake Bridgeport	1.19
2.1.	Seismic time structure map showing the topography of the Vineyard chronostratigraphic surface (base of the Bend Conglomerate).....	2.2
2.2.	Seismic time structure map showing the topography of the Caddo chronostratigraphic surface (top of the Bend Conglomerate).....	2.3
2.3.	Behavior of the seismic reflection amplitude across the Vineyard chronostratigraphic surface	2.5
2.4.	Vertical seismic section along profile ABC shown in Figure 2.3, which traverses three of the white reflection anomalies on the Vineyard surface.....	2.7
2.5.	Structural cross section A-A' of Boonsville project area	2.9

2.6.	Location of the Sealy C-2 well in the northeast part of the project area.....	2.12
2.7.	Expanded view showing Upper Caddo completions near the Sealy C-2 well.....	2.14
2.8.	Stratigraphic cross section A-A', Upper Caddo valley-fill sandstone.....	2.15
2.9.	Stratigraphic cross section B-B', Upper Caddo valley-fill reservoir.....	2.16
2.10.	Stratigraphic cross section C-C', Upper Caddo valley-fill reservoir.....	2.17
2.11.	Initial pressures measured in the Sealy C-2 and Sealy B-3 Upper Caddo completions	2.20
2.12.	Open-hole logs recorded over the Upper Caddo sequence in the Sealy C-2 well	2.21
2.13.	Interpreted log for the Upper Caddo sequence in the Sealy C-2 well.....	2.22
2.14.	Northeast quadrant of the Caddo time structure map showing a ring of karst collapse surrounding the Sealy C-2 well.....	2.24
2.15.	Vertical section along profile B defined in Figure 2.10.....	2.25
2.16.	Vertical section along profile C defined in Figure 2.10.....	2.26
2.17.	History match of production data from the Sealy C-2 well	2.27
2.18.	Structure map contoured on top of MFS90 before drilling of Sealy No. 2 well.....	2.30
2.19.	Structural cross section B-B' before drilling of Sealy No. 2 well	2.31
2.20.	Structure map contoured on top of MFS90 after drilling of Sealy No. 2. well.....	2.32
2.21.	Structural cross section B-B' after drilling of Sealy No. 2 well	2.33
2.22.	Open-hole logs recorded across the Jasper Creek sequences in the Sealy C-3 well....	2.36
2.23.	Net reservoir isopach of the fourth Jasper Creek zone	2.37
2.24.	Stratigraphic cross section 1-1', fourth Jasper Creek sequences	2.38
2.25.	Stratigraphic cross section 2-2', Jasper Creek sequences.....	2.39
3.1.	Lower Caddo net reservoir in the southern third of the project area as determined from well log control, using the criteria that Lower Caddo reservoir facies exist whenever the resistivity exceeds 10 ohm-m, and simultaneously, the SP curve reads less than -30 API units	3.2

3.2. Average instantaneous seismic frequency calculated within the Lower Caddo sequence	3.3
3.3. Well control and cross-section profiles used to analyze Upper Caddo interval	3.4
3.4. Stratigraphic cross section 1-1', Caddo sequences	3.5
3.5. Stratigraphic cross section 2-2', Caddo sequences	3.6
3.6. Upper Caddo sandstone thickness in the northwest third of the Boonsville project area as defined by well log control	3.9
3.7. Log cross section 3	3.10
3.8. Log cross section 4	3.11
3.9. Log cross section 5	3.12
3.10. Map of a seismic amplitude attribute calculated within the Caddo sequence in the northwest third of the project area	3.14
3.11. Seismic profile along the surface track labeled "Line 1" in Figure 3.10	3.16
3.12. Seismic profile along the surface track labeled "Line 2" in Figure 3.4	3.17
4.1. Location of several closely spaced Jasper Creek completions in the southeast portion of the project area	4.2
4.2. Middle Jasper Creek log cross section (1-1') and facies interpretation spanning the IG YTS 33 well	4.3
4.3. Middle Jasper Creek log cross section (2-2') and facies interpretation spanning the IG YTS 33 well	4.5
4.4. Middle Jasper Creek net reservoir sandstone	4.9
4.5. Net reservoir of Middle Jasper Creek transgressive systems tract	4.10
4.6. Middle Jasper Creek interpretation, net reservoir sandstone	4.11
4.7. Expanded view of the wells presented in Figure 4.1, showing the status of the Jasper Creek completions	4.13
4.8. Additional completion and production information on the IGY A9 and 33 wells and the WD 2 and 3 wells	4.14

4.9.	Comparison of initial pressures measured in the IGY 33 and WD 3 wells to initial pressures reported in other Jasper Creek completions	4.16
4.10.	Production histories from the IGY A9 and 33 wells and the WD 2 and 3 wells	4.18
4.11.	Log-log plot of test data from the April 1993 pressure buildup test conducted in the IGY 33 well.....	4.20
4.12.	Semilog analysis of the April 1993 pressure buildup test conducted in the IGY 33 well.....	4.21
4.13.	History match of the April 1993 pressure buildup test conducted in the IGY 33 well.....	4.23
4.14.	Section view showing seismic heterogeneity associated with Middle Jasper Creek reservoirs near IG YTS 33 and Dewbre 3 wells	4.25
4.15.	Horizon slice passing approximately through the two ES34 boundary picks shown in Figure 4.14	4.26
5.1.	Location of the C Yates 9 well in the north-central portion of the project area	5.2
5.2.	Expanded view of wells offsetting the C Yates 9 location	5.4
5.3.	Interpreted log for the Trinity sequence penetrated by the C Yates 9 well	5.6
5.4.	Trinity-only production history from the C Yates 9 well	5.7
5.5.	History match of production data from the C Yates 9 well	5.8
5.6.	An uninterpreted east-west seismic section connecting the C Yates 9 well with neighboring wells.....	5.10
5.7.	An interpreted version of the seismic line shown in Figure 5.6	5.11
5.8.	An uninterpreted northwest-southeast seismic section connecting the C Yates 9 well with neighboring wells.....	5.12
5.9.	An interpreted version of the seismic line shown in Figure 5.8	5.13
5.10.	The data in Figure 5.6 converted to instantaneous phase	5.14
5.11.	The data in Figure 5.7 converted to instantaneous phase	5.15
5.12.	The data in Figure 5.8 converted to instantaneous phase	5.16

5.13.	The data in Figure 5.9 converted to instantaneous phase	5.17
5.14.	Reflection amplitude behavior on the interpreted Trinity surface near the C Yates 9 well	5.19
5.15.	Instantaneous frequency behavior on the interpreted Trinity surface near the C Yates 9 well	5.21
5.16.	Reflection profile along Line 1	5.22
5.17.	Reflection profile along Line 2	5.23
6.1.	Location of the B Yates 18D well in the central part of the project area.....	6.2
6.2.	Expanded view of wells offsetting the B Yates 18D location	6.3
6.3.	East-west seismic profile showing the seismic response of a productive Caddo reservoir penetrated by the Robinson A5 well (JMR-A5) and east-west seismic profile showing the seismic response of a Caddo look-alike to the JMR-A5 response	6.8
6.4.	A northwest-southeast seismic profile passing through the B Yates 18D drill site	6.9
6.5.	Comparison of log data from the productive Caddo interval at the Robinson A5 well with the log data from the Caddo interval at the B Yates 18D	6.10
6.6.	Open-hole logs run across the upper portion of the Bend intervals in the B Yates 18D well showing no Lower Caddo sand development.....	6.11
6.7.	Open-hole logs run across the Trinity, Bridgeport, Runaway, and part of the Beans Creek sequences in the B Yates 18D well	6.12
6.8.	Open-hole logs run across the Jasper Creek and Vineyard sequences in the B Yates 18D well	6.13
6.9.	Flow rates and pressures for the Upper Runaway interval in the B Yates 18D well...	6.17
6.10.	Pressure data recorded during the 2-week buildup test conducted in the Upper Runaway reservoir in the B Yates 18D well.....	6.19
6.11.	History match of B Yates 18D Upper Runaway well test. These data suggest a reservoir size of about 8 acres	6.20

6.12.	Schematic diagram of reservoir model used to history match B Yates 18D Upper Runaway well test data	6.21
6.13.	Initial production from the Jasper Creek reservoirs in the B Yates 18D well	6.23
6.14.	Seismic line traversing the BYTS 18D well and illustrating the distinctive, low- amplitude reflection facies associated with the Jasper Creek interval in the immediate vicinity and northwest of the 18D well	6.25
6.15.	Map of seismic reflection across the MFS32 (Lower Jasper Creek) sequence boundary near the BYTS 18D well	6.26
6.16.	Map of instantaneous seismic frequency values across the MFS (Lower Jasper Creek) sequence boundary near the BYTS 18D well	6.27
6.17.	Location of the B Yates 17D well in the west-central part of the project area	6.29
6.18.	Seismic profile passing through the B Yates 17D well location showing the Caddo look-alike response to the Robinson A-5 well at about 0.88 s and several vertically stacked entrapment possibilities highlighted by arrows down to 1.03 s	6.30
6.19.	Expanded view of wells offsetting the B Yates 17D location	6.31
6.20.	Interpreted log for the Jasper Creek sequences penetrated by the B Yates 17D well..	6.35
6.21.	Initial production from the Lower Jasper Creek in the B Yates 17D well.....	6.36
6.22.	Log-log analysis of the pressure buildup test conducted in the Lower Jasper Creek reservoir in the B Yates 17D well	6.38
6.23.	Semilog analysis of the pressure buildup test conducted in the Lower Jasper Creek reservoir in the B Yates 17D well	6.39
6.24.	North-south profile through the B Yates 17D well location showing the position of the Lower Jasper Creek (heavy dash on the well profile) as determined by the depth-to-time calibration function used in the project area and the resulting interpretation of the Lower Jasper Creek sequence boundary	6.42

6.25.	East-west profile through the B Yates 17D well location showing the position of the Lower Jasper Creek (heavy dash on the well profile) as determined by the depth-to-time calibration function used in the project area and the resulting interpretation of the Lower Jasper Creek sequence boundary	6.43
6.26.	Instantaneous frequency behavior across the interpreted Lower Jasper Creek surface.....	6.45
6.27.	Reflection amplitude behavior across the interpreted Lower Jasper Creek surface	6.46

Tables

1.1	Bend Conglomerate characteristics in Boonsville project area	1.14
2.1	Estimated reservoir properties for the Sealy C-2 well	2.18
2.2	RFT pressures measured in the Sealy C-3 well	2.34
4.1	Summary of well test results in I. G. Yates 33 area	4.19
6.1	Reservoir conditions projected at the B Yates 18D location based on offset well data	6.5

VOLUME II FIGURES AND TABLES

Appendix A Figures

A1.	Time-rock stratigraphic column for post-Mississippian strata in the Boonsville Project Area	A.3
A2.	Middle Carboniferous eustatic sea-level changes derived from coastal onlap data.....	A.6
A3.	Pennsylvanian paleogeography and lithofacies distribution of the Midcontinent United States during maximum regression (lowstand)	A.8
A4.	Tectonic and structural framework of the Fort Worth Foreland Basin. Contours represent depth below sea level of the top of the Marble Falls Formation	A.10
A5.	Comparison of stratigraphic nomenclatures for Atokan rocks in the Fort Worth Basin presented by previous workers	A.17
A6.	Crossbed dip orientations based on FMI log data from the Lower Atoka, Billie Yates No. 18D	A.18
A7.	Depth distribution of potassium feldspars determined from infrared spectroscopic analysis of core samples	A.19
A8.	Distribution of well log suites and cores used in the geologic evaluation of the Boonsville Project Area	A.21
A9.	Typical log responses for composite Boonsville Bend Conglomerate genetic sequence	A.25
A10.	Core graphic illustrating key surface-based sequence terminologies in common use	A.28
A11.	Total Bend Conglomerate (= total Atoka) gross isopach (MFS90–MFS10)	A.31
A12.	Boonsville stratigraphic cross section A–A' through Bend Conglomerate using MFS20 (the top of the Vineyard genetic sequence) as a datum.....	A.32

A13.	Boonsville stratigraphic cross section B–B’ through Bend Conglomerate using MFS20 (the top of the Vineyard genetic sequence) as a datum.....	A.33
A14.	Total Bend Conglomerate net reservoir isopach (MFS90–MFS10)	A.34
A15.	Top of Vineyard genetic sequence (MFS20) measured in depth below sea level	A.36
A16.	Top of Trinity genetic sequence (MFS60) measured in depth below sea level	A.37
A17.	Top of Caddo genetic sequence (MFS90) measured in depth below sea level.....	A.38
A18.	Boonsville structural cross section A–A’ through Bend Conglomerate illustrating faults interpreted from 3-D seismic information.....	A.39
A19.	Boonsville structural cross section B–B’ through Bend Conglomerate illustrating faults interpreted from 3-D seismic information.....	A.40
A20.	Map of Boonsville project area showing the relationship between total Atoka (MFS90-MFS10) net reservoir thickness and deep subsurface structure, as indicated by the top of the Marble Falls Limestone interpreted from 3-D seismic data	A.42
A21.	Map of Boonsville project area showing the relationship between modern stream drainage and deep subsurface structure, as indicated by the top of the Marble Falls Limestone interpreted from 3-D seismic data.....	A.44
A22.	Thick sandstone and subtle structural controls on gas production in the Vineyard sequence	A.45
A23.	Semiquantitative relationship established between relative accommodation available during deposition of the Boonsville sequences and compartment size in terms of typical, expected gas reserves	A.50
A24.	Wizard Wells genetic sequence net reservoir isopach (MFS80–MFS70)	A.52
A25.	Stratigraphic cross section A–A’ of Wizard Wells genetic sequence (MFS80–MFS70) illustrating clinofolds (thin black lines between MFS80–MFS70) comprising this highstand delta system	A.53
A26.	Jasper Creek “Exxon” sequence total gross interval isopach (ES40–ES30)	A.55
A27.	Jasper Creek “Exxon” sequence total net reservoir isopach (ES40–ES30)	A.56

A28.	Stratigraphic cross section A–A’ illustrating the Jasper Creek “Exxon” sequence (ES30–ES40).....	A.57
A29.	Lower Jasper Creek “Exxon” sequence total net reservoir isopach (ES34–ES30).....	A.58
A30.	Middle Jasper Creek lowstand valley fill net reservoir isopach (FS34–ES34).....	A.59
A31.	Upper Jasper Creek “Exxon” sequence net reservoir isopach (ES38–ES36)	A.60
A32.	Fourth Jasper Creek “Exxon” sequence net reservoir isopach (ES40–ES38)	A.61
A33.	Middle Jasper Creek genetic sequence from Threshold Development I. G. Yates No. 33 core	A.62
A34.	Caddo genetic sequence total net reservoir isopach (MFS90–MFS80)	A.64
A35.	Stratigraphic cross section B–B’ illustrating Lower Caddo shingling clinofolds and limestone erosionally truncated by ES95	A.65
A36.	Lower Caddo lowstand wedge net reservoir isopach (ES95–MFS80)	A.66
A37.	Upper Caddo genetic lowstand wedge net reservoir isopach (MFS90–ES95)	A.67
A38.	Upper Caddo sequence from OXY, U.S.A., Sealy C No. 2 core	A.68

Appendix A Tables

A1.	Accommodation settings of marine sedimentary basins.....	A.11
A2.	Logging suites from 222 wells available for geological evaluation of Boonsville Project Area.....	A.20
A3.	Semiquantitative relationship between relative accommodation and typical compartment size	A.49

Appendix B Figures

B1.	Completion frequency in various stratigraphic sequences for all wells in the Boonsville project area.....	B.4
-----	--	-----

B2.	Completion frequency in various stratigraphic sequences for wells drilled since 1980 in the Boonsville project area.....	B.6
B3.	Completion frequency in various stratigraphic sequences for wells drilled since 1990 in the Boonsville project area.....	B.7
B4.	Best estimates of original reservoir pressure available from wells in the Boonsville project area	B.8
B5.	Comparison of initial pressures measured in more recent Upper Caddo completions to original pressures reported in the Upper Caddo sequence in the 1950's	B.10
B6.	Comparison of initial pressures measured in more recent Jasper Creek completions to original pressures reported in the Jasper Creek sequence in the 1950's.....	B.11
B7.	Pressures measured in various stratigraphic sequences in wells drilled since 1990 in the Boonsville project area.....	B.12
B8.	Distribution of estimated ultimate gas recoveries from wells in the project area drilled in the 1950's through 1970's	B.14
B9.	Distribution of estimated ultimate gas recoveries for wells in the project area drilled in the 1980's.....	B.15
B10.	Distribution of estimated ultimate gas recoveries, not including behind-pipe opportunities, for wells in the project area drilled in the 1990's	B.17
B11.	Distribution of net pay and net hydrocarbons among the Bend intervals in the project area	B.19
B12.	Distribution of net pay thickness in all zones between the Lower Caddo and the Vineyard; the median net pay is 30 ft	B.22
B13.	Distribution of net hydrocarbon thickness in all zones between the Lower Caddo and the Vineyard; the median net hydrocarbon thickness in 1.9 ft.....	B.23
B14.	Nomograph for the Boonsville project area, showing the net hydrocarbon feet required as a function of pressure and drainage area to obtain recoverable gas reserves of about 400 MMscf.....	B.25

B15.	Nomograph for the Boonsville project area showing the net pay required as a function of pressure and drainage area to attain recoverable gas reserves of about 400 MMscf	B.26
B16.	Estimated drainage areas computed for the major stratigraphic sequences using production data from wells in the project area	B.27
B17.	Range of net pay and net hydrocarbons found in each major sequence throughout the project area	B.29
B18.	Range of potential gas reserves associated with an 80-acre drainage area in each major sequence throughout the project area	B.30
B19.	Distribution of net hydrocarbons between the Lower Caddo and the Vineyard mapped across the project area	B.32
B20.	Distribution of the number of net pay intervals between the Lower Caddo and the Vineyard mapped across the project area	B.33
B21.	Flattening of the p/z curve with time may suggest communication with an incompletely drained reservoir compartment in high-permeability gas reservoirs.....	B.36
B22.	p/z curves may flatten in lower permeability reservoirs but primarily because 24-hr shut-in pressures do not reflect average reservoir pressure.....	B.38
B23.	Example of a Fetkovich type curve that can be used for quantitative production data analysis to estimate reservoir properties, predict drainage area and gas in place, and forecast future performance	B.41
B24.	Example production data analysis using the Fetkovich type curves.....	B.42
B25.	Semilog plot of flow rate vs. time for the Trinity interval in the C Yates 9 well; this production decline behavior is typical of many wells in the project area	B.45
B26.	Log-log plot of production data from the C Yates 9 well showing significant depletion of the Trinity reservoir	B.46
B27.	Log-log plot of production data from the F Yates 9 well showing significant depletion of the Upper Jasper Creek reservoir	B.48

B28.	Production data from the Runaway interval in the B Yates 2 well.....	B.49
B29.	History match of production data from the Runaway interval suggests that the B Yates 2 well may be in communication with a larger gas volume than it can drain effectively.....	B.50
B30.	Map showing drainage areas estimated for Middle Jasper Creek completions from production data analysis.....	B.52
B31.	Time slice of instantaneous seismic frequency.....	B.53
B32.	Comparison of well performance and permeabilities determined from production data analysis for the Sealy C-2 and Sealy B-3 wells.....	B.55
B33.	History match of the actual pressure buildup test data from the April 1993 well test conducted on the I. G. Yates 33 well	B.58

Appendix C Figures

C1.	Time line showing available tool types and a graph of the drilling activity in the general area of the study	C.2
C2.	Porosity vs. permeability cross plot of all sample plugs from the four cored wells	C.11
C3.	Porosity vs. permeability cross plot of all sample plugs from the four cored wells' zones.....	C.12
C4.	Diagrammatic representation of the dual-water model used to interpret resistivity data for water saturation.....	C.16
C5.	Raw log data from one of the test wells used to develop the IES log-analysis technique	C.19
C6.	Log interpretation of the Tarrant A-4 well using all available curves in a standard log analysis.....	C.20
C7.	Log interpretation of the Tarrant A-4 well using only the SP and deep resistivity curves in the IES log analysis	C.21

C8.	In bad hole, a density point is relocated along the line of the neutron porosity value until it intercepts the appropriate shale volume value.....	C.28
C9.	Cross plot of UMA/RHOG used to determine the proportions of up to four minerals in the rock.....	C.30
C10.	Histogram of the SP curve in the “A” facies	C.34
C11.	Histogram of the PEF curve in the “K” facies	C.35
C12.	Histogram of the neutron curve in the “A” facies.....	C.36
C13.	Geocolumn display of all core data stacked on top of one another to the left of the depth track and the corresponding log-derived facies using the FaciesR model to the right of the depth track	C.39
C14.	Geocolumn display of all core data stacked on top of one another to the left of the depth track and the corresponding log-derived facies using the FaciesG model to the right of the depth track	C.40
C15.	Geocolumn display of all core data stacked on top of one another to the left of the depth track and the corresponding log-derived facies using the FaciesU model to the right of the depth track	C.41
C16.	Geocolumn display of all core data stacked on top of one another to the left of the depth track and the corresponding log-derived facies using the FaciesN model to the right of the depth track	C.42
C17.	Geocolumn display of all core data stacked on top of one another to the left of the depth track and the corresponding log-derived facies using the FaciesP model to the right of the depth track	C.43
C18.	A geocolumn display cross section. This section is through the Caddo sequence	C.46
C19.	Interpreted version of the cross section shown in Figure C18.....	C.47
C20.	Cross plot of porosity vs. permeability for all core plugs from the four cored wells ..	C.48
C21.	Cross section through the Upper Caddo in the northeast part of the study area	C.49

C22. Production histories of the Sealy C-2 and Sealy B-3 wells; both wells are completed in the Upper Caddo.....	C.50
--	------

Appendix C Tables

C1. The 12 primary facies identified from the core data for the Bend Conglomerate	C.8
C2. Results of infrared spectroscopy analysis on selected core samples	C.9
C3. Log curves used to construct petrophysical models.....	C.33
C4. Ideal values for each curve in each facies, as chosen from histograms of these data sets.....	C.37
C5. Accuracy of electrofacies model predictions	C.38

Appendix D Figures

D1. The source-receiver grid used to record the Boonsville 3-D seismic data.....	D.2
D2. The construction requirements for shot holes in Texas when the hole depth is less than 20 ft and 20 ft or more.....	D.5
D3. The C-10 directional charge used as the seismic energy source in the Boonsville 3-D survey	D.6
D4. The five-hole source array geometry used at each source station within the Boonsville grid.....	D.7
D5. The geometry used to record vertical wavetest data in the Billy Yates 11 well	D.9
D6. Some of the vertical wavetest data generated by C-10 directional charges detonated in five-hole patterns constructed as shown in Figure D4 and recorded in the Billy Yates 11 well.....	D.10
D7. Amplitude spectra of the pentolite-generated vertical wavetest data shown in Figure D6	D.11
D8. Vibroseis vertical seismic profile recorded in the Billy Yates 11 well.....	D.13

D9.	Amplitude spectra of vibroseis vertical wavetest data recorded at the same receiver depths as the pentolite data in Figure D6	D.14
D10.	Geometrical theory used to design the dimensions of the surface-positioned seismic receiver arrays at Boonsville field	D.16
D11.	The geometrical relationships between the reflected raypaths that arrive at two receiver arrays separated a distance DX and how this receiver interval DX can be calculated by defining the maximum time moveout DT that should exist for a reflection signal recorded by these two arrays	D.17
D12.	Horizontal wavetesting concepts implemented at Boonsville field	D.19
D13.	An example of the horizontal wavetest data recorded using the point receiver option.....	D.21
D14.	Horizontal wavetest data recorded using a moderately long receiver array	D.22
D15.	The horizontal wavetest data recorded on east-west receiver line 1, the f-k spectrum of the 110-ft long receiver arrays, and the f-k spectrum of the clustered receiver array responses	D.23
D16.	The horizontal wavetest data recorded on north-south receiver line 2, the f-k spectrum of the 110-ft long receiver arrays, and the f-k spectrum of the clustered receiver arrays	D.24
D17.	The staggered-line geometry used at Boonsville field.....	D.26
D18.	Stacking fold for the 110- × 110-ft bins as determined by trace sorting during data processing.....	D.28
D19.	Stacking fold for the 55- × 55-ft bins as determined by trace sorting during data processing.....	D.29
D20.	The receiver aperture ABCD used at Boonsville field	D.30

D21.	The Boonsville data recorded using multiple shooters positioned at preplanned locations S_1 , S_2 , and S_3 and state-of-the-art recording system, which allowed receiver apertures $A_1B_1C_1D_1$, $A_2B_2C_2D_2$, and $A_3B_3C_3D_3$ to be quickly activated about S_1 , S_2 , and S_3 as soon as the shooters at these locations were ready to power their shooting boxes	D.33
D22.	Typical field data recorded across the Boonsville 3-D grid.....	D.35
D23.	Deconvolution test of the far-offset traces of a Boonsville field record to determine the usable bandwidth of the reflection signals	D.38
D24.	Deconvolution test of the near-offset traces of a Boonsville field record to determine the usable bandwidth of the reflection signals	D.39
D25.	Refraction statics, first pass and second pass, applied to the Boonsville 3-D data.....	D.40
D26.	Residual statics, first pass and fourth pass, applied to the Boonsville 3-D data	D.44
D27.	South-north profiles of the final stacking velocities along inlines 100 and 200	D.46
D28.	West-east profile of the final stacking velocities along crossline 100	D.47
D29.	A time slice cutting the 3-D stacking velocity volume at 1.1 s	D.48
D30.	A comparison between Boonsville data stacked without spectral balancing and with spectral balancing	D.50
D31.	A second comparison between Boonsville data stacked without spectral balancing and with spectral balancing	D.51
D32.	The frequency content of a hypothetical seismic trace before and after the numerical process of spectral balancing	D.52
D33.	Flow chart showing the numerical steps involved in spectral balancing	D.54
D34.	The specific bandpass filters created in computation loop A for the Boonsville data.....	D.55

Appendix D Table

D1.	Boonsville 3-D data-processing sequence	D.36
-----	---	------

Appendix E Figures

E1.	Graphical illustration of a complex seismic trace	E.2
E2.	Graphical illustration of seismic attributes—instantaneous amplitude $a(t)$, instantaneous phase $\phi(t)$, and instantaneous frequency $\omega(t)$	E.4
E3.	Illustration of the instantaneous amplitude seismic attribute calculated for an actual seismic trace	E.6
E4.	The instantaneous phase seismic attribute function	E.7
E5.	The instantaneous frequency seismic attribute function calculated for the same seismic trace discussed in Figure E4.....	E.9
E6.	A time slice cutting through the Boonsville 3-D instantaneous frequency volume at a two-way time of 900 ms.....	E.12
E7.	Inline profile 52 showing that the anomalous instantaneous frequency values in the vicinity of crossline coordinate 80 are associated with a stratigraphic pinch-out	E.14
E8.	Inline profile 111 showing that the anomalous instantaneous frequency values in the vicinity of crossline coordinate 165 are associated with a stratigraphic mound (reef?)	E.15
E9.	Crossline 186 showing that the anomalous instantaneous frequency values in the vicinity of inline coordinate 45 are associated with a structural, karst-generated collapsed zone	E.16
E10.	A time slice cutting through the Boonsville 3-D instantaneous frequency volume at a two-way time of 980 ms.....	E.18
E11.	Inline profile 147 showing that the anomalous instantaneous frequency values in the vicinity of crossline coordinate 170 are associated with a fault.....	E.19

Appendix F Figures

F1.	The concept of positioning thin beds in 3-D seismic images	F.2
F2.	Location of wells where velocity checkshots and VSP data were recorded	F.7
F3.	Time-vs-depth functions measured for vibroseis and pentolite (C-10 directional charges) wavelets inside the Boonsville 3-D seismic grid	F.9
F4.	Variance in depth predictions associated with the travelttime functions shown in Figure F3	F.10
F5.	Time-vs-depth functions derived from pentolite-wavelet checkshot data recorded in different wells within the Boonsville 3-D seismic grid	F.12
F6.	Variation in depth predictions associated with the travelttime functions shown in Figure F5	F.13
F7.	Comparison between contractor-delivered VSP images and 3-D seismic images at the B Yates 18D well	F.15
F8.	Comparison between wavelet-equalized VSP and 3-D images at the B Yates 18D well	F.17
F9.	Comparison between contractor-delivered VSP image (northeast source offset location) and 3-D seismic image at the B Yates 17D well	F.18
F10.	Comparison between wavelet-equalized VSP image (northeast source offset location) and 3-D seismic image at the B Yates 17D well.....	F.19
F11.	Comparison between contractor-delivered VSP image (southwest source offset location) and 3-D seismic image at the B Yates 17D well	F.20
F12.	Comparison between wavelet-equalized VSP image (southwest source offset location) and 3-D seismic image at the B Yates 17D well	F.21
F13.	Stratigraphic nomenclature used to define depositional units and sequence boundaries in Boonsville field	F.25

F14. A map showing some of the wells used to identify the time positions of chronostratigraphic surfaces inside the Boonsville 3-D gridF.26

F15. Arbitrary seismic line following the path labeled Line 2 in Figure F14F.28

F16. Arbitrary seismic line following the path labeled Line 5 in Figure F14F.29

F17. The seeding grid for the Caddo chronostratigraphic surfaceF.31

EXECUTIVE SUMMARY

Major Conclusions

This investigation of reservoir compartmentalization in the Bend Conglomerate interval of Boonsville field in the Fort Worth Basin has resulted in the following major conclusions.

1. Ellenburger-related karsts (that is, dissolution of buried Ellenburger carbonates) have produced subterranean voids that collapsed when a sufficient overburden accumulated. These collapse zones extend to great heights above the depth at which the carbonate dissolution occurred, and they have affected Bend Conglomerate sedimentation and created reservoir compartments in the clastic Bend Conglomerate interval as far as 2,500 ft above the Ellenburger. These collapsed chimneys pervade our Boonsville study area **but can be conclusively identified only when 3-D seismic images are available. These important karst phenomena were unknown to exist in the area before our 3-D seismic data were interpreted.**
2. The areal distribution of reservoir facies in the topmost Bend Conglomerate sequence (the Caddo sequence) can be determined from areal maps of key seismic attributes. Instantaneous frequency was the best attribute for mapping Lower Caddo reservoir sandstone, and reflection amplitude was the best attribute for depicting the presence of Upper Caddo reservoir facies. In contrast, seismic attributes could not indicate the presence of reservoir facies in some of the deeper Bend Conglomerate sequences.
3. The complex stratigraphy that is created in low- to moderate-accommodation basin conditions, such as those in the Bend Conglomerate section and in many other Pennsylvanian sections of Midcontinent reservoirs, is best revealed by applying

the **concepts of sequence stratigraphy** to all available well log and core control.

4. Analysis of production and pressure history data demonstrates that a wide range of reservoir compartment sizes exists in Boonsville field, and integration of these engineering analyses with sequence stratigraphy results shows that, in general, **large compartments exist in low-accommodation sequences, and small compartments in high-accommodation sequences.**
5. Although well log control in Boonsville field has spanned a period of 40 yr and many different vintages of logging technology, algorithms can be developed that allow consistent rock facies to be interpreted from these diverse logs. The petrophysical analysis concepts developed in this study should be helpful in other Midcontinent basins.
6. Wells drilled as a result of this study confirm that **reservoirs often exist as vertically stacked compartments in several of the Bend Conglomerate genetic sequences.** These stacked completion opportunities are best found by integrating maps of facies distributions developed from a sequence stratigraphic analysis of logs using 3-D seismic images of selected sequences and using engineering analyses that predict compartment sizes and probable fluid-flow paths.

Methods and Tools

The fundamental objective of the Boonsville study was to demonstrate how to characterize a complex reservoir system by **integrating and applying off-the-shelf technologies**, not to develop fundamental new technologies that industry has not been exposed to nor can readily duplicate. Geologically, the critical analytic method used was **sequence stratigraphy**, and the geological analyses described in this report demonstrate

how sequence stratigraphic principles can be implemented in the complex stratigraphy of Midcontinent-type basins.

The reservoir engineering analytic methods used in this study are practiced by many people in industry and academe and are replicated in various commercial software packages. The reservoir models developed and discussed herein were simply done with great care, and then integrated with geologic and geophysical control to determine which reservoir models best agreed with the pressure and production data.

One of the more important tools used in the Boonsville study was **3-D seismic imaging**. In fact, the complexity of the Bend Conglomerate reservoir systems could not have been fully realized without 3-D seismic imaging technology. Several concepts were tested during seismic data acquisition and processing, such as the use of small directional charges as an energy source, staggered-line recording geometry to create smaller acquisition bins, and spectral balancing to increase stratigraphic resolution. These concepts are discussed in Volume II, Appendix D.

A second important geophysical tool was **vertical seismic profile (VSP) data, which were used to calibrate stratigraphic depth to seismic traveltimes accurately**. These calibration data allowed thin sequences to be positioned in the correct narrow seismic time windows during workstation interpretation sessions. This depth-to-time calibration technique is described in Volume II, Appendix E.

General Comments

This report documents an assessment of Midcontinent sandstone natural gas reservoirs in Boonsville field, Fort Worth Basin, Texas, conducted as part of the Secondary Gas Recovery (SGR) Infield Reserve Growth Joint Venture between the Gas Research Institute (GRI) and the U.S. Department of Energy (DOE). Additional support was provided by the State of Texas. **The objectives of this SGR project were to define undrained or incompletely drained reservoir compartments controlled primarily by**

depositional heterogeneity in a complex, Midcontinent fluvial-deltaic depositional setting, and, afterward, **to develop and transfer strategies for infield reserve growth of natural gas to producers.** Reserve growth resources in the Midcontinent region total as much as 41 Tcf. The region contains the second-largest natural gas reserve growth resource after the Texas Gulf Coast and is thus an appropriate resource target for SGR research.

Midcontinent gas production is dominantly derived from Pennsylvanian sandstones laid down as fluvial and deltaic deposits (23 plays in Texas, Oklahoma, Arkansas, and Kansas). These are the primary facies in the Atokan Caddo and Bend Conglomerate at Boonsville field, our laboratory for defining heterogeneity in these reservoir types. In this project, interpretation of these complex reservoirs was aided by a 26-mi² 3-D seismic survey collected to test methods of reservoir delineation in thin-bed, hard-rock environments.

The thickness of the Atoka Group (Lower and Upper) in the project area varies between 900 and 1,300 ft and has been divided into 13 third-order genetic stratigraphic sequences for purposes of this study. These genetic sequences are defined and bounded by impermeable deep-shelf shales that represent maximum flooding events and are similar in nature to the cycles or cyclothems used in other contexts to describe similarly repetitive, late Paleozoic strata. To our knowledge, this is the first public, comprehensive genetic sequence analysis that relates these prolific Pennsylvanian reservoirs to their seismic response and to gas productivity on a sequence-by-sequence basis.

Pressure and production data confirm the existence of compartmented or poorly drained gas reserves throughout much of the Bend Conglomerate interval in the project area. New wells drilled through the Bend frequently find pressures in one or more of the Bend sequences that are at or near the original pressures encountered more than 40 yr ago when the field was first developed. Most of these compartmented or poorly drained gas reserves are found in sequences between the Lower

Caddo and the Vineyard (the most prolific, basal conglomerate in the Bend section). Median drainage areas in these sequences were found to be 80 acres or less, further confirming the likelihood that compartmented or poorly drained gas reserves will continue to be found as well spacing is reduced to 80 acres (currently the optional well spacing in Boonsville field).

Critical Observations

From comprehensive analysis of the Boonsville project area, **three styles of reservoir compartmentalization were identified in Midcontinent clastic gas reservoirs: structural, stratigraphic, and a combination of these two styles.** Structural compartments in Boonsville field are caused by low-displacement faulting, most commonly associated with karst collapse in deeper carbonate rocks, that produces structurally isolated fault blocks. The faulting is widespread, but subtle, and neither vertical displacements nor fault-block geometries can be mapped without 3-D seismic data. The importance of this karst-induced structure to reservoir development in the Bend Conglomerate was previously unknown.

Stratigraphic compartments may be surface bounded, facies bounded, or cement bounded. Surface-bounded compartments result from superposition of reservoir sandstones and other, diachronous impermeable facies at key surfaces. Facies-bounded compartments are caused by high-frequency, autocyclic processes within depositional systems tracts that result in permeability barriers. These facies changes may occur over fairly short, lateral distances. Cement-bounded compartments result from postdepositional interfacies barriers caused by diagenetic processes (for example, the development of CaCO_3 and SiO_2 cements).

Combination-style compartments have both structural and stratigraphic elements. Although they are most commonly surface and fault bounded, some combination

compartments result from syntectonic deposition—that is, the preferential buildup of reservoir facies in response to subtle fault-block lows.

The best natural gas reservoirs in Boonsville field occur predominantly as lowstand, valley-fill conglomeratic sandstones. They owe their existence to erosional downcutting (incisement), which occurs during relative sea-level lowstands, followed by subsequent aggradation during the early phase of relative sea-level rises. Highstand deltaic and shoreface sandstones are also important reservoirs that occur as progradational lobes. Lowstand fluvial and deltaic deposits overlie and erosionally truncate highstand deposits; however, their respective sandstone bodies typically occur as separate compartments. A relationship has been developed between compartment size (hence, volume of the gas resource) and accommodation space. Caddo and Vineyard sequences contain the largest gas-bearing compartments because lateral reworking was maximized in a low-accommodation space setting.

Isopach mapping of net pay within the total Bend Conglomerate section indicates a strong relationship between sandstone reservoir distribution and structurally low areas on the pre-Atoka seismic time structure surface. This fact suggests that subtle differences in the structural elevation at the pre-Atoka, Paleozoic carbonate, stratigraphic level controlled the geographical location of incised valleys, which are the fluvial and fluvio-deltaic axes in which high-energy reservoir facies were concentrated. In addition, **many of the thickest valley-fill sandstone reservoirs occur above, or immediately adjacent to, the vertically faulted, karst collapse zones identified by means of 3-D seismic,** although this is not the rule for all Boonsville sequences. Karst collapse appears to have occurred throughout Bend deposition such that slightly different structurally controlled physiographies existed during the deposition of each Bend sequence. In some cases, drainage areas inferred from production data analysis and from analysis of 3-D seismic data correlated closely in relict high areas surrounded by karst collapse.

Older ES and IES (resistivity-only) log suites comprised more than half of the available well log data in the project area. In order to include these data in the project analysis, **we developed an algorithm for estimating porosity and lithologies from IES logs**, and we interpreted the ES logs using commercially available software. In addition, **we developed detailed facies identification algorithms for all vintages of well log suites commonly available in the Midcontinent**. These log-calculated facies curves were based on careful calibration of geological core observations and multivariate statistical analysis and were useful in backing up the sequence stratigraphic correlations of reservoir zones.

The interpretation of 3-D seismic data and their application to Bend Conglomerate reservoir types were the cornerstone of this project. In acquiring the 3-D survey, we maximized data resolution using specialized (10 oz), directional explosive charges and a high data-sampling rate (1 ms). A unique staggered source and receiver-line geometry was implemented that allowed data to be stacked into high-fold 110- × 110-ft bins for geological interpretation or into lower fold 55- × 55-ft bins for interpretations requiring detailed lateral resolution. We calibrated thin-bed depths to seismic traveltime by recording detailed vertical seismic profile (VSP) data and explosive-source velocity checkshot data at several locations within the 3-D seismic grid.

At Boonsville, the **3-D data identified a structural component important to reservoir compartmentalization that was unexpected beforehand, which was the aforementioned low-displacement faulting that was often (but not always) associated with karst collapse in deeper carbonate rocks**. These karst collapse features extend vertically as much as 2,500 ft and tend to occur in dominantly north-northwesterly linear groups, suggesting a genetic relationship between karst-dissolution processes and preexisting, subtle basement faulting. **Recent Boonsville wells drilled in these small (about 100 acres), structurally high fault blocks have encountered higher than expected pressures in some sequences,**

suggesting that these low-displacement faults can act as partial barriers to gas flow. Similar karst collapse features occur in Paleozoic outcrops in far West Texas, and hydrocarbon production is known to occur in Ellenburger karst zones in the Val Verde Basin, suggesting that these features may be a widespread influence on the deposition of younger sediments in the Midcontinent.

The ability of the 3-D seismic data to identify stratigraphic entrapments at Boonsville was highly variable. Some sequences, such as the Upper and Lower Caddo, were well imaged in the 3-D data volume, once calibrated to existing well control. **Seismic-attribute analysis based on reflection amplitude and instantaneous frequency behavior in the Upper and Lower Caddo sequences provided excellent agreement with net reservoir distributions generated from the well-log-based sequence stratigraphic interpretations.** In some sequences, the 3-D seismic data can thus be highly predictive for identifying interwell properties and siting new wells, although first there needs to be an adequate number of wells to allow a relationship between seismic attributes and stratigraphic and lithologic facies to be established.

In these complex, surface-dominated stratigraphies that have thin, discontinuous reservoirs, 3-D seismic data do not always provide conclusive answers. Some individual systems tracts and some reservoir sandstones that are subsets of genetic sequences are difficult to trace in the 3-D data, when the targeted units have subtle changes of acoustic impedance or are extremely thin. We found some stratigraphically trapped Bend Conglomerate reservoirs to be seismically nondescript and difficult to distinguish even when well control was used to guide the seismic interpretation. In such instances, the 3-D seismic data cannot be used reliably to locate new infield well locations.

An important use of the 3-D seismic survey in this project was in identifying and tracing the geometries of key chronostratigraphic surfaces that manifest themselves as

seismic reflectors. This is interpretive seismic stratigraphy at a high resolution, which integrates well control with the sequence stratigraphic models developed by the geologist. In Midcontinent rocks, it is particularly important to recognize major erosional features that have cut out previously deposited sequences, as well as shingling, clinoform geometries in which several individual sandstone compartments can occur (and that appear to be only a single unit in log-based cross sections). Integration of the 3-D seismic data is critical to identifying true reservoir architecture, which typically contains significant lateral heterogeneities.

Ultimately the key to successful infield development in an older Midcontinent field such as Boonsville is the volume of gas reserves associated with these compartmented or poorly drained areas of the field. Judging from the hydrocarbon distribution in the project area, the expected gas reserves associated with an individual reservoir compartment or a poorly drained area in any particular Bend sequence will be on the order of 200 MMscf or less (on average) as well spacing is reduced to 80 acres, whereas gas reserves of at least 400 MMscf will typically be required for new wells to be economically attractive (depending on operator and completion practices). Although it is still possible that an individual Bend completion may encounter gas reserves in excess of 400 MMscf (some have in recent wells), it is more likely that multiple stacked completion opportunities will be needed to yield gas reserves sufficient for a viable infield well as spacing is reduced. Highest remaining pressures will most likely be found in sequences below the Caddo and above the Vineyard. The Vineyard sequence in the lower Bend in particular is likely to be substantially drained, given its estimated median drainage area of 160 acres calculated for completions in the project area. However, even a low-pressure reservoir (500 to 1,000 psi) in the Vineyard is often worth completion and contributes to the economics of a new well.

Analysis of the 3-D seismic data volume in the project area leads us to conclude that **stacked trapping geometries commonly exist.** Further, the influence of the vertical, karst collapse features of Bend Conglomerate stratigraphy also suggests the opportunity

and likelihood of finding multiple stacked, and at least partially isolated reservoirs. In the absence of clear geologic or seismic evidence of undeveloped reservoirs, a reasonable approach to identifying new well locations is to focus 3-D seismic evaluation on these apparent, stacked trapping geometries in areas having the highest likelihood of multiple completion opportunities (that is, multiple pay zones). An alternate strategy for siting new wells is to use 3-D seismic data to identify fault-bounded blocks having no well penetrations in those subregional or field-scale areas where the pre-Atoka time structure is low and total Atoka net reservoir isopachs are thick, again increasing the potential for finding multiple vertically stacked completion opportunities.

Technology Transfer

This report summarizes the technical results of the Boonsville investigation, but it represents only one facet of the technology transfer from this project. Three short courses based on these results have already been presented and have been well received by industry audiences, not to mention numerous presentations of aspects of the Boonsville project to a variety of professional organizations. Three to six more short courses are anticipated through early 1996, as well as additional technical papers and presentations.

Seven technical summaries have been published that highlight innovative technological applications in both seismic acquisition and facies determination. Several more technical summaries are planned in the coming months. Executable versions of personal-computer software for applying the IES algorithm are available in both Windows and Macintosh formats. Finally, a digital subset of the 3-D survey data, as well as selected elements of the well data base and digital log curves, will also be made available to industry (by February 1996) as part of the technology transfer process. For further information about the technology transfer products generated by this study, contact the Bureau of Economic Geology at (512) 471-1534 or refer to the Bureau's Internet Web site at <http://www.utexas.edu/research/beg> or to GRI's home page at <http://www.gri.org/>.

1. OVERVIEW

The Context for a Natural Gas Reserve Growth Study of Midcontinent Gas Reservoirs

This report documents an assessment of Midcontinent sandstone natural gas reservoirs in Boonsville field, Fort Worth Basin, Texas. The Boonsville test site centers on a 26 mi² 3-D seismic survey within the field that has been the focal point of this study. The objective of the work, a part of the Secondary Gas Recovery (SGR) Infield Reserve Growth Joint Venture between the Gas Research Institute (GRI) and the U.S. Department of Energy (DOE), is to define advanced approaches to infield natural gas reserve growth. Boonsville field, ranked 28th among U.S. gas fields in cumulative production (as of year-end, 1992), was selected as representative of Pennsylvanian Midcontinent sandstone reservoirs. Pennsylvanian sandstones dominate Midcontinent gas production; 23 out of 41 plays in the region are Pennsylvanian in age and consist dominantly of sandstone reservoirs.

Reserve growth resources in the Midcontinent region total as much as 41 Tcf. The region contains the second-largest gas reserve growth resource after the Texas Gulf Coast and is thus an appropriate resource target after completing the SGR Gulf Coast project. The Midcontinent reservoirs selected for study have more deltaic depositional components than the dominantly fluvial reservoir targets at Stratton field of South Texas (Kleberg and Neuces Counties) that were the focus of a previous Gulf Coast SGR project. The Midcontinent reservoirs studied were deposited in a cratonic basin with relatively low accommodation space and a higher frequency of sea-level fluctuation compared with depositional patterns in the Tertiary of the Gulf Coast Basin. Pennsylvanian Midcontinent sandstone reservoirs are therefore complex and difficult to characterize, but it is this complexity that creates the opportunity for additional infield gas recovery. The purpose of the project is to demonstrate approaches to overcoming that complexity and targeting the gas resource, and pursuing the work using integrated state-of-the-art techniques, such

as sequence stratigraphy, 3-D seismic imaging, and vertical seismic profiling, that can be used by a large cross section of Midcontinent operators.

Project team members have worked with three cooperating companies in assessing reserve growth opportunities at Boonsville: OXY USA, Inc., Enserch Operating Limited Partnership, and Threshold Development/Arch Petroleum Company. These companies provided more than 90-percent cofunding of the 3-D seismic survey, made substantial volumes of existing data available, allowed use of proprietary software for reservoir analysis (OXY USA), and cofunded collection of new data as new wells were drilled, completed, and tested. The participation of these companies was an essential and integral part of the SGR Midcontinent project.

Volume I of this two-volume report is organized around a series of case studies that follow a brief overview of the Boonsville test site. The project was driven by application of 3-D seismic data to Boonsville reservoir types within the Bend Conglomerate, an interval generally 1,000 to 1,200 ft thick that contains at least twelve depositional cycles. However, **the technical details of the applications made in this seismic analysis and in each of the other major disciplines—geology, reservoir engineering, and petrophysics—are contained in a series of appendices in Volume II of this report.** This report structure was adopted so that the case studies would not be burdened with excessive methodological detail. Yet it is this detail that operators will want to understand if they are to examine the results of this study and incorporate the insights gained into their efforts to develop existing fields for gas reserve growth.

It should be noted that the case studies highlight both insights that have been gained and problems that remain unresolved. Whereas the stratigraphic character of key sequences such as the Upper and Lower Caddo was clearly imaged in the seismic volume, the 3-D seismic data did not provide conclusive answers in all sequences within the Bend Conglomerate. In these complex, surface-dominated stratigraphies with thin, discontinuous reservoirs, not all analogs to prolific reservoirs showed an analogous

production response. Structure, related to carbonate dissolution and karst collapse at depth, was found to play a role in reservoir development that was not previously known. Cases are described where different data, namely engineering analyses of reservoir size compared with geophysical images, gave similar results for reservoir dimensions, whereas in other cases such coherence was not achievable. Initial results from two new wells sited early in the interpretation of the 3-D data are also presented, illustrating the seismic features that suggest reservoir compartmentalization and the procedures used to identify these features in the 3-D seismic image. The authors believe that **in documenting these case studies operators will gain a realistic sense of the difficulties, as well as the potential, for successful infield development.** One short course participant commented that he liked the case study approach and liked seeing the real problems presented "warts and all."

Extension to Other Locations and Technology Transfer to Industry

This report documents the technical results of the Boonsville investigation. Three short courses based on these results have already been presented and have been well received by industry audiences. A technology transfer period will follow, with additional short courses and the generation of additional technology transfer products. The second generation of short course notes will provide additional detail for the case studies and will better integrate geophysical and sequence stratigraphic interpretations with other aspects of the investigation. The latter material will reconcile reservoir extent with engineering tests of reservoir volumes that are in communication with a given completion interval. No new data will be incorporated into this additional integration. The focus will be on greater depth of analysis of existing data to develop key relationships that have extrapolation potential to wider areas within Midcontinent cyclic reservoir sequences.

The technology transfer products that will be created include (1) a low-cost digital copy of part of the Boonsville 3-D seismic data, together with digitized well log curves,

vertical seismic profile data, and spreadsheets of production information and pressure data; (2) several free Technical Summaries that provide nonspecialist explanations of key seismic, petrophysical, and engineering concepts; and (3) a how-to manual that describes the factors and procedures required for characterizing a complex reservoir. Updated information about these technology transfer products can be obtained by telephone (Bureau of Economic Geology [512] 471-1534) or by the World-Wide Web (Bureau of Economic Geology at <http://www.utexas.edu/research/beg> and Gas Research Institute at <http://www.gri.org/>). Other comments about our technology transfer plans are provided on page 0.10 of this report.

Overview of the Boonsville Project Area

Introduction

The primary focus of this study was Boonsville (Bend Conglomerate Gas) field located in the Fort Worth Basin of north-central Texas. Figure 1.1 shows the location of the field, which covers most of Wise and Jack Counties, Texas. Actually there are several Boonsville field designations in the area, depending on the particular completion interval(s), but the area of primary interest in the study is officially designated as Boonsville (Bend Conglomerate Gas) field by the Railroad Commission of Texas. This field covers several hundred thousand acres and is one of the largest natural gas fields in the United States. To date, the field has produced in excess of 2.6 Tscf (trillion standard cubic feet) of natural gas; there are just over 2,000 active wells in the field.

In Figure 1.1, the region designated by the solid rectangle on the Wise-Jack County line is the primary area of interest in this project. This is where 26-mi² of 3-D seismic data were gathered and where the vast majority of research work reported here was performed. This location will be referred to as the Boonsville project area throughout this report.

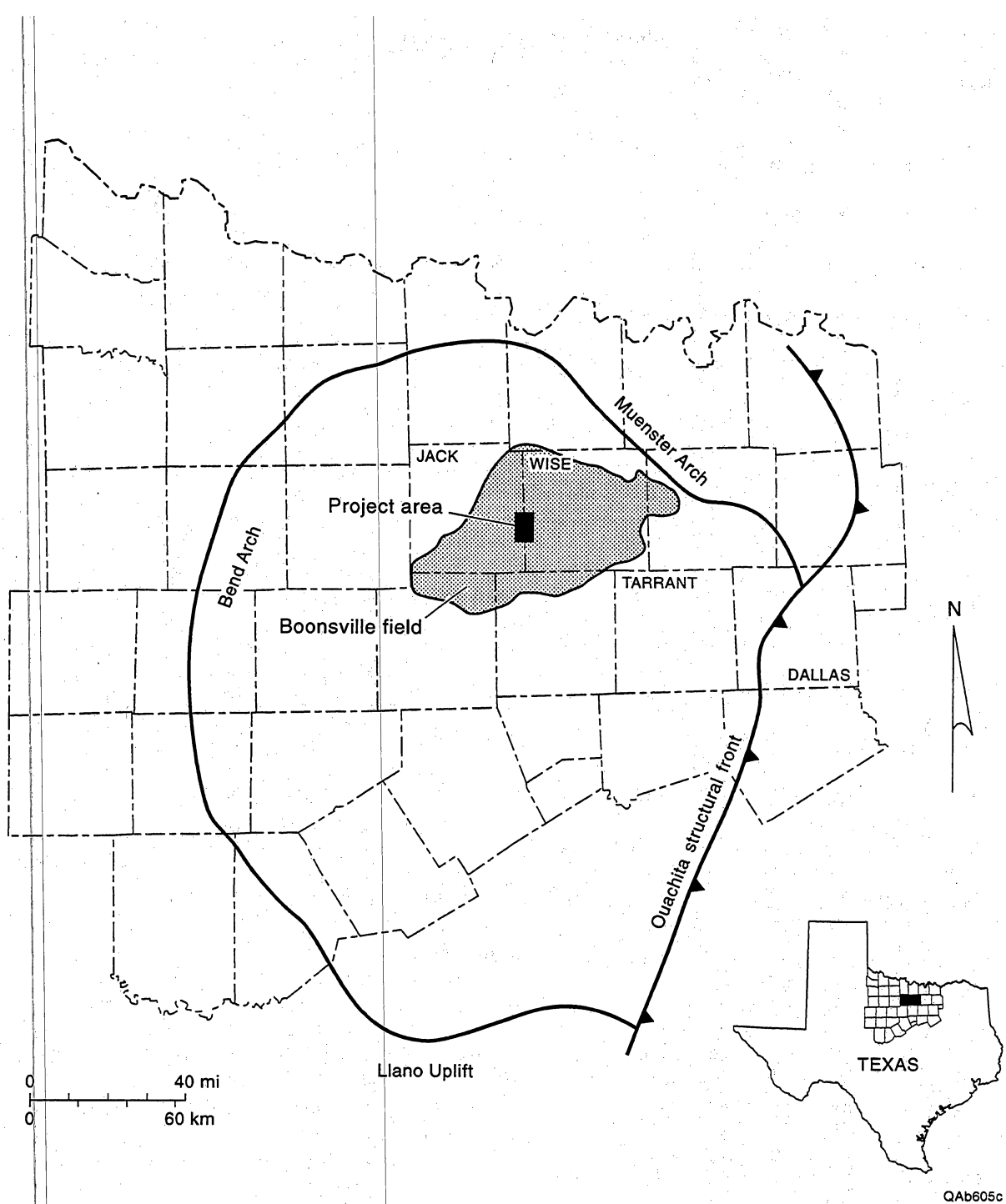


Figure 1.1. Location of Boonsville field in Wise and Jack Counties, Texas. The solid rectangle on the Wise–Jack County line designates the area where the 3-D seismic data were gathered and where the vast majority of the research work was performed.

Figure 1.2 shows a history of drilling activity in the Boonsville project area. This figure plots the number of wells drilled in, and immediately adjacent to, the project area against the year drilled. This figure does not include all wells in the field, but the trends shown in the figure are representative of the field as a whole.

Boonsville field was discovered in 1945, but in the late 1940's and early 1950's, there was not much market for the gas. In fact, operators commonly abandoned, or shut in and temporarily abandoned, a number of gas-producing wells in this time period. Drilling boomed in the mid- to late 1950's, following the construction of a large gas pipeline that went from Wise County to Chicago. Figure 1.2 illustrates the large increase in drilling activity in the project area in the mid- to late 1950's owing to the existence of the new pipeline market.

In November 1957, the Railroad Commission of Texas officially established field rules for Boonsville (Bend Conglomerate Gas) field. These initial field rules permitted one well to be drilled on a 320-acre unit. This field designation consolidated more than 29 separate fields in existence at the time, and other fields have been merged with Boonsville (Bend Conglomerate Gas) field since then.

Drilling activity tapered off in the 1960's and 1970's; then in 1980, the Railroad Commission of Texas modified the field rules to permit wells to be drilled on optional 160-acre units. As Figure 1.2 shows, this ruling sparked new drilling activity in the field in the early- to mid-1980's. Recently, in 1991, the Railroad Commission reduced the spacing requirements again, permitting wells to be drilled on optional 80-acre units. Again, there has been a small upturn in the drilling activity as a result of this reduced spacing.

Geologic Setting

Natural gas production in Boonsville field comes from conglomeratic sandstones deposited in the Fort Worth Basin during the Atoka stage of the Middle Pennsylvanian

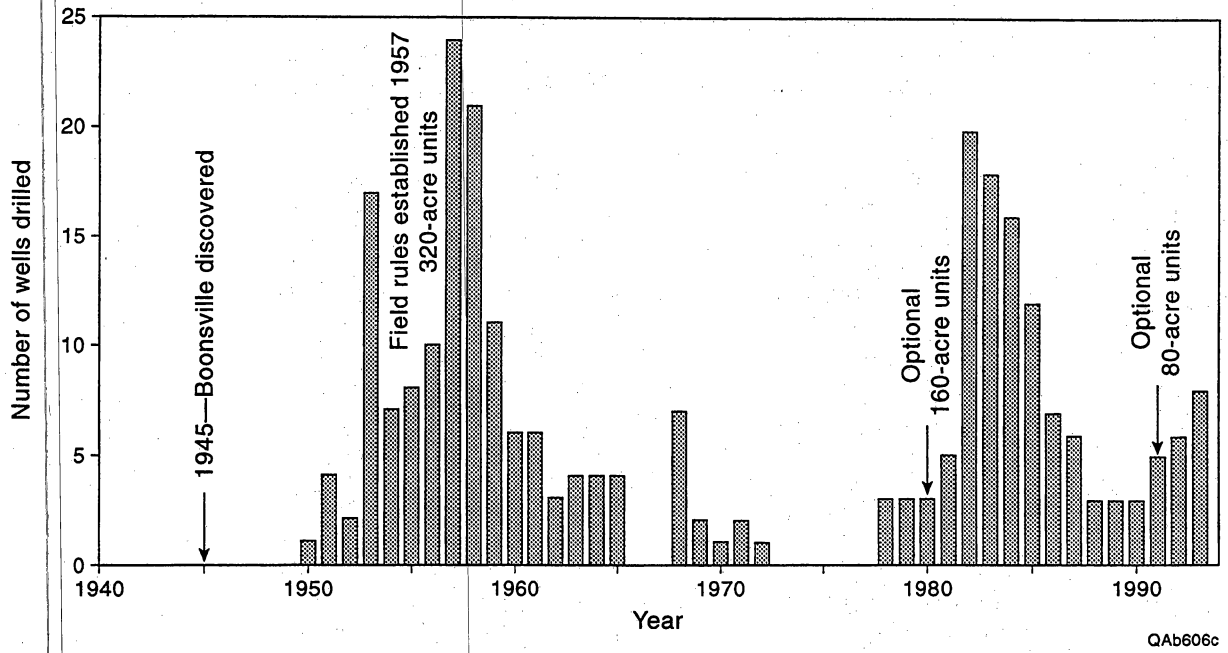


Figure 1.2. History of drilling activity for wells drilled in, and immediately adjacent to, the Boonsville project area.

period (Figs. 1.3 and 1.4; Blanchard and others, 1968; Thompson, 1982). The primary trapping mechanisms are facies and permeability pinch-outs (Glover, 1982; Lahti and Huber, 1982; Thompson, 1982), and effective exploitation of these fields is difficult because the typically thin and discontinuous sandstone reservoirs represent a variety of complexly intermingled depositional environments and facies and commonly contain pore-occluding diagenetic cements. The complexities found in many Upper Paleozoic sandstones of the U.S. Midcontinent are the result of unique fundamental geological controls that combined to produce complex, compartmentalized reservoirs.

Specifically the primary geological controls were:

- relatively low accommodation setting (i.e., shallow basin),
- high-amplitude, high-frequency sea level fluctuations,
- tectonic jostling during sedimentation,
- temporal variations in sediment source material,
- high rates of sediment supply, and
- tropical paleoclimate.

The Fort Worth Basin is a late Paleozoic foreland basin that contains a maximum thickness of approximately 13,000 ft (~4,000 m) of sedimentary strata, the majority of which are Pennsylvanian in age (Turner, 1957; Thompson, 1988). In addition to the dominantly Pennsylvanian basin fill, major sequences of Cambrian, Ordovician, Mississippian, and Permian rocks are also present. The Paleozoic units are unconformably overlain and onlapped by Cretaceous strata in the eastern and southeastern parts of the basin (Flawn and others, 1961; Lahti and Huber, 1982; Thompson, 1982).

In map view, the Fort Worth Basin is an asymmetric, inverted triangle that is approximately 80 mi across and 250 mi long, from apex to base (Figure 1.3). Fault-bounded structural uplifts define the eastern (Ouachita Thrust Belt) and northern limits (Muenster Uplift, Red River-Electra Uplift) of the basin, but the less distinct western

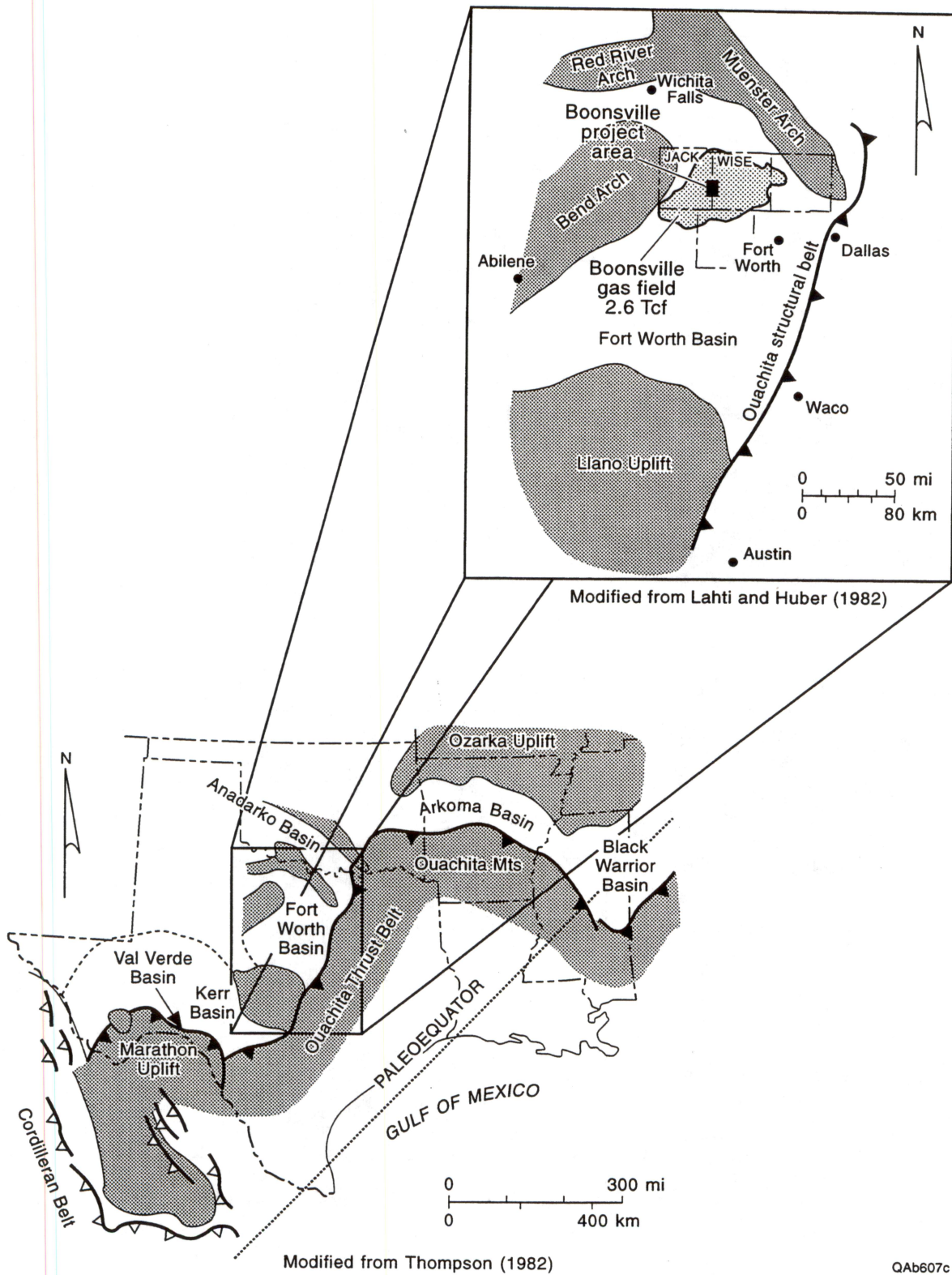
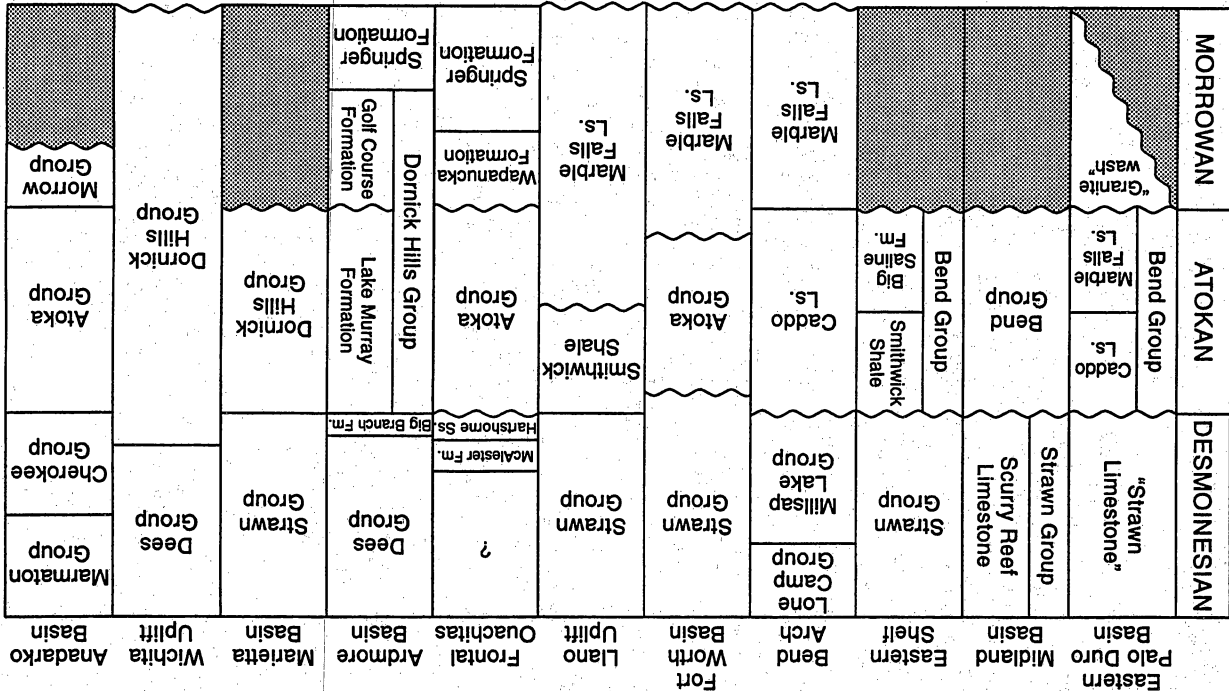
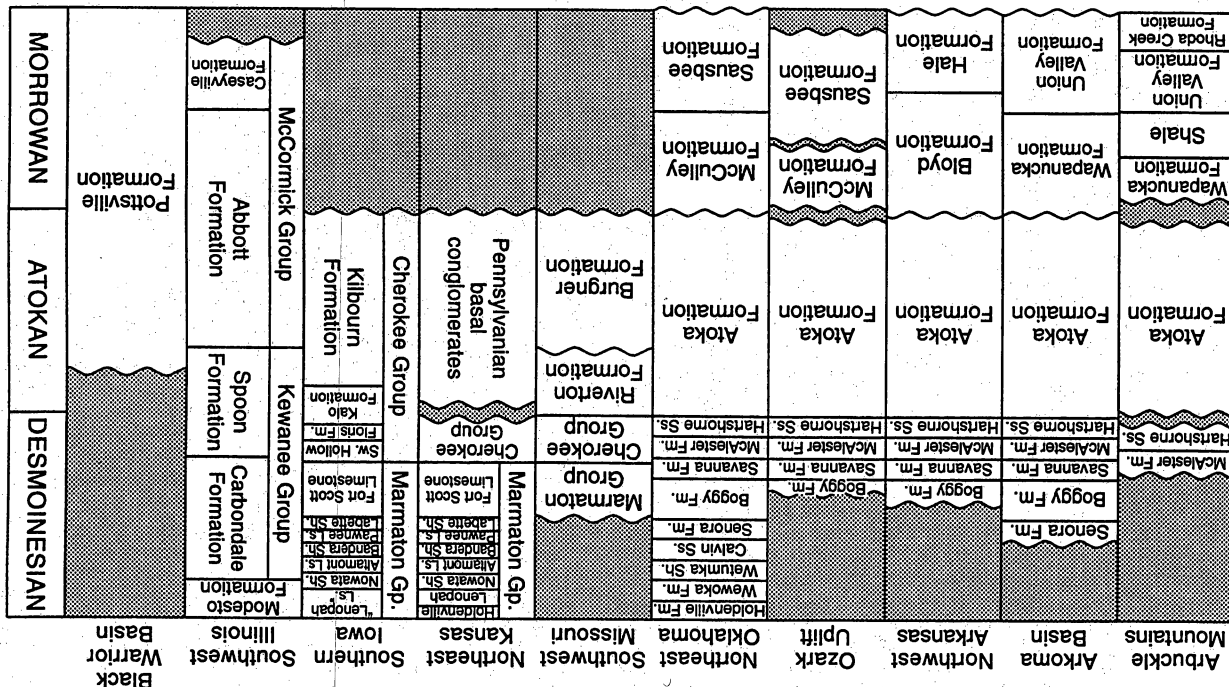


Figure 1.3. Middle Pennsylvanian paleogeographic map showing Fort Worth Basin and Boonsville project area.

Figure 1.4. Time-stratigraphic correlation for Middle Pennsylvanian rocks of the U.S. Midcontinent region. Based on Sutherland and others (1982), Thompson (1982), Chapin and others (1983), Ravn and others (1984), Shaver and others (1984), Zachy and Sutherland (1984), Adler and others (1986), Carlson and others (1986), Grayson (1990), Manger and others (1992), and Sutherland and Grayson (1992).

QAB608c



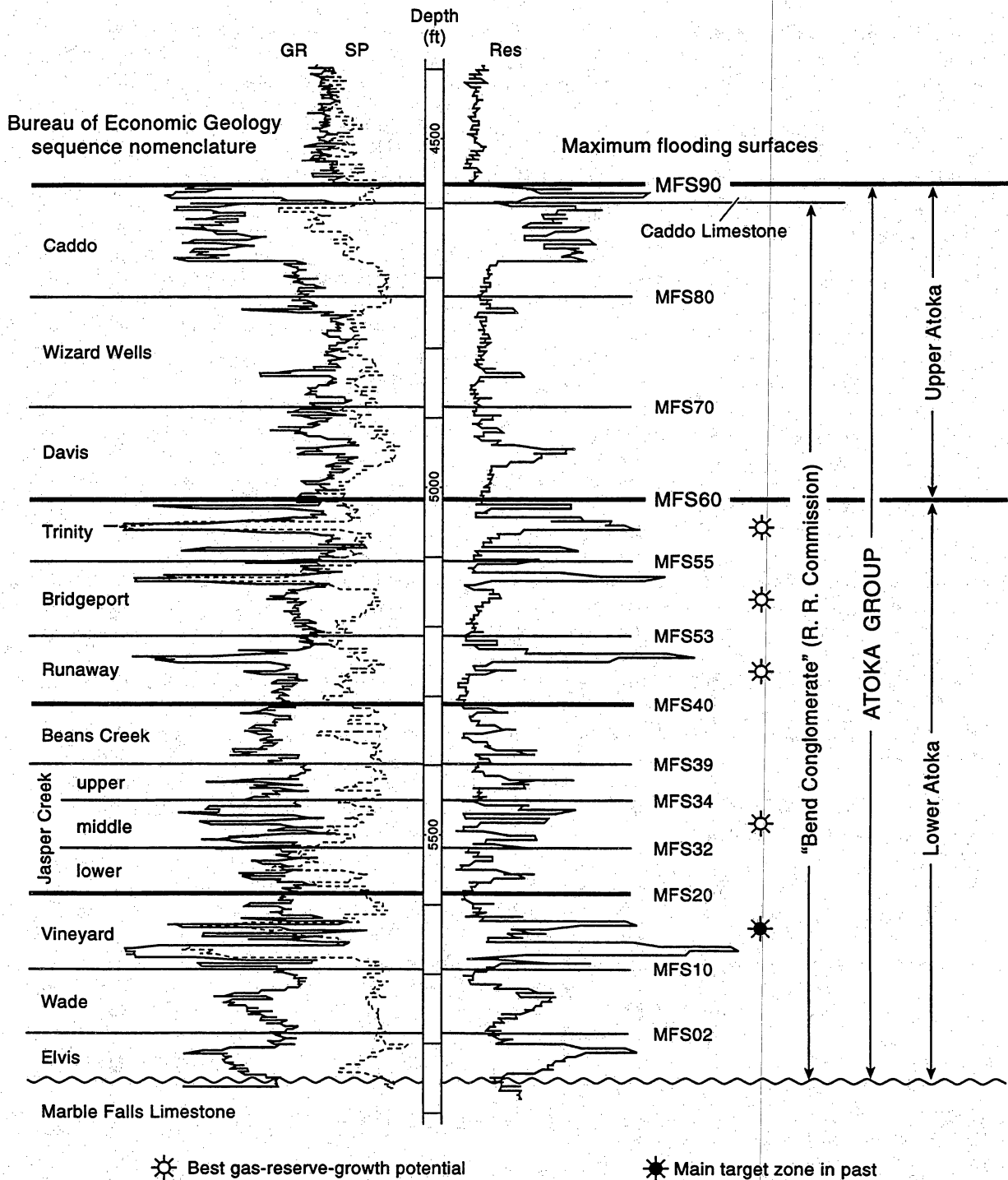
limit is bounded by the Bend Arch, which is a low, north-plunging fold. The Muenster and Red River–Electra Uplifts are both thought to be part of the northwest-trending Amarillo–Wichita Mountain Uplift, which resulted from reactivation of Precambrian boundary faults when Ouachitan compressive stresses were transmitted to the craton (Walper, 1977).

Ouachita foreland basin gas accumulations, including Bend Conglomerate gas in the Fort Worth Basin, occur as large, pervasive, deep basin accumulations (Masters, 1979; Meckel and others, 1992). Pennsylvanian gas reservoirs in these basins, typically underpressured, are rarely water productive, are relatively tight (typically less than 10 md), and are hydraulically separated from updip–overlying, more permeable, normally pressured water-bearing units (Meckel and others, 1992). The source of the natural gas is probably the abundant humic materials (land-derived, macerated plant material) in shales that encase the sandstone reservoirs (Meckel and others, 1992). Other Ouachita foreland basins having similar habitats include the Arkoma, Val Verde, and Black Warrior Basins, and possibly the Kerr and Marfa Basins.

Stratigraphy and Nomenclature

Figure 1.5 presents a typical log from the Bend Conglomerate interval in the project area. The Bend Conglomerate is defined as those intervals between the base of the Caddo Limestone and the top of the Marble Falls Formation (Railroad Commission of Texas, 1991). The Bend interval is treated as a common source of supply, and wells completed in more than one of the Bend productive sequences may be commingled and produced from a single wellbore. Recently the Railroad Commission has also allowed operators to commingle both Caddo and Bend Conglomerate production in a single wellbore, especially when necessary for economic reasons.

For practical purposes, the terms “Bend Conglomerate” and “Atoka Group” are essentially synonymous and can be used interchangeably. We have retained Thompson’s



QAb609c

Figure 1.5. Type log from Boonsville project area, Threshold Development, Fayette Yates No. 11. Major reservoir zones were defined by genetic sequences, which are upward-coarsening units bounded by impermeable, maximum-flooding shales.

(1982) "Lower Atoka" and "Upper Atoka" division, which splits the Bend Conglomerate interval into two geologically distinctive halves. A time-stratigraphic correlation chart for comparing units across the many basins of the U.S. Midcontinent appears in Figure 1.4.

A variety of nomenclatures have been developed to divide the major intervals of the Bend Conglomerate, but the complex stratigraphy, lack of outcrop exposures, and paucity of good index fossils have led to a proliferation of schemes that are not rigorously correlative to one another. As a result of the confusion in the published literature, individual operating companies have developed their own local nomenclatures. Even within the Boonsville project area, there were considerable differences in interval definitions, correlations, and names used by our operator partners.

To facilitate communication between the project participants, and to permit unrestricted geological interpretation of the Bend Conglomerate interval, it was necessary to construct a new, more broadly applicable nomenclature, in which **major reservoir intervals were divided by using the concepts of sequence stratigraphy** (see discussion that follows and Appendix A). The log section shown in Figure 1.5 illustrates the stratigraphic framework we used to define the major reservoir zones in the Boonsville project area. These intervals represent major, time-equivalent sequences that were subsequently named for local cultural and geographic features in the project area; the widely used terms Caddo and Davis were preserved because they fit within our sequence stratigraphic framework.

Reservoir Characteristics

The Bend Conglomerate ranges from 100 to 1,700 ft thick across Boonsville field, and in the project area, the interval is 900 to more than 1,300 ft thick. As Figure 1.5 illustrates, there are numerous potentially productive sequences throughout the Bend. Of these intervals, the Caddo and the Vineyard have been by far the most prolific producing reservoirs in the project area, but there have been completions in all the major sequences.

Typically these intervals are gas productive, but several of these sequences are also oil productive in the northeast and southeast portions of the project area. The Caddo sequences are primarily oil productive in the project area.

Table 1.1 lists some of the key characteristics of the Bend Conglomerate in the project area. As shown, the Bend Conglomerate is found at depths ranging between 4,500 and 6,000 ft and is somewhat underpressured. Depending on the interval and the depth, the best estimate for initial pressure ranges from 1,400 psi to 2,200 psi, which is a pressure gradient of about 0.35 to 0.4 psi/ft. The reservoir temperature is about 150° F, and the typical gas gravity is 0.65 to 0.75 (1,100 to 1,200 BTU/MMscf).

Table 1.1. Bend Conglomerate characteristics in Boonsville project area.

Property/item	Typical values
Depth	4,500 to 6,000 ft
Initial pressures	1400 to 2200 psi - somewhat underpressured
Temperature	150°F
Gas gravity	0.65 to 0.75
Gross thickness	900 to 1,300 ft
Net thickness	Multiple pays from a few ft to 20–30 ft each
Permeability	Varies from <0.1 md to >10 md; 0.1 to 5 md typical
Porosity	5 to 20 percent
Production	Varies from 10 MMscf to 8 Bscf; 1.5 Bscf Median

Net pay thickness ranges from several feet to 20 to 30 ft in each sequence; thus, a typical well may have anywhere from just a few feet of net pay to more than 100 ft of net pay. Permeabilities vary widely from less than 0.1 md to greater than 10 md, but values in the range of 0.1 to 5 md are typical. Gas production also varies widely. In the project area alone, gas recoveries range from as little as 10 MMscf to as much as 8 Bscf, with a median per-well recovery of about 1.5 Bscf.

Major reservoir intervals in the Bend Conglomerate strata correspond to “genetic sequences” (similar to cycles or cyclotherms in other terminology) averaging approximately 100 ft in thickness. Genetic sequences consist of upward-coarsening facies successions that are defined and bounded by impermeable marine shales marking key

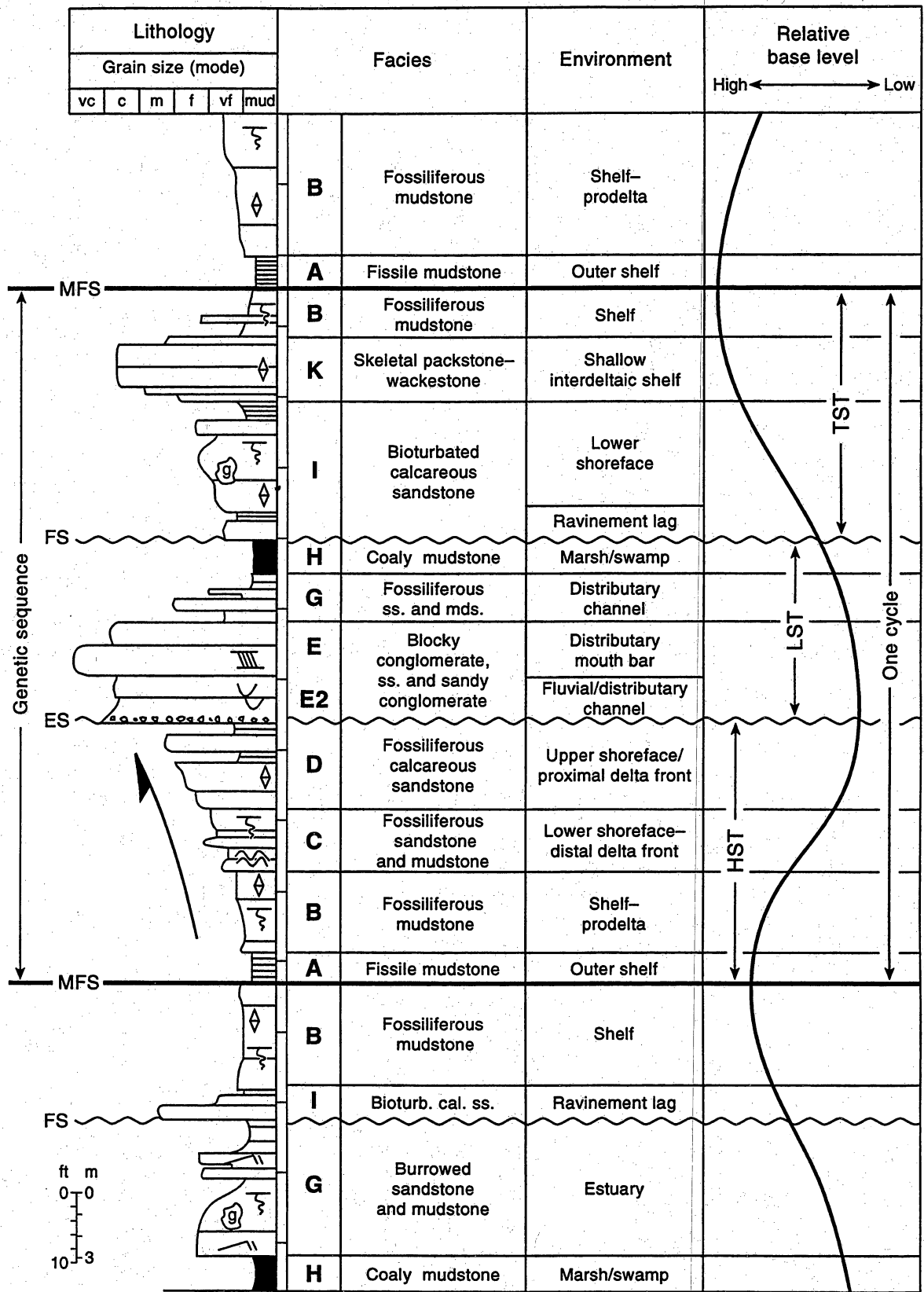
maximum flooding surfaces (Figure 1.6). Natural gas reservoirs at Boonsville occur predominantly in lowstand, valley-fill, conglomeratic sandstones; they owe their existence to erosional downcutting, which occurs during relative sea-level lowstands, followed by subsequent aggradation during the early phase of relative sea-level rises. Highstand deltaic and shoreface sandstones are also important reservoirs that occur as progradational lobes. Lowstand deposits overlie and erosionally truncate highstand deposits; however, their respective reservoir sandstone bodies typically occur as separate compartments.

Completion Practices

Figure 1.7 illustrates the typical completion practices in the Boonsville project area over the years. New wells drilled in the 1950's were most likely completed as (1) single or multiple, commingled completions in the Bend only or (2) dual completions in the Bend and the Caddo, with the latter typically being oil productive. Operators generally pumped small, hydraulic fracture treatments to stimulate production from the Bend reservoirs. Typical fracture treatments in the 1950's consisted of a treated lease oil with 10,000 lb of sand per zone.

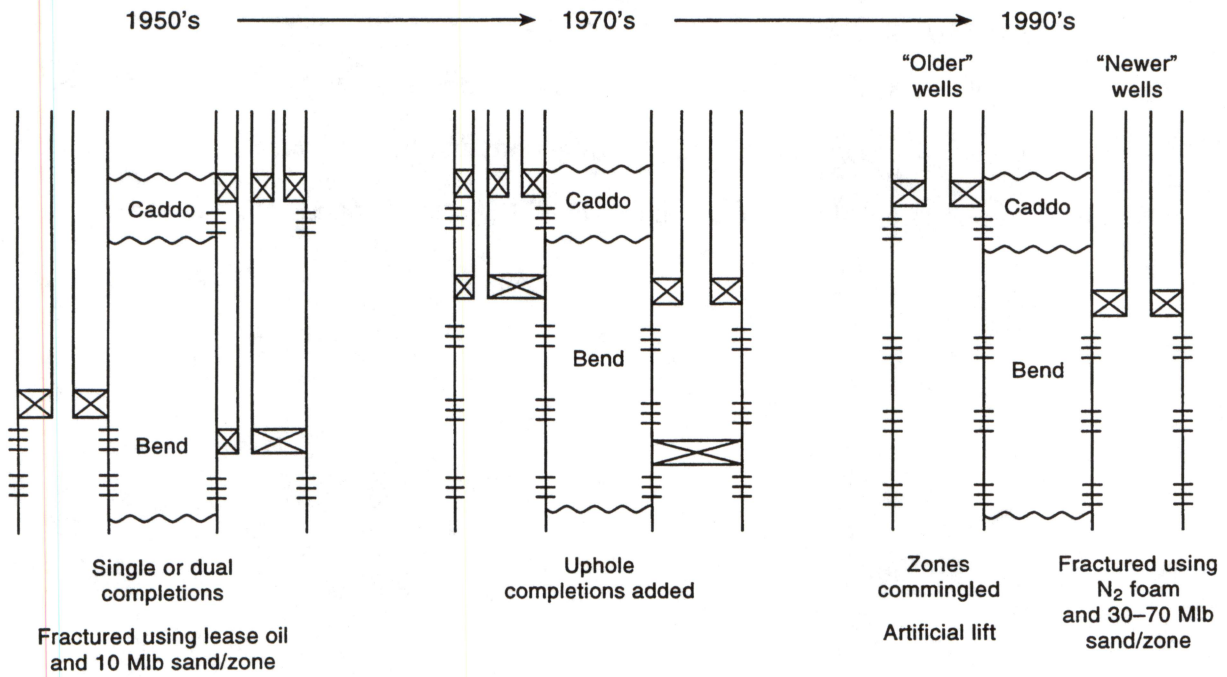
As the productivity of the lower Bend intervals declined over time (into the 1970's), additional intervals were commonly added up-hole. Sometimes operators abandoned the original completion intervals. At other times, production from these zones was simply commingled with that from the newly completed zones up-hole.

Today, production from multiple zones is commingled in most of the older, original completions. As mentioned previously, the Bend Conglomerate may now also be commingled with production from the Caddo in certain instances. Many of these older wells are on some sort of artificial lift, such as beam pumps or plunger lifts. The newer completions may be either single or dual completions. Often multiple Bend Conglomerate intervals may be completed together. Today these intervals are usually



QAb610c

Figure 1.6. Composite genetic sequence illustrating key chronostratigraphic surfaces and typical facies successions. Constructed from actual core data spanning four Boonsville sequences. One relative base level cycle is commonly represented by highstand (HST), lowstand (LST), and transgressive (TST) systems tracts. Cycles beginning and ending with maximum flooding surfaces (MFS), typically contain one or more erosion surfaces (ES) and flooding surfaces (FS), which are commonly ravinement surfaces. Reservoir sandstone facies, if present, usually occur in the LST.



QAb611c

Figure 1.7. History of typical completion practices in the Boonsville project area.

fractured by means of a 70- to 75-quality nitrogen foam carrying 30,000 to 70,000 lb of sand per interval treated.

Detailed Project Area

Figure 1.8 is a detailed map of the project area showing all wells having a total depth of more than 4,000 ft, which includes all wells that have penetrated the Caddo or below. The project area is just to the west of Lake Bridgeport, and the outline shown on the map illustrates the boundaries of the 26-mi² area where 3-D seismic data were recorded.

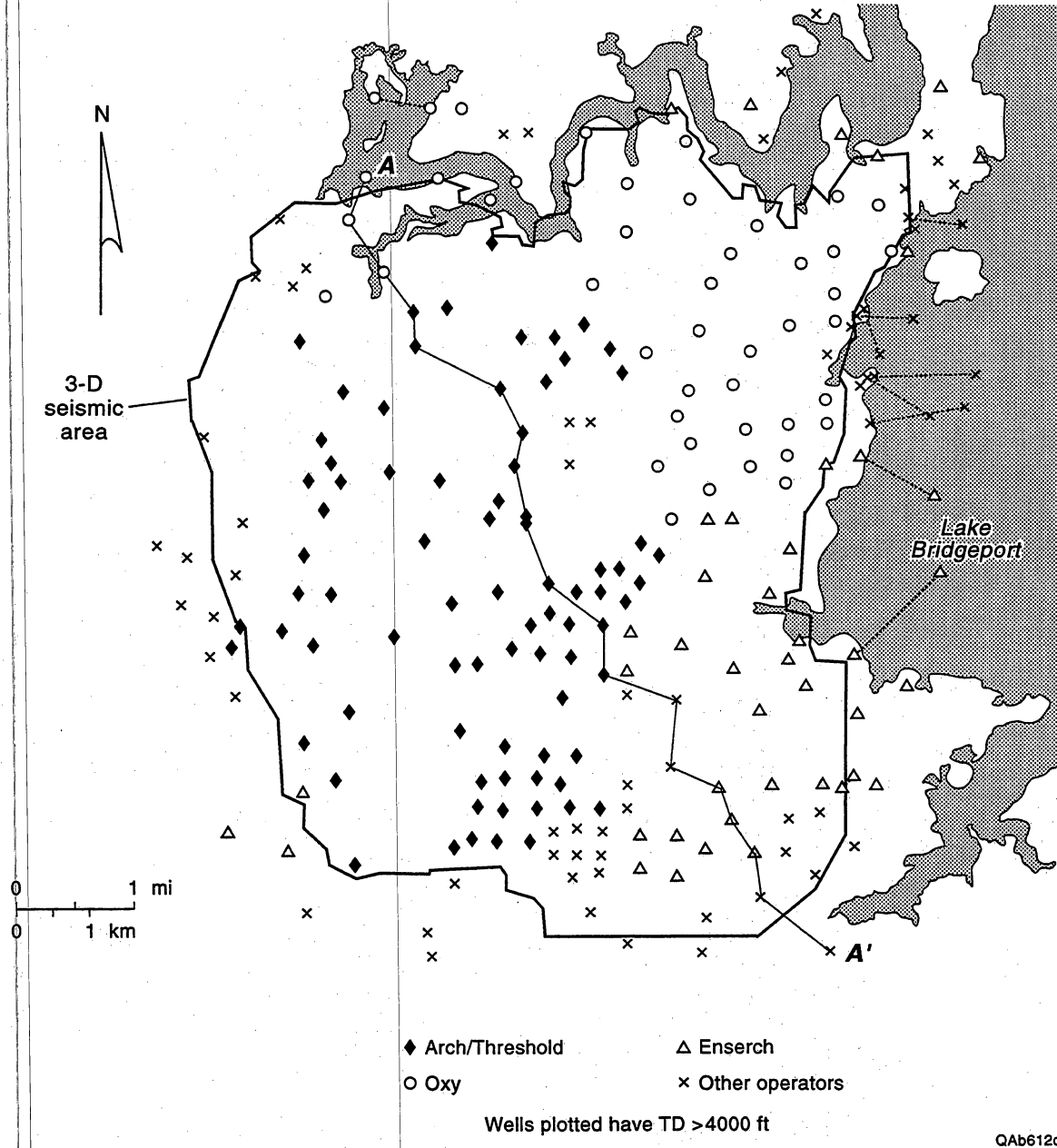


Figure 1.8. Detailed map of the Boonsville project area, located just to the west of Lake Bridgeport. Threshold Development/Arch Petroleum Co., OXY USA, Inc., and Enserch Operating Limited Partnership were the key operating partners in the project area. Cross section A-A' shown in Figure 2.5.

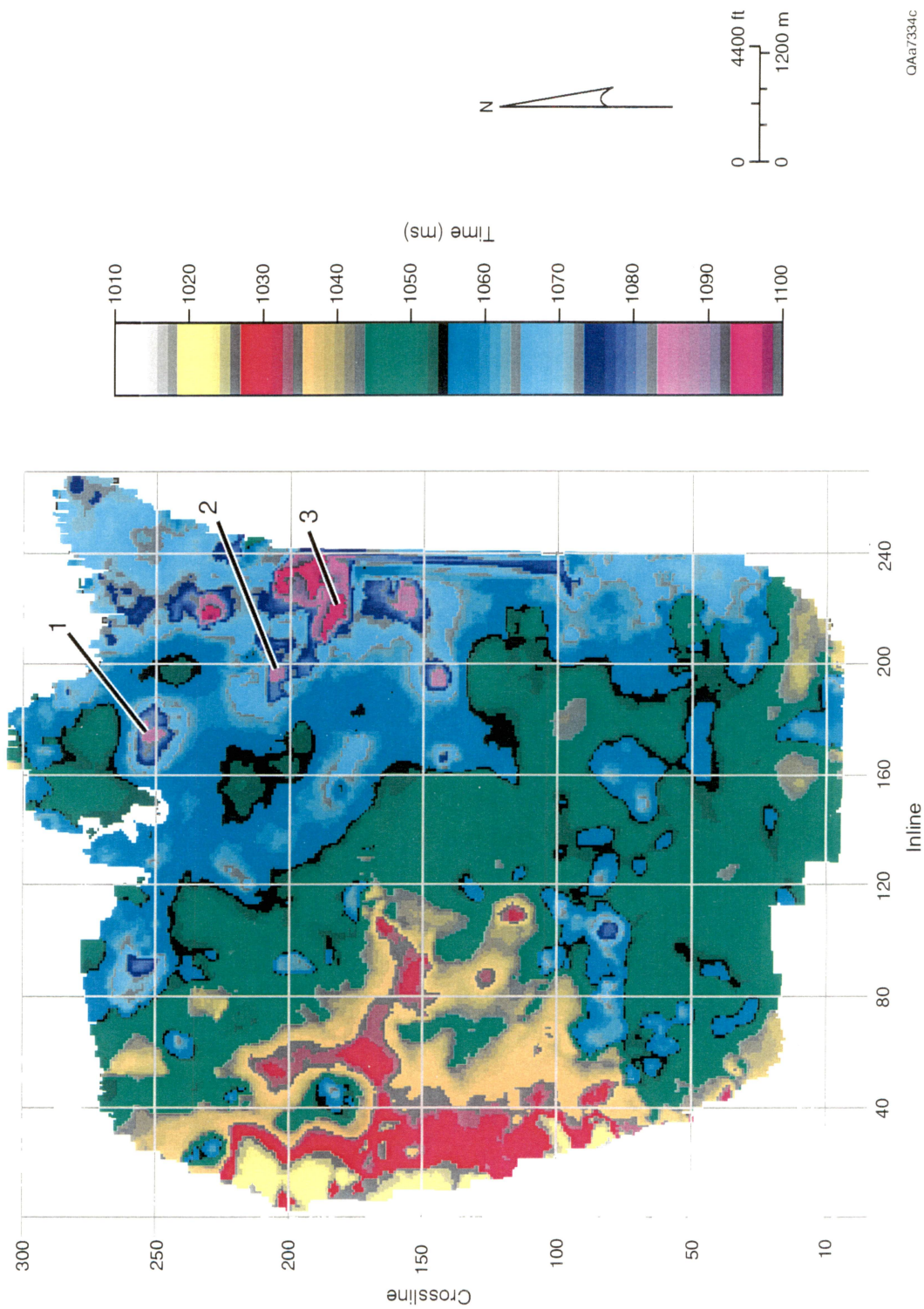
2. INFLUENCE OF PALEOZOIC CARBONATE KARST COLLAPSE ON BEND CONGLOMERATE STRATIGRAPHY AND RESERVOIR COMPARTMENTALIZATION

One unique aspect of Bend Conglomerate stratigraphy which is best revealed by 3-D seismic imaging is the manner in which Atokan-age sedimentation has been influenced by karsting in deep, Ordovician age and perhaps younger Paleozoic carbonate rocks. **Although there are hints that small grabenlike structural features are present in well control, neither the vertical displacements nor the fault-block geometries can be mapped without 3-D seismic data.** This karsting phenomenon can be illustrated by inspecting seismic-derived structure maps traversing the base and top of the Bend Conglomerate interval. The maps produced during the course of the Boonsville 3-D seismic interpretation are presented as Figures 2.1 and 2.2 and show, respectively, the topography at the base of the Bend Conglomerate (or the Vineyard surface) and the topography at the top of the Bend Conglomerate (or the Caddo surface).

Structural Evidence of Karsts

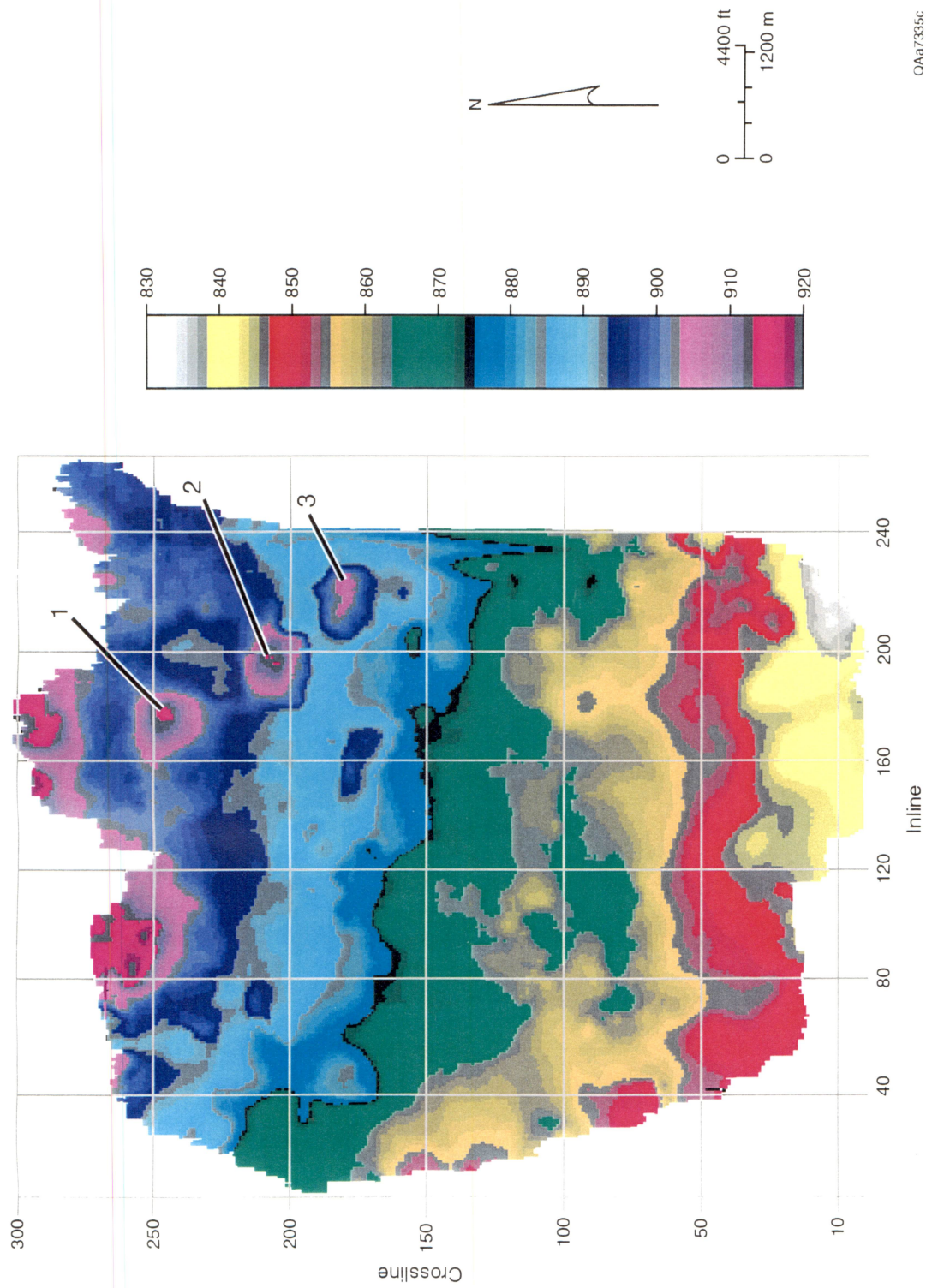
Inspection of the Vineyard structure map (Fig. 2.1) shows that several depressions occur in a seemingly random pattern across the Vineyard chronostratigraphic surface. These depressions tend to have circular to oval shapes, with diameters ranging from about 600 to about 3,000 ft. Figure 2.1 identifies the locations of three of these interesting structural depressions. Groups of karst collapse features sometimes occur along poorly defined linear trends, suggesting that subtle north-northwest-trending basement faults provided favorable sites for carbonate dissolution that often resulted in “rows” of sinkholes.

Inside the 3-D seismic grid, well log control defines the Caddo surface (top of the Bend Conglomerate) to be 1,000 to 1,200 ft above the Vineyard surface (basal unit of the



0Aa7334c

Figure 2.1. Seismic time structure map showing the topography of the Vineyard chronostratigraphic surface (base of the Bend Conglomerate). The numbered features identify only three of the numerous karst collapse areas observed in the 3-D seismic data volume.



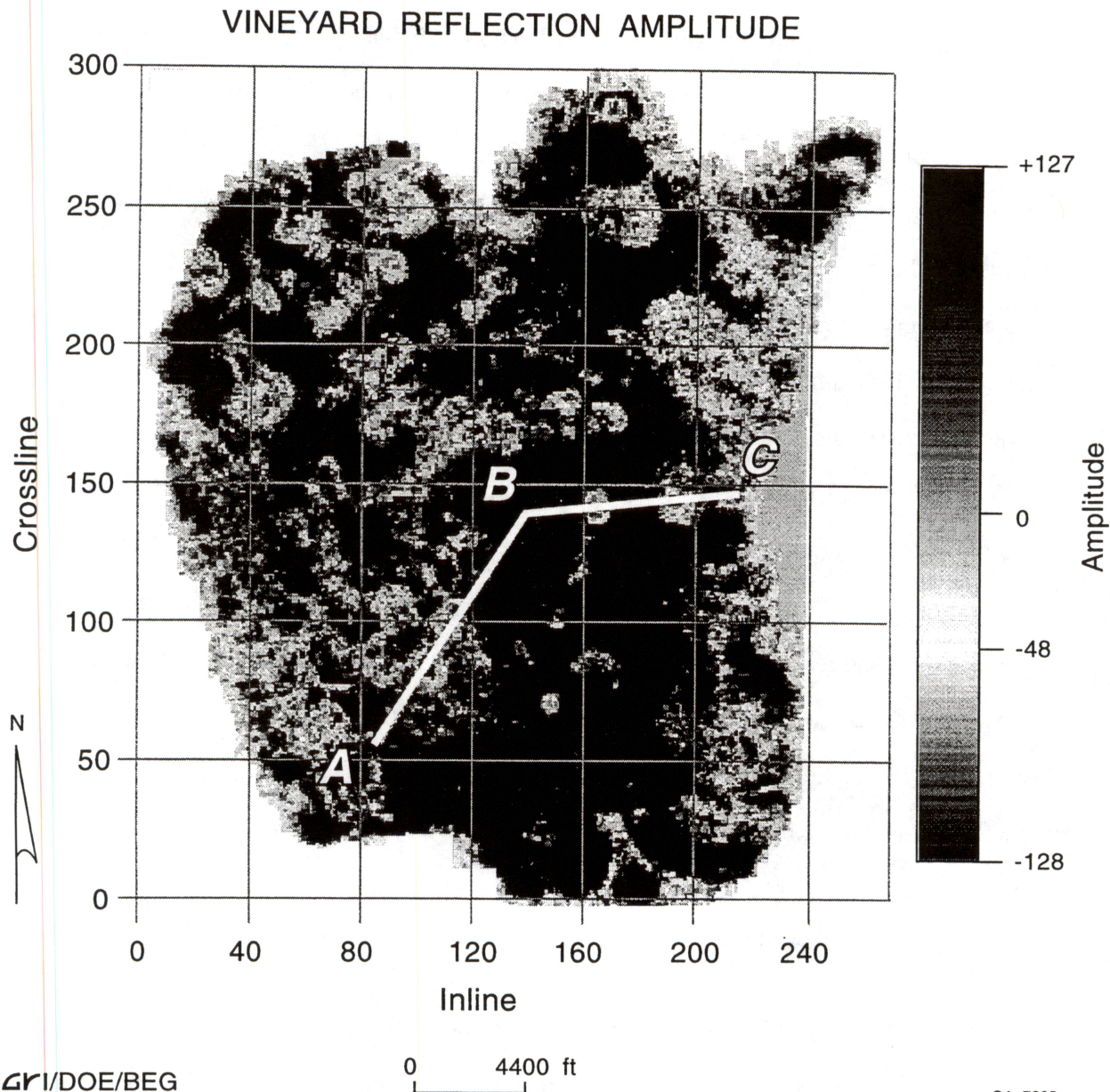
QAa7335c

Figure 2.2. Seismic time structure map showing the topography of the Caddo chronostratigraphic surface (top of the Bend Conglomerate). The numbered features identify three karst collapse areas. Note that these karst depressions are positioned directly above the labeled depressions in the Vineyard surface (previous figure).

Bend Conglomerate). The seismic-interpreted Caddo surface developed in this study is displayed in Figure 2.2. This map shows that depressions similar to those at the Vineyard level also occur across the Caddo surface. An important observation is that these Caddo depressions, particularly the three prominent ones labeled 1, 2, and 3, are positioned directly above equivalent depressions in the Vineyard surface, approximately 1,000 ft deeper, implying that there is a genetic relationship between the Caddo depressions and the older Vineyard depressions.

Seismic Reflection Anomalies Associated with Karsts

The seismic reflection response inside each of these structural depressions differs significantly from the reflection response in nondepressed areas. This variation in seismic reflection behavior is best documented by viewing the reflection response across an interpreted chronostratigraphic surface. One example of the seismic sensitivity to these surface depressions is shown in Figure 2.3, which is a display of the reflection amplitude magnitude on the Vineyard time structure surface (Fig. 2.1). Because this chronostratigraphic surface is interpreted so that it follows the apex of a reflection peak, the reflection amplitudes on the surface have the same algebraic sign but variable magnitudes. When the seismic wiggle trace data are displayed so that all positive reflection amplitudes are one color (dark) and all negative reflection amplitudes are a different color (white), as is done in this instance, the reflection amplitude map should have the same color, but with varying intensity, across the entire surface (refer to the shading bar in Fig. 2.3). Inspection of this map shows that quasi-circular disruptions (appearing as white areas) occur across this seismic amplitude response map, and correlating this disruption pattern with the Vineyard structure map (Fig. 2.1) confirms that each of the dramatic alterations in the seismic reflection response corresponds to a depression in the Vineyard surface topography.



GRI/DOE/BEG

QAa7365c

Figure 2.3. Behavior of the seismic reflection amplitude across the Vineyard chronostratigraphic surface. The reflection response on this surface should have a constant polarity, shown by the dark color. The white areas define regions where the polarity of the Vineyard reflection changes algebraic sign. Each white area corresponds to a karst depression in the Vineyard surface.

The location of the arbitrary profile ABC shown in Figure 2.3 is chosen so that it traverses three of these seismic reflection anomalies on the Vineyard surface. A section view of the seismic behavior along this profile is provided as Figure 2.4, and, in this view, the consistently near-vertical attitude and the extreme height of these stratigraphic disruptions are striking. Each structural depression begins at seismic basement (not far below 1.2 s), which is the Ellenburger (Ordovician age), and extends vertically into, or completely through, the Bend Conglomerate (Pennsylvanian Atokan age), causing the vertical extent of these disrupted zones to vary from 2,000 to 2,500 ft throughout the Boonsville 3-D seismic grid. In a few instances, a disruption continues into the Strawn above the Bend Conglomerate.

These structural collapse zones occur at a rather high spatial density, with adjacent collapses often separated by only 1 mi or less (see Fig. 2.3), and as noted, each zone extends completely through the Bend Conglomerate, or at least through a significant part of the Bend interval. Because of the severe stratigraphic disruption that these features cause within the Bend Conglomerate, some of these basement-related collapses had to be a significant influence on Bend sedimentation and, thus, these basement-related phenomena need to be considered when evaluating Bend Conglomerate prospects.

General Observations about Fort Worth Basin Karsts

The karst collapse features are inferred to be low displacement, faulted, and complexly fractured zones. The zones are near vertical, and displacements within the Bend Conglomerate interval, as inferred from 3-D seismic sections, are typically 25 to 50 ft. A few faults approach 100 ft of displacement, and most of the deformation occurs in the Lower Atoka (Trinity and deeper), although some faults extend into the Strawn Group. Fault displacement and karst collapse both increase with depth, with greater collapse occurring below the Bend Conglomerate than within the Bend interval. The limited core and FMI/FMS data that exist in the project area support the fault/fracture

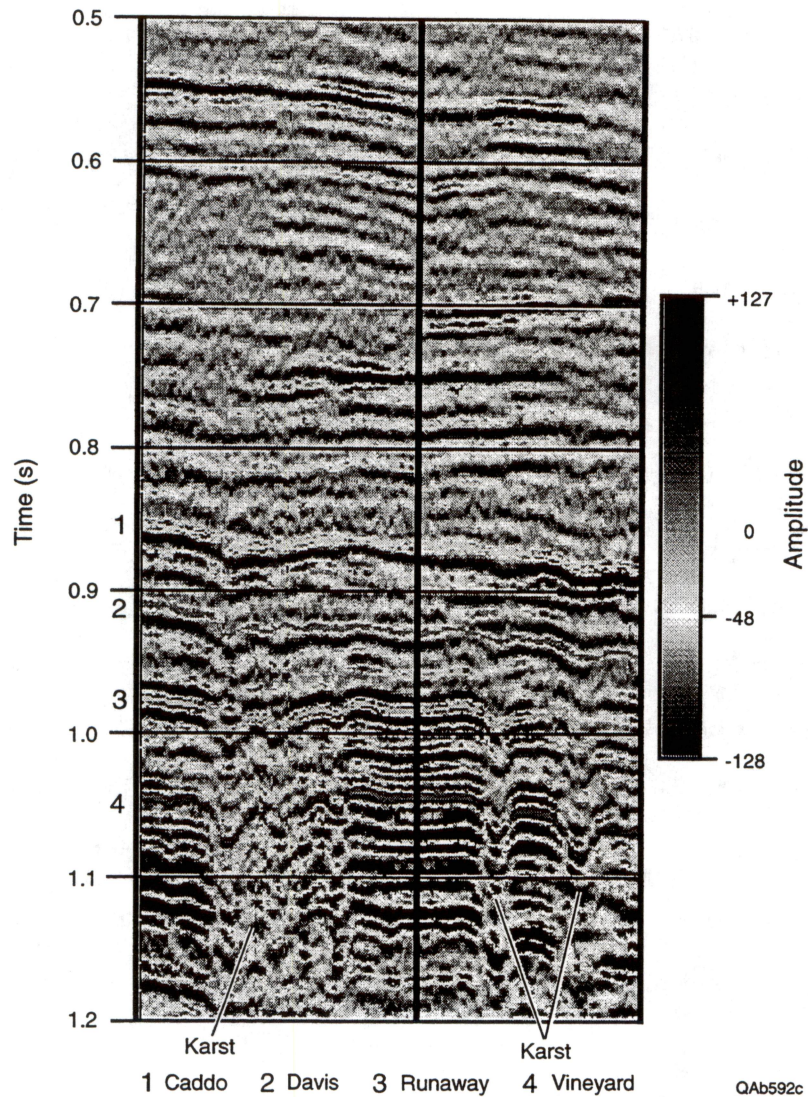


Figure 2.4. Vertical seismic section along profile ABC shown in Figure 2.3, which traverses three of the white reflection anomalies on the Vineyard surface. This section view shows that these reflection disturbances are vertical collapse zones that start at seismic basement (just below 1.2 s) and extend all the way to the Caddo level (surface 1). These features are thought to be karst-driven phenomena that initiated at the Ellenburger level (seismic basement) and continued for an unknown length of time.

zone interpretation. The three wells that have FMI/FMS data available, the I.G. Yates 33 and the Billie Yates 17D and 18D, are located in relatively undisturbed areas; however, natural fractures are common even in these FMI/FMS images, and a few faults having a few feet of displacement were observed.

A part of the geological research data base was a core from the Jasper Creek sequences in the Enserch J. D. Craft–Water Board 3, which is located in the southeast corner of the project area on the margin of a circular sinkhole feature. This core contained numerous natural fractures, and core recovery in some of the calcareous fossiliferous mudstones was uncommonly poor. The rubble appeared to contain clean, regular fractures unlikely to have been induced by the coring process.

Structural evaluations using only standard well log control cannot identify the karst collapse zones, nor can potentially isolated fault blocks be identified (Fig. 2.5). Panel (a) of Figure 2.5 illustrates the seemingly gentle, undeformed attitude of the Atoka section through the well log filter. Hints of vertical deformation zones are represented as gentle undulations and sags; however, specific evidence defining interwell structural displacements and geometry of fault blocks is absent. Only with the aid of 3-D seismic can the interpreter confidently identify and map these subtle structural features (panel [b]).

Proposed Geological Mechanism for Collapse Structures

The extensive vertical collapse zones shown in Figure 2.4 are interpreted to be the result of Ellenburger and post-Ellenburger karsting. This karst model is adopted because karst-generated vertical collapse zones can be observed in Ellenburger outcrops in the Franklin Mountains at El Paso, Texas, and because Ellenburger karst plays are pursued by some West Texas operators. In the Franklin Mountains outcrops, the measured lateral dimensions of the collapsed features correspond to the diameters of the disrupted zones observed in the 3-D seismic image at Boonsville. The outcrop features

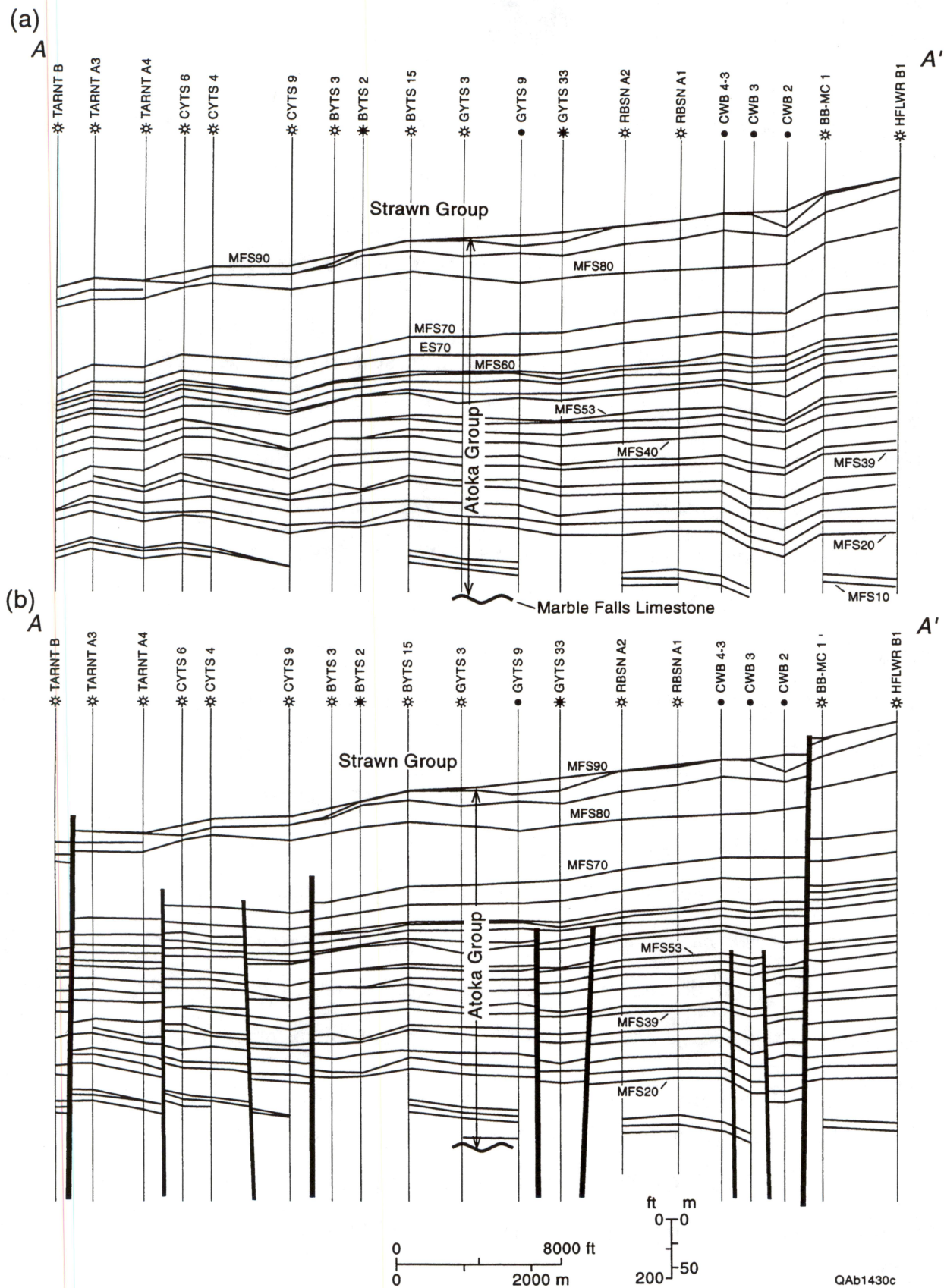


Figure 2.5. Structural cross section A–A' of Boonsville project area. (a) Well control: gentle structural undulations can be detected, but fault interpretations are difficult to justify; (b) structural interpretation guided by 3-D seismic: many small vertical displacement faults are present. Line of section shown in Figure 1.8.

also have extensive vertical dimensions, as do the seismically imaged collapses at Boonsville, with some of these outcrop collapses extending vertically for at least 1,200 ft in the larger outcrop exposures.

It is important to note that the Ellenburger karst collapse zones observed in outcrops in the Franklin Mountains and the Ellenburger-related collapse zones observed in the Boonsville 3-D data document that **this Paleozoic karsting phenomenon spans a distance of at least 400 mi.** The influence of this deep karsting on younger sedimentation needs to be studied at several sites between these two widely separated control points to better document how this karsting phenomenon affects hydrocarbon production and exploration strategy throughout the Permian and Delaware Basins.

Although no Ellenburger cores are available within the Boonsville project area, these regional outcrop observations and the Boonsville seismic images allow the following karst-related hypothesis to be put forward regarding the genesis of the Boonsville collapse structures.

1. Post-Ellenburger/pre-Bend basement faulting (apparently strike-slip(?) faults trending north-northwest) occurred across the Boonsville area.

2. Karst solution weathering then ensued, particularly along subtle faults where water seepage was enhanced, and produced large caverns in some carbonate units.

3. As Atokan clastic sediment accumulated, sediment loading by the Bend Conglomerate sequences caused sporadic and intermittent collapsing of these karst-induced caverns.

4. The presence of the resultant collapse structures influenced the distribution of sandstone reservoir facies within the various Atokan sequences. Periods of active collapse would have produced a hilly, hummocky physiography; downcutting fluvial systems would occupy these subtle, collapsed areas and allow site-preferential aggradation of high-energy, active-fluvial and deltaic facies to be deposited during late phases of base-level lowstands.

5. The locations of active collapsing apparently varied with time and caused each Bend Conglomerate sequence to be affected differently. For example, the Davis and Wizard Wells genetic sequences appear to have been relatively unaffected by underlying karst collapse; however, the Caddo and some members of the Jasper Creek were strongly influenced by some of these features. Without doubt, the distribution of reservoir sandstone facies was significantly affected by the karst collapse features, and even today, surface streams seem to be affected by basement structure (see Structure and Sedimentation section of Appendix A).

Fault-Bounded Reservoir Compartmentalization Resulting from Karst Collapse Processes

The previous section presented an important factor that needs to be considered when evaluating the compartmentalization of Bend Conglomerate reservoirs—**deep Paleozoic karsting significantly influenced shallower sedimentation processes and often created partial interwell flow barriers.** One example of deep-seated karsts creating a partial reservoir compartmentalization at the Caddo level, some 2,500 ft above the onset of the karsting, is the situation associated with the Sealy C-2 well inside our study area.

Overview of Production History in Sealy C-2 Area

Figure 2.6 shows the location of the OXY Sealy C-2 well in the northeast portion of the project area. This well is currently producing gas from the Upper Caddo. There are 32 Upper Caddo completions in the project area, the majority of which are oil productive. Oil recoveries from the Upper Caddo are quite variable, ranging from as little as 5,000 STB to as much as 200,000 STB. The gas completions in the Upper Caddo have estimated ultimate recoveries ranging from only about 50 MMscf to as much as

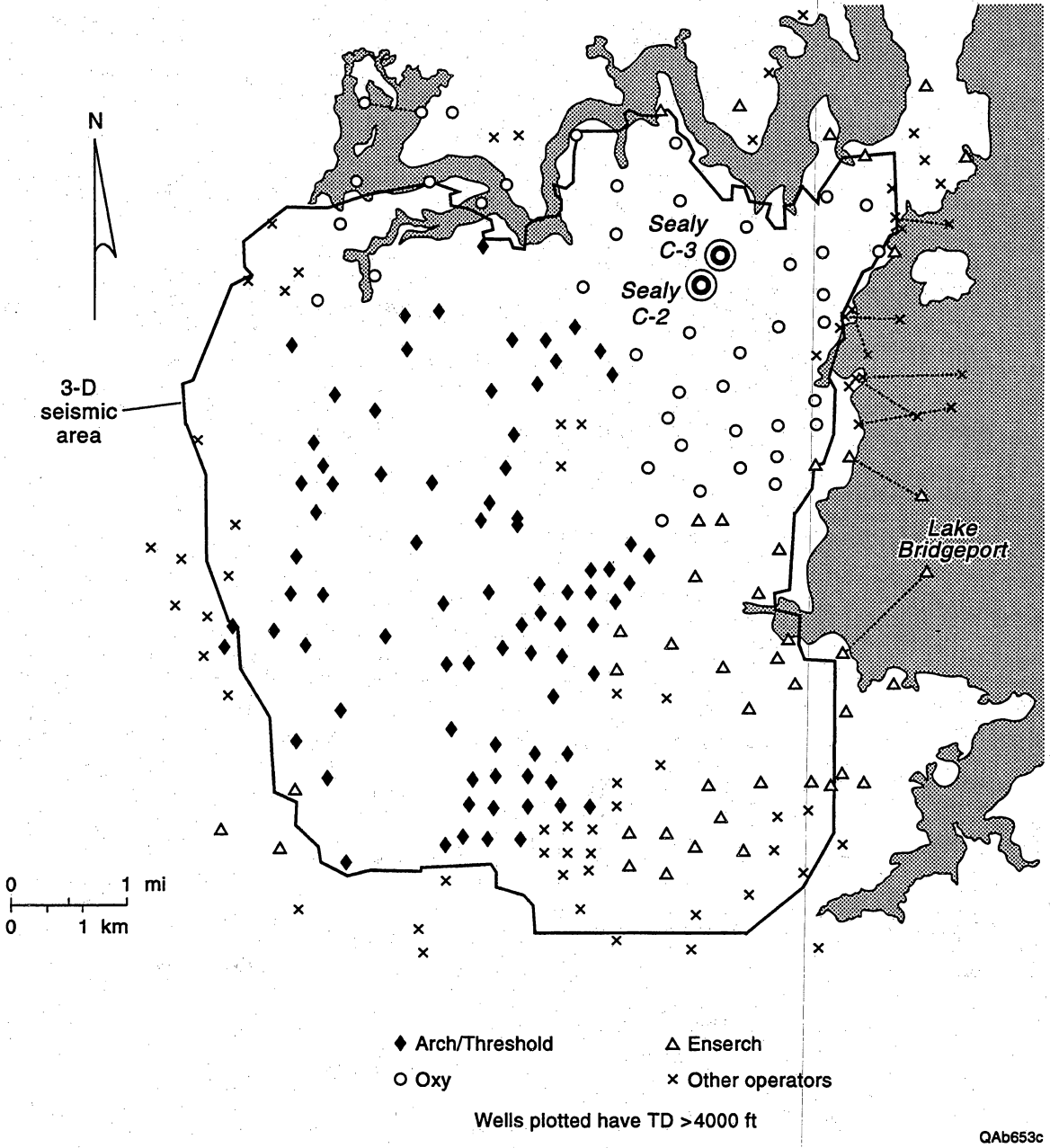


Figure 2.6. Location of the Sealy C-2 well in the northeast part of the project area.

700 MMscf. Drainage areas tend to range anywhere from about 10 to 170 acres; typical values are about 40 to 60 acres.

Figure 2.7 presents an expanded view of the area around the Sealy C-2 well. The Sealy B-3 well to the north is also a fairly recent Upper Caddo gas completion, having produced 346 MMscf of gas since June 1991. There are also a number of Upper Caddo completions immediately to the southwest and updip of the Sealy C-2. Most of these wells produce oil, and some, like the OXY Ashe B-2 and the OXY Ashe B-4, have been quite prolific, producing 129,000 STB and 83,000 STB, respectively, from the Caddo.

Most of these wells were completed in the Upper Caddo in the mid- to late 1950's, but some, such as the Threshold Development Cap Yates 3, 10, and 11 wells are more recent Upper Caddo recompletions during the late 1980's and early 1990's. Many of these recompletions found significant depletion in the Upper Caddo and produced only 5,000 to 10,000 STB of oil. The Sealy B-2 to the northeast tested the Upper Caddo when drilled in the mid-1960's, but despite testing gas, the well was completed in several lower intervals in the Bend Conglomerate. In addition to the Upper Caddo, there are also a number of other Bend intervals completed in wells in the immediate vicinity of the Sealy C-2, including the Lower Caddo, Trinity, Bridgeport, Runaway, Beans Creek, Lower Jasper Creek, and Vineyard.

Sealy C-2 Drilling Results

The Sealy C-2 penetrated a broad, southeast-trending valley-fill complex. Surrounding offset wells had also penetrated 10 to more than 40 ft of net reservoir sandstone (Figs. 2.8 through 2.10), except for the Ashe A-5, which encountered part of a small Caddo limestone erosional remnant (or outlier), and the Sealy B-1, in which the valley-fill sandstones are tight, probably because of a facies change adjacent to the limestone outlier. Stratigraphic compartmentalization, except to the northwest (Fig. 2.9),

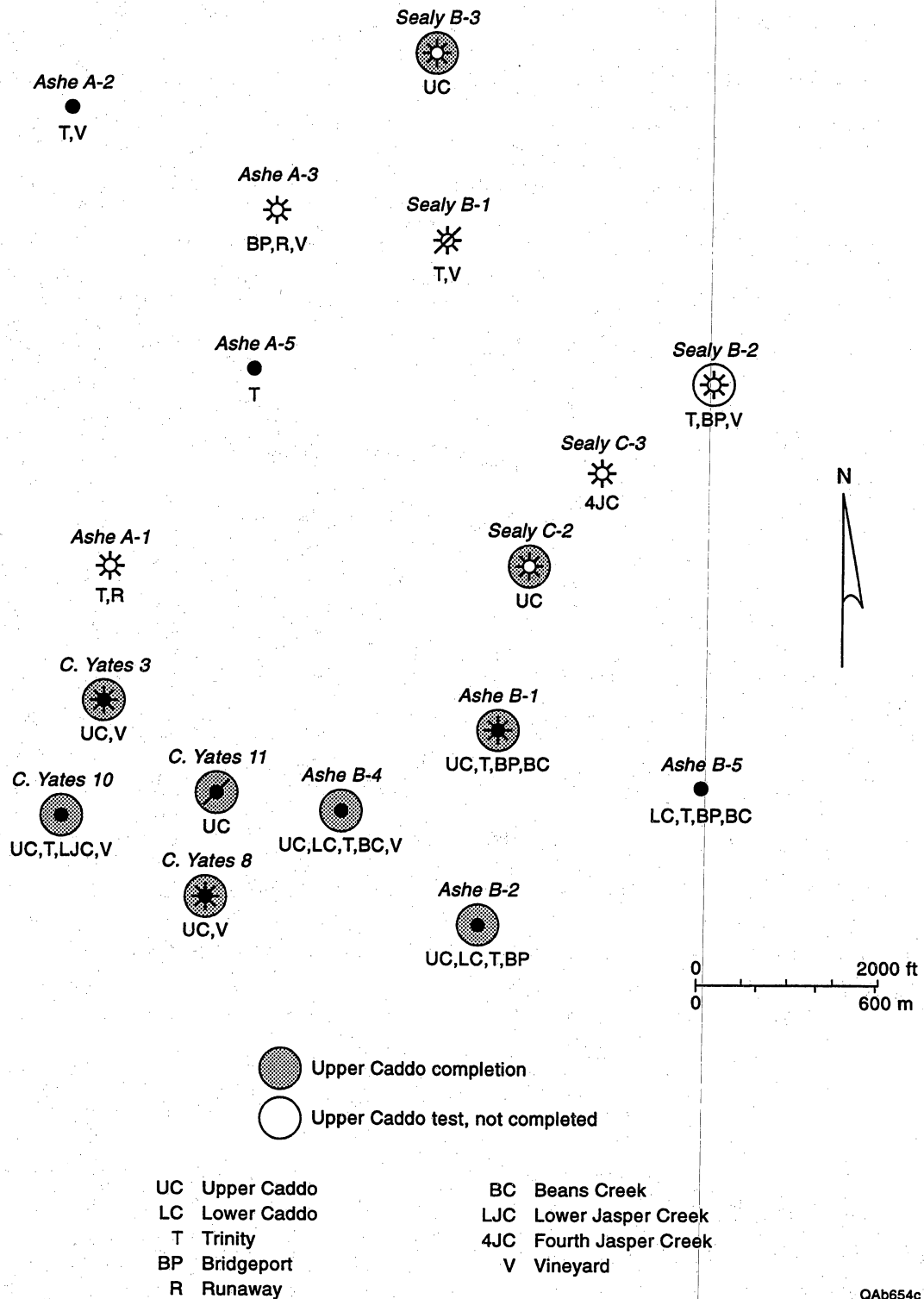


Figure 2.7. Expanded view showing Upper Caddo completions near the Sealy C-2 well. Most are southwest of the Sealy C-2 location and tend to be oil wells. Many other Bend zones are also completed in nearby wells.

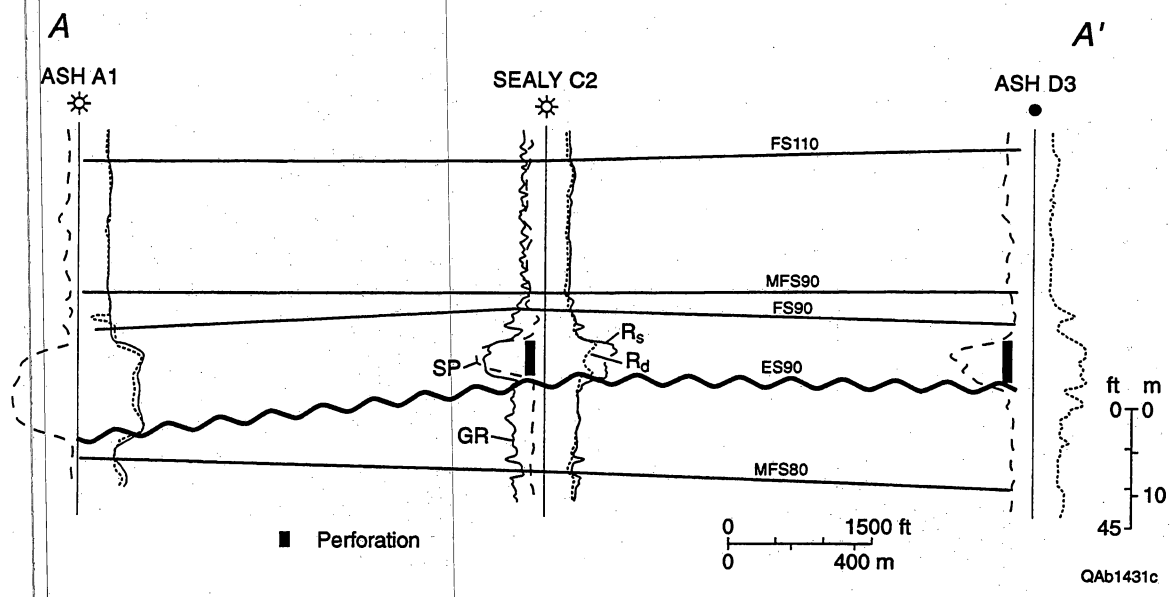


Figure 2.8. Stratigraphic cross section A-A', Upper Caddo valley-fill sandstone reservoir. Cross section parallels 3-D seismic Line A in Figure 2.14.

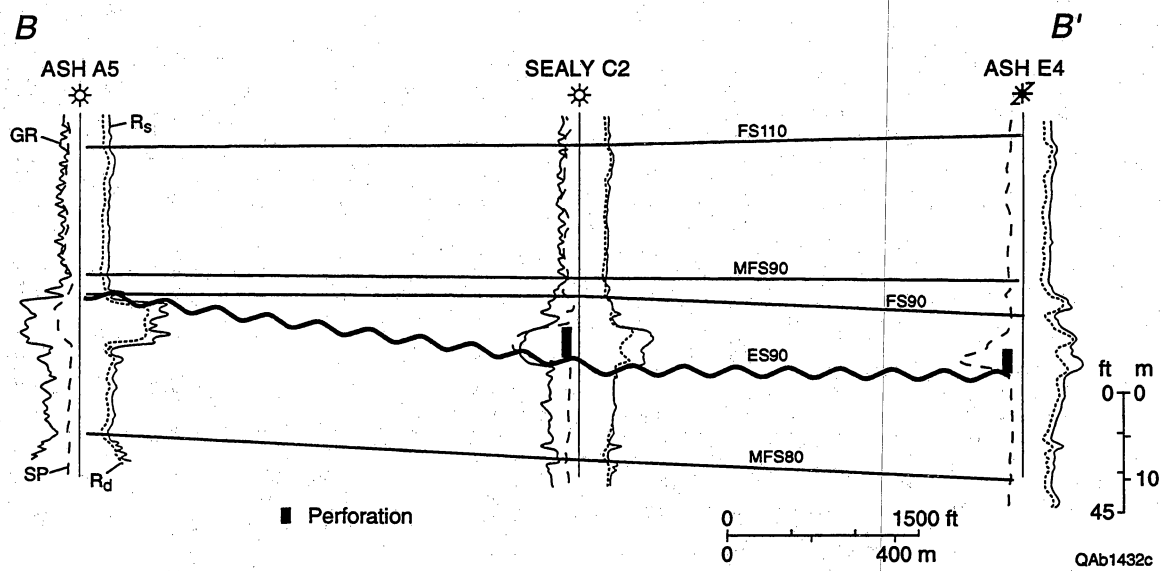


Figure 2.9. Stratigraphic cross section B-B', Upper Caddo valley-fill sandstone reservoir. Cross section parallels 3-D seismic Line B in Figure 2.15.

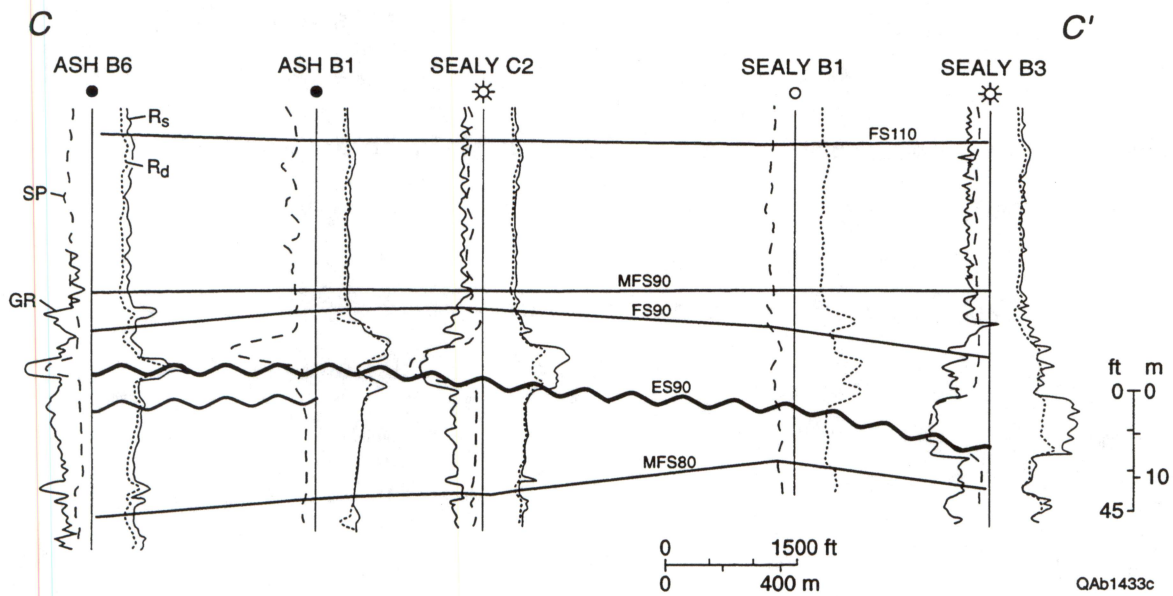


Figure 2.10. Stratigraphic cross section C-C', Upper Caddo valley-fill sandstone reservoir. Cross section parallels 3-D seismic Line C in Figure 2.16.

is probably negligible. Similar log curve patterns and consistently negative SP response suggest that the Upper Caddo sandstone is hydraulically well connected in the area.

The Sealy C-2 was spudded in September 1992 and drilled through the Vineyard to a total depth of 5,830 ft. Table 2.1 presents the log-derived reservoir properties, as well as the bottomhole pressures measured in the various Bend intervals. The pressures measured in the Vineyard and the Upper Caddo were higher than expected and suggested only partial pressure depletion in these intervals. The Trinity and Bridgeport intervals appear to be more pressure depleted based on the RFT results, but both zones still offer behind-pipe completion opportunities.

Table 2.1. Estimated reservoir properties for the Sealy C-2 well.

Sequence	Net pay (ft)	Porosity (%)	Water saturation (%)	Bottomhole pressure (psi)	Source of pressure data
Upper Caddo	16.5	11.7	44.5	1,300*	PBU**
Lower Caddo	0	—	—	—	
Wizard Wells	3	10.6	51.7	—	
Davis	0	—	—	—	
Trinity	11.5	11.5	35.1	750	RFT
Bridgeport	7.5	11.8	37.1	540/660	RFT's
Runaway	0	—	—	—	
Beans Cr	0	—	—	—	
U Jasper Cr	0	—	—	—	
M Jasper Cr	0	—	—	—	
L Jasper Cr	0	—	—	—	
Vineyard	24.5	9.3	45.6	1129	PBU

* Estimated average reservoir pressure.

** Pressure buildup test.

Initially the Sealy C-2 was completed and tested in the Vineyard. The measured bottomhole pressure of 1,129 psi in the Vineyard was higher than generally found in the project area today; Vineyard pressures of 500 psi or less are far more common. The Vineyard interval produced only a small show of gas following a 2,000-gal acid treatment. This was not surprising, however, because the Sealy C-2 is located in a

northwest-southeast-trending portion of the Vineyard reservoir that appears to have considerably lower permeability and much less productivity than usually observed in the Vineyard throughout the project area. A bridge plug was set above the Vineyard, and the operator moved uphole to complete the Upper Caddo.

The Upper Caddo was perforated from 4,886 to 4,902 ft and treated with 2,000 gal of 15 percent HCl. Following cleanup of the acid treatment, a pressure buildup test was conducted, and an average reservoir pressure of 1,300 psi was estimated for the Upper Caddo (Table 2.1). Following the shut-in period, the Sealy C-2 produced at 1.04 MMscf/d during a 24-h flow test.

Figure 2.11 is a plot of initial pressures in the Upper Caddo measured from wells in the project area over time. The values of initial pressure for the Sealy C-2 and Sealy B-3 wells are similar to those reported in wells drilled and completed in the 1950's. Note that, in each case, the pressures reported are the best estimates that could be obtained for particular wells using available data sources (both operator and public domain records). The estimated initial reservoir pressure for the Sealy C-2 of 1,300 psi represents a pressure gradient of about 0.3 psi/ft. This pressure suggests that although the Sealy C-2 location has been partially drained by surrounding production, the pressure is higher than might have been expected given the extent of the offsetting production from the Upper Caddo.

Figure 2.12 shows the logs recorded in the Sealy C-2 across the Upper Caddo sequence. The Upper Caddo shows good sand development on both the SP and gamma-ray logs. Note, too, the well-developed gas effect on the neutron-density crossover. Below this sand is a marine, shale-dominated sequence. Figure 2.13 presents an interpreted log for the Upper Caddo sequence. A net pay of 16.5 ft, with a porosity of 11.7 percent and a water saturation of 44.5 percent, was calculated for the Upper Caddo sand (see Table 2.1). Facies analysis described the majority of the Upper Caddo sand as

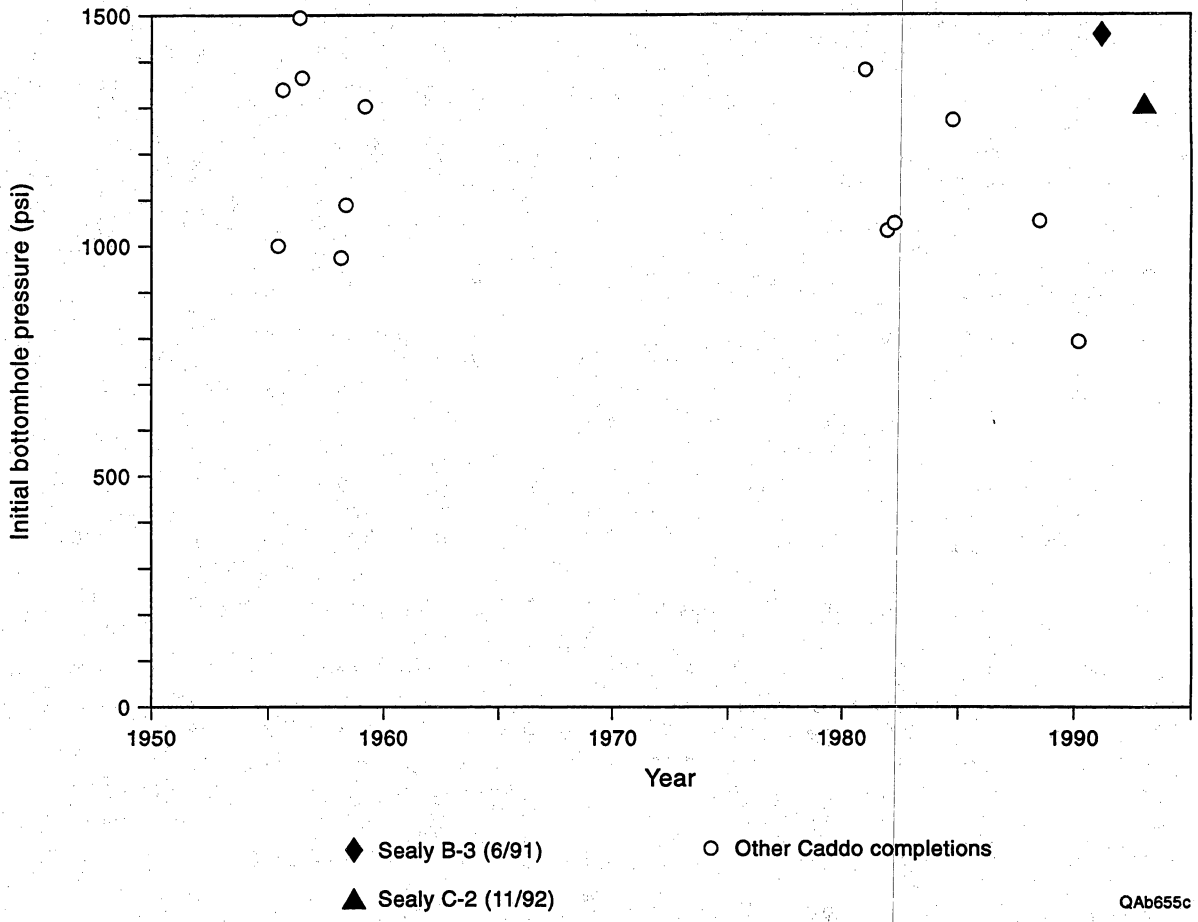
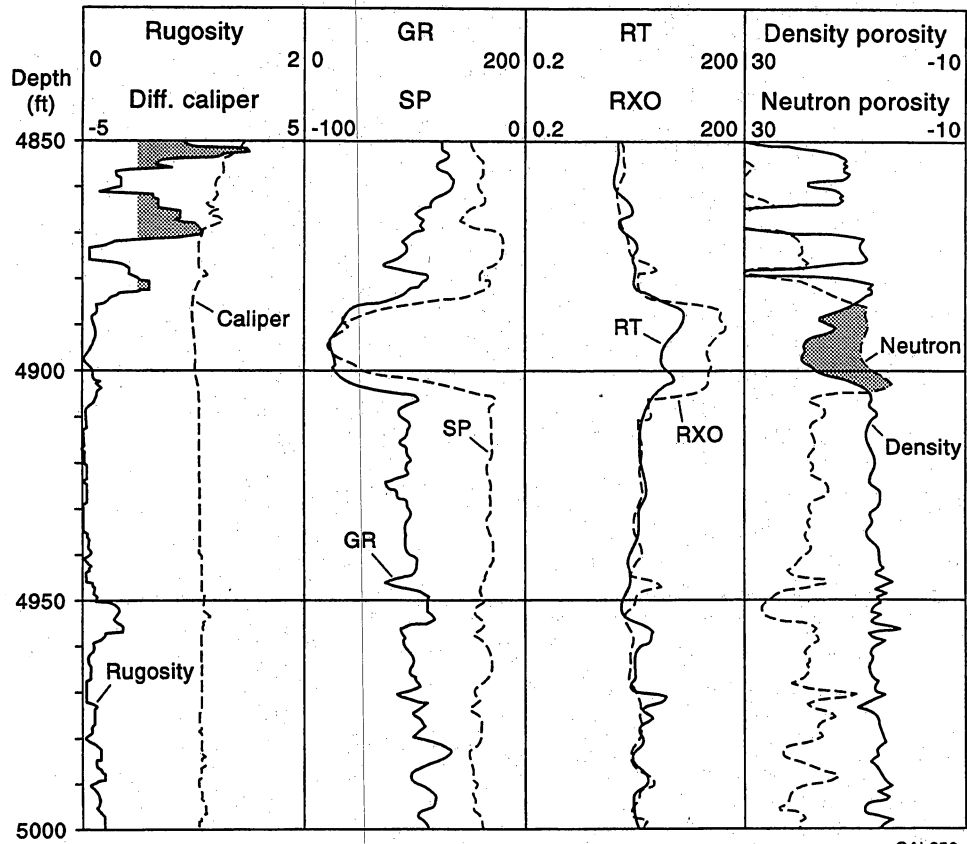


Figure 2.11. Initial pressures measured in the Sealy C-2 and Sealy B-3 Upper Caddo completions. These pressures are comparable to initial pressures reported in other wells drilled in the Upper Caddo sequence over the past 40 yr.



QAb656c

Figure 2.12. Open-hole logs recorded over the Upper Caddo sequence in the Sealy C-2 well.

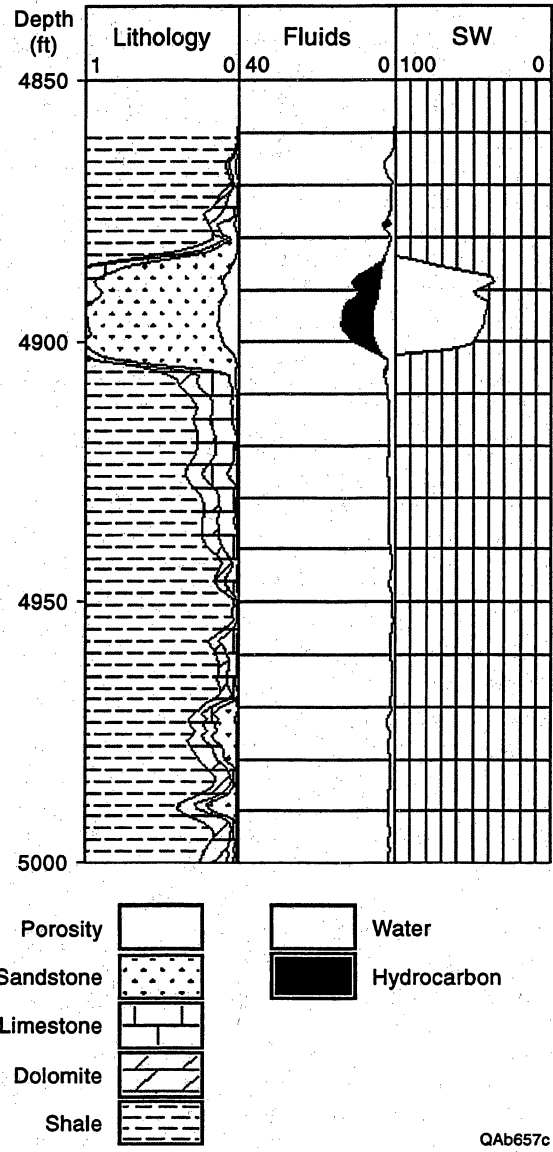


Figure 2.13. Interpreted log for the Upper Caddo sequence in the Sealy C-2 well.

facies "E," the cleanest, most productive sand facies in the project area (see Appendix C for additional details on the facies analysis).

Seismic Interpretation of Sealy C-2 Area

The northeast quadrant of the Caddo time structure map (Fig. 2.2) is enlarged in Figure 2.14, and the locations of the Sealy C-2 and several neighboring wells are identified. This map shows that the Sealy C-2 well was drilled on the flank of what appears to be a structural high. However, when the structural and stratigraphic details associated with the Sealy C-2 well are viewed in section views along profiles such as A, B, C, or D (Fig. 2.14), it is apparent that **the well is not positioned on a structural high created by tectonic uplift, but rather is on a portion of the Caddo surface where the terrain completely surrounding the well collapsed because of underlying karsting.**

Seismic profiles B and C are presented as Figures 2.15 and 2.16, respectively, to support this karst compartmentalization model. Both profiles show that vertical, seismically disrupted, collapse zones extend from the Caddo surface down to the Ellenburger (approximately 1.2 s), and that these collapse zones surround and isolate the Sealy C-2 well. These vertical seismic sections indicate that numerous low-displacement, vertical faults (often with throws of only 20 to 30 ft) separate the Sealy C-2 fault block from the surrounding terrain.

The estimated Upper Caddo reservoir pressure of 1,300 psi encountered in the C-2 well and the subsequent production history (Fig. 2.17) suggest that these low-displacement faults acted as at least partial barriers to fluid flow. The area inside the circumference defined by this ring of collapse is approximately 130 acres; thus if it is assumed that the karst collapse zones are partial flow barriers at the Caddo level, then the Sealy C-2 well is producing from a Caddo reservoir compartment that appears to span about 130 acres.

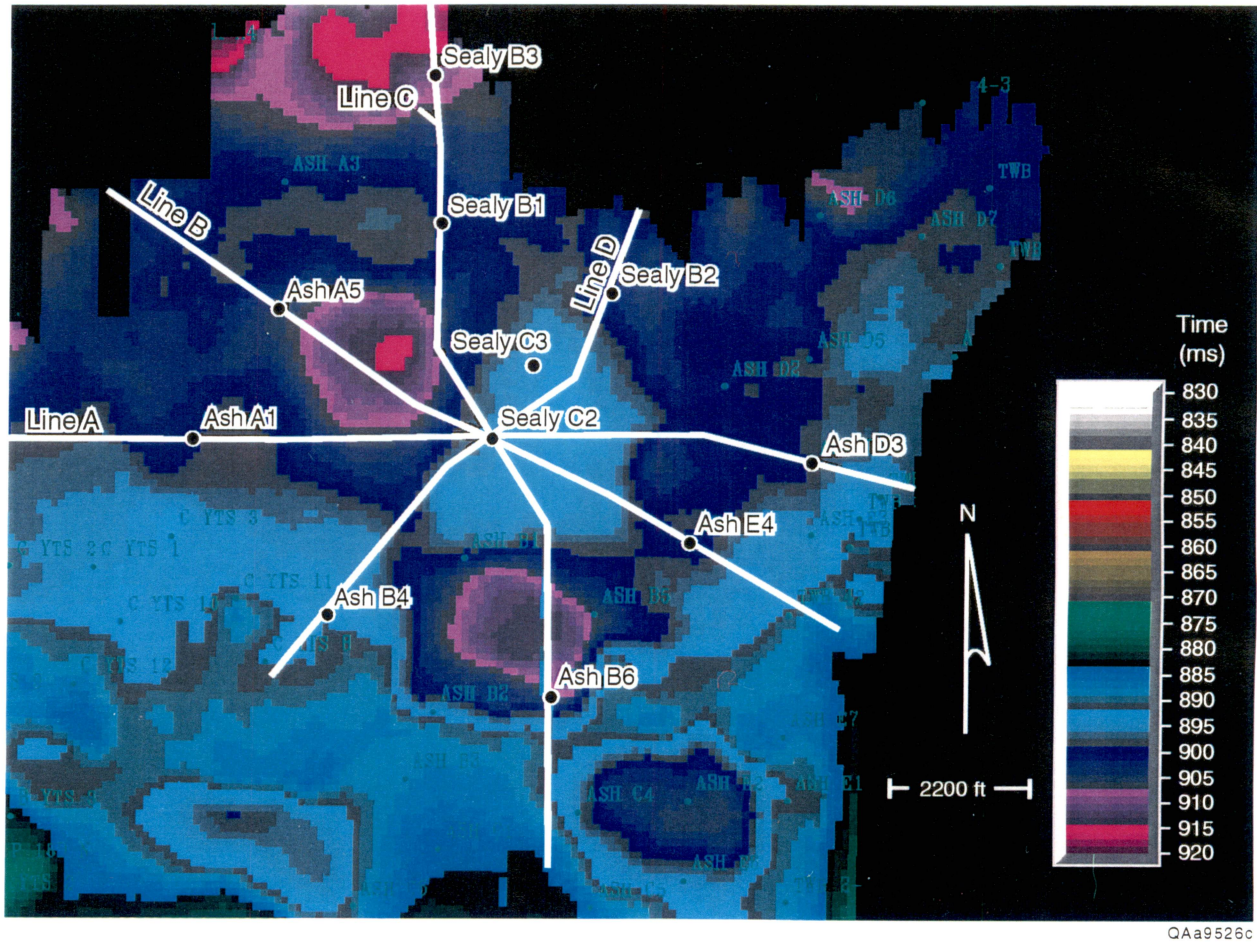
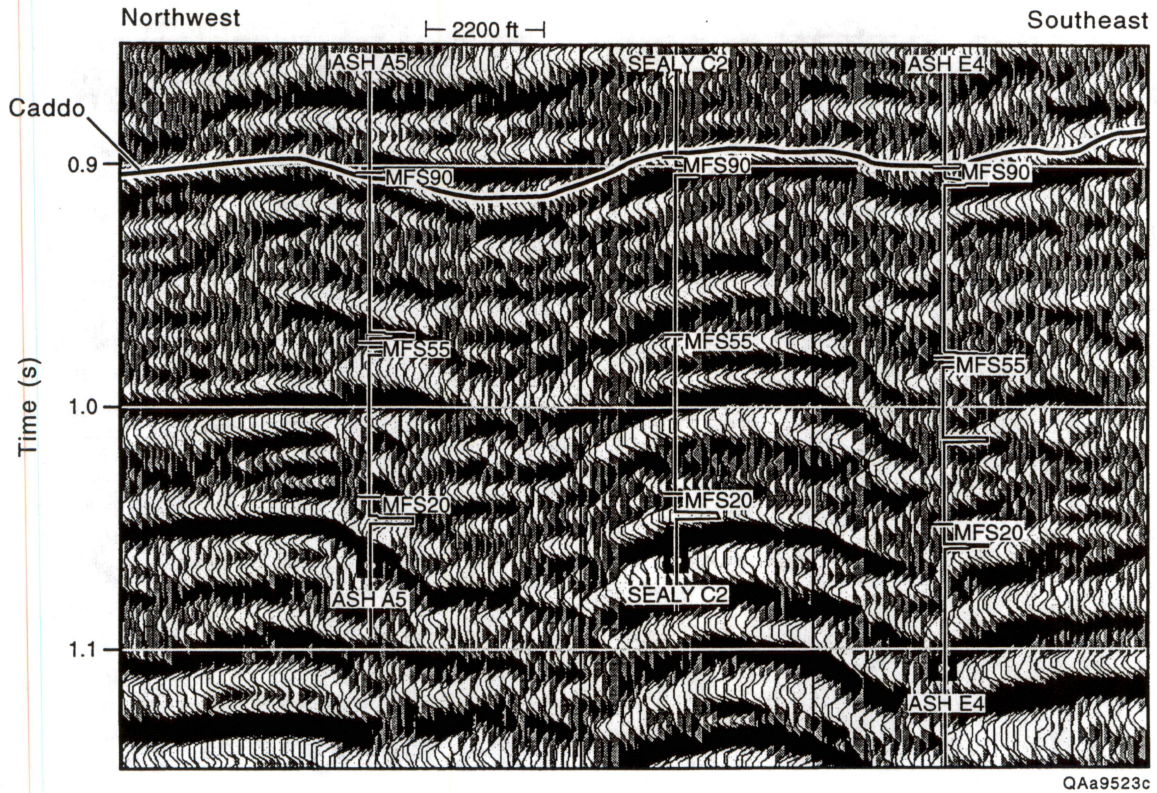


Figure 2.14. Northeast quadrant of the Caddo time structure map showing a ring of karst collapse surrounding the Sealy C-2 well. The Sealy C-3 well was drilled at the conclusion of this study.



QAa9523c

Figure 2.15. Vertical section along profile B defined in Figure 2.14. This section view emphasizes how the Sealy C-2 well is positioned on an apparent structural high, which actually is not a structural uplift, but rather is an area that remained in place after the surrounding terrain fell into a series of karst collapses. The curve plotted at each well location identifies where reservoir quality facies occurs within the Bend Conglomerate section.

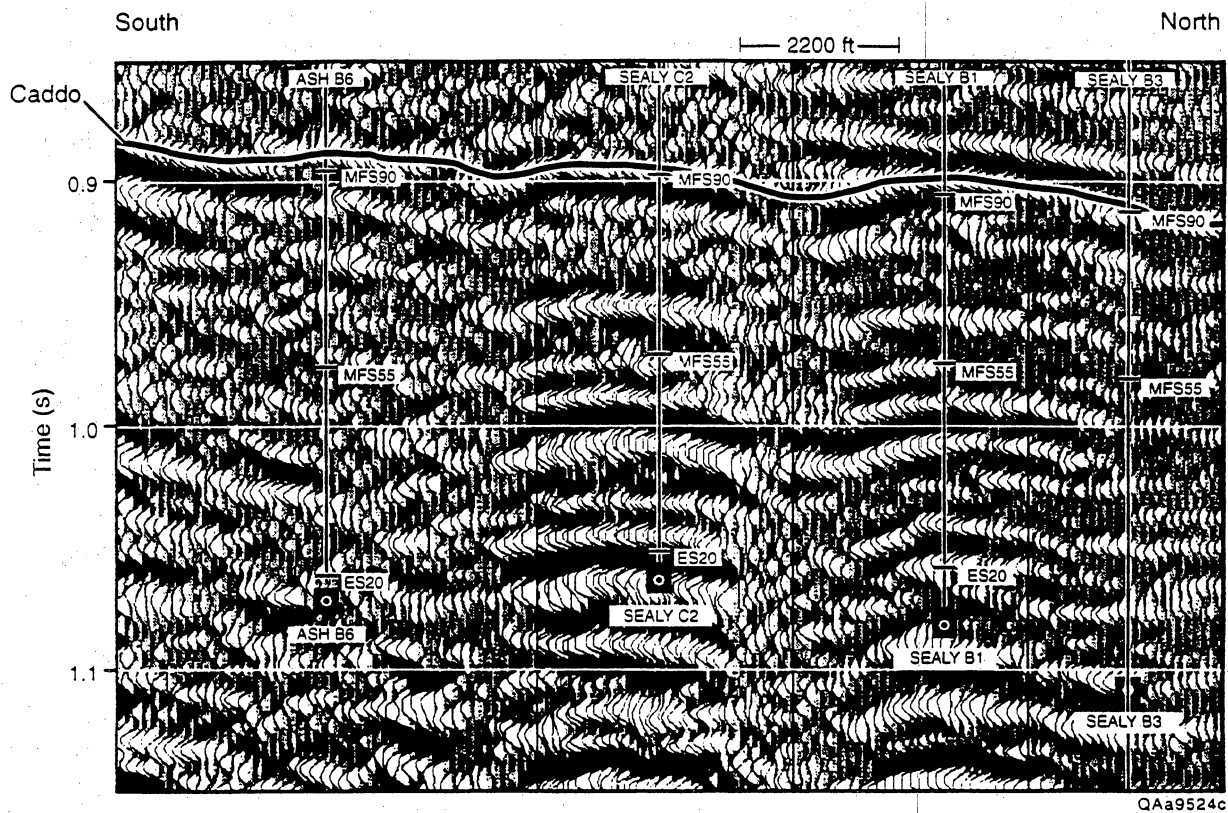


Figure 2.16. Vertical section along profile C defined in Figure 2.14. See caption of previous figure for explanation of key features.

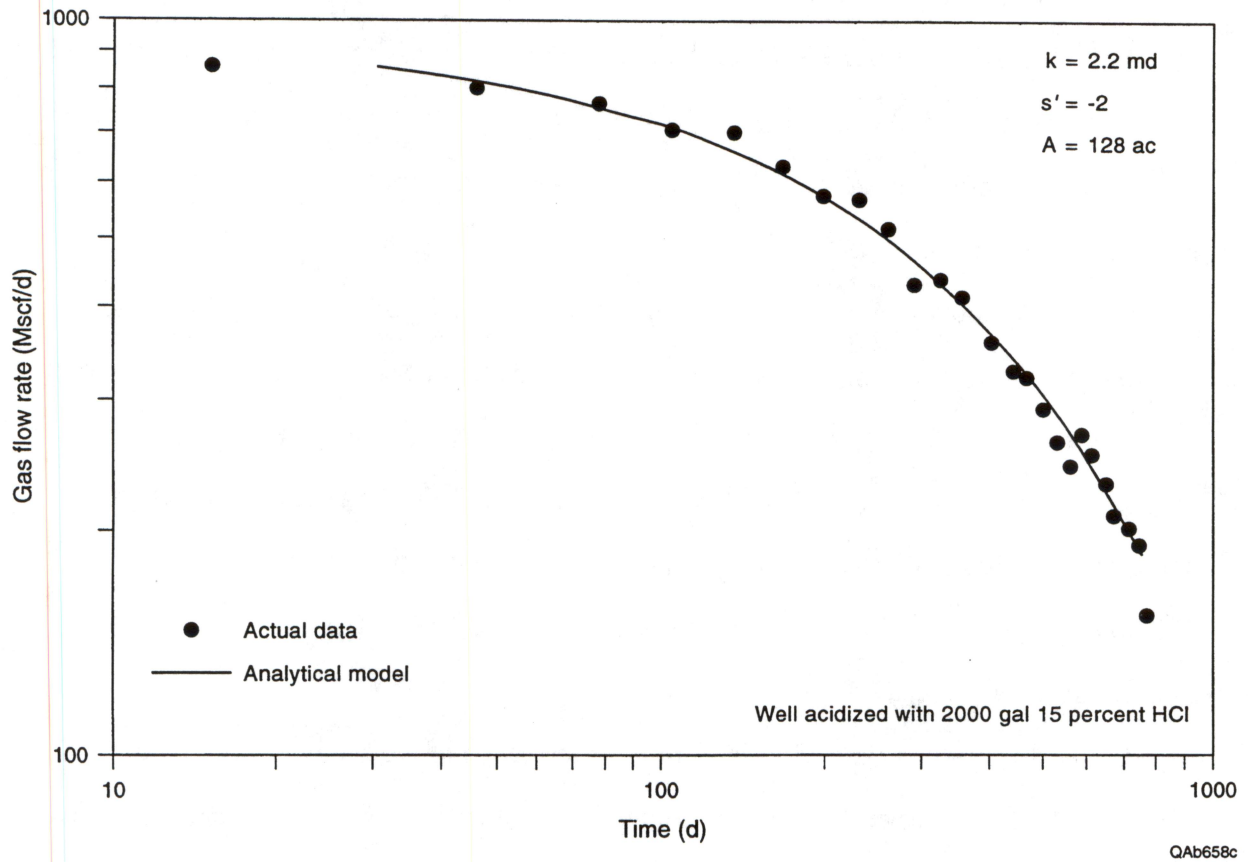


Figure 2.17. History match of production data from the Sealy C-2 well.

Analysis of Sealy C-2 Production Data

Figure 2.17 shows the actual production from the Sealy C-2 well. This is a log-log plot of gas flow rate versus time. The well came on line in November 1992 and produced 800 to 900 Mscf/d for the first couple of months. Since then, the gas flow rate has gradually declined to about 200 Mscf/d, after just over 2 yr of production. The Sealy C-2 has produced about 350 MMscf of gas to date. The production data, when plotted this way, show the influence of reservoir boundaries, as evidenced by the concave downward shape of the later-time data.

The production data were history-matched with an analytical reservoir model to estimate reservoir properties and gas in place. As Figure 2.17 shows, the analytical model provides a good match of the actual production data. From this analysis, a permeability of 2.2 md, a skin factor of -2 (indicating slight stimulation following the acid treatment), and a drainage area of 128 acres were determined. The estimated reservoir area of 128 acres agrees well with the 130-acre reservoir size identified from the seismic interpretation, as described previously.

Using this reservoir description, future performance of the Sealy C-2 was projected. The Sealy C-2 is expected to recover another 200 MMscf over the next several years, resulting in an ultimate gas recovery of about 550 MMscf. This projected ultimate recovery is at the high end of what might be expected statistically from an Upper Caddo gas completion in the project area (see Appendix B). In addition, this projected future recovery is for the Upper Caddo reservoir only; there still appear to be behind-pipe opportunities in both the Trinity and Bridgeport sequences, which may lead to additional gas recovery from this well.

Integration of Seismic and Engineering Data

As mentioned earlier, **the reservoir size estimated from the production data analysis was essentially the same as that predicted from the 3-D seismic interpretation.** The reservoir performance supports the seismic interpretation of an Upper Caddo reservoir compartment created by the karst-collapse zones surrounding the Sealy C-2 well. None of the reservoir pressures measured in the Bend intervals from the Caddo through the Vineyard, however, could be considered initial reservoir pressures; all indicated varying degrees of pressure depletion at this location. Therefore, the low-displacement faults associated with these karst collapse features may act as partial, but not total, barriers to gas flow, at least in this case. The degree of isolation caused by this low-scale faulting may also vary from sequence to sequence.

Structure mapping using only well control did not give any indication that a small structural high would be present at the Sealy C-2 site (Figs. 2.18 through 2.21). In fact, many geologists may have inferred the site to be in a saddle, on the basis of the nearest offset wells in the Ashe lease (to the south) (Fig. 2.7). However, the top of the MFS90 came in 15 to 50 ft higher than offset wells, and inspection of the 3-D seismic lines (Figs. 2.15 and 2.16) indicates the presence of subtle vertical faulting on the order of 25 ft of throw. This small displacement and the presumed complexity of the fault or collapse zone appear to have formed a partial barrier to fluid flow in an otherwise well-interconnected Upper Caddo reservoir.

Sealy C-3 Drilling Results

In May 1995, OXY USA drilled the Sealy C-3 well approximately 1,500 ft northeast of the Sealy C-2, as shown in Figure 2.7. This well penetrated the northern part of the structure shown in Figure 2.14. A key objective of this well was to test the hydrocarbon potential of the Ellenburger Formation below the Bend Conglomerate. Repeat Formation

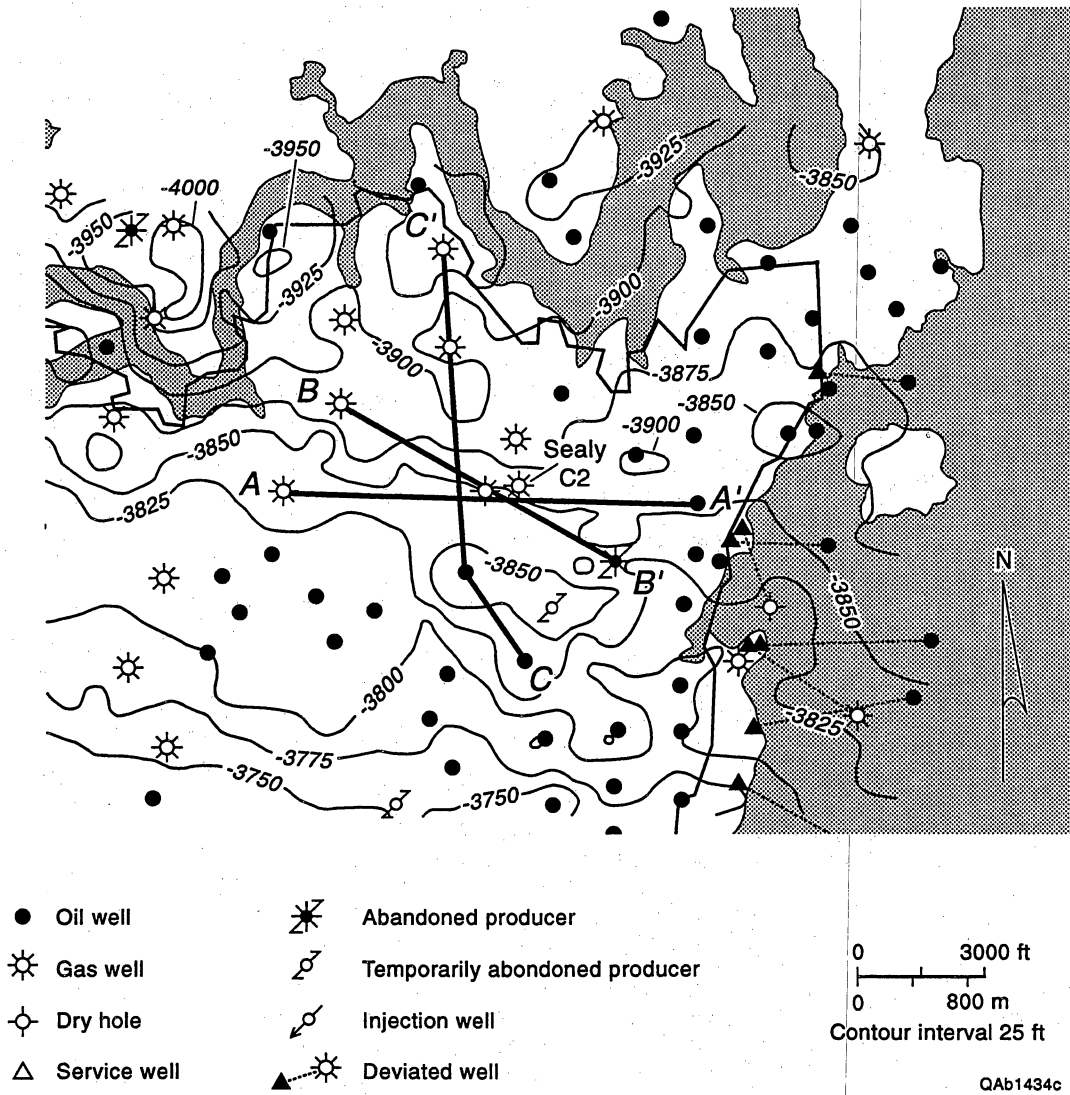


Figure 2.18. Structure map contoured on top of MFS90 (top of Caddo) before drilling of Sealy C-2 well. Well control gives no hints that a small high block occurs at the Sealy C-2 location.

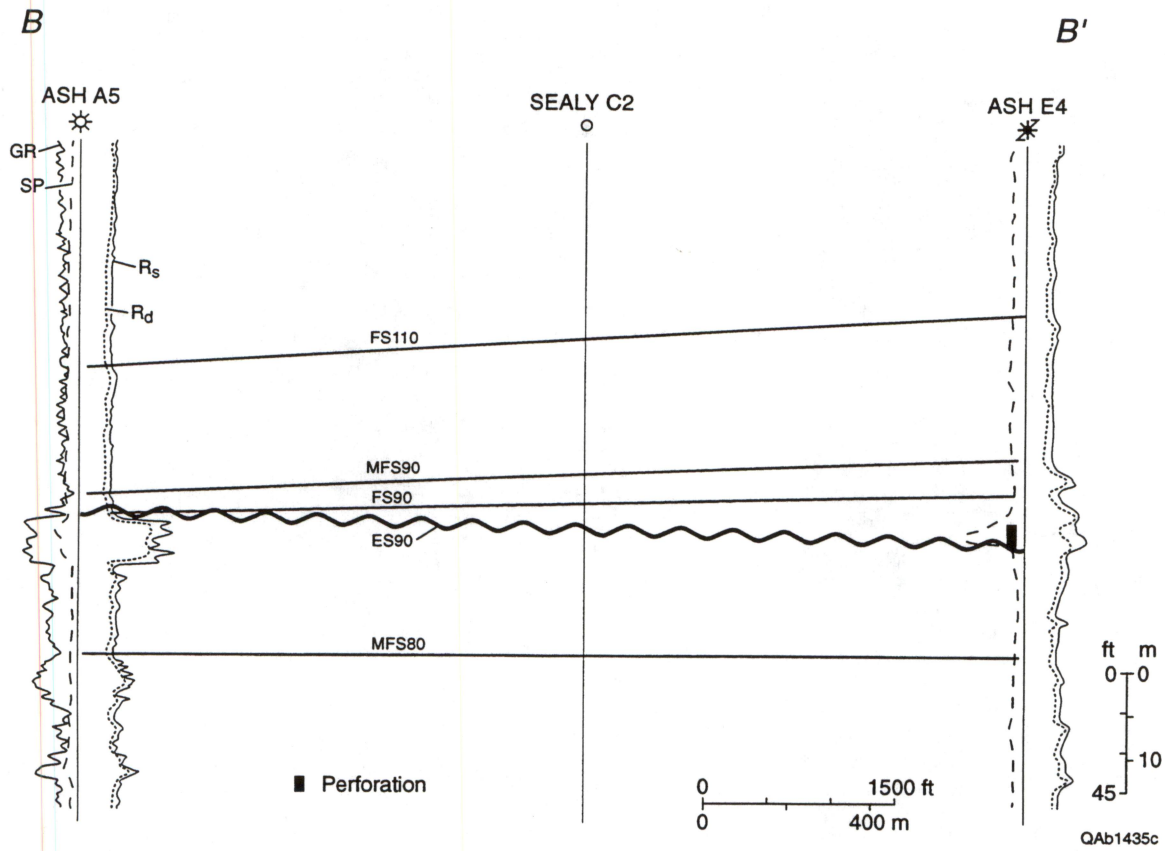


Figure 2.19. Structural cross section B-B' before drilling of Sealy C-2 well. Cross section parallels 3-D seismic line B-B' in Figure 2.15.

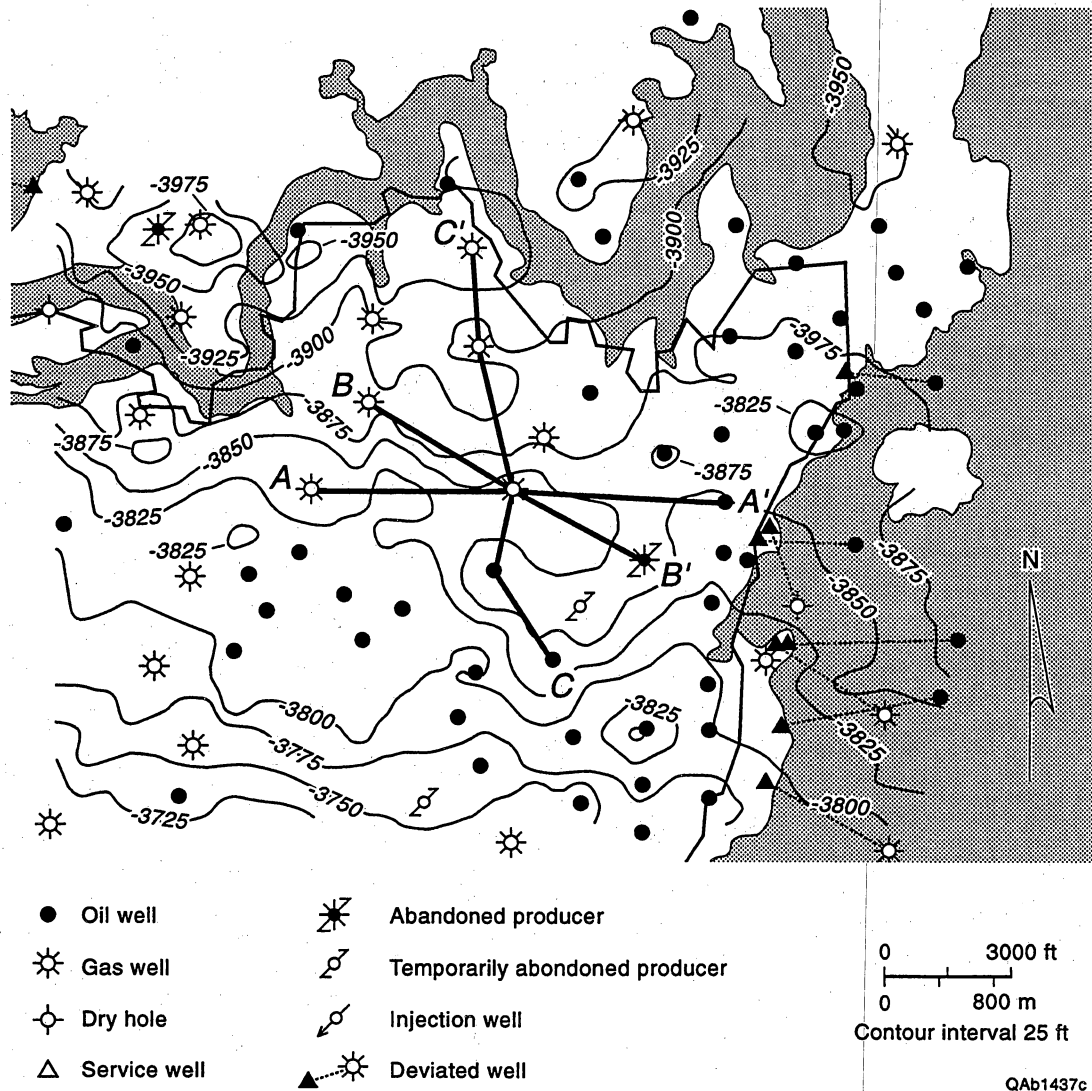


Figure 2.20. Structure map contoured on top of MFS90 (top of Caddo) after drilling of Sealy C-2 well. Contours represent subsea elevations in feet.

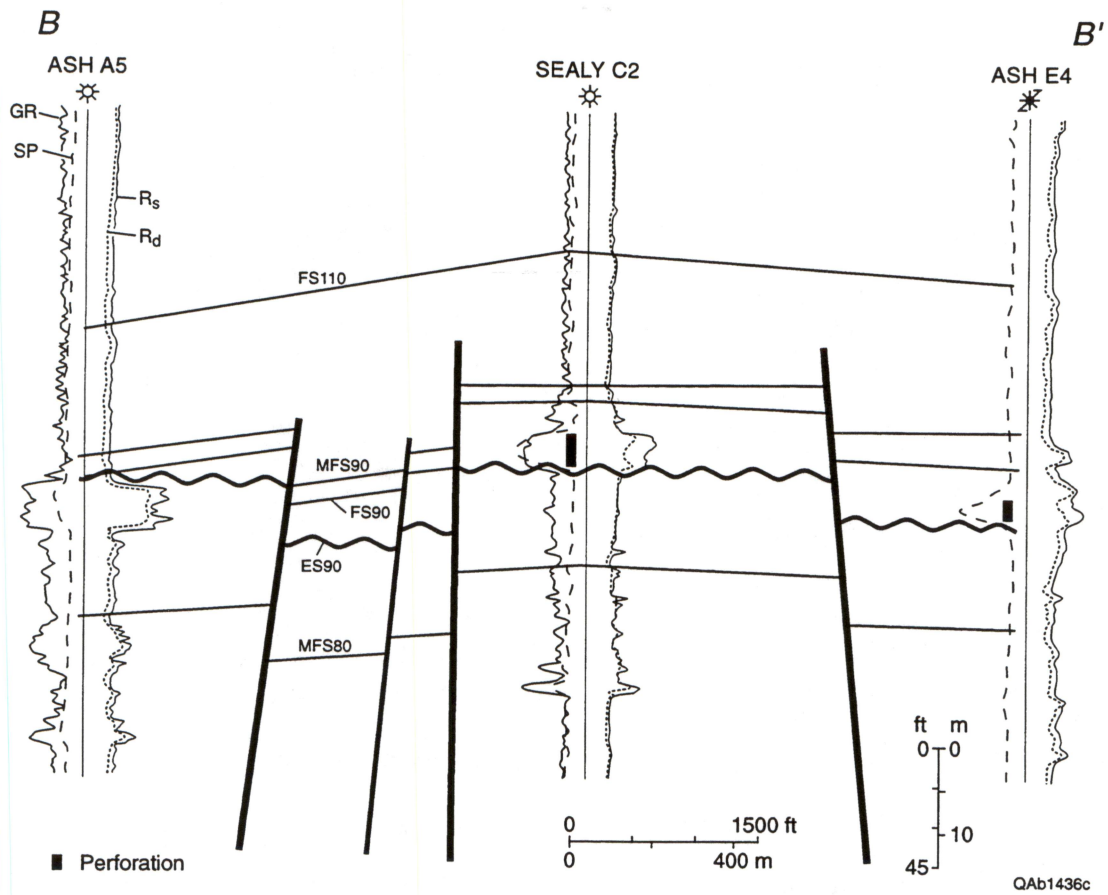


Figure 2.21. Structural cross section B-B' after drilling of Sealy C-2 well. Neither the subtle structural high nor small-scale faulting could have been inferred with well control: 3-D seismic is necessary to delineate subtle, fault-bounded compartments.

Tester (RFT) measurements were run throughout the Bend section, however, to evaluate potential completion zones in these sequences as well. Table 2.2 presents these RFT results.

Table 2.2. RFT pressures measured in the Sealy C-3 well.

Sequence	RFT pressure (psi)
Upper Caddo	1005
Lower Caddo	—
Wizard Wells	—
Davis	—
Trinity	708
Bridgeport	902
Runaway	—
Beans Cr	—
Fourth Jasper Creek	2,196/2,200
Middle Jasper Creek	—
Lower Jasper Creek	—
Vineyard	840

Similar to the Sealy C-2 (see Table 2.1), potential completion opportunities were identified in the Upper Caddo, Trinity, Bridgeport, and Vineyard sequences. As in the Sealy C-2, the Vineyard interval was found to be a low-permeability, low-productivity reservoir at this location. Pressures in the Trinity and Bridgeport sequences suggest partial drainage of the gas in these intervals, but both still offer behind-pipe completion opportunities. The pressure of 1,005 psi in the Upper Caddo reflects communication with the gas production from the Sealy C-2 well. This pressure value supports the seismic interpretation of the structural feature shown in Figure 2.14 and is in line with the value expected at this location given the size of the structure, the well locations, and the total production (degree of depletion) from the Sealy C-2 well.

Unlike the Sealy C-2, however, an excellent 10-ft sand in the upper part of the Jasper Creek sequence (later designated as the fourth Jasper Creek zone) was also

encountered in the Sealy C-3. As shown in Table 2.2, pressures of 2,196 and 2,200 psi were measured during two RFT tests in this interval. Pressure built up rapidly during both RFT's, indicating good permeability in this zone as well. These pressures are considered to be initial pressure at this depth, and, thus, the Sealy C-3 has encountered a previously undrained portion of the Jasper Creek or an isolated, reservoir compartment. Figure 2.22 shows the open-hole logs recorded across this interval. Notice the excellent SP development and the gas effect observed from the density–neutron crossover.

The Sealy C-3 encountered pay in the updip edge of a fourth Jasper Creek valley-fill sandstone (Figs. 2.23 through 2.25). Karst collapse faulting may provide a partial fluid-flow barrier; however, the elongate geometry of the fourth Jasper Creek sandstone may also have prevented drainage by the Ashe D2 and D3 wells in this zone. The latter wells penetrated thick (~20 ft net reservoir) sandstones, which appear to have been preferentially deposited in, and adjacent to, a significant karst collapse low (Figs. 2.2 and 2.14). The Sealy C-3 fourth Jasper Creek sandstone may be draining a much larger reservoir sandstone body lying downdip to the east (Fig. 2.23).

Middle Jasper Creek valley-fill reservoir sandstone is also well developed in the Ashe D2 area, particularly in the Ashe D5, whereas this area was a site of erosion during early Jasper Creek time. Increased sandstone thickness in the area centered on the Ashe D2 suggests that an episode or episodes of karst collapse occurred between (but not including) early Jasper Creek and Beans Creek time.

Following an Ellenburger test, OXY elected to complete the Sealy C-3 well in the Vineyard from 5,742 to 5,752 ft. Only a small gas show was reported after an acid treatment, and this interval was subsequently abandoned. Next, in mid-June 1995, OXY completed the Jasper Creek sand from 5,540 to 5,550 ft. This zone tested 3 MMscf/d at 1,500 psi flowing tubing pressure. As of the end of June, this well was still making in excess of 1 MMscf/d at about 1,600 psi flowing tubing pressure.

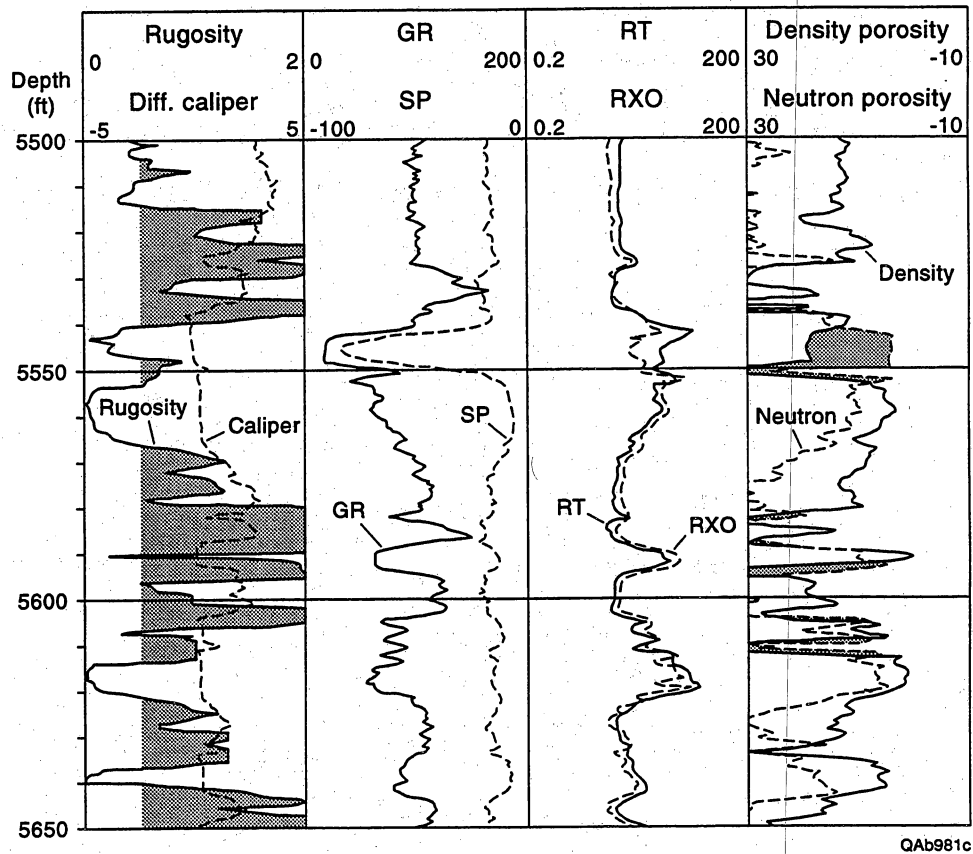


Figure 2.22. Open-hole logs recorded across the Jasper Creek sequences in the Sealy C-3 well.

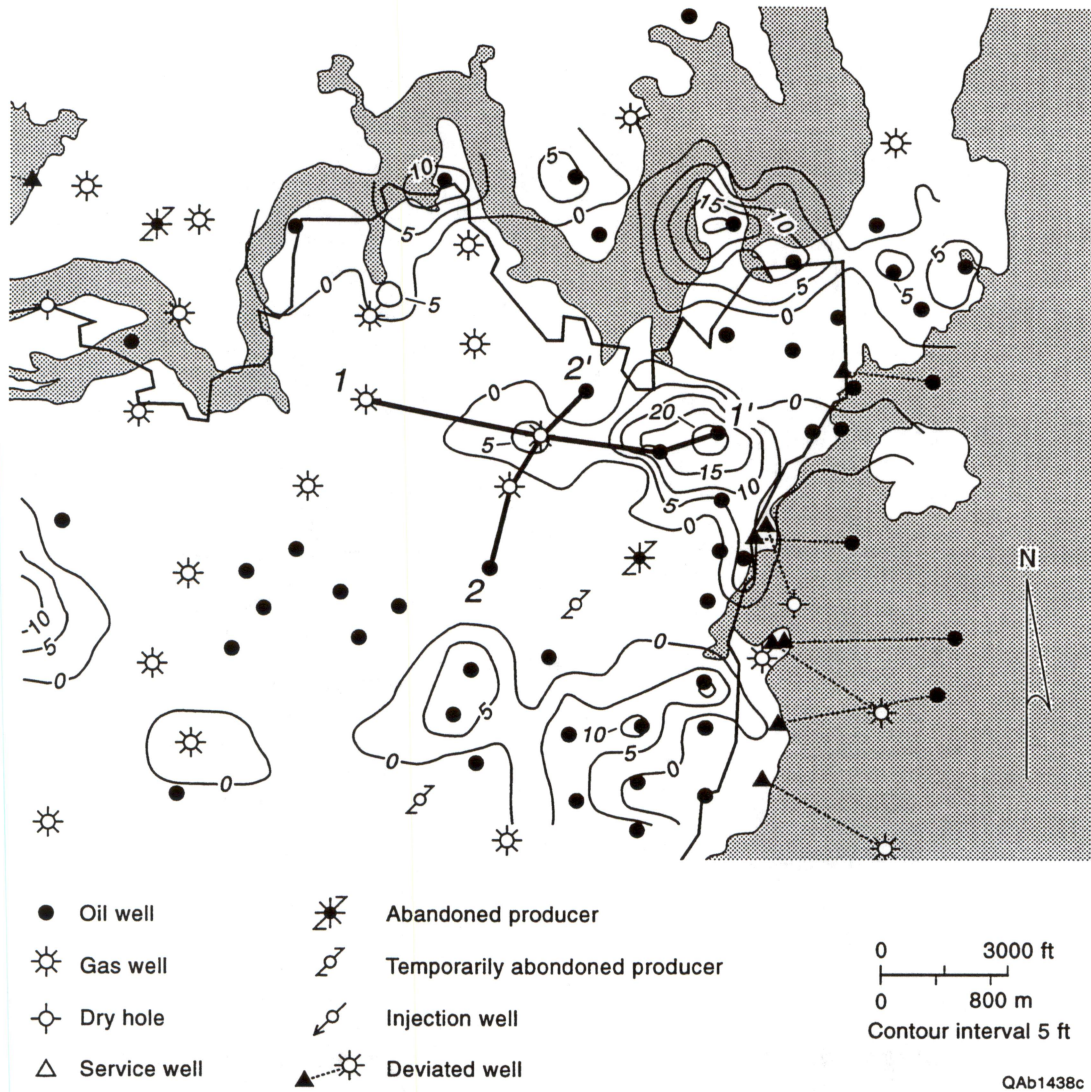


Figure 2.23. Net reservoir isopach of the fourth Jasper Creek zone.

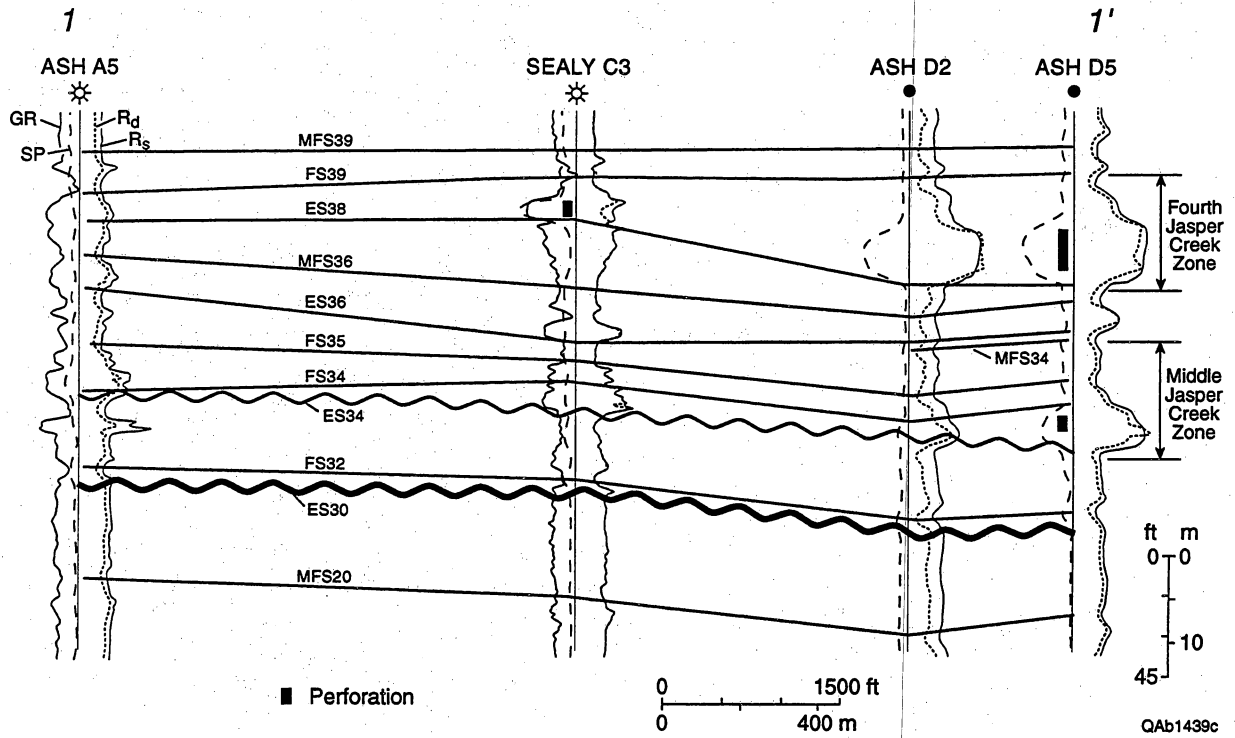


Figure 2.24. Stratigraphic cross section 1-1' of the Jasper Creek sequences (MFS39-MFS20). The fourth Jasper Creek zone (FS39-ES38) appears to be the updip edge of the large valley-fill complex to the east.

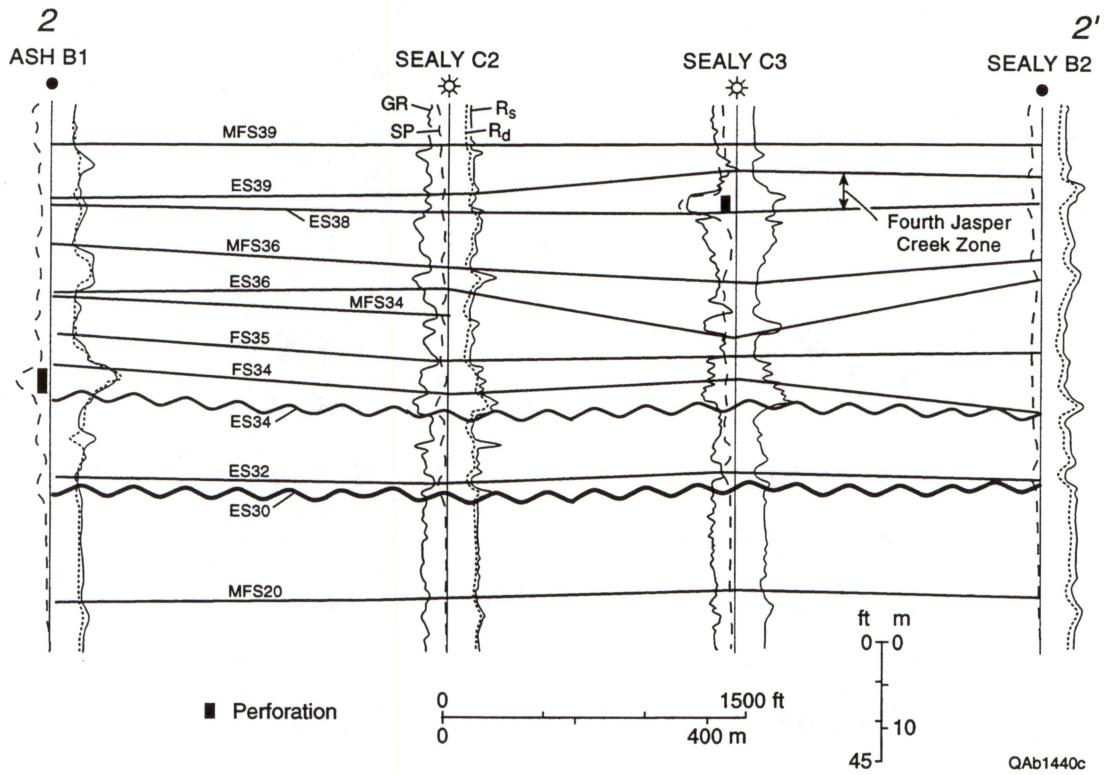


Figure 2.25. Stratigraphic cross section 2-2' of the Jasper Creek sequences (MFS39-MFS20).

We will continue to monitor the performance of the Sealy C-3 well to determine the effective size of this Jasper Creek reservoir. If this sand should cover most of the structure illustrated in Figure 2.14, as did the Upper Caddo in the Sealy C-2, the gas reserves associated with this Jasper Creek reservoir could be in excess of 500 MMscf. The discovery of this reservoir in the Sealy C-3 well further illustrates the influence of these karst collapse features on stratigraphy and potential reservoir compartmentalization in the Bend Conglomerate.

Summary

The 3-D seismic data identified a previously unknown, but important structural component influencing reservoir compartmentalization in the form of low-displacement faulting often associated with karst collapse in deeper carbonate rocks. The Sealy C-2 and C-3 examples illustrate that this deep Paleozoic karsting significantly influenced shallower sedimentation processes and often created at least partial interwell flow barriers throughout the Bend Conglomerate. Furthermore, it can be inferred that this Paleozoic karsting phenomenon may be a widespread control on younger sedimentation in areas such as the Permian and Delaware Basins as well. Given this finding, one strategy for siting new infield wells in Boonsville field is to use 3-D seismic data to identify these karst-bounded or fault-bounded blocks having no well penetrations in regional areas where the time structure is low, the sands are thickest, and the highest likelihood exists for encountering multiple completion opportunities.

3. CORRELATION BETWEEN SEISMIC ATTRIBUTES AND CADDO RESERVOIR PROPERTIES

One research activity that was pursued in the Boonsville seismic interpretation was to investigate whether any seismic parameter could be found that was a reliable indicator of the presence of reservoir facies. This effort focused on the Caddo interval because Caddo reservoirs are among the most productive in the area and because the Caddo sequence creates a relatively good seismic response across the study area. Numerically the investigation concentrated on analyzing the Hilbert transform seismic attributes described in Appendix E. These attributes are commonly referred to as instantaneous amplitude, instantaneous phase, and instantaneous frequency.

Lower Caddo

One of the better correlations discovered in this investigation was the relationship between instantaneous seismic frequency and the amount of net reservoir within the Lower Caddo. This correspondence between net reservoir and seismic frequency can be seen by comparing the areal distributions of these two parameters about the labeled well coordinates shown on the maps in Figures 3.1 and 3.2, respectively, which cover the southern third (approximately) of the 26-mi² 3-D seismic grid. The Lower Caddo seismic attribute analysis is limited to this portion of the project area because the Lower Caddo is a pervasive, major producing reservoir only within these bounds; Lower Caddo reservoirs are sparsely distributed in the northern two-thirds of the seismic area.

The Lower Caddo is a south-prograding deltaic system, exhibiting low-angle, shingled clinoforms in log-based cross sections (Figs. 3.3 through 3.5). "The Caddo Limestone" in the project area actually comprises two separate carbonate units representing the abandonment and transgression of two distinct delta-lobe platforms. Figure 3.4 shows a northeast-trending net reservoir thick in the south half of the project

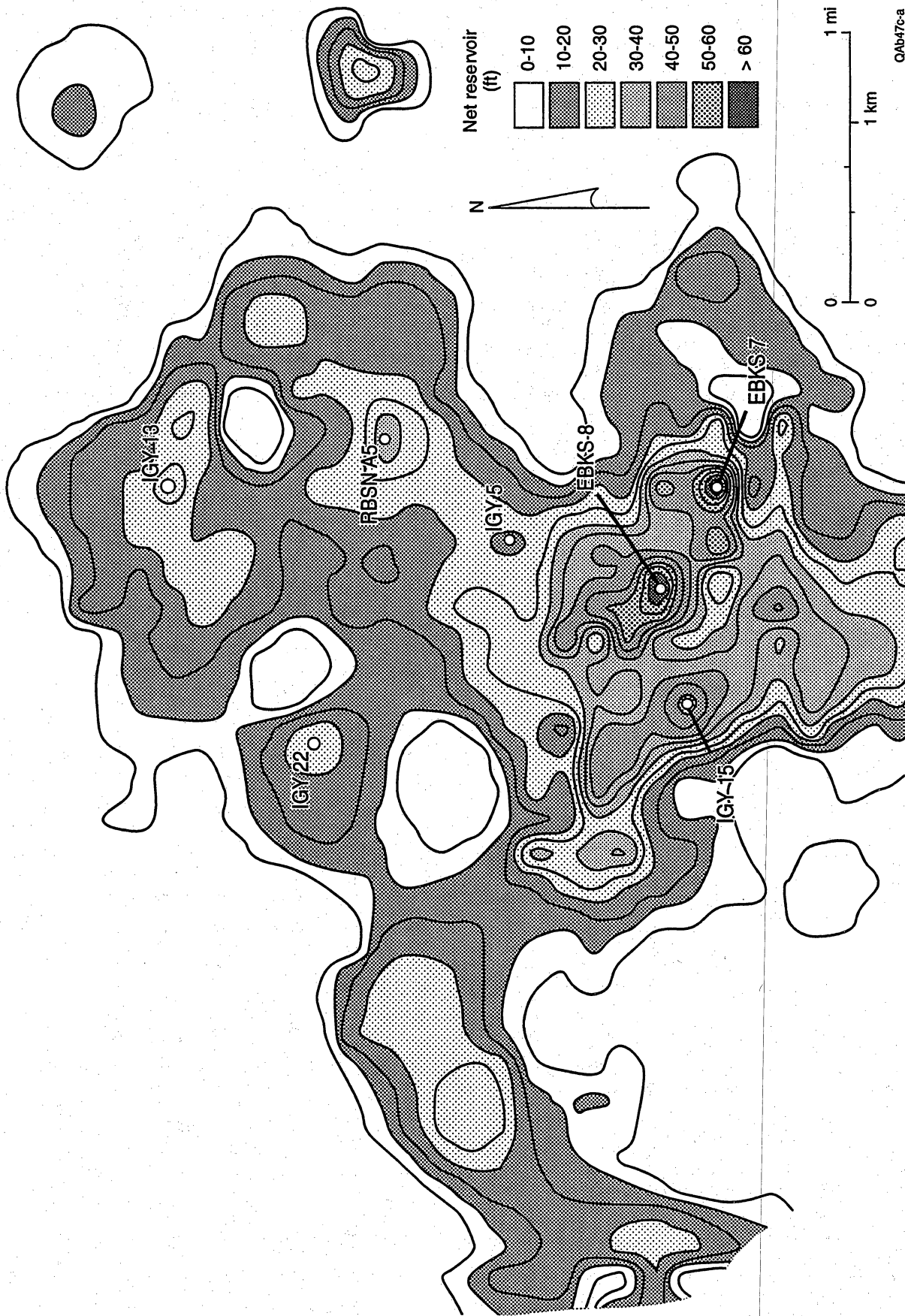


Figure 3.1. Lower Caddo net reservoir in the south third of the project area as determined from well log control, using the criteria that Lower Caddo reservoir facies exists whenever the resistivity exceeds 10 ohm-m and simultaneously the SP curve reads less than -30 API units. This map was created using data from approximately 75 wells; only 7 of the wells are labeled.

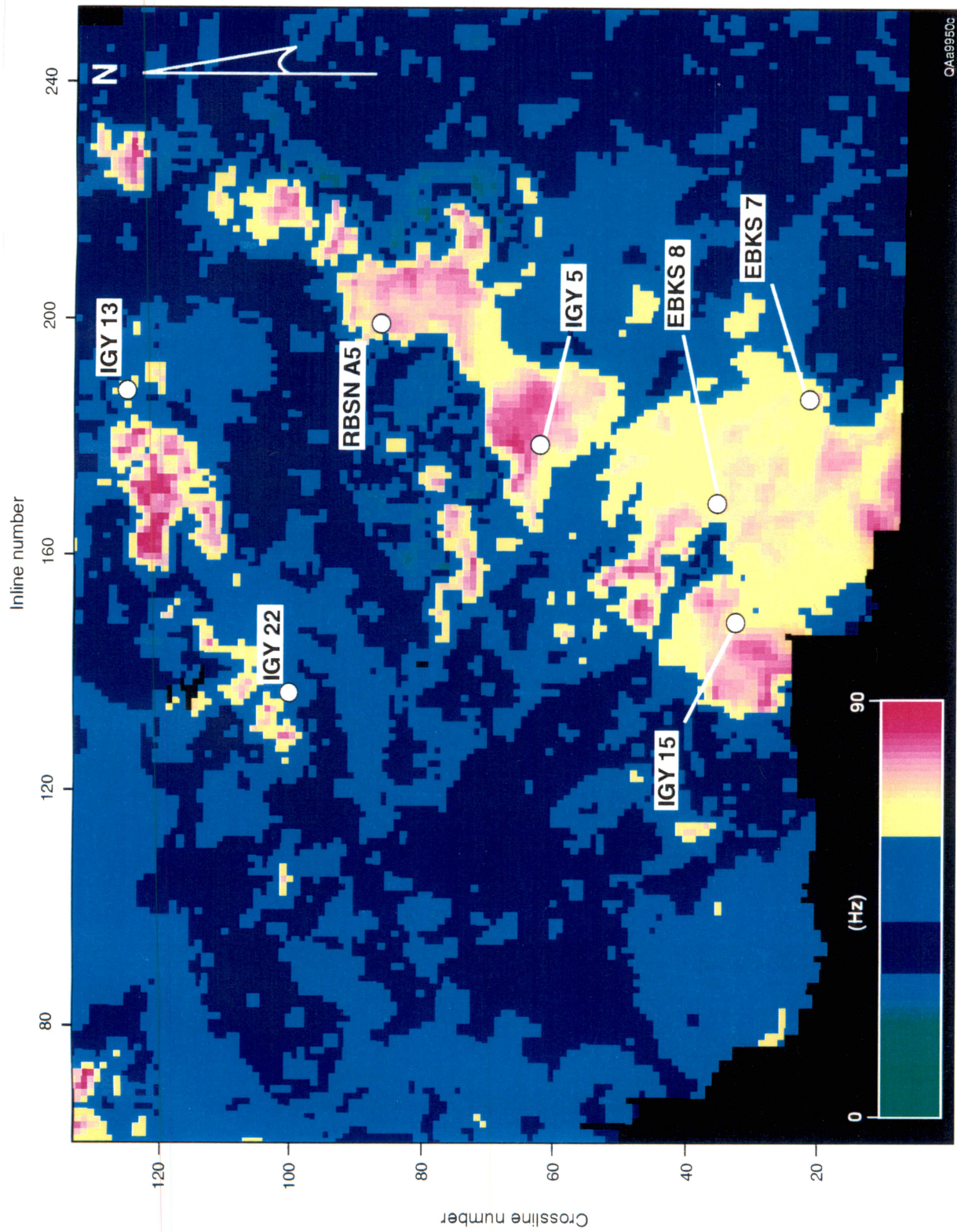


Figure 3.2. Average instantaneous seismic frequency calculated within the Lower Caddo sequence. This map should be compared with the preceding Lower Caddo net reservoir map. The parameter that is mapped is the average instantaneous frequency in a 10-ms window that is conformable to the seismically derived Caddo chronostratigraphic boundary and starting 10 ms below that boundary. The correspondence between this seismic attribute map and the log-based net reservoir map is striking, and shows that, in some circumstances, 3-D seismic data provide a valuable predictive tool for locating stratigraphically trapped reservoirs. The theory of instantaneous frequency is discussed in Appendix E.

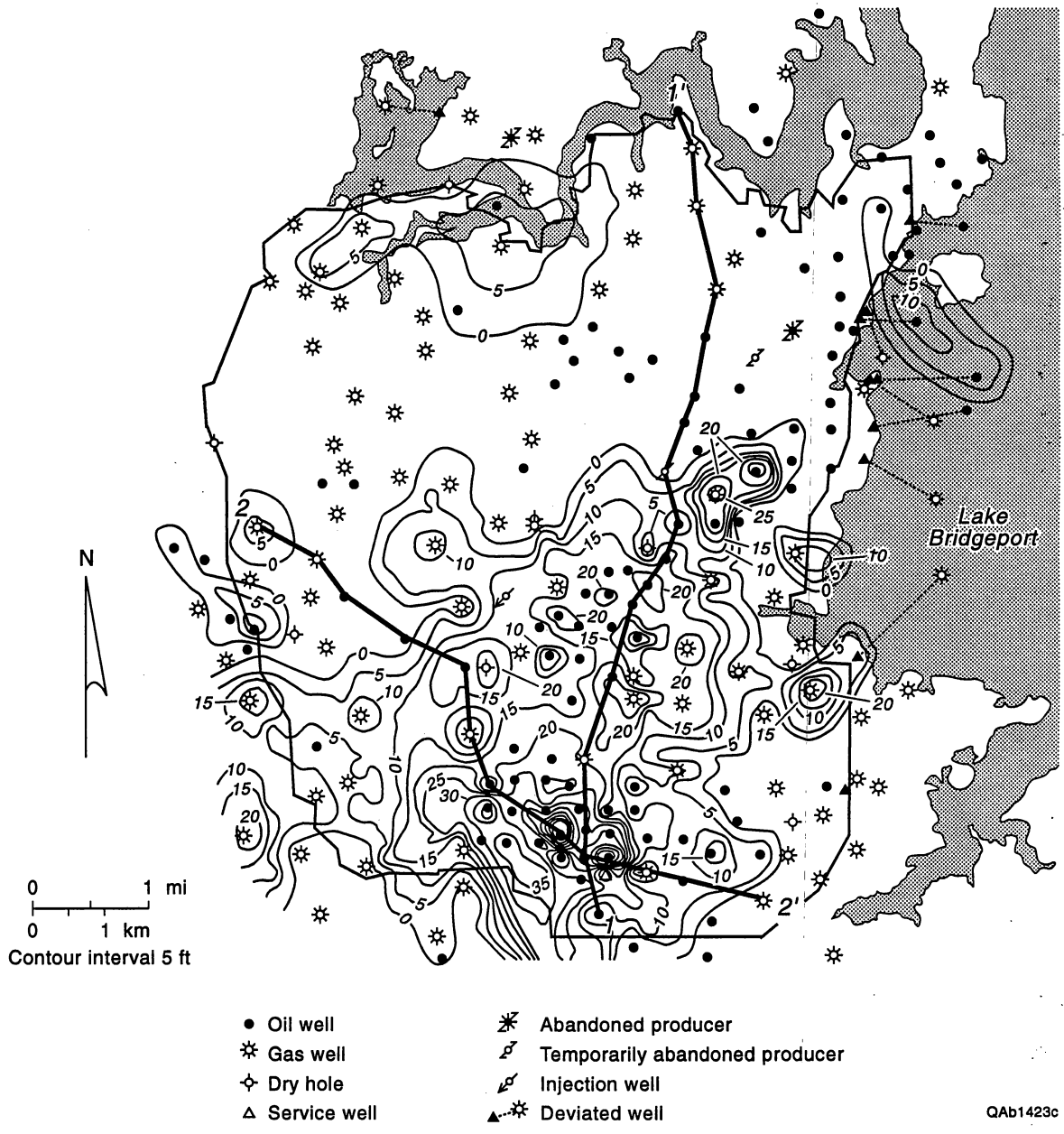
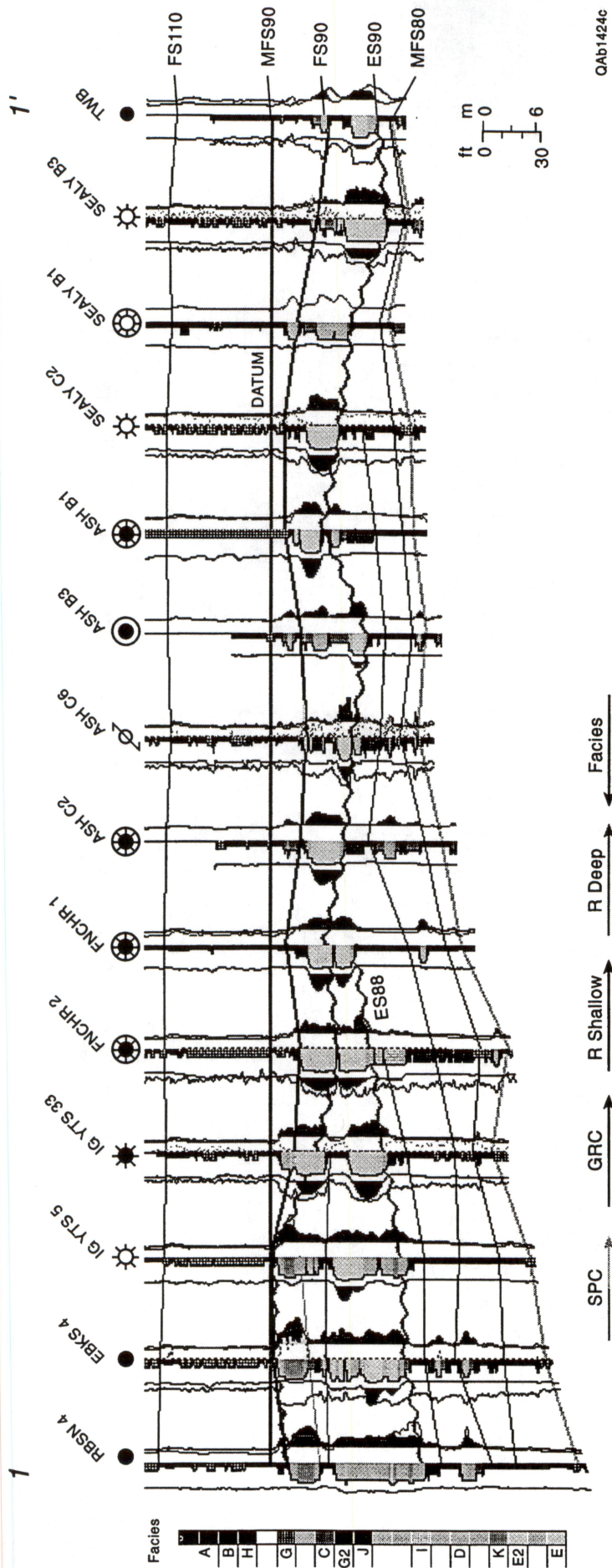


Figure 3.3. Well control and cross-section profiles used to analyze Lower Caddo interval.



QAb1424c

Figure 3.4. Stratigraphic cross section 1-1', Caddo sequences. The Lower Caddo is defined by MFS90 and ES90, which appear to be an unconformity surface representing a significant subaerial exposure event. Fluvial and deltaic sandstone reservoirs filled incised valleys above ES90, cutting deltaic sandstones and abandoned delta platform limestones of the Lower Caddo sequence (ES90-MFS80). The Strawn Group overlies MFS90. This section occurs approximately parallel to depositional strike. Line of section shown in Figure 3.3. See Appendix C for explanation of facies code bar.

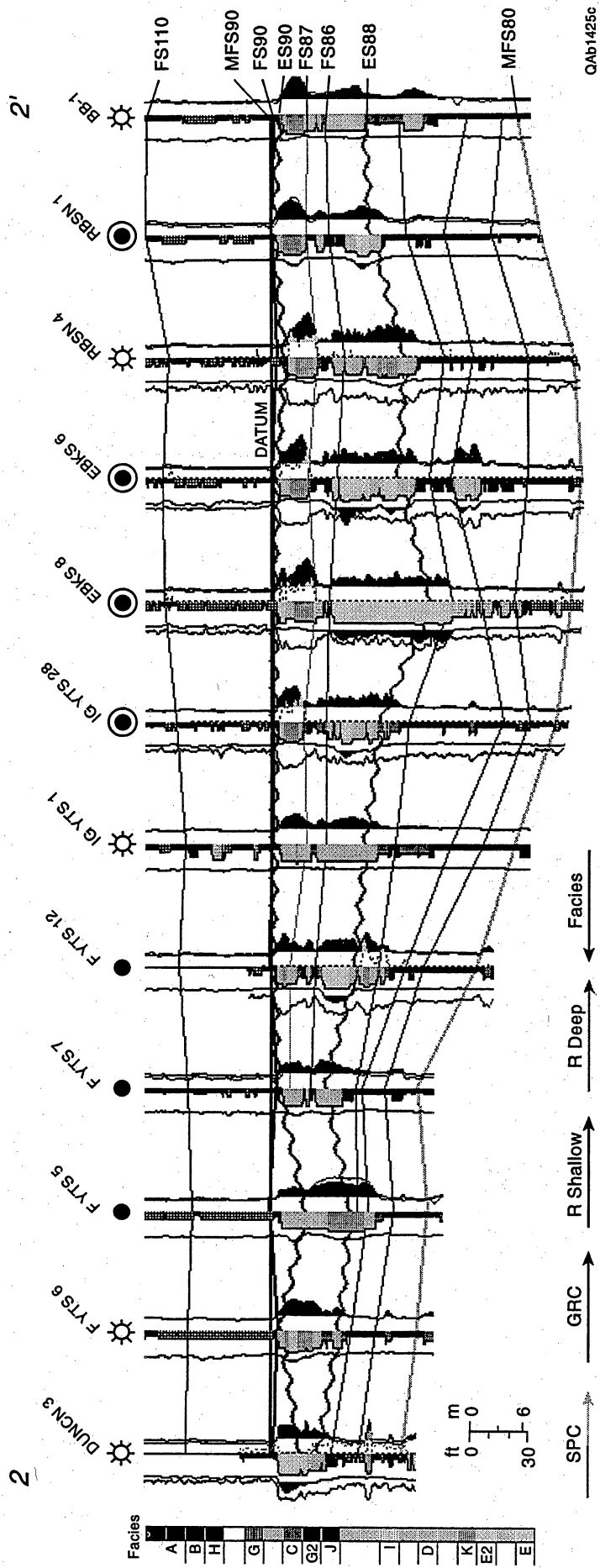


Figure 3.5. Stratigraphic cross section 2-2', Caddo sequences. Depositional dip section through thickest part of Lower Caddo deltaic unit. Line of section shown in Figure 3.3. See Appendix C for definition of facies code bar.

area that is interpreted to be a strike-oriented, delta-front deposit. Sinuous, south-trending ribbons of thin sandstone north of the delta front sandstone may represent minor fluvial or distributary channels. The Lower Caddo is predominantly an oil-productive zone, and it occurs in the area of highest structural elevation at the Caddo level (Fig. A17).

The value, net reservoir feet, plotted in Figure 3.1 is a log-based parameter determined by summing the cumulative number of vertical feet within the Lower Caddo where the deep resistivity exceeds 10 ohm-m, the SP value is less than -30 API units, and the facies curves (see Appendix C) indicate either facies E or E2. The seismic frequency value in Figure 3.2 is the average instantaneous frequency in a 10-ms window starting 10 ms below, and remaining conformable with, the interpreted Caddo sequence boundary, which is the seismic time window where several Lower Caddo reservoirs are located. Comparing the two maps and noting where the labeled well coordinates occur in each plot show that this **average instantaneous frequency parameter produces an areal pattern that is strikingly similar to the areal distribution of the Lower Caddo net reservoir map**. This correlation leads to the conclusion that there are some stratigraphically trapped reservoirs in the Boonsville study area that can be seismically imaged with considerable accuracy if seismic attributes have been selected carefully. To produce reliable seismic maps of these stratigraphic reservoir facies, we found that several seismic attributes, but principally just reflection amplitude and instantaneous frequency, had to be calculated within the narrow, precisely defined seismic time window that spanned the targeted sequence, and that each calculated attribute then had to be displayed with a variety of color bars until a color bar was found that caused a certain numerical range of the attribute to be distributed in an areal pattern that reasonably matched the areal facies pattern implied by key control wells.

In this Lower Caddo example, the best seismic attribute for mapping net reservoir was instantaneous frequency, and the best choice for a color bar seemed to be the one

shown in Figure 3.2. **This interpretational approach requires that two forms of supporting data be available to the interpreter:**

1. An accurate depth-to-time conversion function must exist so that the log-derived depths of the thin Lower Caddo sequence can be converted into the correct narrow time window in the Boonsville 3-D seismic data volume.
2. A reasonable number of wells must exist so that the amount of Lower Caddo net reservoir can be determined at several locations and so that a color bar can then be found that will cause the areal distribution of a certain numerical range of instantaneous frequencies to reasonably match the areal net reservoir pattern suggested by these control wells.

In addition to these requirements, the stratigraphic horizon that contains the seismic imaging objective must be laterally traceable in the 3-D data volume, which fortunately was possible for the Caddo (MFS90) sequence boundary. Several geologic factors affect the lateral continuity of the seismic reflection event that exists at a targeted sequence, such as the acoustic impedance contrast across the bed boundary and the thickness of the bed. These conditions were also favorable at the Caddo boundary.

Upper Caddo

Upper Caddo reservoirs are found primarily in the north half of the Boonsville study area, and a particularly important trend of Upper Caddo producers occurs in the northwest third of the 3-D seismic grid. A well-log-based map defining the distribution of the Upper Caddo sandstone thickness in this northwest area is shown in Figure 3.6. From log and core analyses, these Upper Caddo sandstones are interpreted to be valley-fill, fluvial, and deltaic sandstones. Log control indicates that a small arm of a large southeast-trending system (Fig. A36 of Appendix A, Volume II) runs northeast-southwest between the CYTS5 and DUNCN3 wells (Fig. 3.6). Well log cross sections (Figs. 3.7 through 3.9) illustrate the interpretation that a significant erosion surface (ES90) separates fluvio-

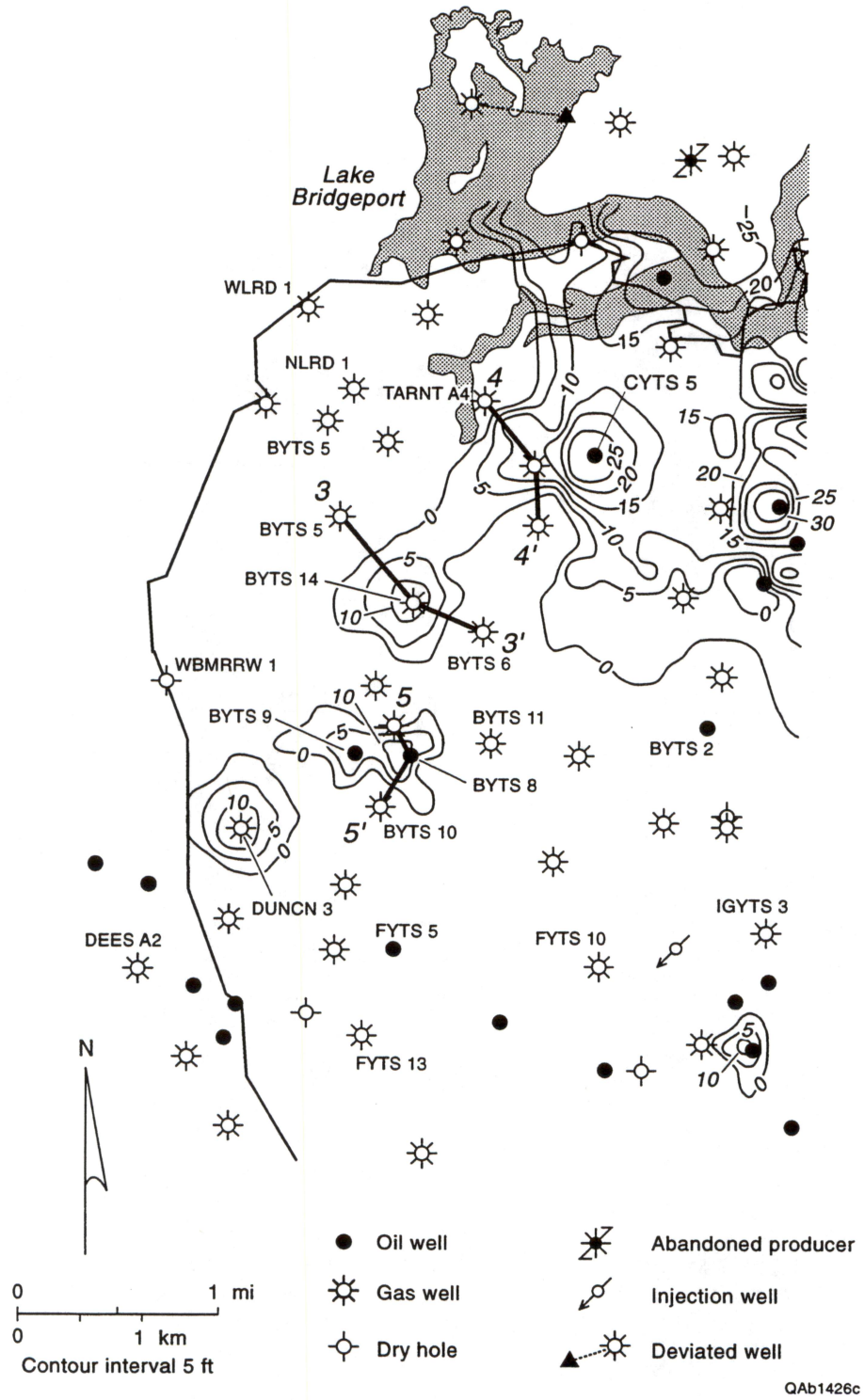


Figure 3.6. Upper Caddo net reservoir sandstone thickness in the northwest third of the Boonsville project area as defined by well log control. This map is a computer-contoured product generated from only 40 (approximately) control points. Note the series of bullseyes centered on the BY 14, 8, 9, and Duncan 3 wells, suggesting that an elongate valley-fill sandstone extends southwestward from the main valley-fill complex in the north part of the 3-D survey (see Figure A37). Stratigraphic cross sections 3, 4, and 5 shown in Figures 3.7 through 3.9, respectively.

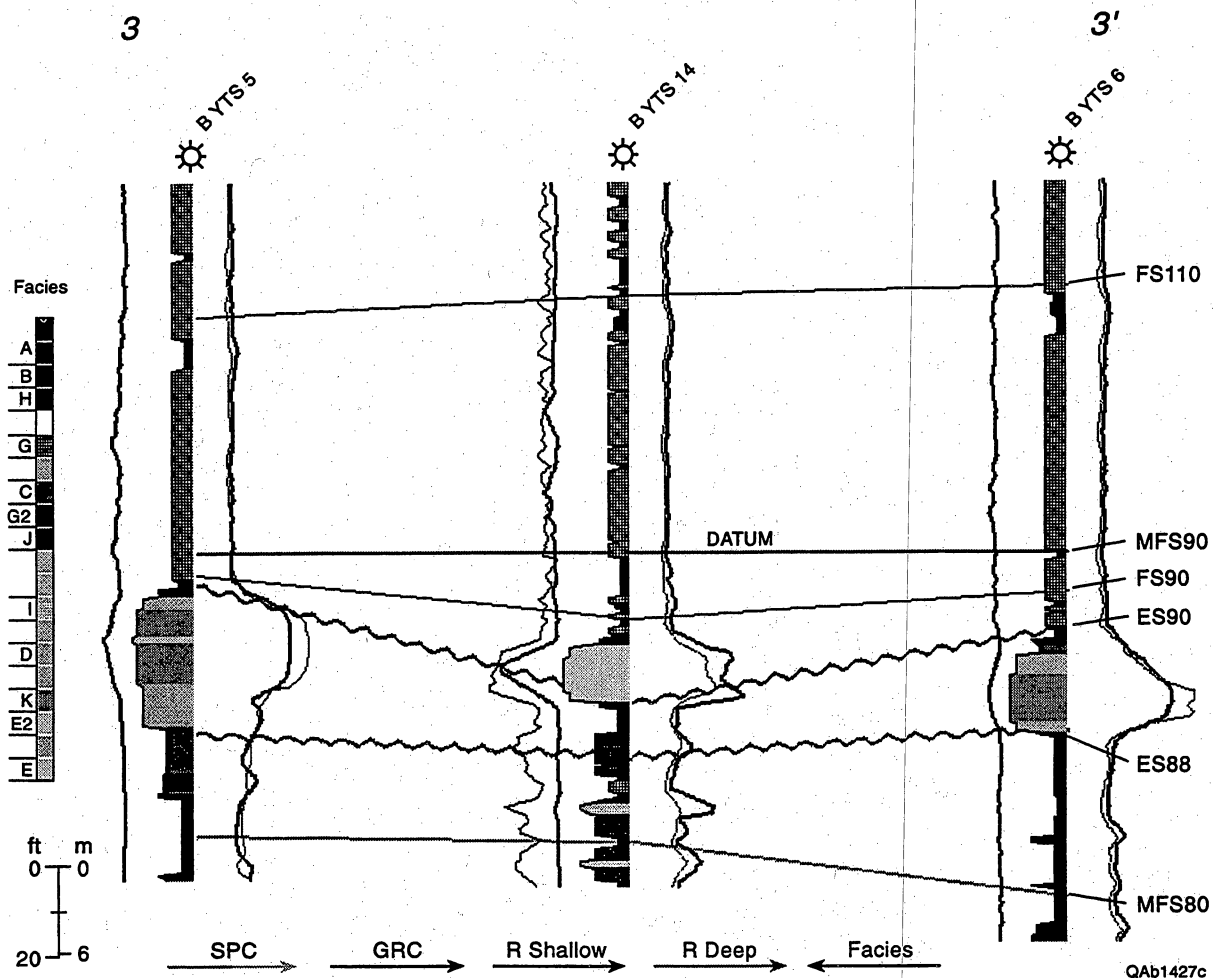


Figure 3.7. Log cross section 3. Line of section shown in Figure 3.6. Facies code bar is described in Appendix C.

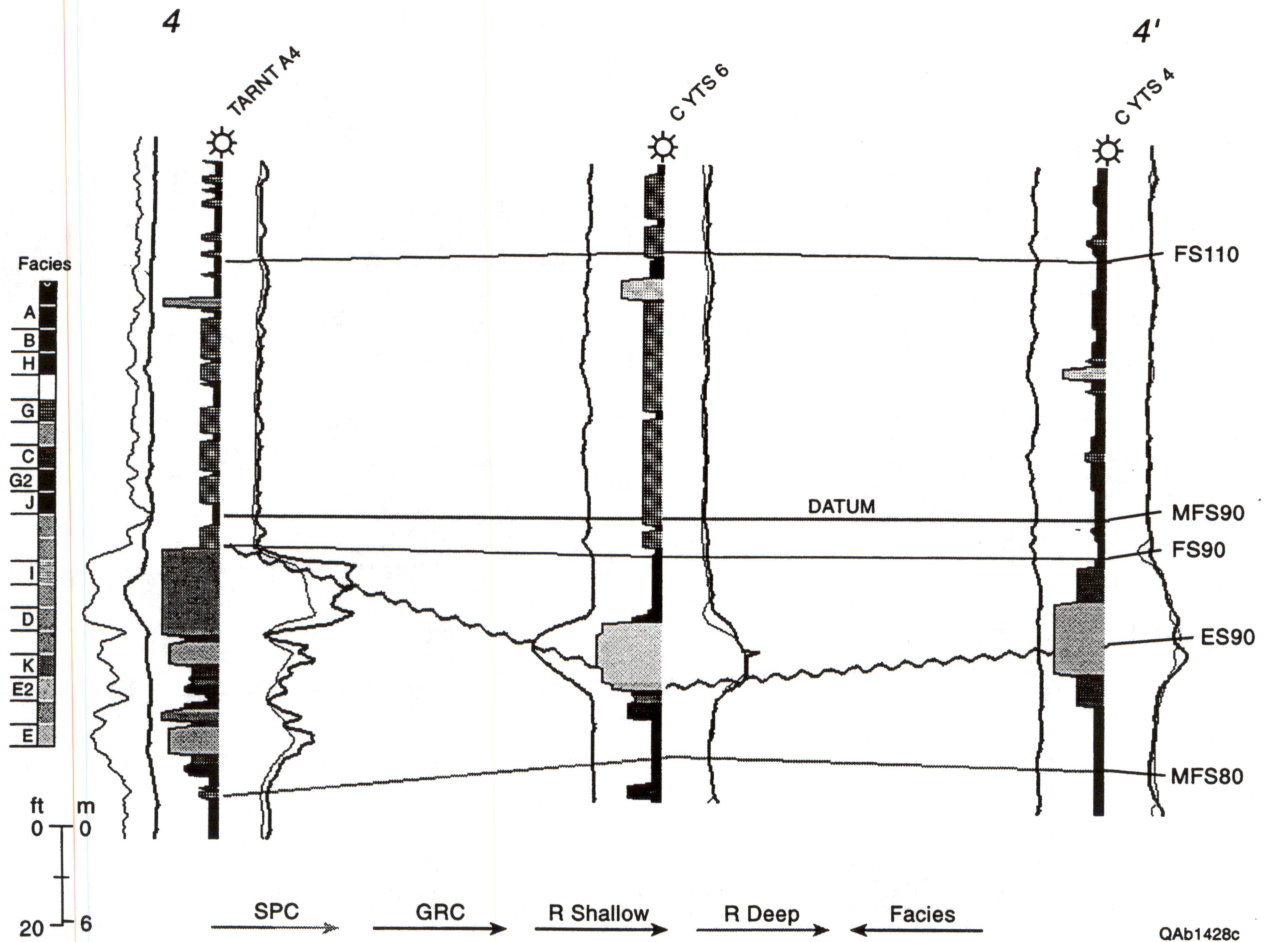


Figure 3.8. Log cross section 4. Line of section shown in Figure 3.6. Facies code bar is described in Appendix C.

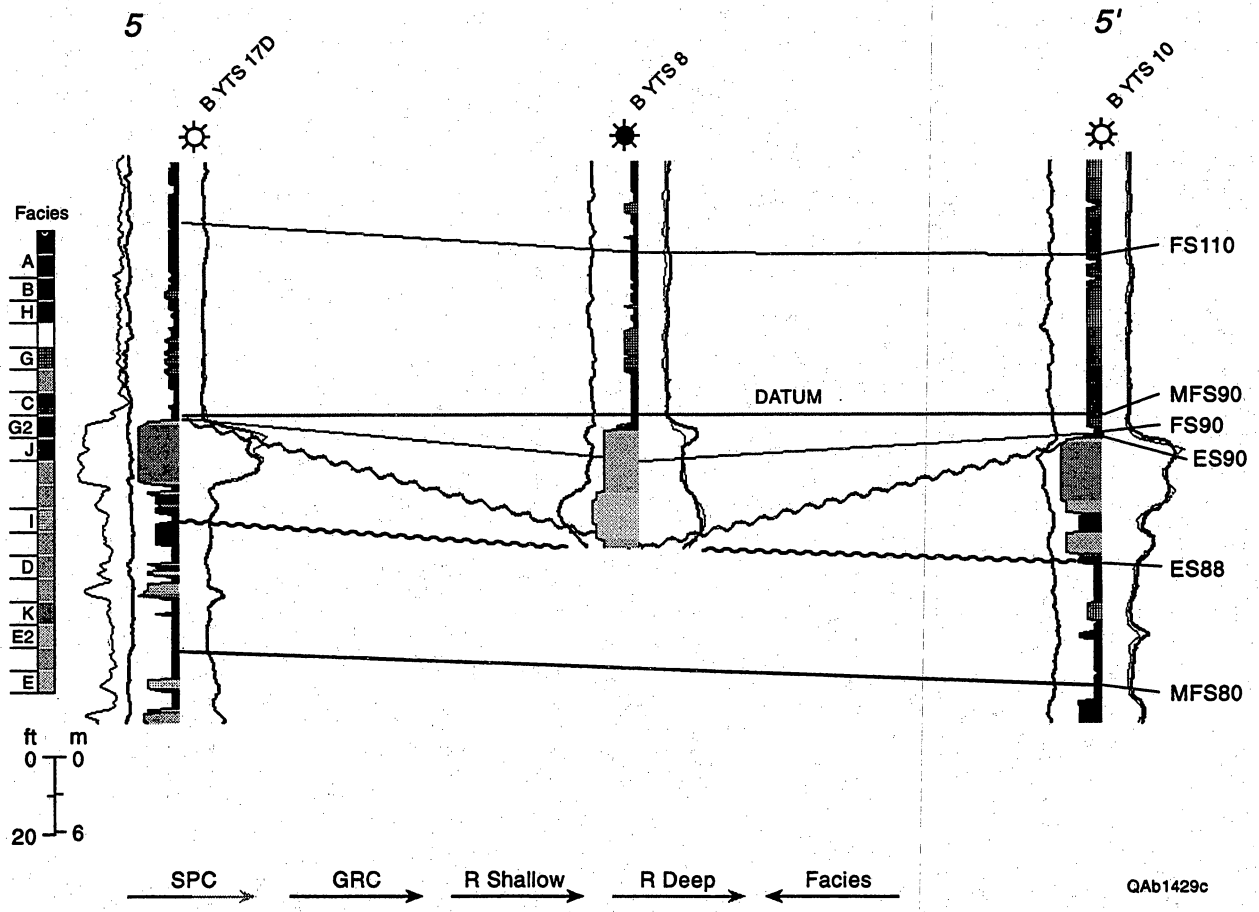


Figure 3.9. Log cross section 5. Line of section shown in Figure 3.6. Facies code bar is defined in Appendix C.

deltaic sandstone reservoir facies from previously deposited marine limestone. The sporadic occurrence and consistent, sublinear trend of net reservoir sandstone encounters in well bores suggest that an incised river valley, in most places less than 2,000 ft in width, meanders in and out of the well control in the area. The ES90 may represent an unconformity surface, in turn representing a significant time period of subaerial exposure and downcutting of a small sinuous canyon. Fluvial and perhaps estuarine and deltaic sands accumulated in the valley as the transgression ensued. This lowstand landscape would have featured a sinuous canyon having depths of 10 to 50 ft meandering through a limestone-capped plateau.

Examination of the Boonsville 3-D seismic data shows that in the northwest portion of the seismic grid, the seismic reflection associated with the Caddo sequence boundary (MFS 90) undergoes a significant amplitude reduction along the trend where the well-log-based map shows that the Upper Caddo net reservoir sandstone exists. A display of this Caddo reflection behavior is shown as Figure 3.10, and the northeast-southwest trend of low-amplitude responses in this seismic attribute map is similar to the trend in the log-derived sandstone thickness map in Figure 3.6.

The particular seismic attribute displayed in Figure 3.10 is the average of the negative reflection amplitudes occurring in a 30-ms window immediately below the Caddo sequence boundary. This seismic analysis window slightly exceeds the thickness of the Caddo sequence, but the average negative amplitude in this data window differs little from the average negative amplitudes calculated in shorter data windows. Other estimates of the Caddo seismic reflection amplitude might be equally as diagnostic of Upper Caddo sandstone thickness as is the parameter displayed in Figure 3.10.

One principal difference between the maps in Figures 3.6 and 3.10 is that the sandstone distribution shown in Figure 3.6 is a computer generated contouring of only 40 (approximately) widely separated data points calculated in the existing control wells, whereas the seismic display is a composite of approximately 30,000 reflection amplitude

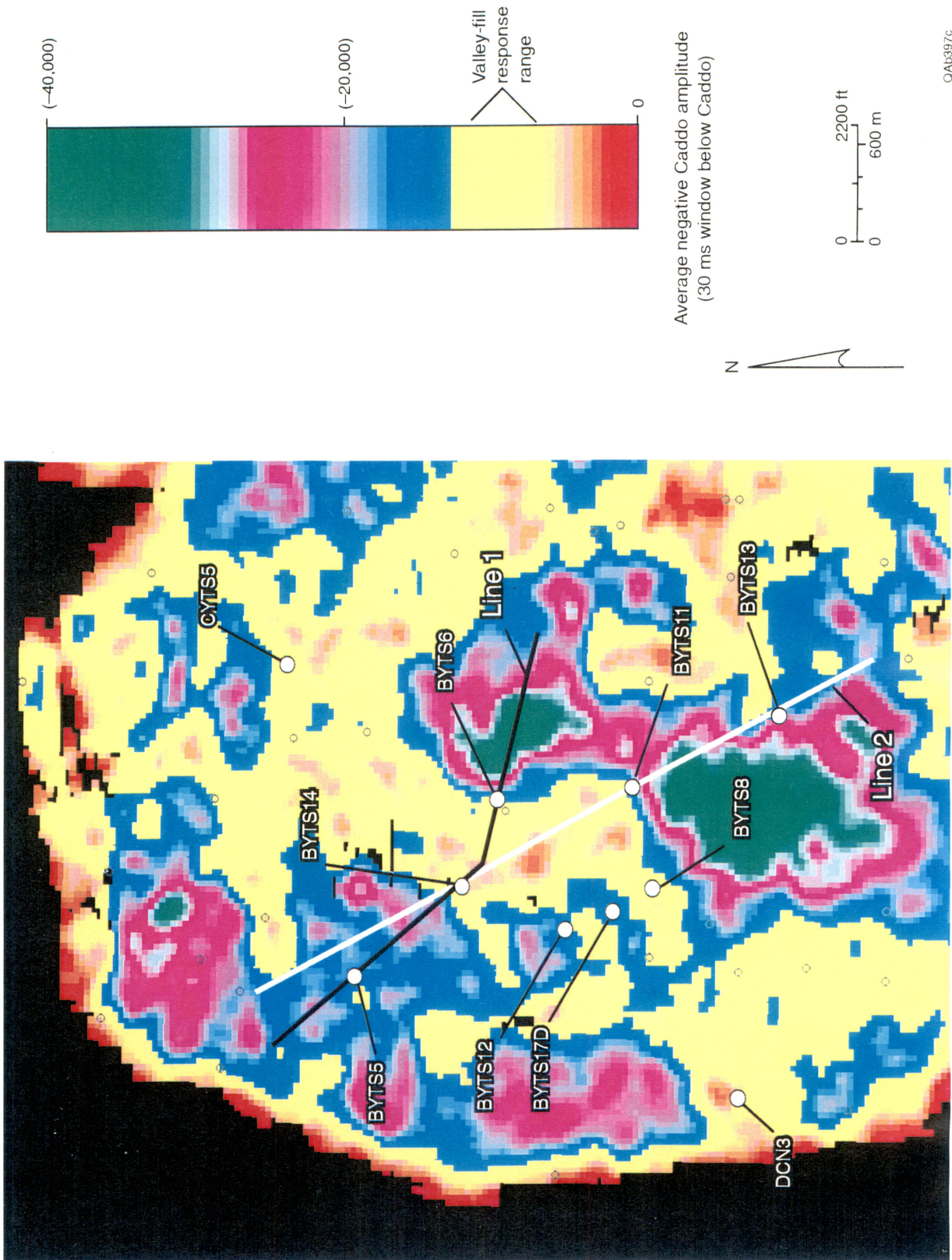


Figure 3.10. Map of a seismic amplitude attribute calculated within the Caddo sequence in the northwest third of the project area. The parameter that is displayed is the average of the negative reflection amplitudes occurring in a 30-ms window immediately below the Caddo sequence boundary (MFS90). The amplitude values coinciding with the yellow portion of the color bar define a trend that is remarkably similar to the valley-fill trend shown in Figure 3.6, implying that seismic reflection amplitude is a reliable indicator of Upper Caddo valley-fill facies in this portion of the study area.

values measured at closely spaced points (that is, stacking bins) occurring at intervals of only 110 ft across the complete map area. Because of this dense spatial sampling, a display of a facies-sensitive seismic attributes (if that seismic attribute map is carefully calibrated to well control!) can be an accurate depiction of the spatial distribution of reservoir facies in the interwell spaces, whereas a well log based map constructed from control points at 80-acre spacing (or greater) is spatially aliased, by definition.

Two profiles, labeled as Line 1 and Line 2, are shown connecting key control wells on the seismic attribute map, and the seismic images along these two profiles are depicted in Figures 3.11 and 3.12. In each profile, that portion of the Caddo horizon where the reflection amplitude undergoes a significant reduction is enclosed by a dashed circle. This **amplitude dimming is a key seismic attribute that maps this particular Upper Caddo valley-fill sandstone**. The relationship between the low reflection amplitude magnitude where the valley-fill reservoir facies occurs and the high reflection amplitude magnitude at other locations on the Caddo sequence boundary where nonreservoir (limestone) facies occur is probably best illustrated by the color bar in Figure 3.10 that defines the parameter range used to display the Caddo seismic reflection attribute. The valley-fill sandstone facies consistently produces a reflection magnitude that is approximately one-fourth the reflection amplitude occurring on the Caddo surface outside of the valley-fill reservoir trend.

Like the previously discussed Lower Caddo example, this Upper Caddo analysis shows that **by carefully calibrating a series of seismic attributes with well control, a key attribute (reflection amplitude, in this case) can often be found that is sensitive to facies changes** within the targeted sequence. Rarely will an interpreter know beforehand which seismic attribute will exhibit the sensitivity that is necessary for identifying facies variations nor what size seismic time window should be used for attribute calculation. These **specific parameters must be determined by trial and error and by careful calibration to control wells**. One problem that confronts interpreters is

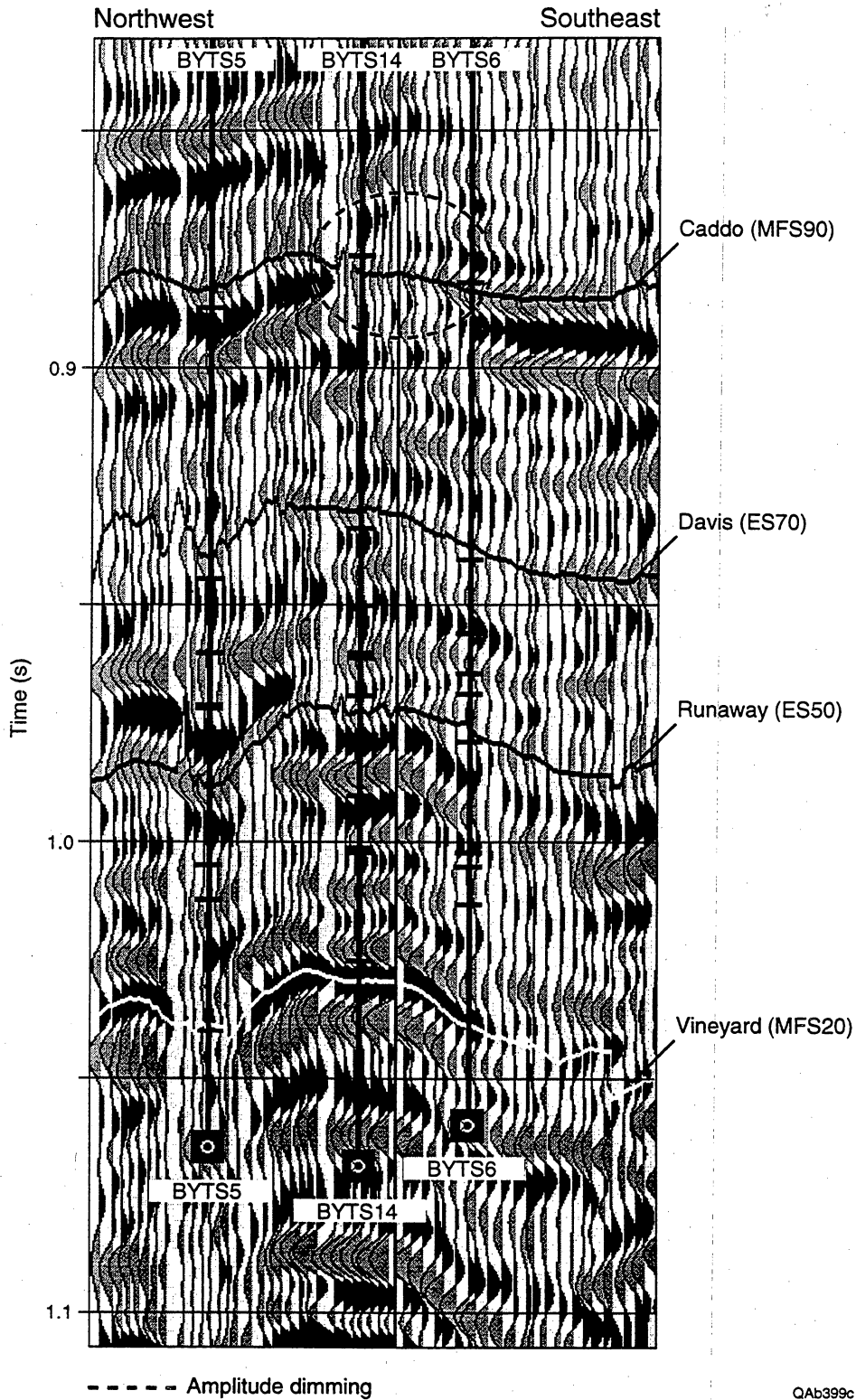


Figure 3.11. Seismic profile along the surface track labeled “Line 1” in Figure 3.10. The amplitude dimming of the Upper Caddo reflection response inside the dashed circle is a key seismic parameter that maps the position of the Upper Caddo valley-fill facies.

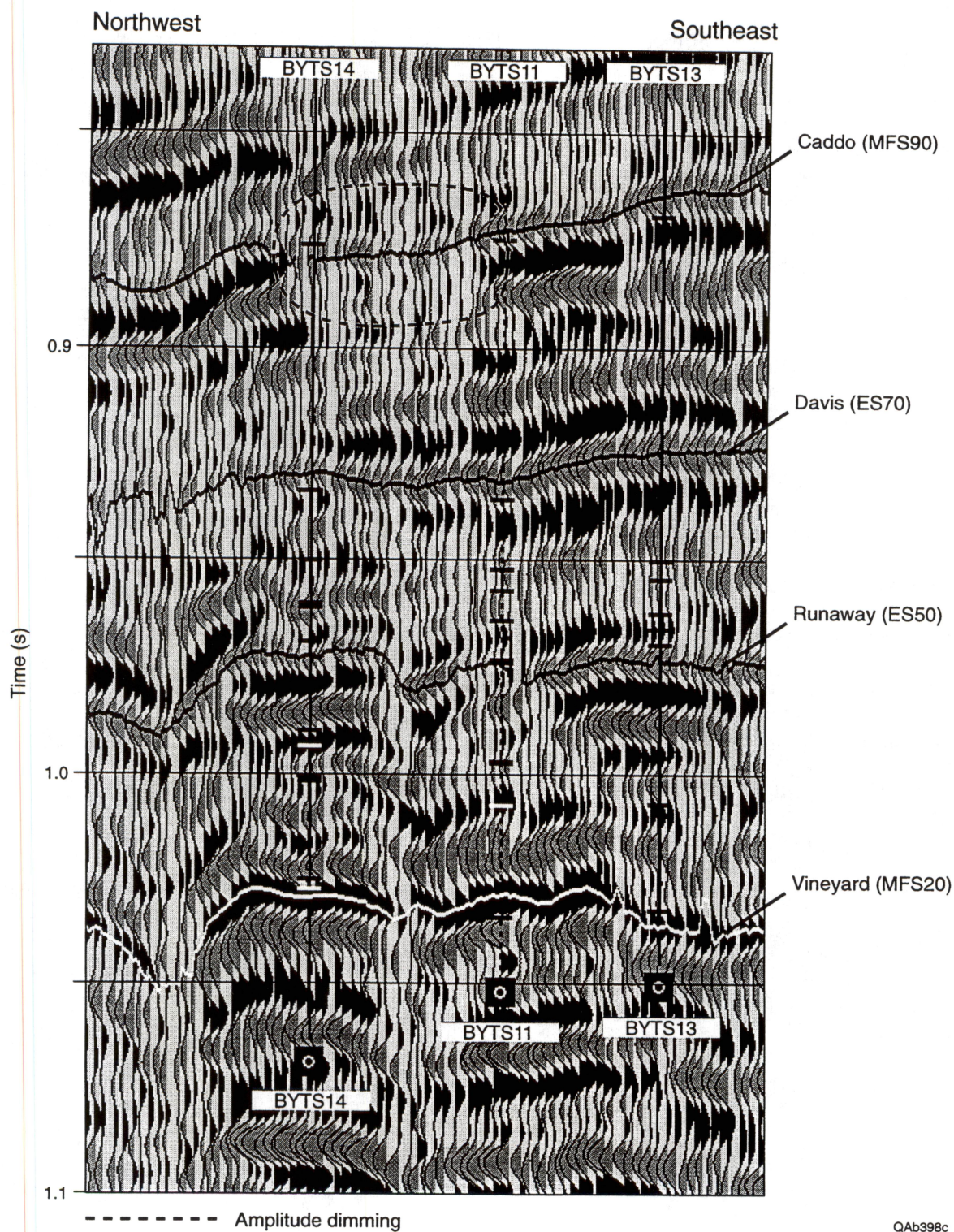


Figure 3.12. Seismic profile along the surface track labeled “Line 2” in Figure 3.10. The amplitude dimming of the Upper Caddo reflection response inside the dashed circle is a key seismic attribute that maps the position of the Upper Caddo valley-fill facies.

that an attribute that exhibits the desired facies sensitivity in one 3-D seismic volume may not do so in another 3-D volume. For example, in the preceding Lower Caddo example, instantaneous frequency was a good seismic attribute for mapping the productive reservoir facies, and the critical frequency range was 75 to 85 Hz (Fig. 3.2). However, if a second 3-D seismic survey had covered the same area and had had an upper signal frequency of only 70 Hz, then instantaneous frequency would not have been an effective mapping parameter for portraying the areal distribution of reservoir facies.

Summary

The Upper and Lower Caddo sequences illustrate the successful application of seismic attribute analysis in identifying the presence of reservoir facies. The apparent correlations between particular seismic attributes and Caddo reservoir facies were obtained by trial and error and by careful calibration to well control. Once such correlations are identified and calibrated, the resulting seismic maps can then be used to identify reservoir facies in interwell spaces and to site infield development wells. The Upper and Lower Caddo were two of the sequences that were most clearly imaged in the Boonsville data set. Other Bend Conglomerate sequences were more difficult to image, as discussed further in Section 5.

4. COMPLEX BEND CONGLOMERATE STRATIGRAPHY CAN LEAD TO SMALL-SCALE RESERVOIR COMPARTMENTALIZATION

One of the best examples illustrating how the complex stratigraphy in the Bend Conglomerate can lead to small-scale reservoir compartmentalization involves several closely spaced wells drilled and completed in the Jasper Creek sequence in the southeast part of the project area. Figure 4.1 shows the location of the four primary wells of interest, the Threshold I. G. Yates 33 (IGY33) and I. G. Yates A9 (IGY A9) wells to the west and the Enserch W. Dewbre 2 (WD2) and W. Dewbre 3 (WD3) wells to the east. What is particularly interesting about this area is that it occurs at the lease boundaries of several operators. As indicated on the map, Threshold's acreage is to the west, Enserch's acreage is to the east, and Mitchell Energy is the operator of the wells immediately to the south (the X's on the map).

Overview and Production History of I. G. Yates 33 Area

In the project area, 72 wells have been completed in one or more of the Jasper Creek sequences. About 75 percent of the Jasper Creek completions are gas productive, but the Jasper Creek does make some oil in the northeast and southeast portions of the project area. Gas recoveries from the Jasper Creek in this vicinity have ranged from as little as 10 MMscf to as much as 3.5 Bscf. Drainage areas calculated for the Jasper Creek range from less than 10 acres to more than 500 acres (see Appendix B of Volume II), so there is quite a range in effective Jasper Creek reservoir size across the project area.

Figure 4.2 is an expanded view of the IGY33 area. In addition to the four wells of primary interest in this discussion, two other offset wells have been completed in the Middle Jasper Creek—the Threshold I. G. Yates 4 (IGY4) and the Mitchell J. M. Robinson A-5 (JMR A5) wells. In the figure, each well completed in the Jasper Creek is designated by a gas symbol. Next to the symbol for each completion is listed the best

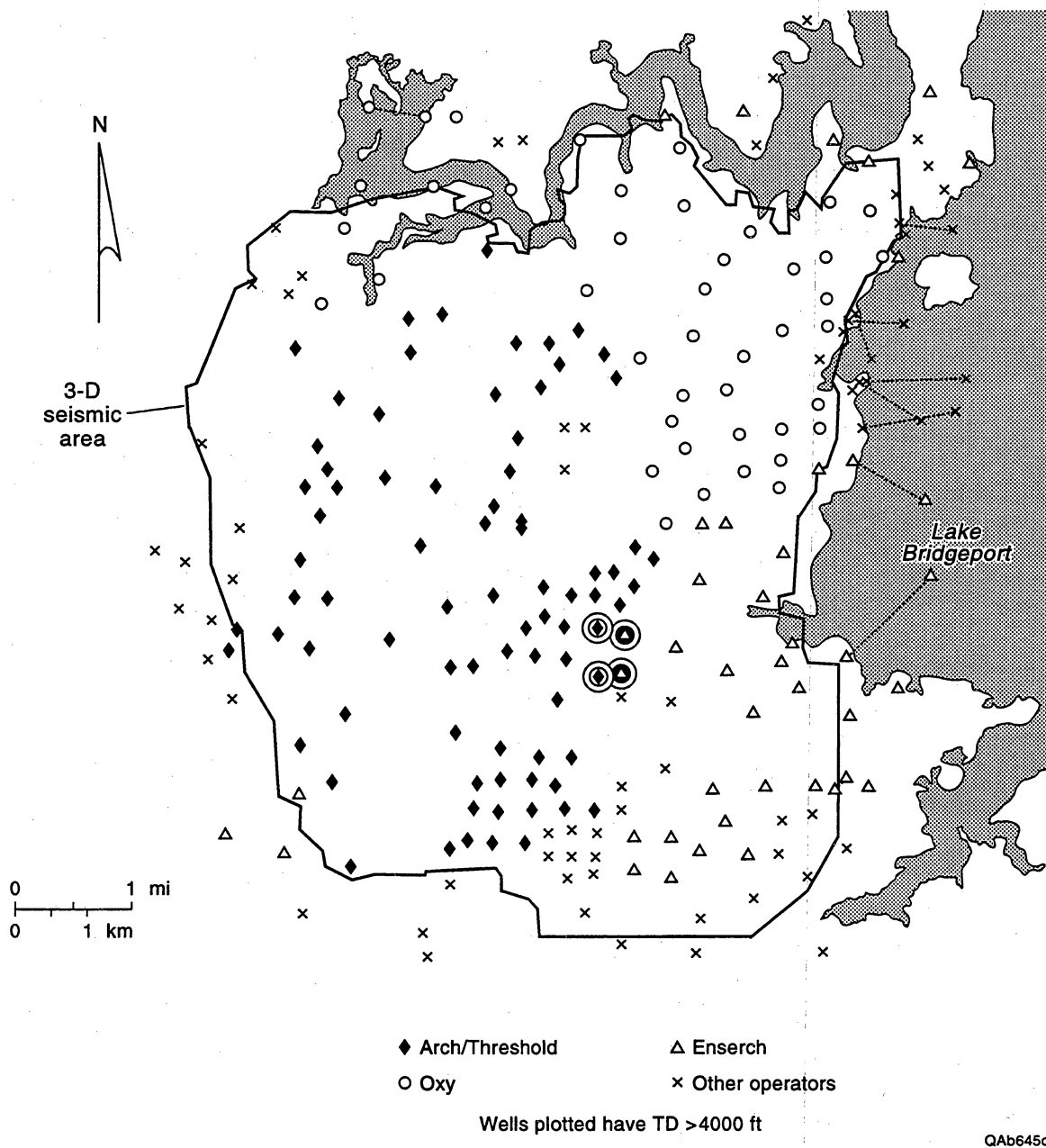


Figure 4.1. Location of several closely spaced Jasper Creek completions in the southeast portion of the project area. Clockwise from the southwest corner, the four wells highlighted on the map are the Threshold I. G. Yates 33 and A9 wells and the Enserch W. Dewbre 2 and 3 wells.

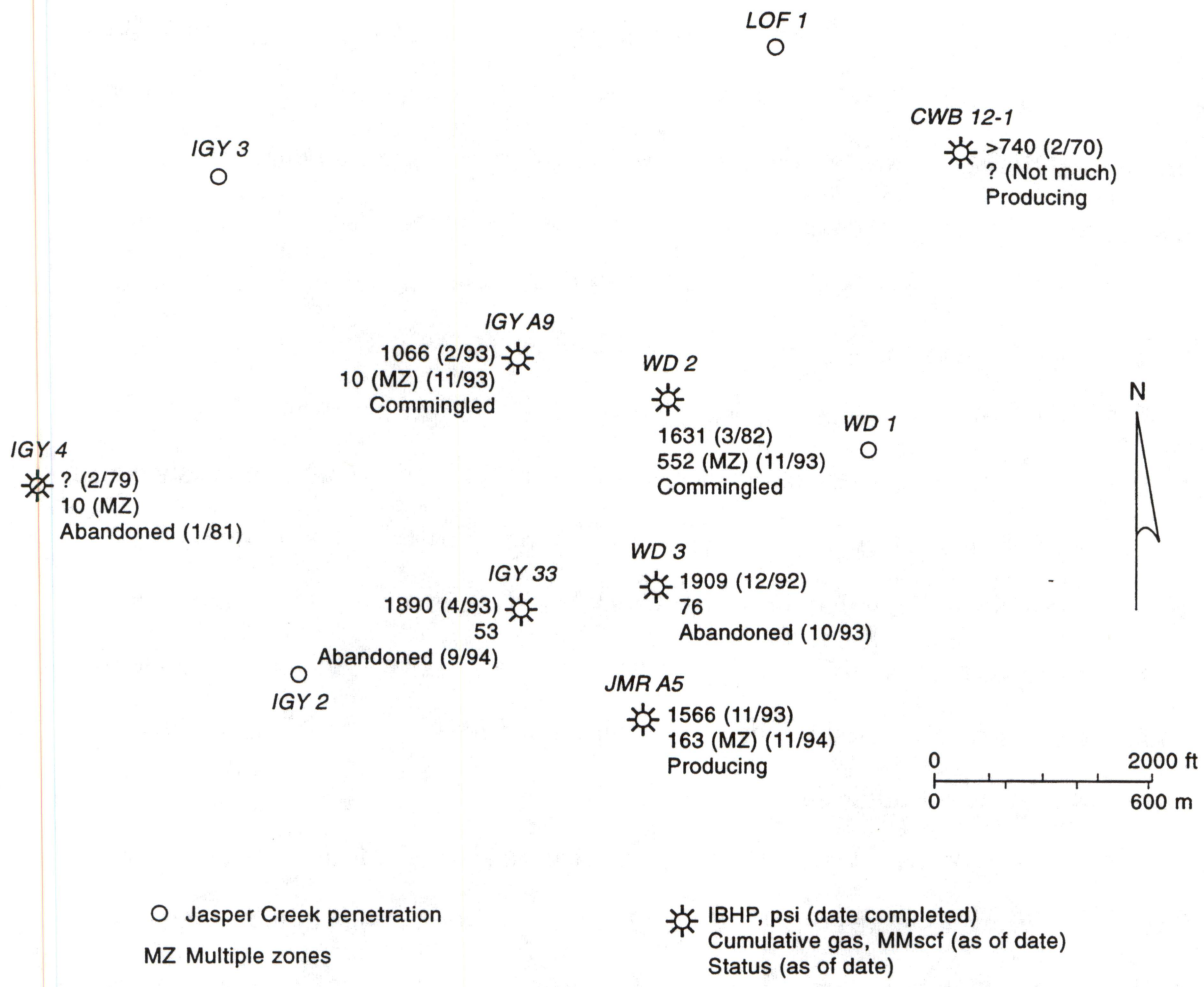


Figure 4.2. Expanded view of the wells presented in Figure 4.1, showing the status of the Jasper Creek completions. Facies code bar is defined in Appendix C.

estimate for initial bottomhole pressure and the date that the Jasper Creek was completed, the cumulative gas produced from the interval, and the current status of the Jasper Creek completion. In some wells, the cumulative production came from multiple zones (in addition to the Jasper Creek); if so, the designation MZ appears after the cumulative production figure. Those wells in the figure shown by open circles penetrated, but were not completed in the Jasper Creek.

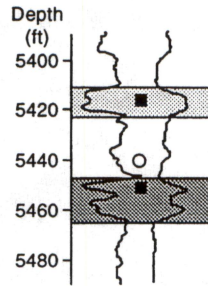
The IGY 4 well produced only about 10 MMscf when recompleted to the Jasper Creek in 1979; this zone was subsequently abandoned in 1981. The Jasper Creek interval in the CWB 12-1 had an initial pressure greater than 740 psi (based on a shut-in surface pressure measurement) when completed in 1970, but this zone would not produce against line pressure on test. Although the zone is still open and part of a commingled Bend completion, it is unlikely that the Jasper Creek has made much gas at this location. The JMR A5 was completed in five different Bend intervals in late 1993 and is producing commingled from all zones; the initial pressure reported is for the well as a whole, not just for the isolated Middle Jasper Creek interval.

Figure 4.3 presents some additional information about the four primary wells of interest. These wells were completed in either one or two intervals in the Jasper Creek; the intervals shown in Figure 4.3 are the Middle and Lower Jasper Creek sequences. As mentioned previously, these wells are fairly closely spaced; the distance between the IGY33 and the WD3 is about 1,200 ft; the distance between the WD2 and the WD3 is about 1,500 ft.

The WD2 well was drilled and completed in the Middle Jasper Creek in March 1982. On completion, the bottomhole pressure in the interval was estimated to be just over 1,600 psi. This zoned tested about 2 MMscf/d initially. The well was completed in two other intervals uphole (both in the Trinity sequence); the Trinity intervals did not test much gas after an acid treatment, and they were not tested separately after a subsequent fracture treatment. All three intervals in the Trinity and Middle Jasper Creek were then

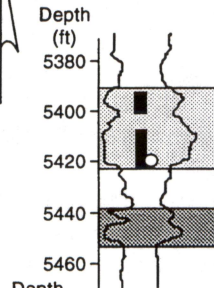
Threshold – I. G. Yates A9

Recompleted: 2/93
 Perforations: 5414–18' and 5450–54'
 IBHP: 1066 psi (PBU)
 Test: 400–500 Mscf/d
 Cumulative: 15 MMscf (11/93)
 Status: Commingled with Caddo (8/93)



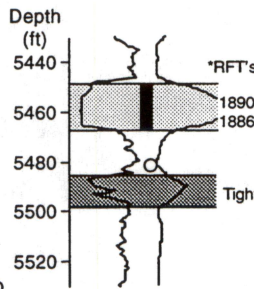
Enserch – W. Dewbre 2

Completed: 3/82
 Perforations: 5394–5400' and 5408–20'
 IBHP: 1631 psi (estimated)
 Test: 2.0 MMscf/d at 600 psi FTP
 Cumulative: 552 MMscf–3 zones (11/93)
 Status: Commingled with Caddo (12/93)



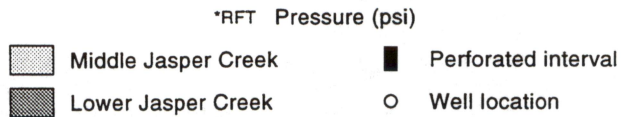
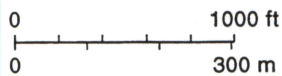
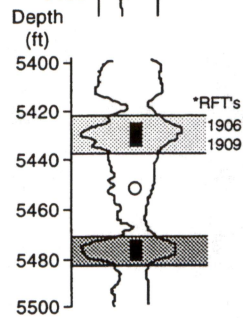
Threshold – I. G. Yates 33

Completed: 4/93
 Perforations: 5449–65'
 IBHP: 1890 psi (RFT)
 Test: 1.8–2.2 MMscf/d at 1200 psi FTP
 Cumulative: 60 MMscf (9/94)
 Status: Abandoned, recompleted to Caddo



Enserch – W. Dewbre 3

Completed: 12/92
 Perforations: 5425–35' and 5473–81'
 IBHP: 1909 psi (RFT)
 Test: 2.2 MMscf/d at 1130 psi FTP
 Cumulative: 76 MMscf (10/93)
 Status: TA; producing uphole in Trinity and Caddo



QAb647c

Figure 4.3. Additional completion and production information on the IGY A9 and 33 wells and the WD2 and 3 wells. Facies code bar is defined in Appendix C.

commingled and produced together. The WD2 produced 552 MMscf from the combined Trinity and Middle Jasper Creek intervals, although it is not possible to determine how much gas came from each interval. In December 1993, the Caddo zone was also commingled with the Trinity and Middle Jasper Creek production.

Almost 10 yr after the WD2 was drilled, Enserch drilled the WD3 well in December 1992. This well was perforated in both the Middle and Lower Jasper Creek intervals. RFT's measured pressures of just over 1,900 psi in the Middle Jasper Creek, which reflects initial pressure in the Jasper Creek sequence, and **it appeared that the WD3 encountered an isolated gas compartment in the Jasper Creek.** This zone tested about 2.2 MMscf/d during a short flow test and came on line making about 1 MMscf/d. Unfortunately the flow rate declined very quickly, and within a few months, the well was making less than 50 Mscf/d. The combined Middle and Lower Jasper Creek intervals produced a total of only 76 MMscf through October 1993, before being abandoned. The well is currently completed uphole in the Trinity and Lower Caddo intervals.

The IGY A9 was recompleted from the Lower Caddo to both the Middle and Lower Jasper Creek in February 1993. The completion interval tested 400 to 500 Mscf/d during a short flow test, but the production from these zones also declined quickly. Within about 6 mo, the IGY A9 was making only 10 to 15 Mscf/d, and through November 1993, the Jasper Creek zones produced only about 15 MMscf. These intervals are now commingled with the original Lower Caddo perforations uphole.

As a result of the encouraging early results from the WD3, Threshold drilled the IGY33 well in April 1993 as a direct offset to the WD3. RFT's run on the IGY33 also recorded pressures of about 1,900 psi in the Middle Jasper Creek, again **suggesting no pressure depletion at this location.** The IGY33 flowed at rates above 2 MMscf/d, without stimulation, during initial flow tests. Unfortunately, as with the WD3 and IGYA9 wells, the production from this zone declined very quickly. The IGY33 came on line making 2 MMscf/d but declined to less than 50 Mscf/d in 2 to 3 mo. This zone also made

a few barrels of oil per day as well, and a pumping unit was installed to help lift the liquids. The Middle Jasper Creek **made only about 60 MMscf of gas before being abandoned** in September 1994; the IGY33 is currently producing from the Caddo uphole.

The results from the WD3 and IGY33 wells suggested that isolated, but very small, reservoir compartments were encountered in each well. More detailed geologic and engineering analyses were conducted to determine the most likely cause of the reservoir compartmentalization.

Geological Analysis of I. G. Yates 33 Area

The Jasper Creek interval is a thick, erosion-surface-bounded sequence that consists of four subsequences, each one of which contains sinuous belts of reservoir sandstone (Figs. A27 and A28 of Appendix A, Volume II). The Jasper Creek represents an intermediate relative accommodation example in the comparative examination of reservoir types found within Bend Conglomerate sequences. **Intermediate relative accommodation type reservoirs are the most attractive targets for future gas reserve growth because they are highly compartmentalized and thus likely to contain untapped reserves.** Reservoir compartments in the Jasper Creek sequences are mostly surface-bounded valley-fill deposits, with varying degrees of internal facies- and cement-bounded barriers.

The example discussed here illustrates a surface boundary between a fluvial valley-fill sandstone reservoir and a transgressive shoreface reservoir sandstone, the lowstand and transgressive systems tracts, respectively, of the Middle Jasper Creek sequence (MFS34–FS32). Well control allows confident interpretation of two separate sandstone bodies, yet there may be additional, finer scale facies changes and diagenetic cementation causing further compartmentalization that cannot be detected using present technologies.

Stratigraphic cross sections (Figs. 4.4 and 4.5) contain standard well log curves and (calculated) facies interpretations of the Middle Jasper Creek sequence. Thick sharp-based sandstones overlying the ES34 surface in the WD2 and IGY33 wells are interpreted to be fluvial valley-fill deposits. A core collected from the IGY33 (Fig. A33 of Appendix A, Volume II) Middle Jasper Creek reservoir sandstone has characteristics of a typical fluvial channel-fill deposit. A crossbedded sandstone sharply overlies fossiliferous (sponges, brachiopods, echinoderms) marine mudstone (facies B) and contains an upward-fining grain-size trend that changes from a basal gravel to very fine sand at the top of the unit. The gamma-ray and resistivity log curves track the grain-size trend faithfully (Figs. 4.4, 4.5, and A38). Sedimentary structures decrease in scale and imply paleoenergy levels that vary from trough crossbedding to planar-tabular beds, which are capped by parallel laminations and current-ripple stratification.

Measured permeabilities of several hundred millidarcys are unusually high for the Bend Conglomerates (Fig. A33, Appendix A, Volume II). Many values exceeding 100 md occur, and one core-plug analysis data point measured 2.7 darcys. Visual examination of the slabbed core provided an answer to this anomalous situation: vuggy secondary porosity resulting from dissolution of pebble-sized clasts (K-feldspar and chert) has greatly enhanced permeability. All Bend Conglomerate sandstones observed from core samples displayed this secondary porosity; however, the degree of porosity enhancement in the IGY33 core far exceeded the typically minor effect seen in other cores.

Figure 4.6 shows the net reservoir sandstone distribution of the Middle Jasper Creek, which displays a sinuous ribbonlike pattern. Log curve patterns superimposed on the net reservoir sandstone map have patterns similar to those observed in the IGY33 (albeit a thinner sandstone was penetrated), suggesting a genetic kinship, namely a fluvial depositional environment.

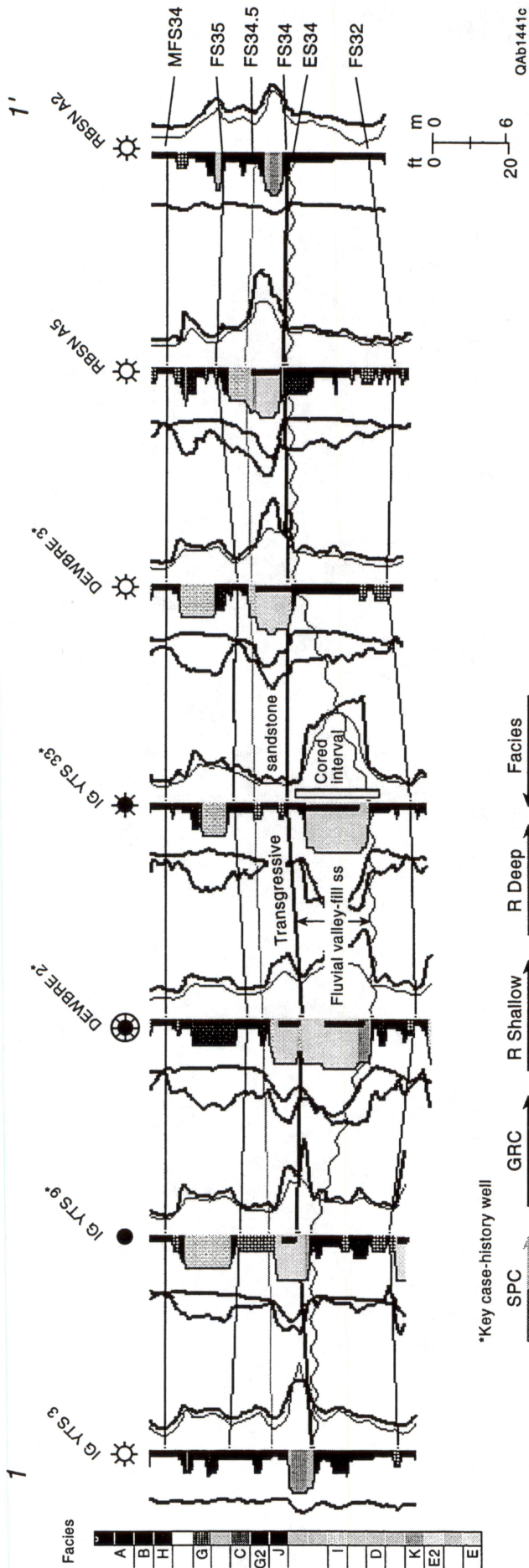


Figure 4.4. Middle Jasper Creek log cross section and facies interpretation spanning the IGYTS 33 well. These data are from profile 1-1' shown in Figures 4.6 and 4.7. See Appendix C for explanation of facies code bar.

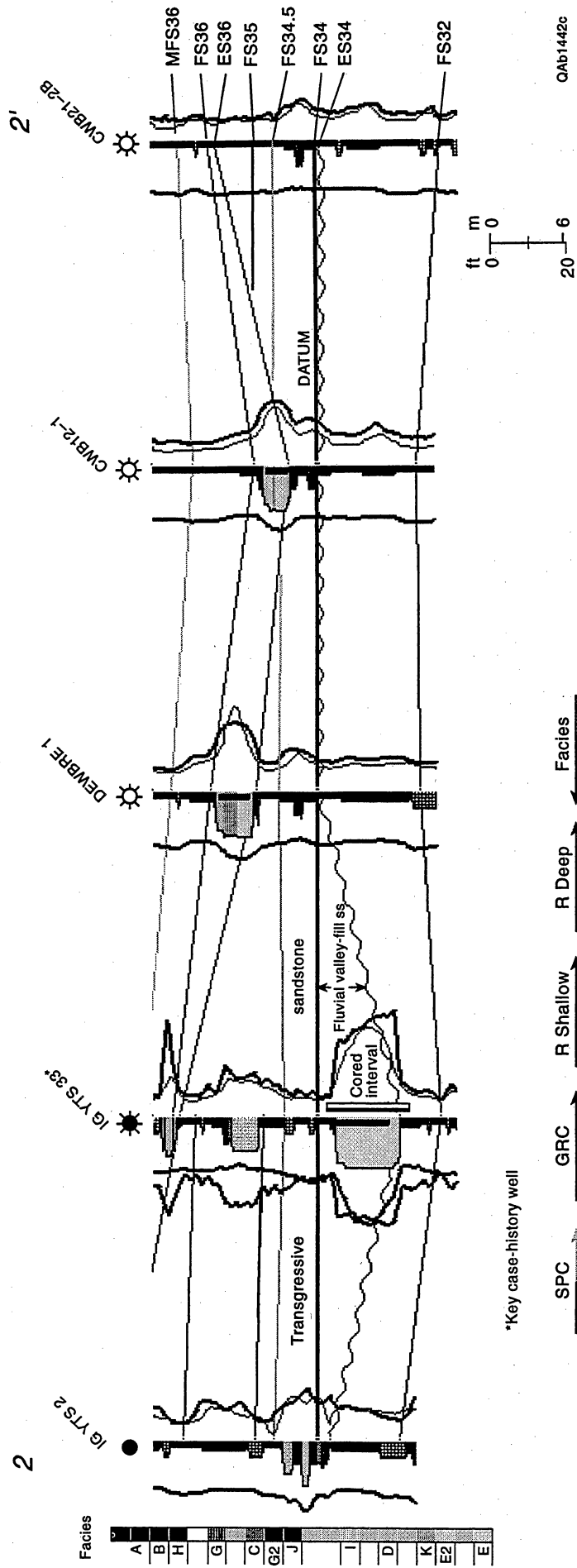
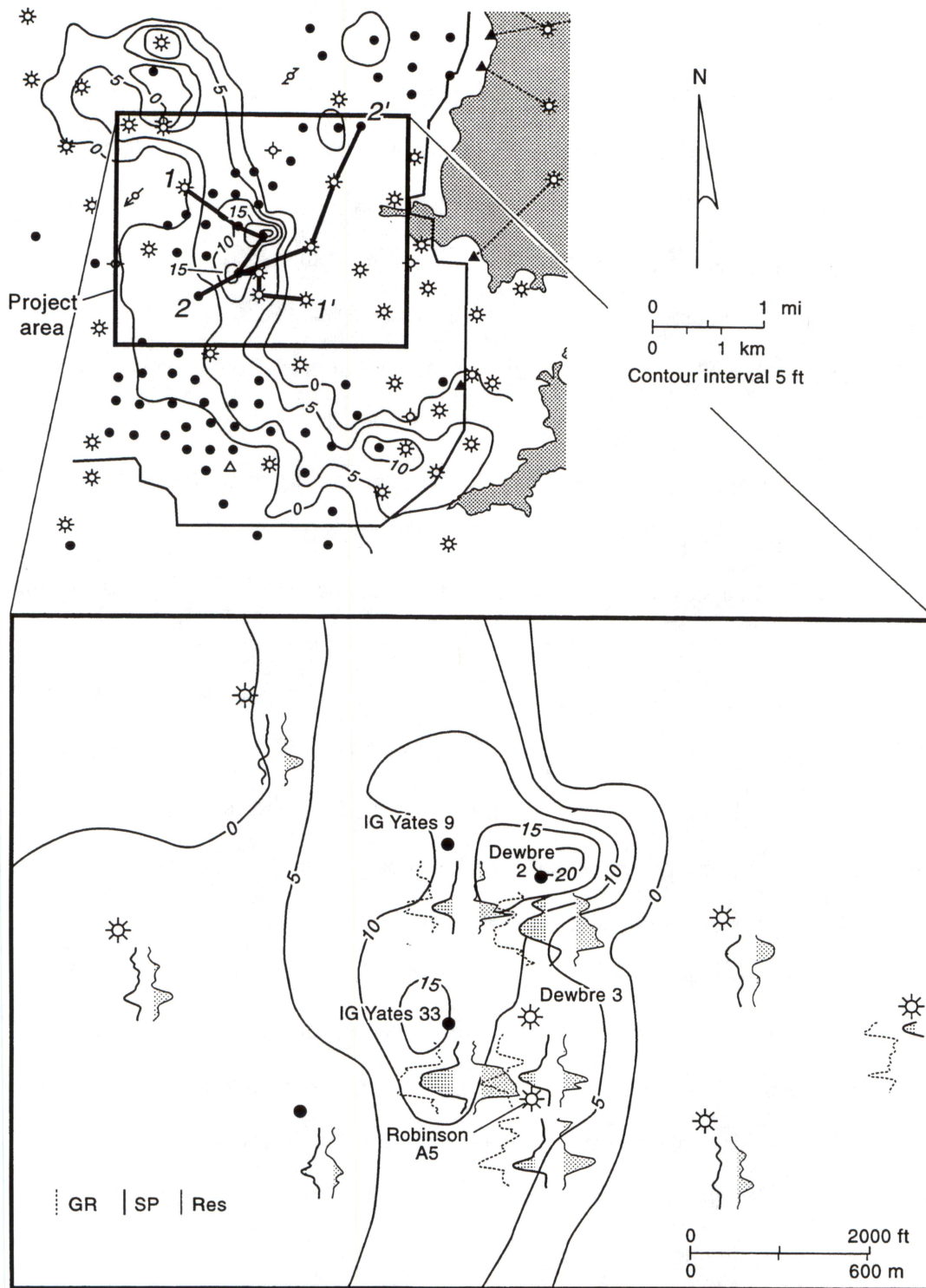


Figure 4.5. Middle Jasper Creek log cross section and facies interpretation spanning the IGYTS 33 well. These data are from profile 2-2' shown in Figures 4.6 and 4.7. See Appendix C for explanation of facies code bar.



GR | SP | Res

- Oil well ▲ Service well ⚡ Temporarily abandoned producer
- ☆ Gas well ▲☆ Deviated well ⚡ Injection well
- ⊕ Dry hole

QAb1443c

Figure 4.6. Middle Jasper Creek net reservoir sandstone.

The superposition of high-energy fluvial facies upon truncated marine-shelf mudstones suggests that the ES34 surface is an unconformity surface that represents a subaerial exposure event. During the base-level lowstand, the sinuous valley was cut by fluvial processes; aggradation of fluvial sands followed as the base level began to rise. Reservoir quality fluvial sands were deposited and preserved in the most deeply incised parts of the valley. Crossbed dip orientations from FMS data collected from the IGY33 (Middle Jasper Creek sandstone) indicate a southwestward sediment transport.

Subsequent transgression, marked by the FS34 surface, appears to have ravined the upper surfaces of the lowstand tract (Dewbre 2 well; Fig. 4.2), and a thin (<10 ft) transgressive shoreface sandstone was deposited. Middle Jasper Creek strata above the FS34.5 boundary represent a mixed terrigenous clastic and carbonate marine shelf. The transgressive shoreface sandstone is permeable, and it has produced gas from the IG YTS9, Dewbre 2 (WD2), Dewbre 3 (WD3), and RBSN A5 wells, but although the sandstone body is widespread, reservoir quality sandstones within it comprise a thin strip (Fig. 4.7). Perhaps they represent a clean shoal sandstone deposited on the margins of subtle paleohighs located on the east bank of the valley (Fig. 4.8).

Core was collected from the Enserch J. D. Craft-Water Board 3, Middle Jasper Creek transgressive unit (in the southeast corner of the project area), which has a sharp base and a coarsening-upward grain-size trend. The sandstone contains abundant CaCO_3 cement, and it is highly fossiliferous. The sharp base marks a significant facies dislocation, but unlike the IGY33 deposit, all of these features are consistent with a transgressive shoreface interpretation.

The evidence presented thus far clearly documents a **surface-boundary mechanism for stratigraphic compartmentalization** of the Middle Jasper Creek zone between the IGY33 and WD3 wells. If a stratigraphic boundary does in fact exist between the thick, lowstand fluvial sandstones penetrated by the IGY33 and WD2 (Fig. 4.4), finer scale mechanisms beyond the data resolution must be called upon to explain it. Two

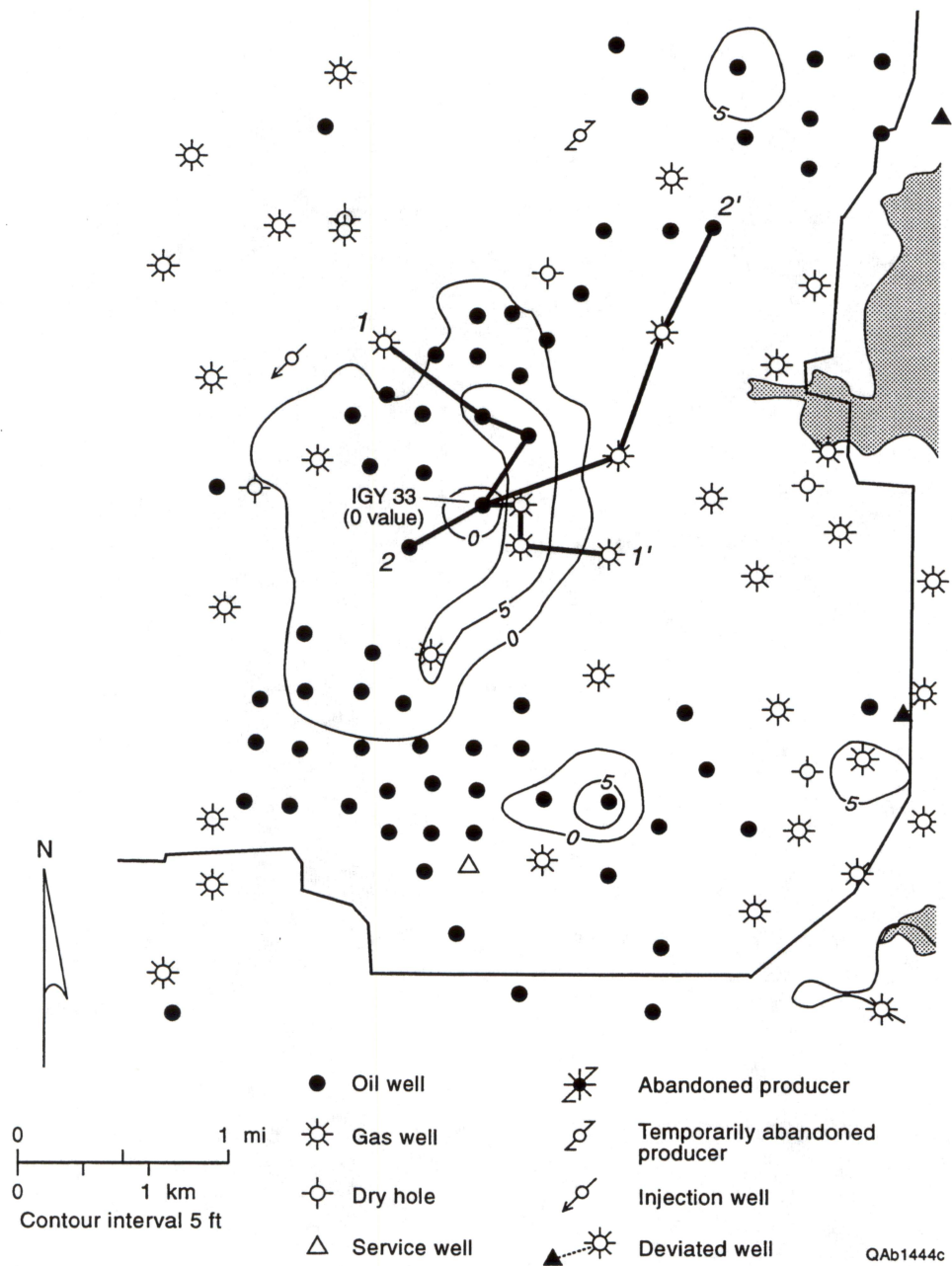


Figure 4.7. Net reservoir of Middle Jasper Creek transgressive systems tract (FS34.5-FS34).

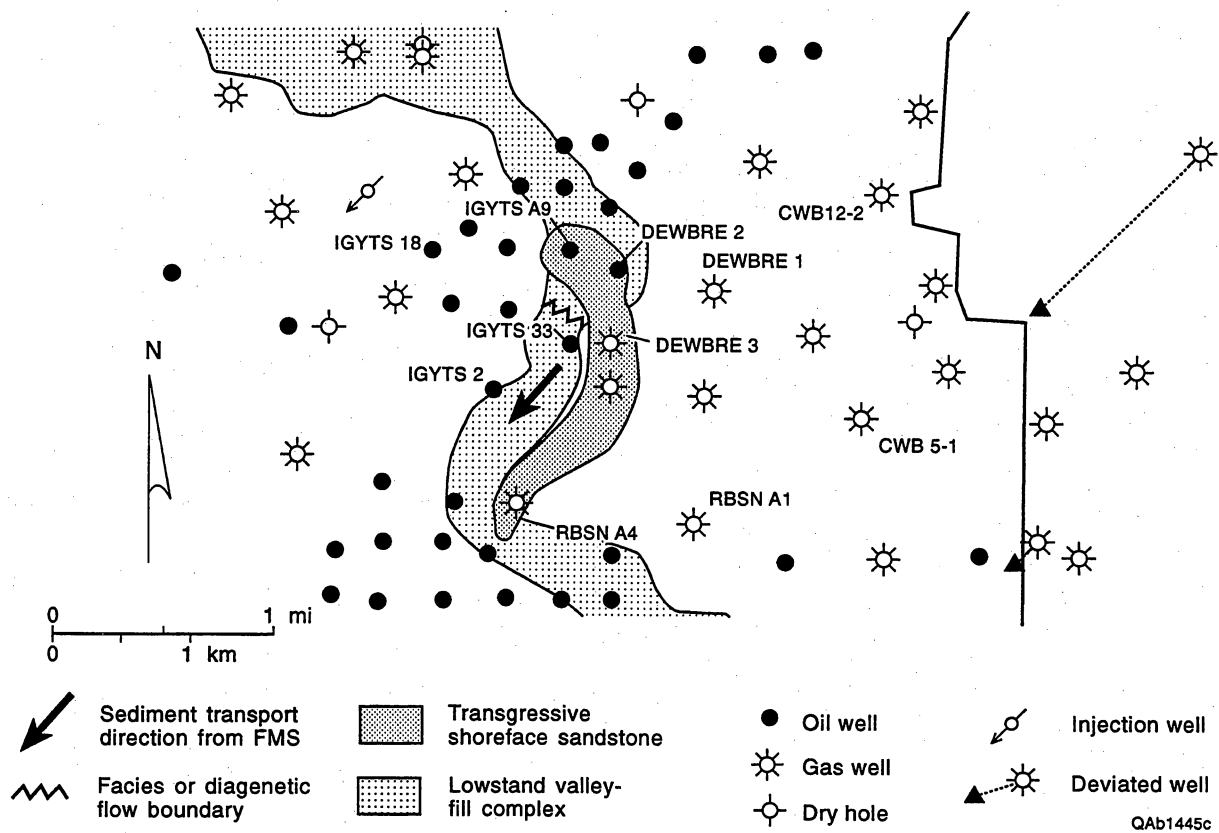


Figure 4.8. Middle Jasper Creek interpretation, net reservoir sandstone.

possibilities are that (1) the thick sandstones represent separate meander-bend pods, similar to point bars, and the high-energy reservoir facies are thus not continuous between the wells, and (2) a diagenetic cement barrier exists between the wells. The high degree of secondary dissolution porosity observed in the IGY33 core indicates a large amount of postdepositional chemical activity. Some of this dissolved material may have been redeposited such that a cement barrier exists between the wells.

The IGYA9 penetrated the Middle Jasper Creek transgressive sandstone unit, which appears to be continuous with the WD2 reservoir; this sandstone may have been at least partly depleted by the WD2. Pressure data measured on the IGYA9 well suggest, but cannot confirm, that communication between the IGYA9 and WD2 wells is possible.

Overall, commingling of zones and ambiguous pressure data make it difficult to assess reservoir communication between wells, with the exception of the IGY33 and WD3 reservoirs, which are stratigraphically compartmentalized—two separate sandstone reservoir bodies that were deposited at different times, in different systems tracts, and were penetrated by the respective wells; pressure and well-test data support this interpretation as indicated in the engineering analysis that follows this discussion.

Geologic analysis of well control suggests that the transgressive sand unit penetrated by the IGYA9, WD2, JMR A5 and WD3 may be connected in all wells. Again, however, the commingling of multiple producing zones and the ambiguity of the available pressure data make this suspected communication difficult to confirm.

Engineering Analysis of I. G. Yates 33 Area

Figure 4.9 is a plot of initial pressures in the Jasper Creek measured from wells in the project area over time. The values of initial pressure measured for the IGY33 and the WD3 wells are similar to those reported in wells drilled and completed since the 1950's. Note, in each case, that the pressures reported are the best estimates that could be obtained for particular wells using available data sources (both operator and public

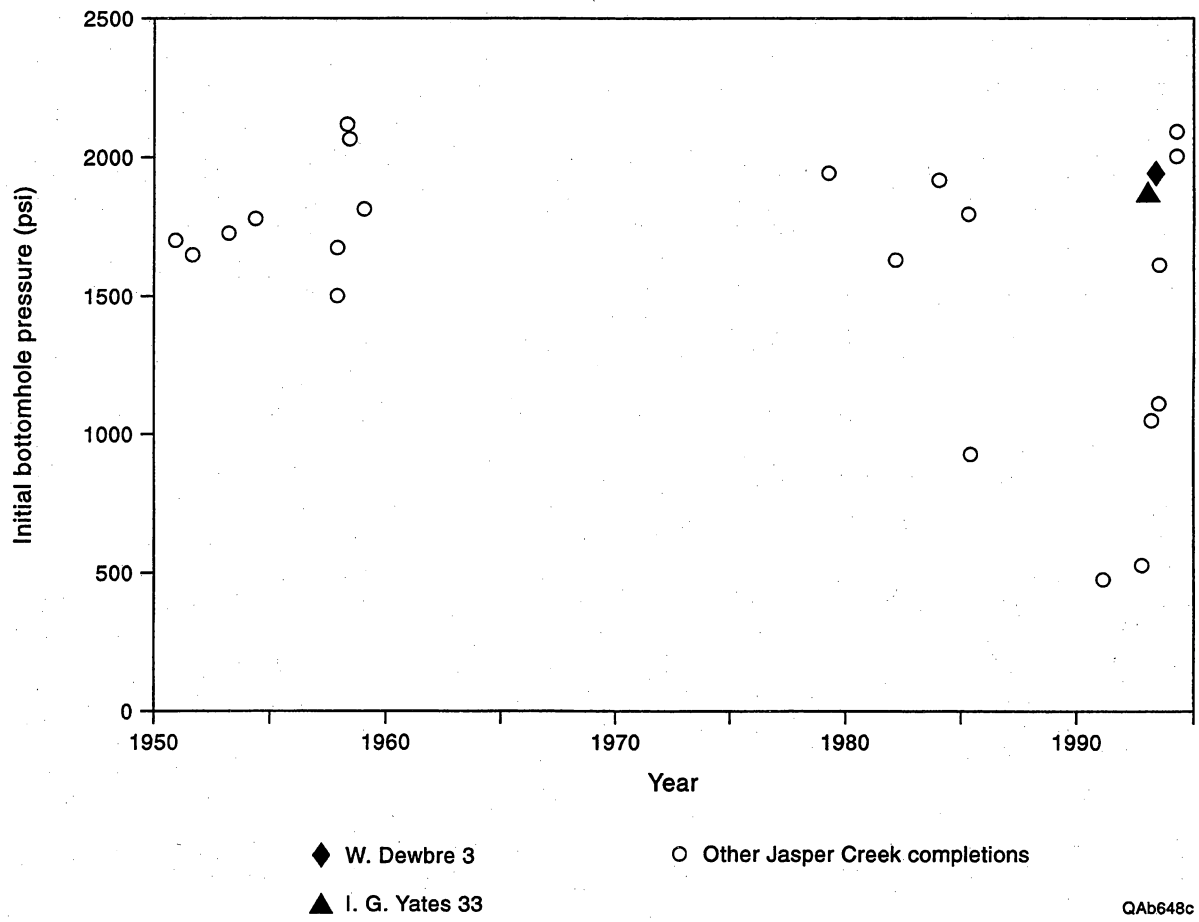
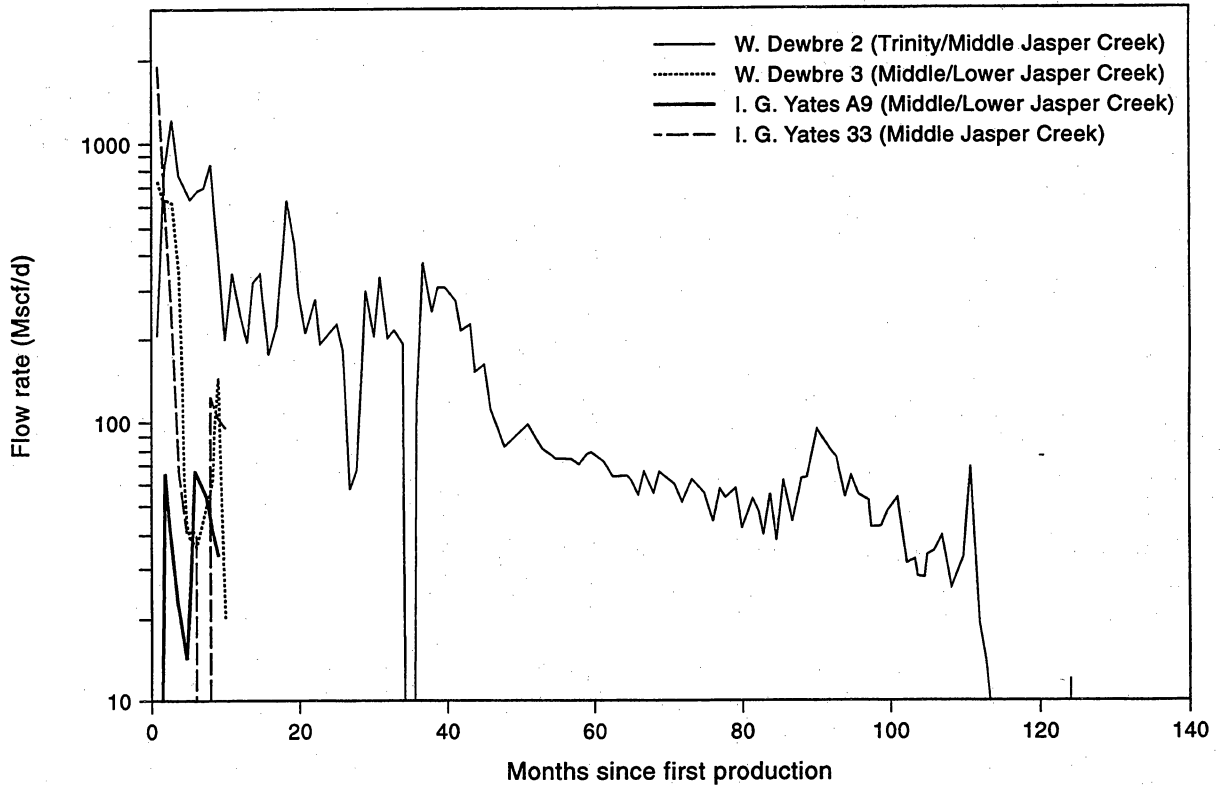


Figure 4.9. Comparison of initial pressures measured in the IGY33 and WD3 wells to initial pressures reported in other Jasper Creek completions.

domain records). This figure suggests that the IGY33 and WD3 encountered original pressure in the Jasper Creek.

Figure 4.10 presents a comparison of production from these four offsetting Jasper Creek completions. As mentioned previously, the WD2, WD3, and the IGY33 wells all tested the Jasper Creek at rates of about 2 MMscf/d initially, but production from the WD3 and IGY33, as well as the IGY A9, declined very rapidly. The WD2 well showed a more typical decline with time, but the data presented in Figure 4.10 reflect commingled production from both the Trinity and the Jasper Creek. Because production from the WD2 has always been commingled, it is not possible to separate the contributions of the Trinity and Jasper Creek intervals. Given the performance of the offsetting Jasper Creek completions, it appears likely that much of the gas produced by the well may have come from the Trinity interval, with the Jasper Creek being a high-productivity, but low volume contributor to the overall production of the well. If most of this gas was produced from the Jasper Creek, however, the Middle Jasper Creek in the WD2 does not appear to have been in communication with the Jasper Creek intervals at the IGY33 and WD3 locations.

Several pressure buildup tests were run on the IGY33, WD3, and IGY A9 wells. Table 4.1 summarizes key results from the test analyses. These buildup tests show considerable variability in reservoir quality over this small area within the Jasper Creek, with permeabilities varying from 28 md in the IGY33 to 0.2 md in the IGY A9. Notice, too, how rapidly reservoir pressure declined in the IGY33 and WD3 wells over a short time period. Tests conducted in the IGY33 well showed a drop in average reservoir pressure of about 1,300 psi in just 4 mo, after only about 40 MMscf of gas had been produced. Likewise, reservoir pressure in the WD3 declined from approximately 1,900 psi to about 700 psi in just 8 mo, after only about 70 MMscf had been produced. Both wells were apparently draining high-productivity, but low-volume Jasper Creek



QAb649c

Figure 4.10. Production histories from the IGY A9 and 33 wells and the WD2 and 3 wells.

reservoirs. Drainage areas of 8 and 20 acres were estimated for the IGY33 and WD3 wells, respectively.

Table 4.1. Summary of well test results in I.G. Yates 33 area.

Well	Test date	k, md	s'	\bar{p} psi	Remarks
I. G. Yates 33	4/93	—	—	1,890	RFT pressure
	4/93	28	+2	1,560	After 7 MMscf produced
	8/93	28	-2	~600	After 42 MMscf produced
Dewbre 3	12/92	—	—	1909	RFT pressure
	8/93	2	+3	~700	After 71 MMscf produced
I. G. Yates A9	2/93	0.2	-3	1,066(?)	Highest pressure measured

In addition to providing estimates for average pressure and reservoir quality, the wells tests also provided insight into the size and shape of the Jasper Creek reservoirs. An example illustrating this type of detailed analysis is shown in Figures 4.11 and 4.12. These figures present the analysis of the first pressure buildup test conducted on the IGY33 well in April 1993. The well flowed for about 4 d before being shut in for this 3-d buildup test.

Figures 4.11 and 4.12 show the log-log and semilog plots prepared to interpret the test data. In the log-log plot shown in Figure 4.11, both the change in pressure and its derivative are plotted versus "time since shut-in" on a log-log scale. In this figure, adjusted pressure change versus equivalent adjusted time is actually plotted. These plotting functions are similar to actual pressure and time but include the corrections necessary to account for changes in gas fluid properties with time (Al-Huissany and others, 1966; Agarwal, 1979; Lee, 1986). The equivalent time correction allows the use of drawdown type curves to analyze buildup test data (Agarwal, 1980).

The earliest data are approximately unit-slope, suggesting a very brief period of wellbore storage. The flattening of the derivative curve at an equivalent adjusted time of about 0.1 h indicates the beginning of pseudo-radial flow, when a straight line would be expected on the semilog plot whose slope is inversely proportional to permeability. The

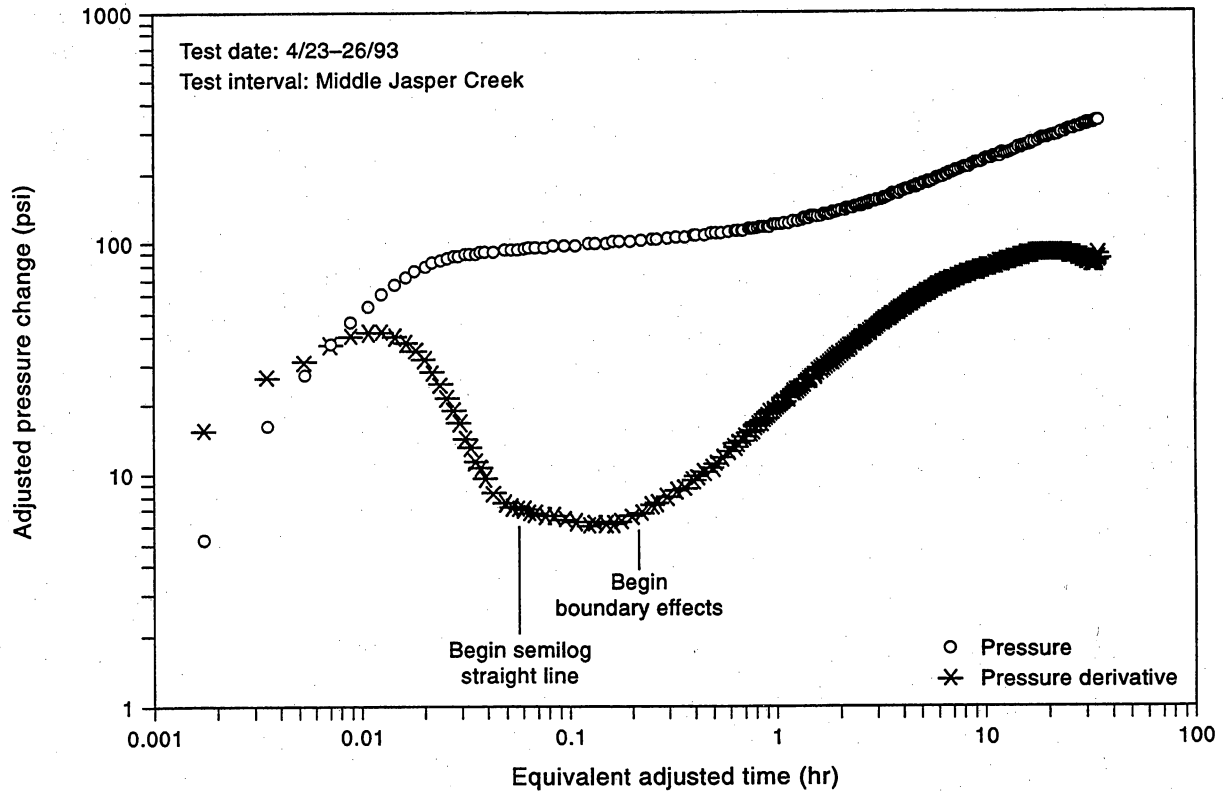


Figure 4.11. Log-log plot of test data from the April 1993 pressure buildup test conducted in the IGY33 well.

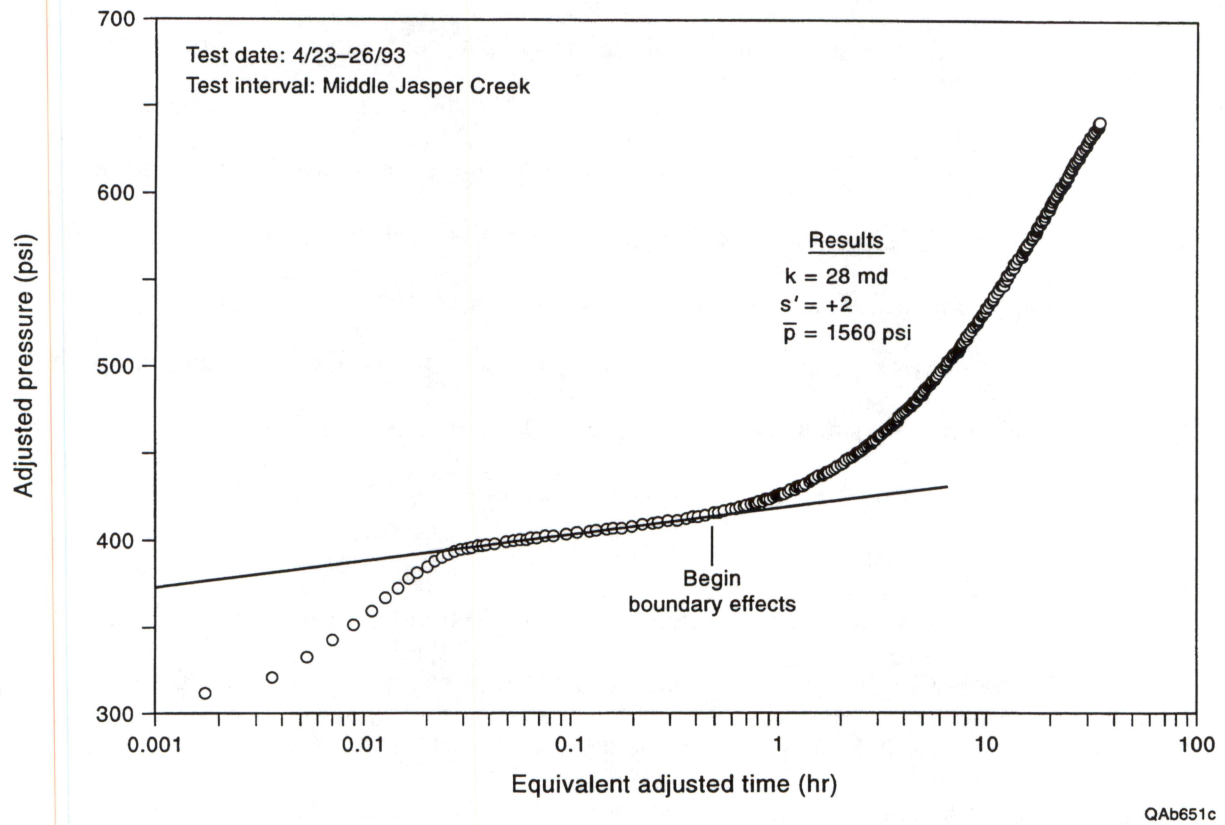


Figure 4.12. Semilog analysis of the April 1993 pressure buildup test conducted in the IGY33 well.

fact that the derivative flattens like this so early in the test suggests a high-permeability sand. The sharp upturn in the pressure derivative data at a time of about 0.3 h indicates that a near-well boundary has been encountered, although not all boundaries have yet been felt. The flattening and subsequent decline in the pressure derivative data during the later stages suggest that all reservoir boundaries may have been encountered during the test.

Figure 4.12 is the semilog plot of the test data. Using the slope of the straight line shown in the figure, a permeability of 28 md was calculated for the Middle Jasper Creek reservoir. This permeability was higher than generally observed for the Bend intervals in this area (permeabilities of 0.1 to 5 md are more typical), but this value is consistent with the abnormally high values measured from core analysis in this well. In addition, as Table 4.1 shows, the same permeability was also calculated from the second pressure buildup test run in August 1993.

Figure 4.13 presents a history-match of the pressure buildup test generated by a reservoir simulator. Although several different reservoir descriptions were tried, the best match of the actual test data was obtained using a long, narrow (16×1) rectangular-shaped reservoir, with the well located near one end of the drainage area. The permeability used in generating the simulated test data was 28 md, the same value calculated from the conventional analyses shown in Figures 4.11 and 4.12. The total reservoir size was about 8 acres. This high-permeability, rectangular-shaped sand body, as deduced from the well test analysis, was considered consistent with the geologic interpretation of the Jasper Creek reservoirs in this immediate vicinity. Whether this rectangular reservoir shape represents a point-bar-type sandstone deposit or whether it is an artifact of diagenesis cannot be deduced from the well test data.

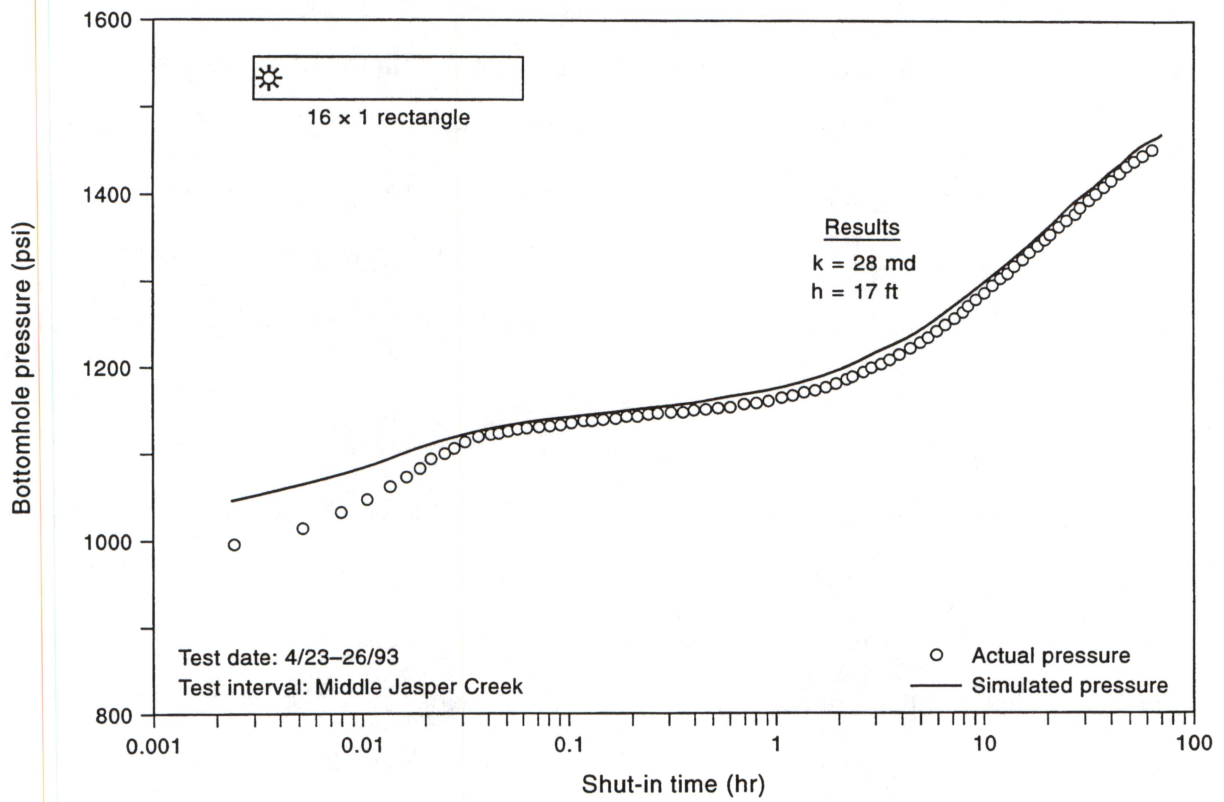


Figure 4.13. History match of the April 1993 pressure buildup test conducted in the IGY33 well.

Seismic Interpretation of I. G. Yates 33 Area

The Boonsville 3-D seismic data confirm that the Jasper Creek sequences are heterogeneous in the vicinity of the IGY33 well. For example, an east-west seismic profile passing through the WD3 and IGY33 wells is displayed in Figure 4.14, and the positions of the Middle Jasper Creek reservoirs associated with the ES34 erosion surface at each well are indicated by a bold horizontal dash on each well profile. In this section view, the Middle Jasper Creek interval appears to consist of shingled clinofolds that propagate westward locally, and each clinofold seems to be segmented into narrow, disjointed reflection units, implying that each depositional cycle has considerable lateral heterogeneity.

A laterally continuous reflection event immediately above the ES34 boundary was chosen as a local flattening surface (see Figure 4.14 for the identification of this reference surface), and numerous horizon views through the Middle Jasper Creek interval, each horizon being conformable to this flattening surface, were extracted from the 3-D seismic data volume. One of these horizon slices, which passed close to the ES34 picks shown at the IGY33 and WD3 wells, is displayed in Figure 4.15. The data that are displayed are reflection amplitude, positive amplitudes shown in red and negative amplitudes in blue. This map view shows that in the area of the targeted four-well complex (IGY9 and 33, WD2 and 3), that the seismic reflection polarity of the Middle Jasper Creek sequence changes abruptly across the surface, creating small, isolated areas of distinct seismic reflection facies. These lateral changes in reflection polarity suggest that lateral variations of rock facies exist across the interpreted horizon; some of these rock facies boundaries probably also create reservoir compartment boundaries.

The seismic data in Figure 4.15 indicate that the Middle Jasper Creek interval in the immediate vicinity of the IGY9, IGY33, WD2, and WD3 wells is highly heterogeneous, and this evidence, in turn, implies that individual reservoir

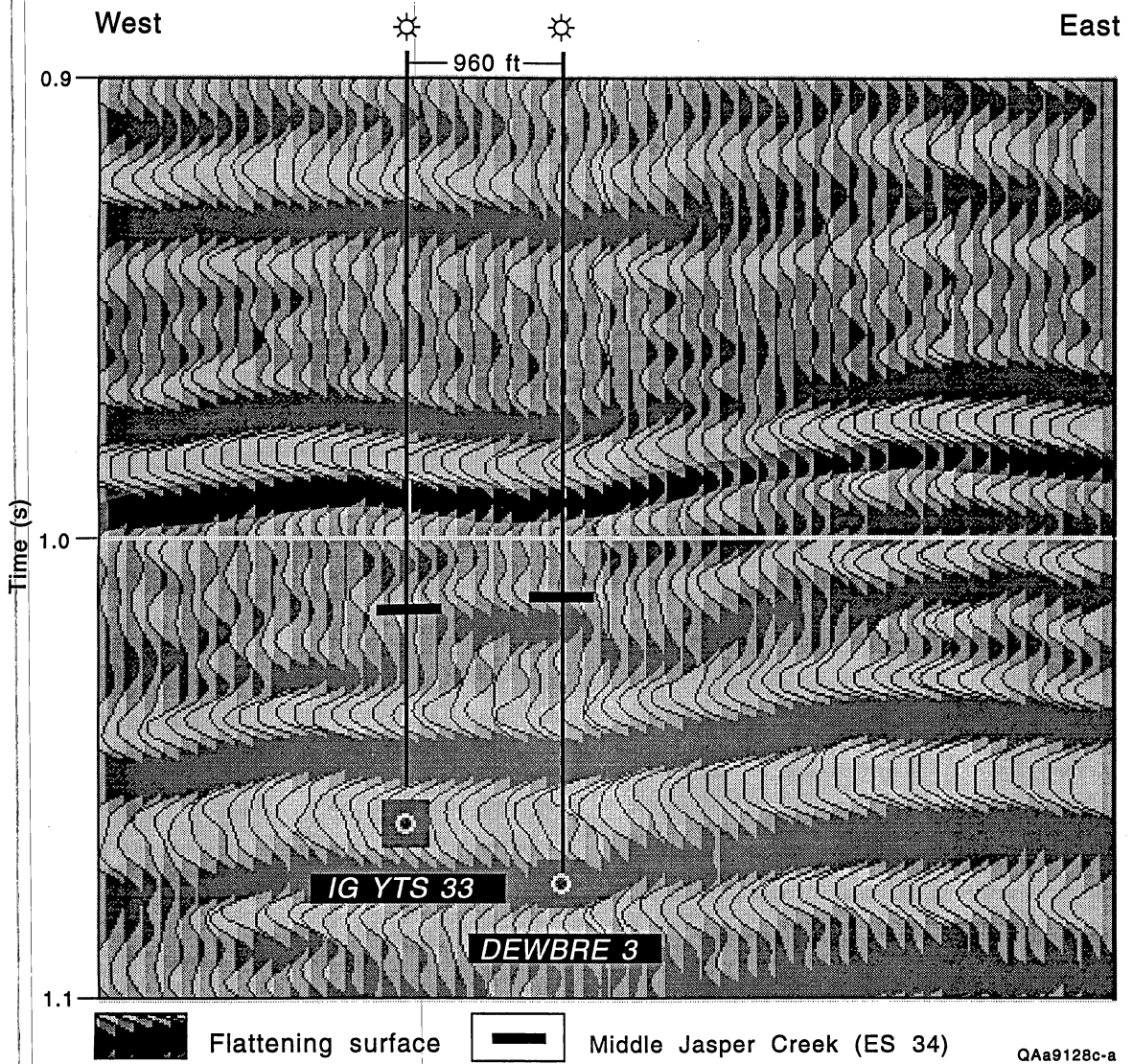


Figure 4.14. Section view showing seismic heterogeneity associated with Middle Jasper Creek reservoirs near IGYTS 33 and Dewbre 3 wells. The ES34 erosional surface at these two well locations is positioned in an interval of west-prograding clinoforms. In the immediate neighborhood of these wells, these clinoforms are disrupted and exhibit numerous lateral discontinuities.

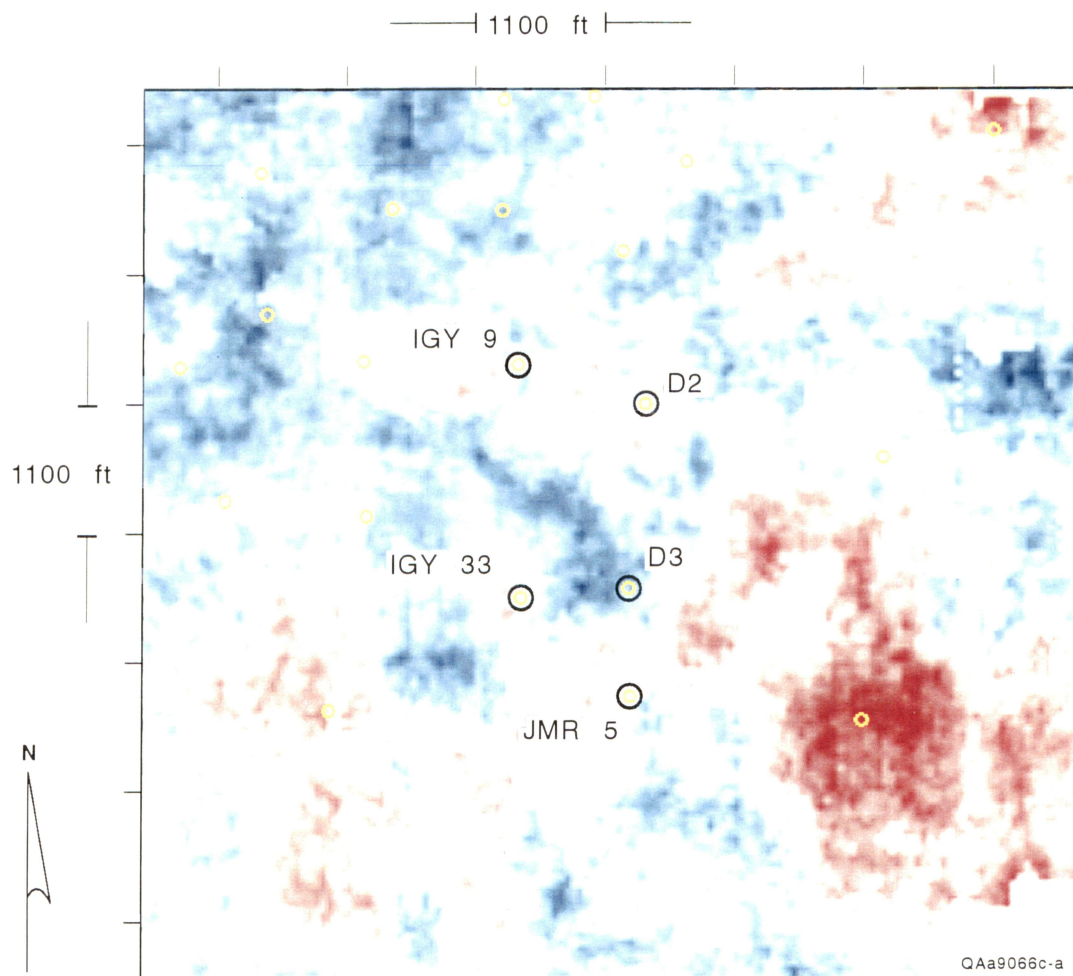


Figure 4.15. Horizon slice passing approximately through the two ES34 boundary picks shown in Figure 4.14. The parameter that is displayed is seismic reflection amplitude, positive reflection values being red and negative values blue. This horizon map shows that the Middle Jasper Creek interval near the IGY9, IGY33, D2, and D3 wells is highly heterogeneous in a seismic sense and that individual reservoir compartments are likely to be small if the imaged changes in reflection polarity are assumed to be possible compartment boundaries. Note that the IGY33 well is located near the north end of a narrow trend of a positive (red) reflection facies that covers about 10 ac. The areal geometry of this particular facies, and the position of the IGY33 well within it, resemble the reservoir geometry implied by pressure data analysis in Figure 4.13.

compartments are likely to be quite small. Note, in particular, that the IGY33 well is located near the north end of a narrow area of positive (red) reflection facies that covers about 10 ac. This small patch of unique Middle Jasper Creek facies has a geometry that is almost identical to the reservoir geometry developed from the pressure data analysis in Figure 4.13, suggesting that this small area may be the compartment that was produced at the IGY33 well.

Summary

In summary, it appears that **both the IGY33 and the WD3 wells encountered original pressure and apparently untapped gas reserves in the Jasper Creek interval, despite being only about 1,200 ft apart.** Unfortunately the drainage areas and, hence, **the volumes of these compartments found in the Jasper Creek are small, on the order of 100 MMscf or less,** which when considered on their own, are insufficient to be economical infill development targets. This example illustrates that the stratigraphic complexity found in the Bend intervals can lead to small-scale reservoir compartmentalization resulting from both surface-boundary mechanisms and possible diagenesis. These results also suggest the need for multiple completion opportunities in any new wells drilled.

5. DIFFICULT-TO-IMAGE RESERVOIRS

One objective of the Boonsville research was to determine what combinations of modern technology, if any, can reliably predict where to find uncontacted Bend Conglomerate reservoirs. Considerable emphasis was placed on determining whether 3-D seismic images, or some combination of numerically derived seismic attributes, could locate isolated Bend Conglomerate compartments. Our conclusion is that the ability to see Bend reservoirs using 3-D seismic data is quite variable, with clear, almost unarguable images produced in some instances (for example, the Upper and Lower Caddo reservoirs discussed in Section 3), whereas in other locations only faint, elusive seismic evidence of certain Bend Conglomerate reservoirs can be seen. This section describes one of these difficult-to-image reservoirs within the Bend Conglomerate.

C Yates 9 Trinity Reservoir—Production History and Engineering Analysis

The Trinity reservoir penetrated by the C Yates 9 well was selected as one example (of many that could have been chosen) that illustrates how 3-D seismic data may not satisfactorily image the lateral heterogeneity associated with a Bend Conglomerate stratigraphic trap compartment boundary. The Trinity interval at the C Yates 9 well is particularly significant because it contains a reservoir that is one of the most prolific Trinity producers within the 26-mi² seismic grid.

The Threshold Development C Yates 9 well was drilled and completed in early 1971. Figure 5.1 shows the location of the well in the north-central part of the project area. The C Yates 9 was initially perforated in the Vineyard interval from 5,688 to 5,701. Following a small fracture treatment (12,000 gal gelled water and 12,000 lb 20/40 sand),

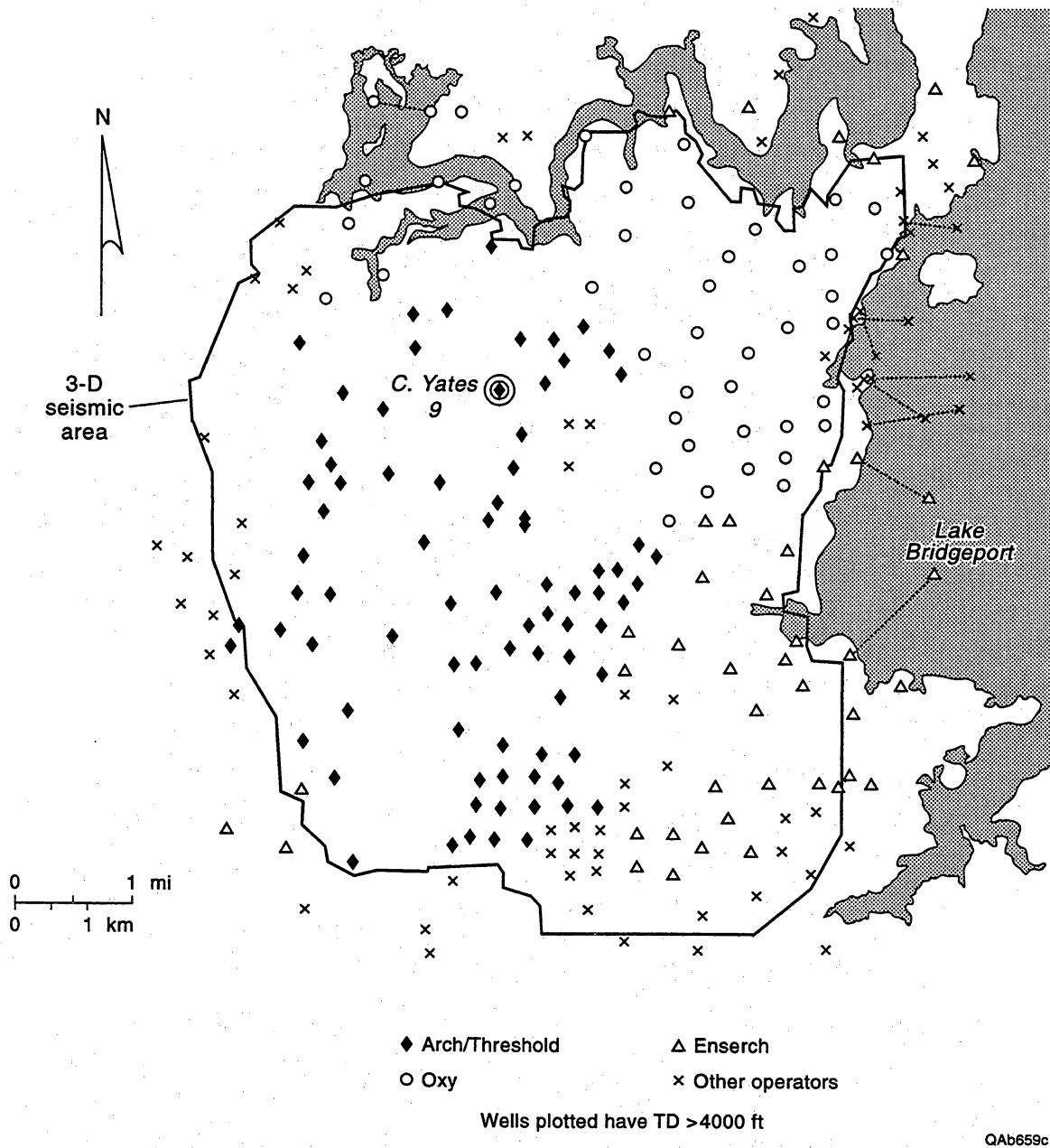


Figure 5.1. Location of the C Yates 9 well in the north-central portion of the project area.

the Vineyard tested 668 Mscf/d and 2 STB/d condensate at 100 psi flowing tubing pressure on a 3/4-inch choke.

Immediately thereafter, a bridge plug was set above the Vineyard, and the Trinity interval was perforated from 5,206 to 5,210 ft. After a small fracture treatment (10,000 gal gelled water and 9,000 lb 20/40 sand), the Trinity reservoir tested 2.45 MMscf/d and 14 STB/d condensate at 580 psi on a 1/2-inch choke. The C Yates 9 was turned to sales and produced only from the Trinity interval from June 1971 to September 1989, making 1.91 Bscf of gas. At that time, the bridge plug was removed, and the lower Vineyard perforations were put on production. Currently both the Vineyard and Trinity zones are commingled, and the well has produced a total of 2.11 Bscf.

Although the C Yates 9 was not drilled until 1971, the nearest Trinity completion at the time was more than 1 mi away, and it had not produced much gas from the Trinity (only about 60 MMscf). It is unlikely that any significant drainage from the Trinity reservoir had occurred at this location at the time the C Yates 9 was completed.

Figure 5.2 presents an expanded view of the area around the C Yates 9 well. The OXY Ashe 1 well was completed in the Trinity interval in January 1961, which was the only nearby well completed in the Trinity before the C Yates 9 was drilled, and it had produced only about 60 MMscf of gas to that time (cumulative Trinity production to date is only 185 MMscf). Trinity perforations were added in the C Yates 6 well in May 1983, but because the Trinity is one of six Bend intervals commingled in this wellbore, it was impossible to estimate its gas production individually.

The C Yates 10 and 12 wells were drilled in 1984 and 1985, respectively. Both wells were multiple completions in the Trinity, Lower Jasper Creek, and Vineyard sequences. Upper Caddo perforations were added in the C Yates 10 in 1990. Both these wells are structurally lower than the C Yates 9 by about 40 to 50 ft, and each tested and produced both oil and gas from the Trinity; both were actually classified as oil wells. The C Yates 10 has produced about 25,000 STB of oil and 184 MMscf of gas from the three

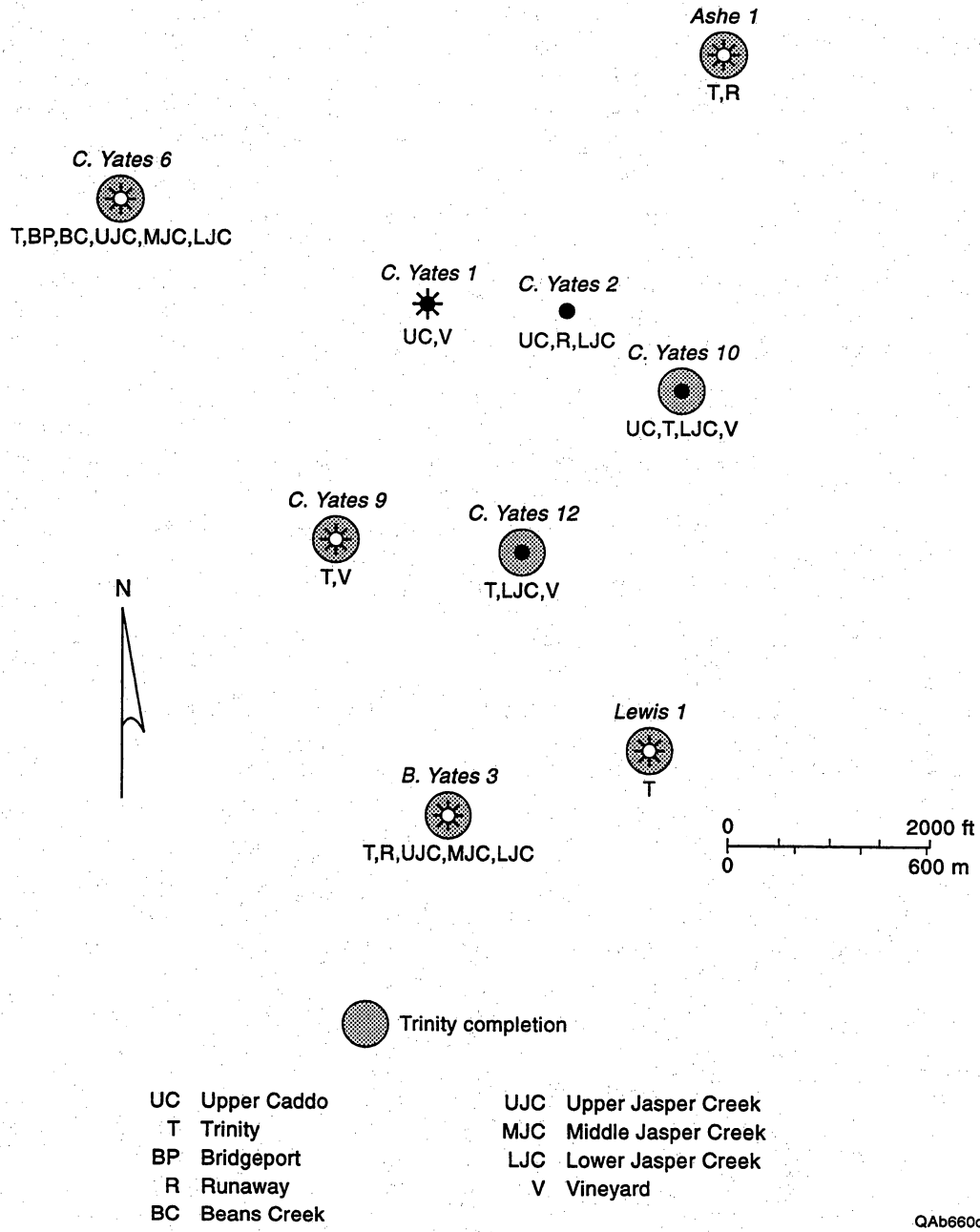


Figure 5.2. Expanded view of wells offsetting the C Yates 9 location.

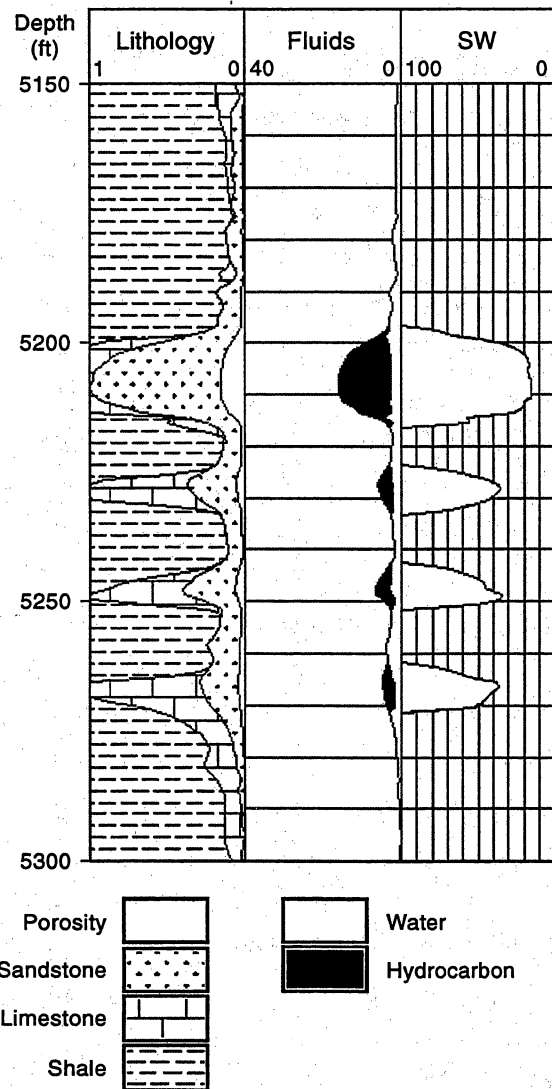
commingled intervals, whereas the Cap Yates 12 has produced only about 3,400 STB of oil and 165 MMscf of gas.

In December 1992, the B Yates 3 well was recompleted in the Trinity. There was significant pressure depletion in the Trinity on recompletion; this zone had an estimated reservoir pressure in the Trinity of about 200 psi on the basis of surface pressure measurements. The C Yates 9 had apparently drained the Trinity reservoir at the B Yates 3 location. The same is true at the Lewis 1 location, where the initial pressure on completion of the Trinity interval was 508 psi in March 1982.

Figure 5.3 presents an interpreted log across the Trinity sequence penetrated by the C Yates 9. The upper part of the sequence from 5,197 to 5,218 ft had excellent sand development and good porosity and gas saturation; this was the interval that was completed. The lower sands are highly carbonate cemented with a resulting loss of porosity and productivity.

Figure 5.4 shows the Trinity-only gas production from the C Yates 9 well and is a semilog plot of gas flow rate versus time. The well came on line making in excess of 2 MMscf/d and declined to a rate of about 20 Mscf/d over an 18-yr period.

Figure 5.5 is a log-log plot of gas flow rate versus time. This plot indicates boundary-dominated flow during most of the well's producing life, as evidenced by the concave downward shape of the production data after about 300 to 500 d of production. Using an analytical model to history-match the production data, the Trinity reservoir was estimated to have a permeability of about 3.3 md and a drainage area of approximately 300 acres. This estimated drainage area is based on a constant, average net pay thickness of 14 ft calculated for the C Yates 9. If the average net thickness of the Trinity reservoir in communication with the C Yates 9 wellbore is less than 14 ft, then the apparent reservoir size of 300 acres is a minimum value. The estimated total gas in place of 2.1 Bscf in the Trinity reservoir, however, should be correct for any combination of net pay thickness and drainage area. Because the Trinity reservoir in the C Yates 9 well had



QAb661c

Figure 5.3. Interpreted log for the Trinity sequence penetrated by the C Yates 9 well.

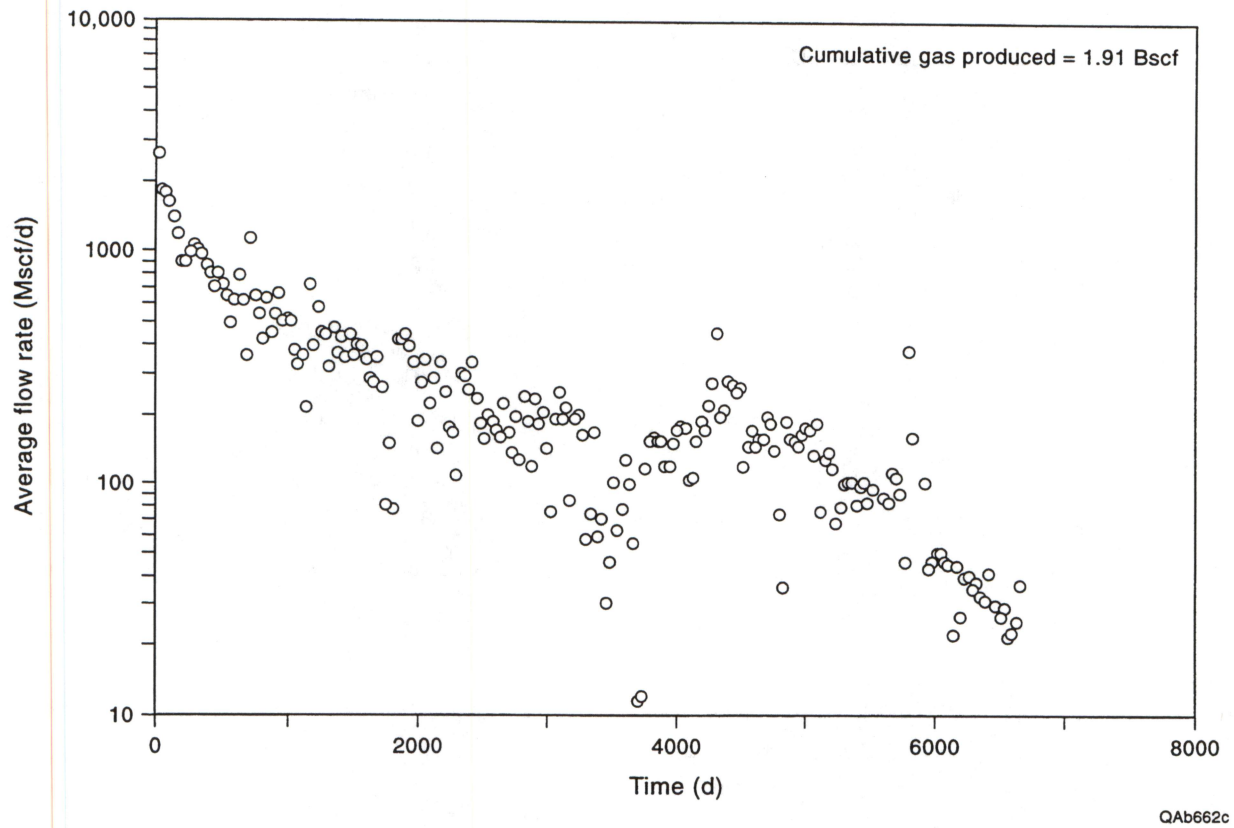
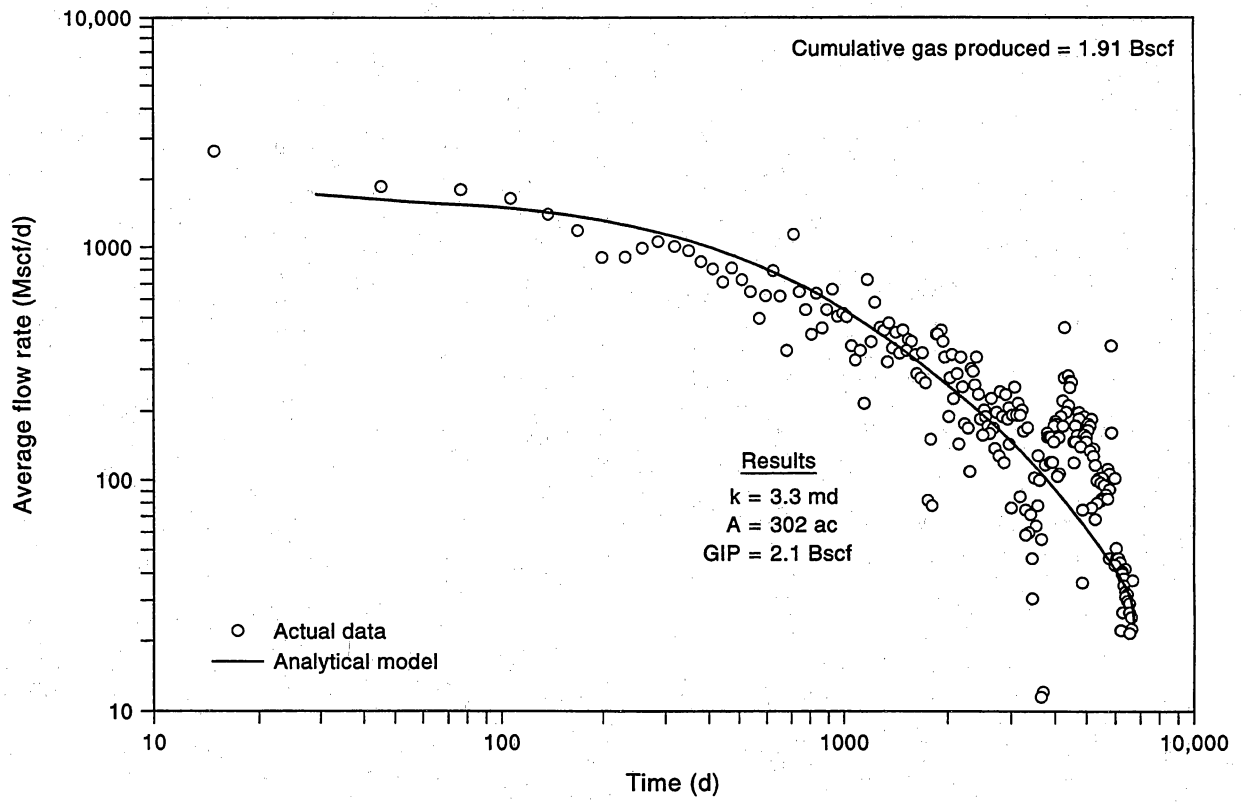


Figure 5.4. Trinity-only production history from the C Yates 9 well.



QAb663c

Figure 5.5. History match of Trinity-only production data from the C Yates 9 well.

such a large areal extent, we anticipated that it would be easy to identify in the seismic data, but as described in the following discussion, this was not the case.

C Yates 9 Trinity Reservoir—Seismic Analysis

Two seismic profiles that traverse the C Yates 9 well and connect with adjacent wells are used to illustrate the seismic subtlety of this particular Trinity reservoir. These vertical seismic sections are shown as uninterpreted and interpreted wiggle trace data in Figures 5.6 through 5.9, and as uninterpreted and interpreted instantaneous phase data in Figures 5.10 through 5.13 (see Appendix E, Volume II, for a discussion of how instantaneous phase is calculated and used).

In this situation, it is easier to use instantaneous phase to interpret the position of the Trinity surface than it is to use the traditional approach of using wiggle trace data. The advantage of instantaneous phase is that the phase behavior of seismic data is independent of the magnitude of the reflection signal amplitude; consequently, **instantaneous phase displays show stratigraphic relationships in low-amplitude portions of a 3-D seismic data volume** with the same degree of fidelity and robustness as they do in high-amplitude portions. Because the reflection response associated with the Trinity surface is low amplitude, the Trinity sequence boundary can be tracked more easily in instantaneous phase displays. In all instances where any Bend Conglomerate sequence boundary had to be interpreted in low-amplitude wiggle trace data, the seismic interpretations were usually done using instantaneous phase volumes.

The seismic two-way traveltime positions of several log-interpreted sequence boundaries are marked by heavy horizontal dashes on each well profile in these seismic displays, and these sequence boundary control points are expanded into continuous sequence boundaries on each interpreted section. The MFS60 (Trinity) surface is the target reservoir that needs to be imaged. The wiggle trace displays in Figures 5.6 and 5.7 show that, along this particular profile, **the Trinity surface is marked by a low-**

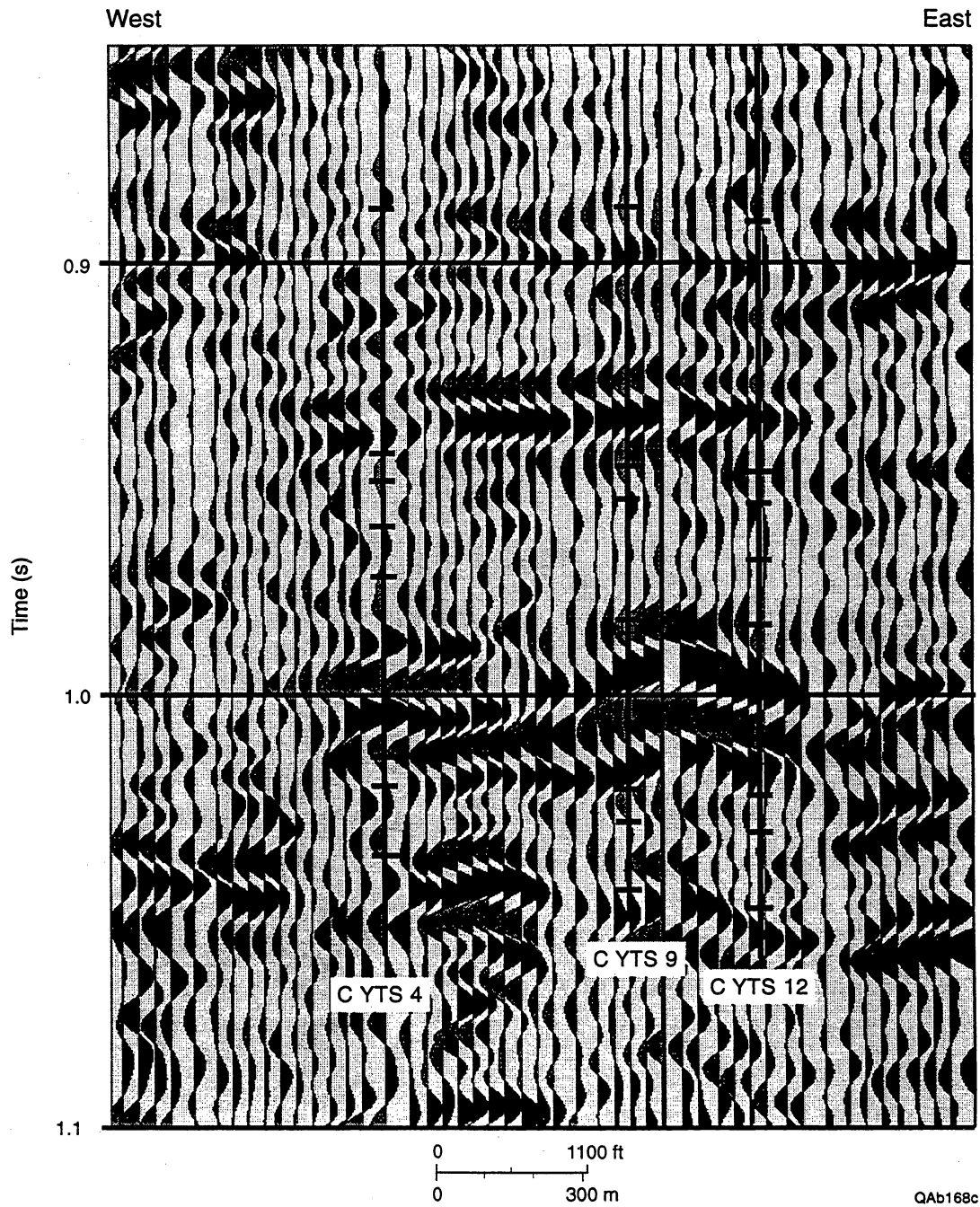


Figure 5.6. An uninterpreted east-west seismic section connecting the C Yates 9 well with neighboring wells. The horizontal dashes on each well profile show where key sequence boundaries are positioned by the depth-to-time conversion function developed for the study area.

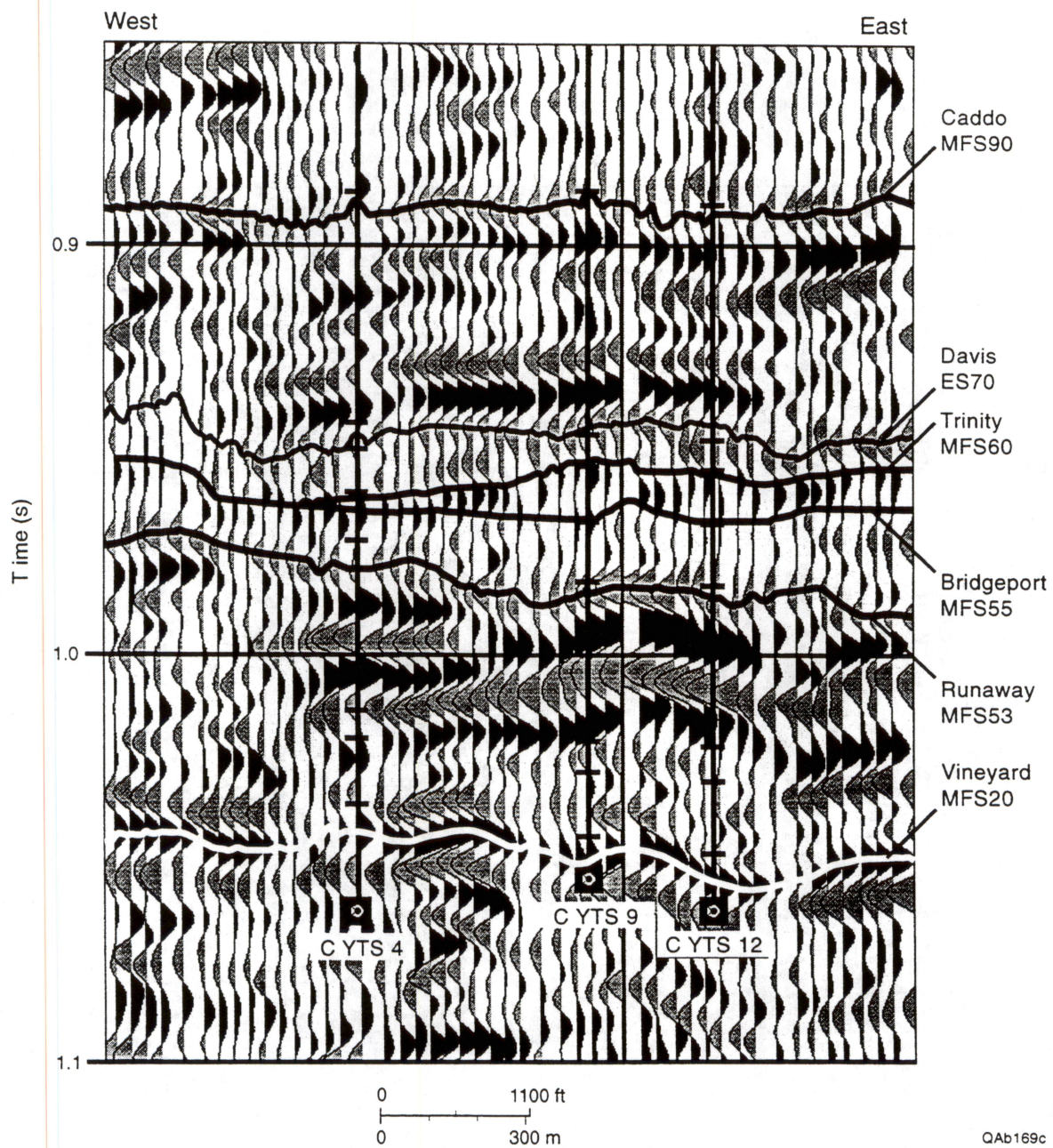


Figure 5.7. An interpreted version of the seismic line shown in Figure 5.6. The imaging objective is a major reservoir immediately below the Trinity (MFS60) sequence boundary.

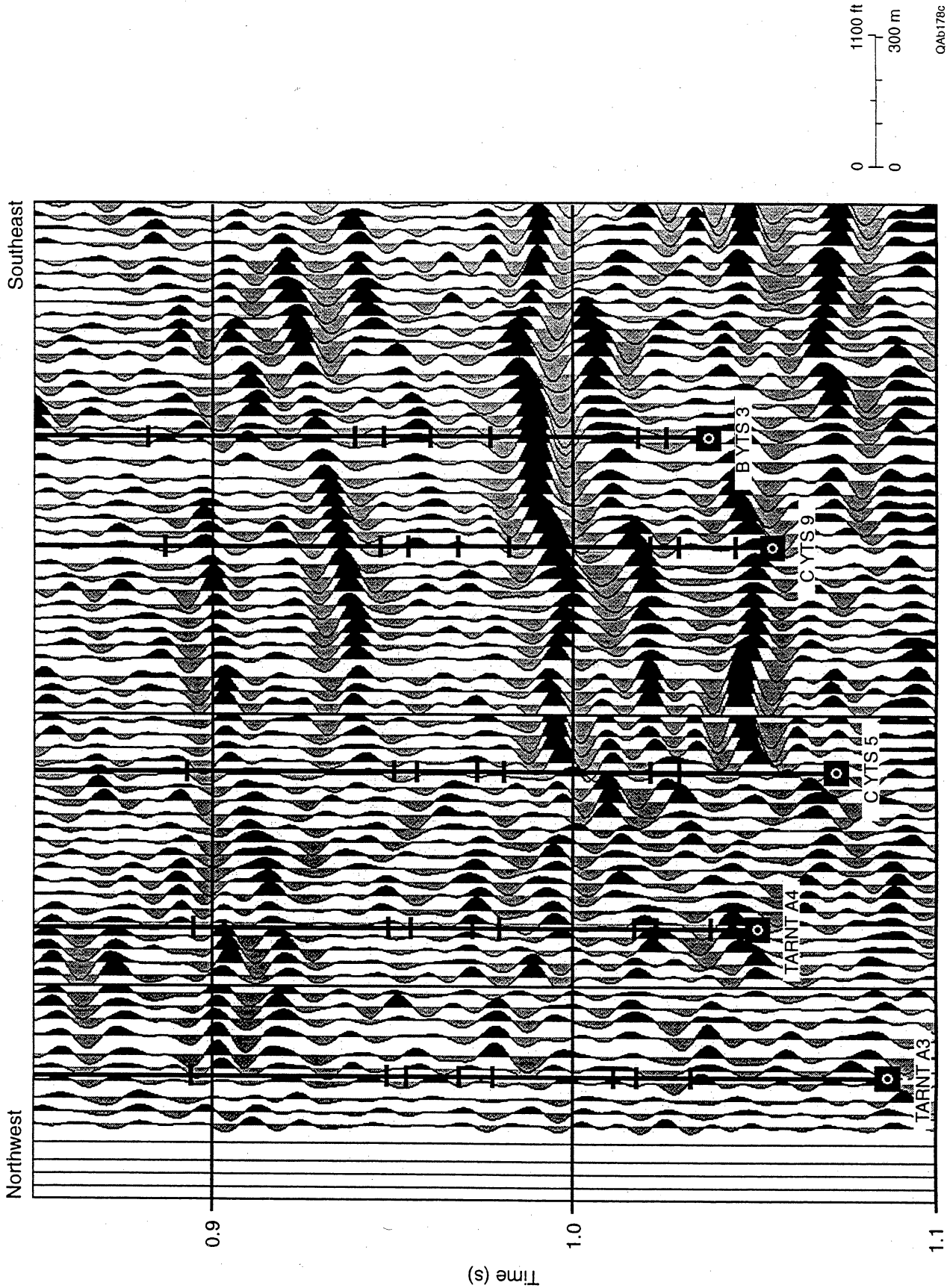


Figure 5.8. An uninterpreted northwest-southeast seismic section connecting the C Yates 9 well with neighboring wells. The horizontal dashes on each well profile show where key sequence boundaries are positioned by the depth-to-time conversion function developed for the study area.

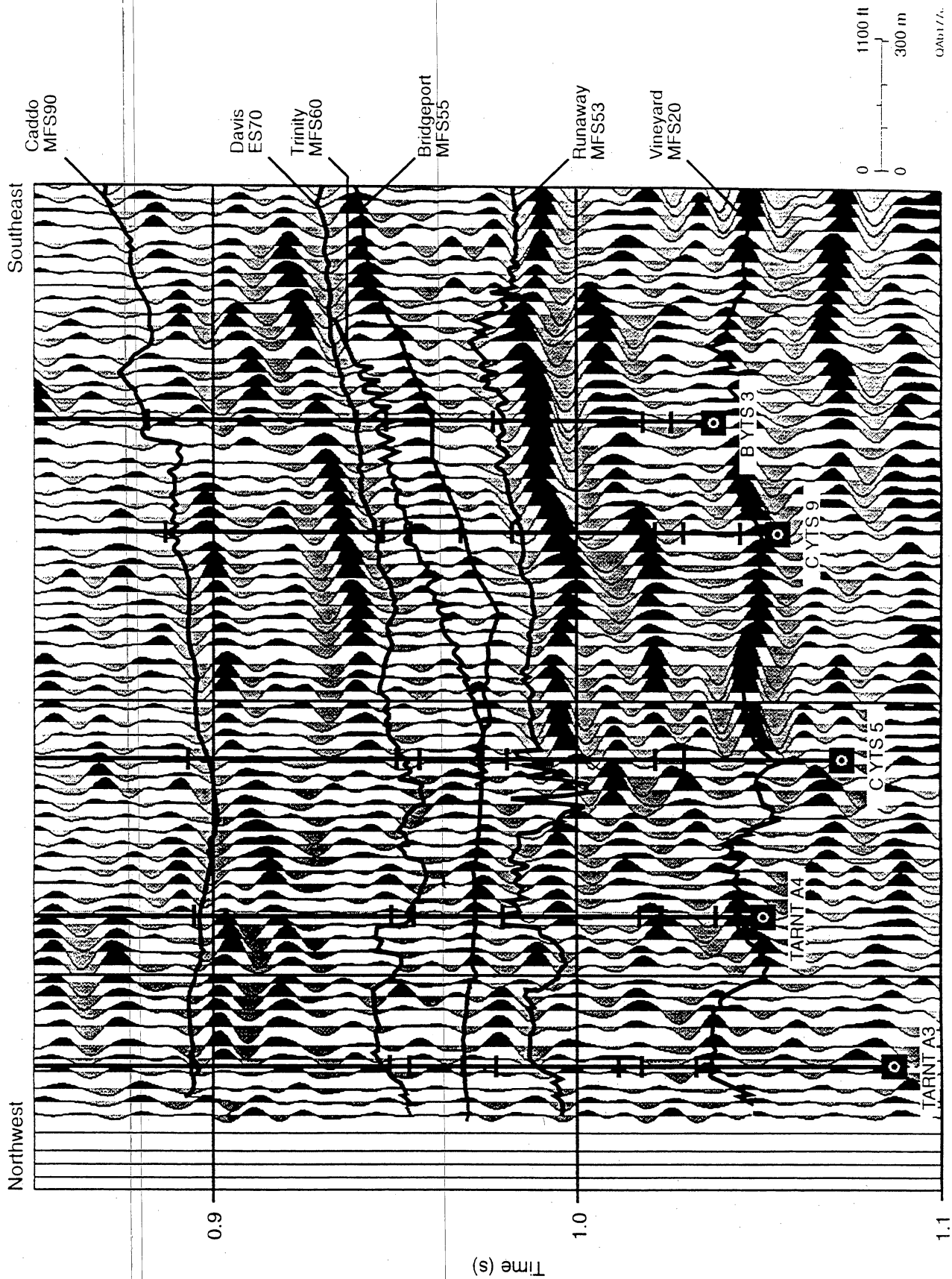


Figure 5.9. An interpreted version of the seismic line shown in Figure 5.8. The imaging objective is a major reservoir immediately below the Trinity (MFS60) sequence boundary.

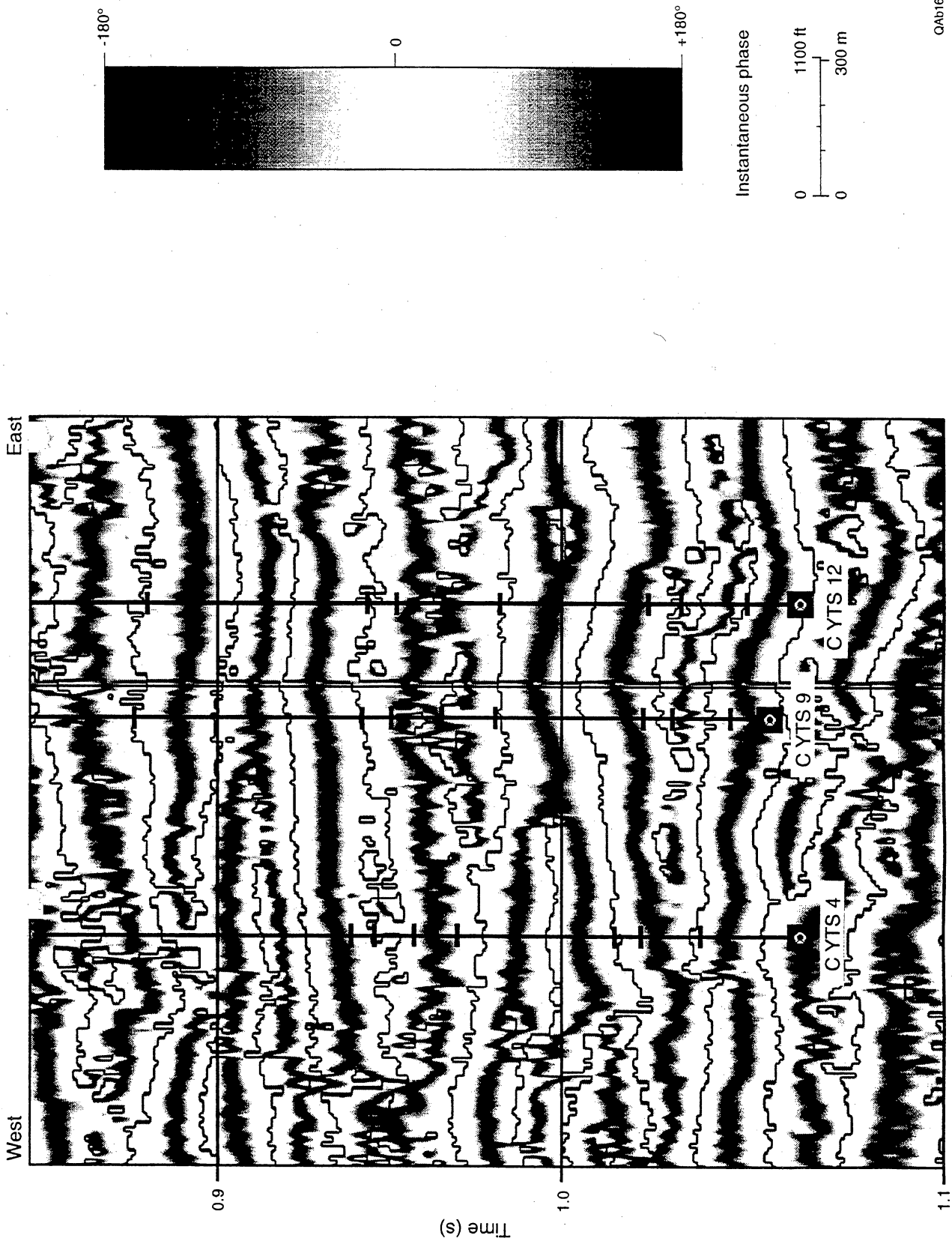
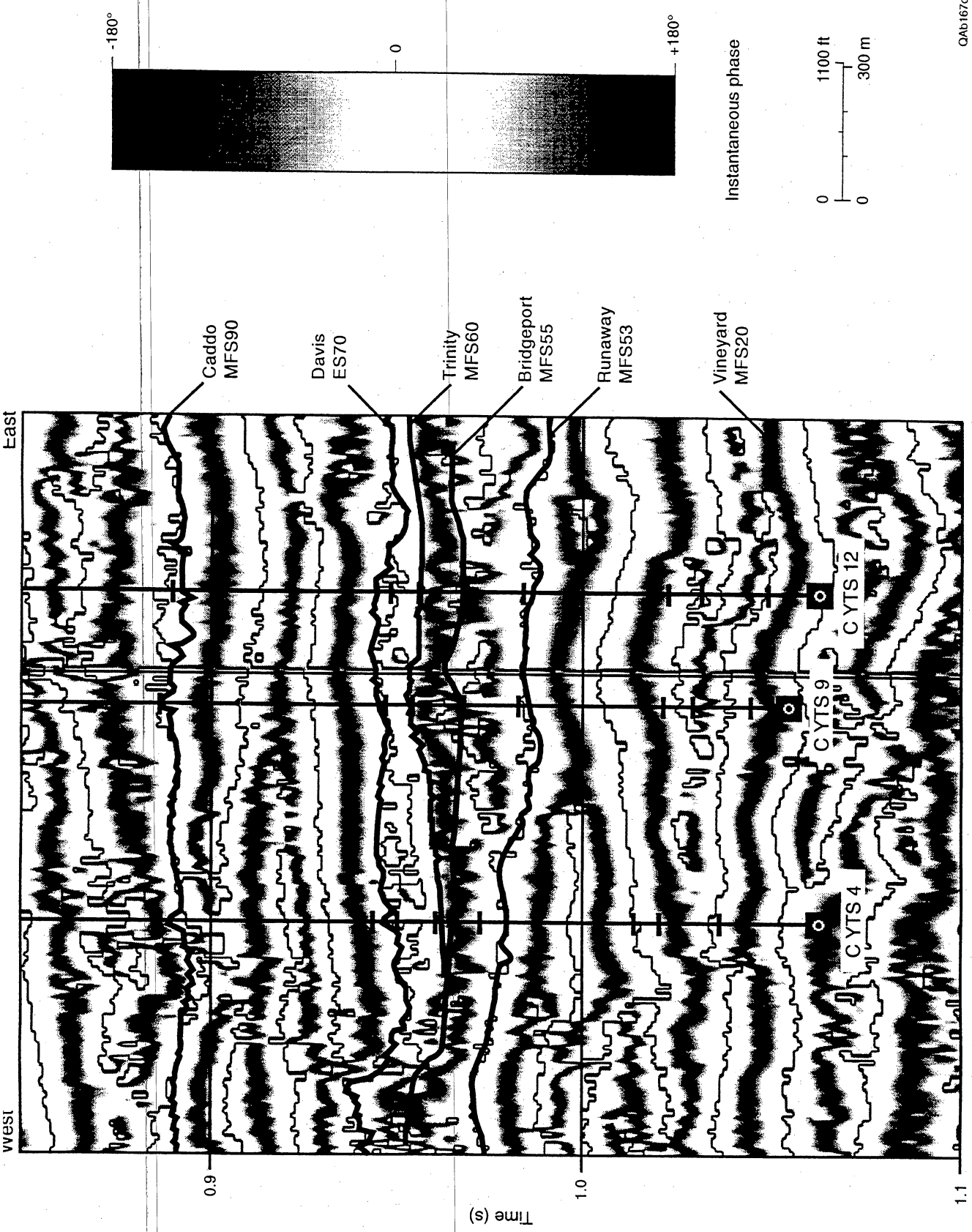


Figure 5.10. The data in Figure 5.6 converted to instantaneous phase. The thin black line passing through the center of each white phase zone shows where the phase function undergoes a 360° wrap-around when the phase function cycles through the 0° value. This helpful phase surface is automatically provided by the Landmark software used to interpret the Boonsville 3-D seismic data.



QA0167c

Figure 5.11. The data in Figure 5.7 converted to instantaneous phase. Note that each sequence boundary, including the Trinity surface, follows a reasonably constant phase surface.

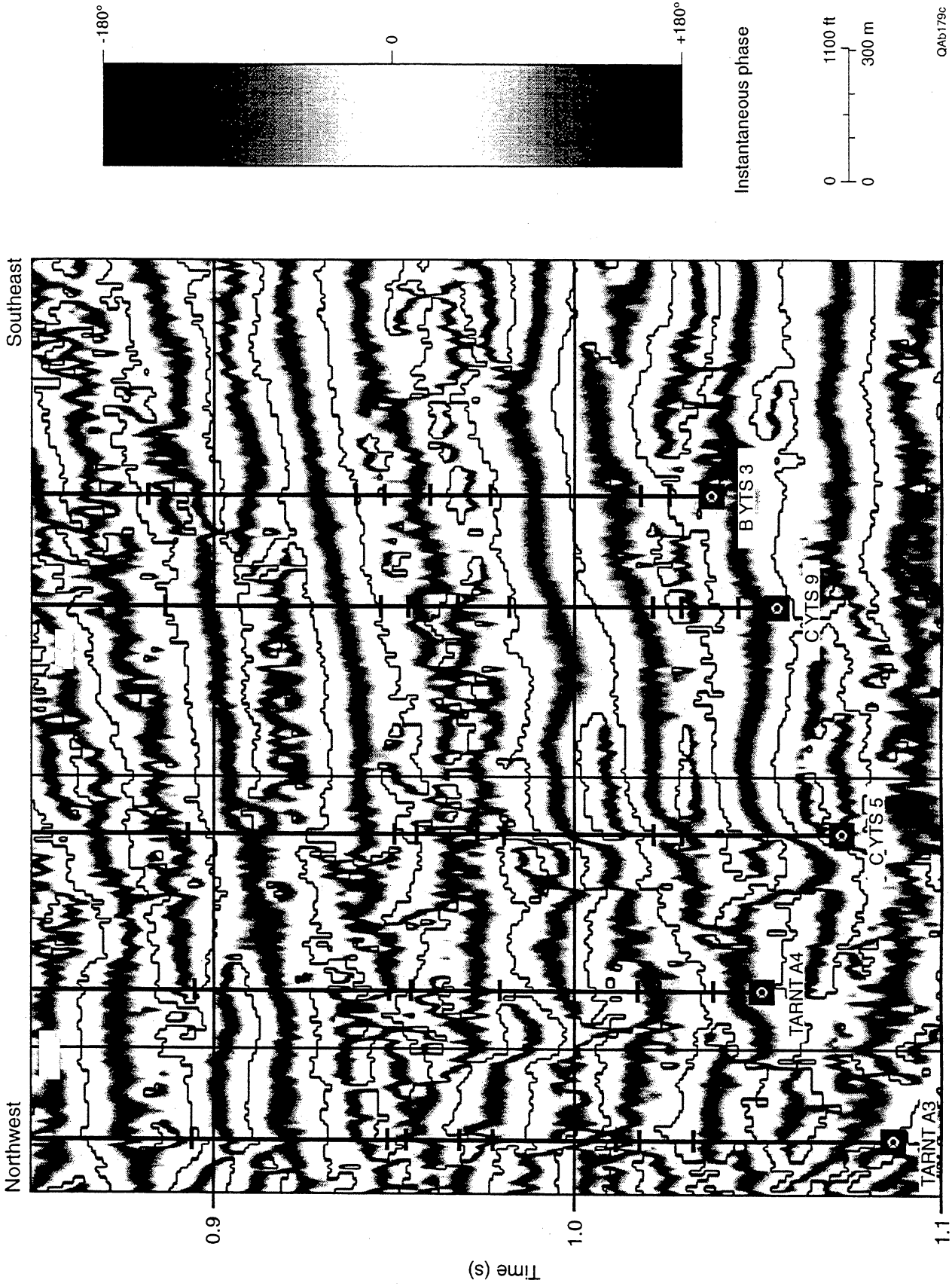
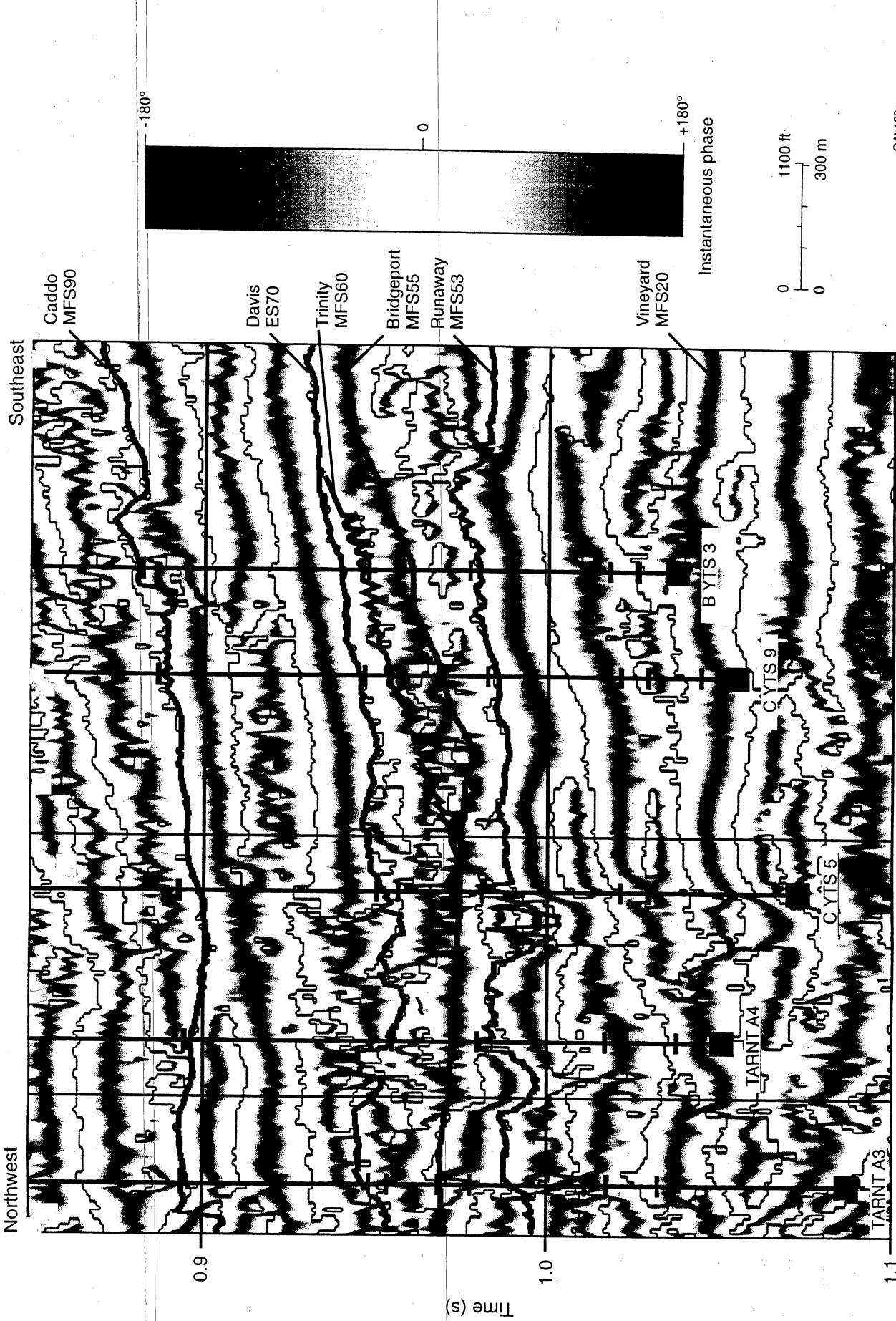


Figure 5.12. The data in Figure 5.8 converted to instantaneous phase. The thin black line passing through the center of each white phase zone shows where the phase function undergoes a 360° wrap-around when the phase function cycles through the 0° value. This helpful phase surface is automatically provided by the Landmark software used to interpret the Boonsville 3-D seismic data.



QAb180c

Figure 5.13. The data in Figure 5.9 converted to instantaneous phase. Note that the Davis and Runaway surfaces that bracket the Trinity sequence follow a reasonably constant phase surface, but the Trinity boundary is located in a time window where the seismic phase has a highly erratic behavior.

amplitude event that has an erratic time onset and a variable waveshape. In this instance, the Trinity surface follows a reasonably consistent phase trend (Figs. 5.10 and 5.11). In contrast, no definitive reflection event is associated with the Trinity surface along the profile shown in Figures 5.8 and 5.9, and in the associated phase displays (Figs. 5.12 and 5.13), the phase exhibits rapid lateral changes along the time surface where well control defines the Trinity sequence boundary to be located. Thus, even though the Trinity sequence penetrated by the C Yates 9 well is a significant reservoir, **the reservoir is quite elusive in a seismic sense,** and some interpreters might refer to the reservoir as being seismically invisible in this particular 3-D seismic data volume.

The principal point to make concerning the seismic image of this stratigraphy is that this Trinity reservoir is not seismically invisible; it is simply nondescript in a seismic sense because **the reflection waveshapes defining the sequence are low amplitude, variable in character, irregular in their time onset, and not conformable to any nearby reflection event.** No distinctive seismic property causes an interpreter to focus on that portion of the 3-D data volume where this Trinity reservoir is located, and well control must be used to identify the precise location of the Trinity sequence boundary.

Once the Trinity sequence boundary is interpreted from the C Yates 9 and neighboring wells and incorporated into the interpretation, the two-way seismic traveltime of the Trinity reservoir can be defined, and the sequence boundary associated with the reservoir can be extended away from the control wells. Maps of seismic attributes calculated on the resulting Trinity horizon show that there is a distinctive reflection amplitude behavior (Fig. 5.14), with the Trinity sequence being expressed by low reflection amplitudes having both positive and negative algebraic signs immediately around the C Yates 9 well, and by larger, positive-only reflection amplitudes at greater distances from the well. We assumed that the low-amplitude seismic facies indicated the productive Trinity reservoir facies, and that the larger valued, positive seismic amplitude facies mapped nonreservoir Trinity facies. The exact way to position the boundary that

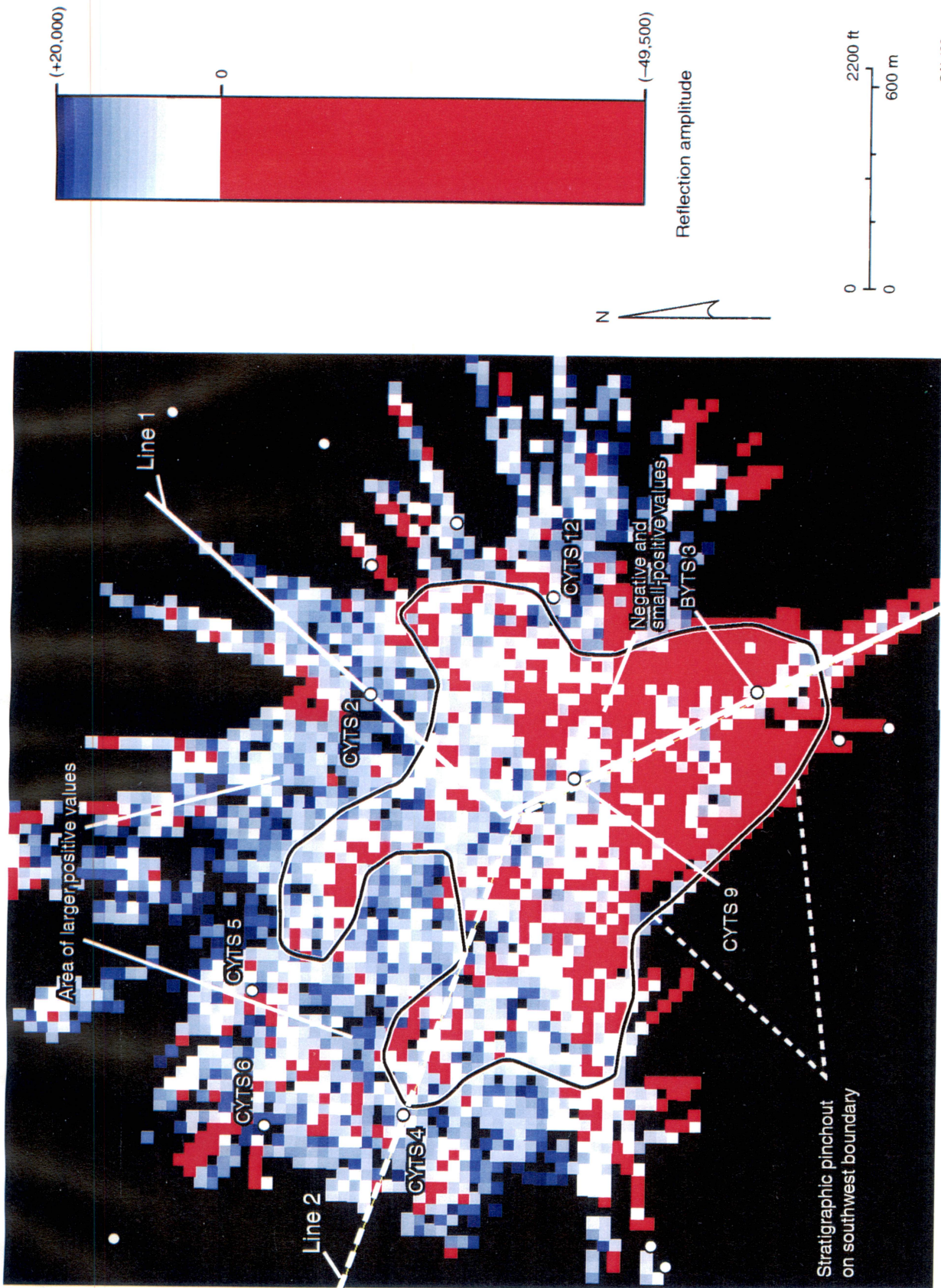


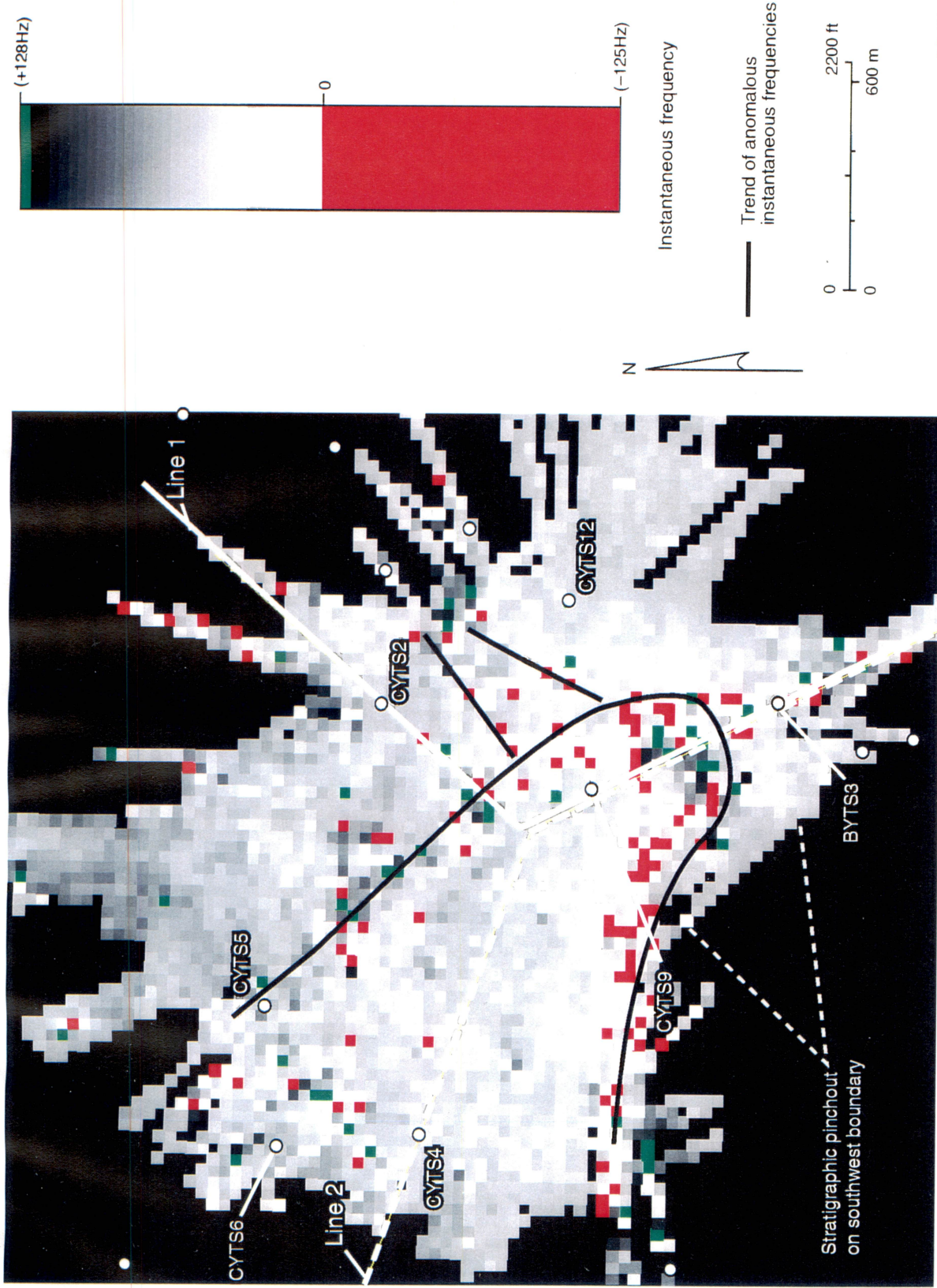
Figure 5.14. Reflection amplitude behavior on the interpreted Trinity surface near the C Yates 9 well. The heavy outline encloses an area of approximately 300 ac, where the reflection amplitude is either positive or negative, but always of quite low amplitude. Outside of this boundary, the reflection amplitudes are positive and have relatively high amplitudes. Seismic reflection profiles along Line 1 and Line 2 are displayed as Figures 5.16 and 5.17.

segregates these two seismic amplitude facies is a matter of subjective judgment, but the configuration shown in Figure 5.14 is thought to be reasonably consistent. This boundary encloses an area of almost 300 acres, which is a reservoir size similar to what the production data imply. The B Yates 3 well is positioned inside the south edge of this interpreted Trinity compartment.

A distinctive boundary of anomalous frequency values (Fig. 5.15) also encircles the C Yates 9 well. If we assume that the boundary defined by the anomalous frequencies also marks the lateral extent of the C Yates 9 reservoir compartment, as is suggested by the data examples presented in Appendix E, then the seismic data imply that the areal size of this Trinity reservoir is a little over 100 acres, which is not as large a reservoir as the production data imply. Reflection profiles along Lines 1 and 2, shown on the seismic amplitude and frequency maps, are provided as Figures 5.16 and 5.17 to support the claim that this particular Trinity reservoir is a highly elusive target in the 3-D seismic image. Both profiles show that the MFS60 sequence boundary follows an inconsistent seismic phase and that reflection amplitudes are weak and highly variable along the Trinity surface. No definitive seismic character can be related to this sequence in these section views.

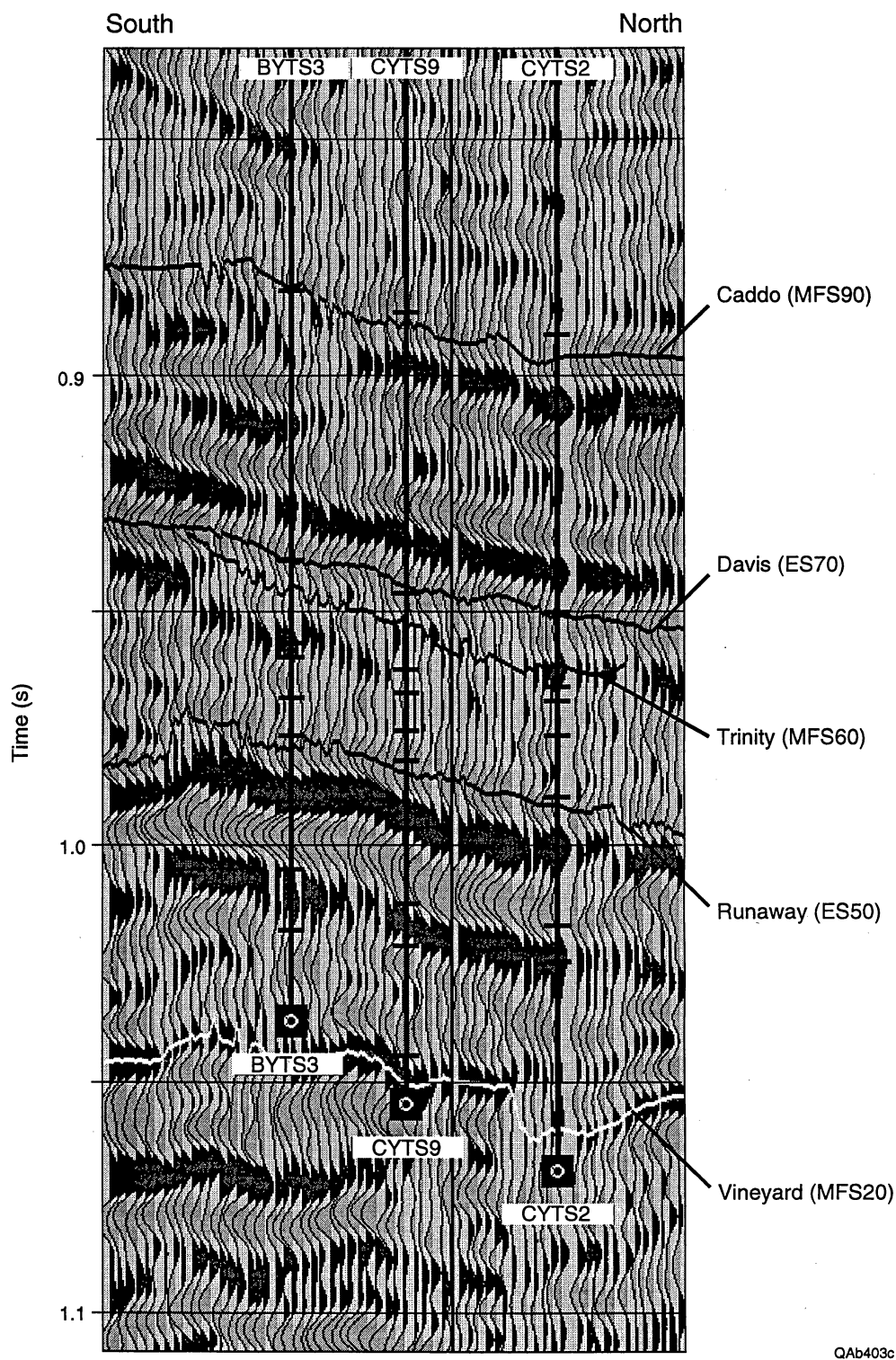
Summary

A significant conclusion provided by this C Yates 9 reservoir analysis is that other Bend Conglomerate reservoirs, not just Trinity reservoirs, may also not be easily seen in 3-D seismic images, even when seismic attributes such as instantaneous frequency and amplitude are used in the analysis. Stated another way, **it will be difficult for 3-D seismic data to be used as a predictive tool to site exploration wells for some, but not all, Bend Conglomerate reservoirs in undrilled areas if the reservoir trapping mechanism is caused strictly by lateral facies change rather than by some type of structural disruption.** Even when an elusive reservoir of this type is the primary



OAB401c

Figure 5.15. Instantaneous frequency behavior on the interpreted Trinity surface near the C Yates 9 well. The east-west linear trend of red and green points, which passes between the CYTS12 and BYTS3 wells and then turns northwest to reach the CYTS5 well, indicates where there are anomalous negative and positive frequency values, and these anomalous frequencies, in turn, indicate trends where the reflection waveform is distorted (App. E). Such distorted waveforms often imply compartment boundaries, but if that interpretation rule is invoked here, the Trinity reservoir inside the region circumscribed by this trend of anomalous frequencies covers an area only slightly greater than 100 ac, which does not agree with the production data. Thus, the reservoir size implied by the amplitude image (Fig. 5.14) agrees more closely with the size implied by the production performance. Seismic reflection profiles along Line 1 and Line 2 immediately below.



QAb403c

Figure 5.16. Reflection profile along Line 1. Note that the Trinity surface is essentially invisible in a seismic sense in the interval from near the BYTS3 well to near the CYTS2 well. To the right of the CYTS2 well (toward the northeast), the Trinity surface follows a positive peak of reasonable amplitude.

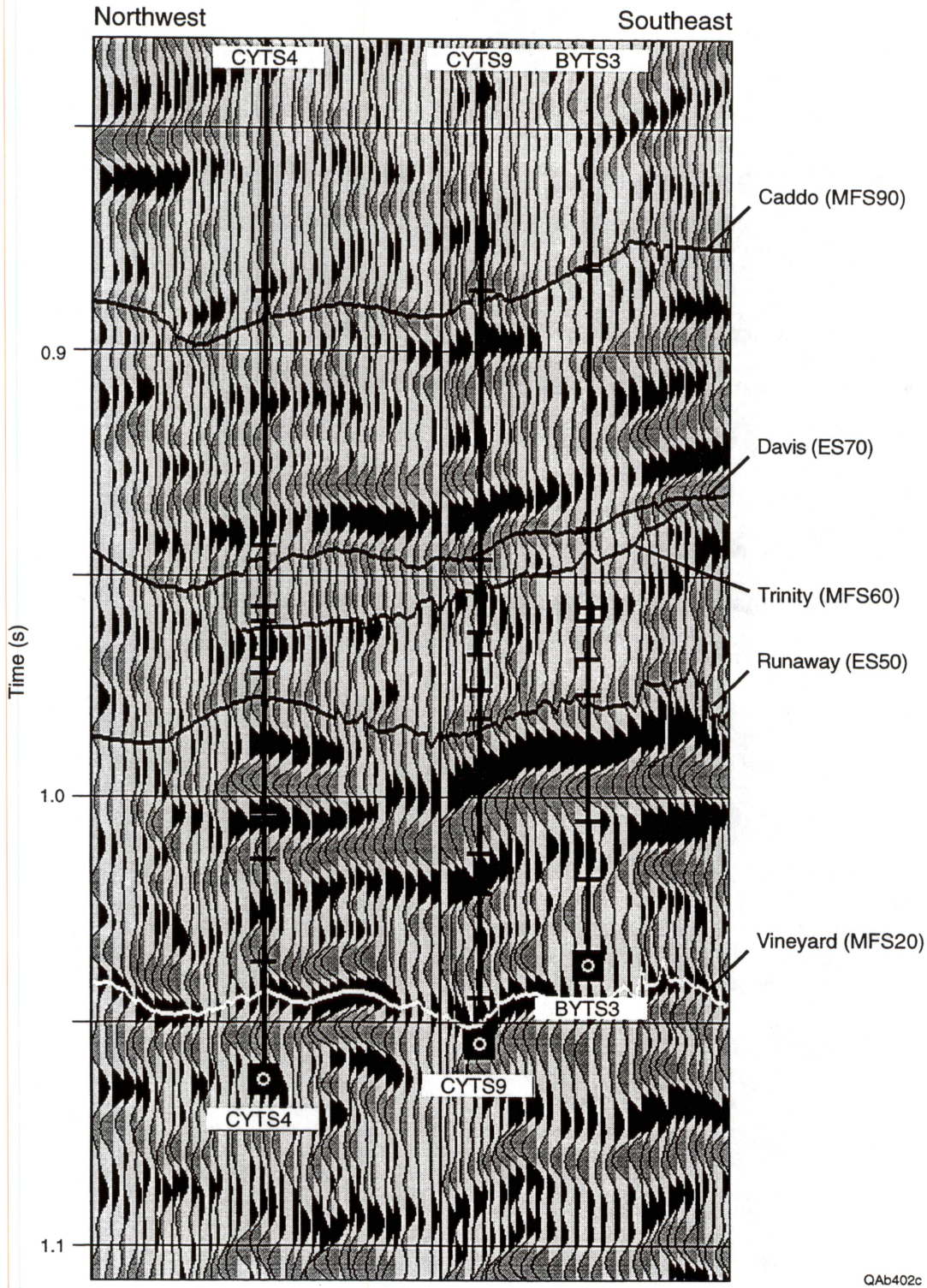


Figure 5.17. Reflection profile along Line 2. Again, the Trinity surface along much of this profile is a trend of low-amplitude responses of variable waveshapes that have either positive or negative amplitudes, which indicates that the low-amplitude Trinity reflection signal is contaminated by noise and by interference from nearby reflecting surfaces.

interpretation target, however, 3-D seismic imaging is still valuable for estimating the areal size of the stratigraphic trap, because once the reservoir has been penetrated by a well, the reservoir sequence can then be accurately positioned in the 3-D data volume and seismic attribute maps can be made to imply compartment size and shape.

Thus, the role of 3-D seismic technology in low-accommodation Midcontinent fields similar to Boonsville seems to be the following.

1. 3-D seismic imaging can be used as a predictive tool for siting exploration wells when the reservoir trapping mechanism is associated with a structural disruption, such as a fault or a karst collapse zone, and also for many stratigraphic traps, such as has been documented for the Upper and Lower Caddo (see Section 3).

2. 3-D seismic imaging may not serve as a reliable predictive tool for some subtle stratigraphic traps, but in such cases, seismic imaging can still be used as a valuable property management tool to estimate the areal size and shape of these subtle stratigraphic traps once the reservoir has been penetrated by a well. This increased value of 3-D seismic data at the production phase of an elusive reservoir play occurs because once well data become available, they can be coupled with reliable seismic velocity control to position the sequence boundary of the reservoir in the 3-D seismic data volume accurately, even if the seismic response at that boundary has no obvious, distinctive waveform character.

6. SITING BOONSVILLE DEVELOPMENT WELLS—CASE HISTORIES

Two wells, the B Yates 17D and 18D, were drilled inside the 26-mi² Boonsville 3-D seismic survey area shortly after interpretation of the seismic data was initiated, but before 3-D interpretation was completed and properly integrated with the geologic and engineering control. There are numerous reasons why a drilling program must be started before a prospect is fully interpreted, so the urgency to select drill sites for the B Yates 17D and 18D wells before a detailed Bend Conglomerate stratigraphic model was constructed is typical of situations that confront many operators. In this instance, the Boonsville 3-D seismic program was delayed several months because of logistical problems, and the operating company delayed its drilling program as long as practical in an attempt to have some 3-D seismic guidance in siting the wells. This section describes the procedures we followed to help the operator (Threshold Development) site the first two development wells involved in this research program.

B Yates 18D—Engineering Overview

Figure 6.1 shows the location of the B Yates 18D well in the central part of the project area. This well was drilled by Threshold Development in November and December 1994 and is the first of several infill development wells that Threshold has planned in the immediate project area. The B Yates 18D was the first well drilled in the project area following collection of the 3-D seismic data.

Figure 6.2 presents an expanded view of the B Yates 18D location and the surrounding wells. Of the two closest wells, the B Yates 4 did not penetrate the Bend interval, and the B Yates 1 was drilled in the late 1940's, found gas, but was abandoned owing to a lack of market and pipeline facilities at the time. The other nearby wells produce from a variety of intervals from the Caddo through the Vineyard.

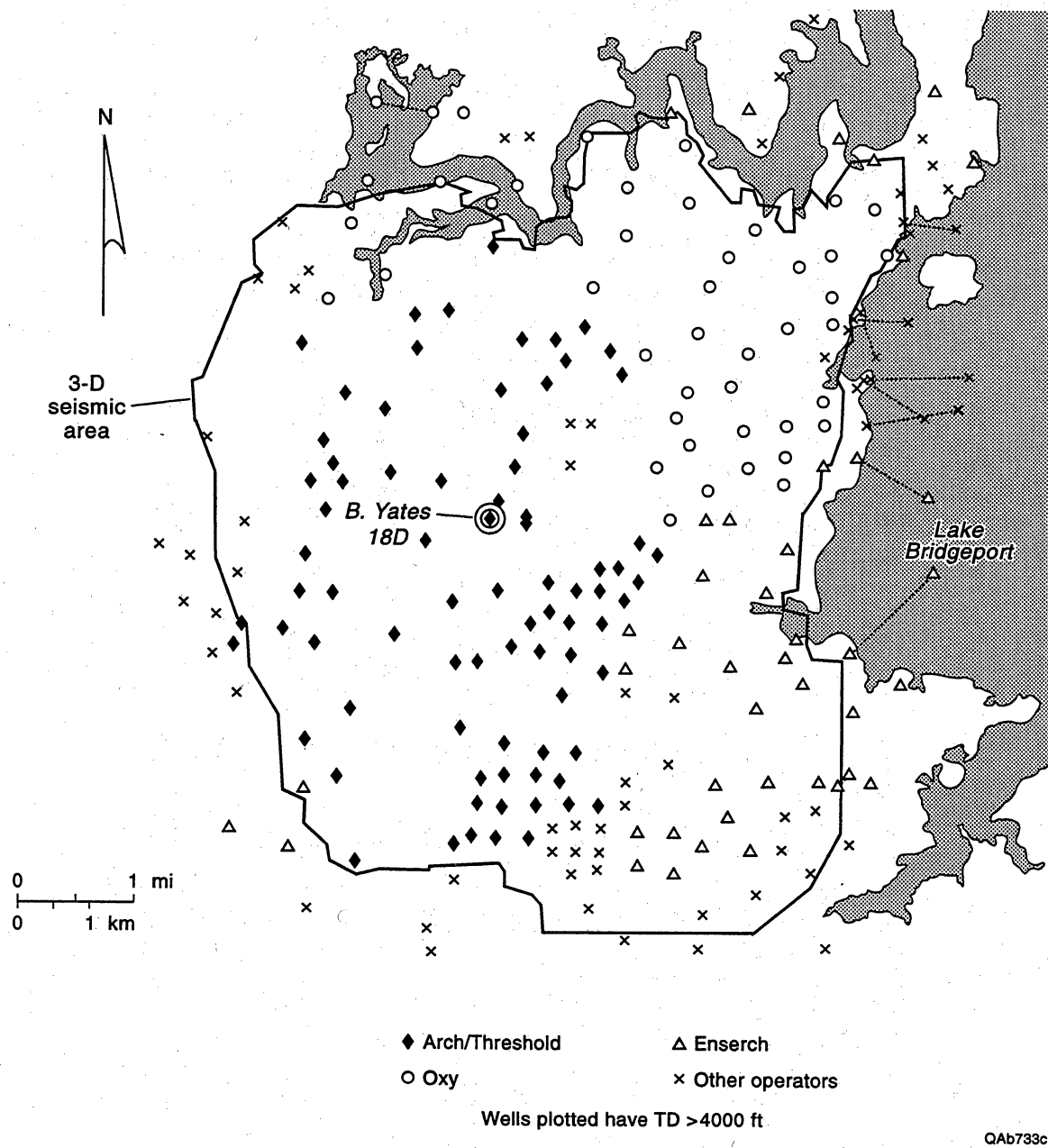


Figure 6.1. Location of the B Yates 18D well in the central part of the project area.

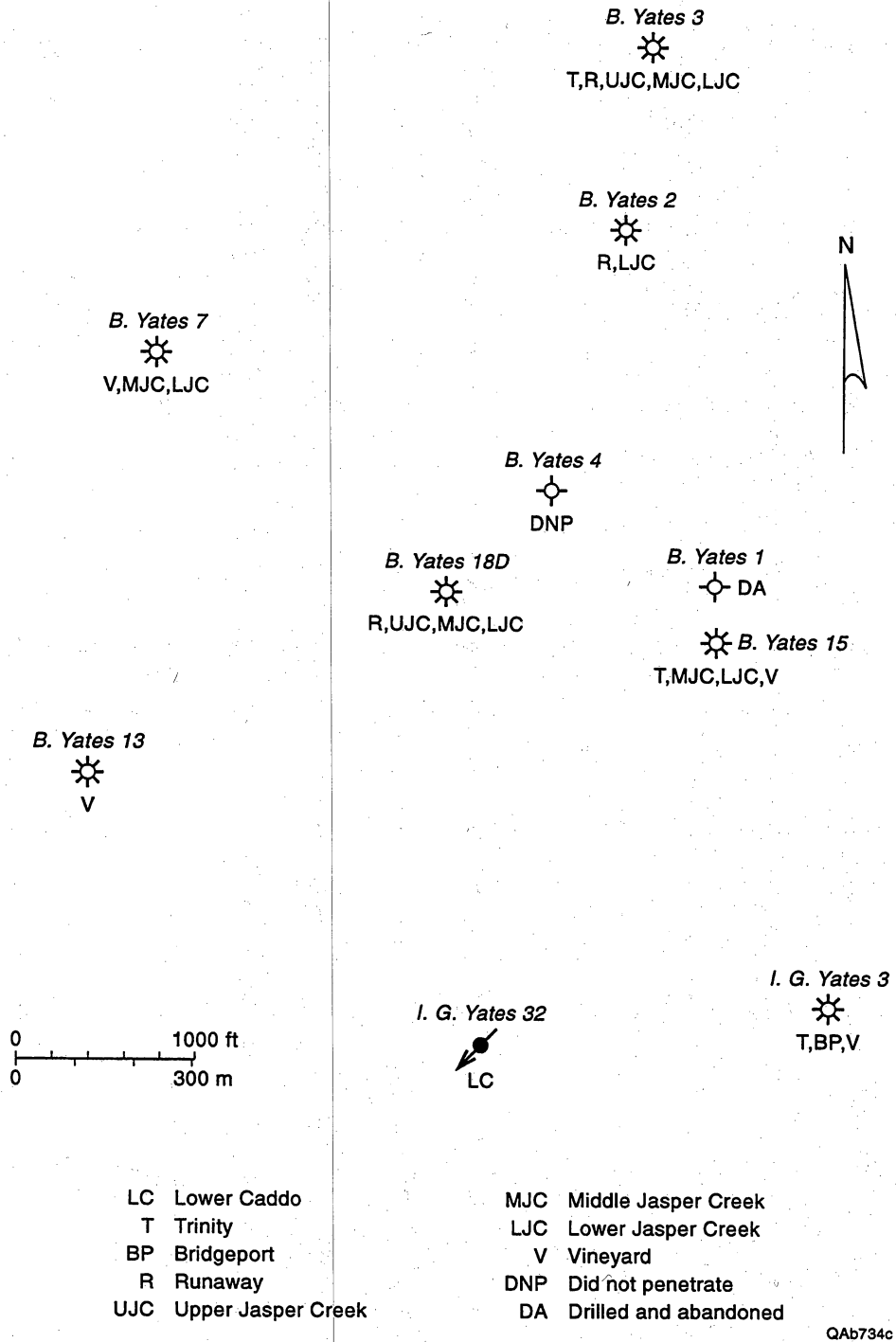


Figure 6.2. Expanded view of wells offsetting the B Yates 18D location.

The B Yates 2 was initially completed in the Lower Jasper Creek in 1950 but did not produce much gas. This well was tested unsuccessfully in the Vineyard in 1956 and then was recompleted successfully in the Runaway shortly thereafter. The B Yates 2 has produced over 1.1 Bscf from the Runaway interval and is still actively producing.

The B Yates 3 produced in excess of 3.4 Bscf from the Middle and Lower Jasper Creek from 1951 through 1992. In 1992, the well was recompleted in the Trinity, Runaway, and Upper Jasper Creek sequences, but these intervals have not contributed much, if anything, to the overall production from the well.

The B Yates 7 is one of the best Vineyard wells in the project area, producing over 5.7 Bscf. That interval is now abandoned, and the well has recently been recompleted in the Middle and Lower Jasper Creek. These zones were partially drained when recompleted, apparently from the B Yates 3 but are still producing about 200 Mscf/d.

The B Yates 13 was drilled and completed in the Vineyard in 1984. Despite being substantially drained at this location and finding only 457 psi bottomhole pressure in the Vineyard, the well has still produced about 350 MMscf to date. The B Yates 15 was drilled and completed in the Trinity, Middle and Lower Jasper Creek, and the Vineyard in 1985. The well has produced 544 MMscf from the combined intervals.

The I. G. Yates 3 was completed in the Trinity, Bridgeport, and Vineyard intervals in 1958. It is one of the best wells in the project area, producing in excess of 5.4 Bscf from these commingled zones. The I. G. Yates 32 was drilled to the Lower Caddo in 1992. This well found a bottomhole pressure of 618 psi, indicating significant depletion in the Lower Caddo. The I. G. Yates 32 was oil productive and was converted to a water injection well as part of a Lower Caddo waterflood project being conducted just to the southeast of the area shown in this figure.

B Yates 18D—Geological Perspective

From a review of the offsetting production history and the distribution of net pay and net hydrocarbon in the vicinity, Table 6.1 provides the projected reservoir conditions expected at the B Yates 18D location prior to drilling. Less than 5 ft of pay was expected in the Caddo, and the interval was expected to have poor reservoir quality and limited productive potential. Only 2 to 3 ft of net pay was anticipated in the Wizard Wells; this interval was expected to exhibit poor reservoir quality. There was no sand development projected in the Davis sequence.

Table 6.1. Reservoir conditions projected at the B Yates 18D location based on offset well data.

Interval	Net pay (ft)	Projected reservoir conditions
Caddo	<5	Poor reservoir quality, limited productive potential
Wizard Wells	2-3	Very poor reservoir quality, no potential
Davis	0	No sand development
Trinity	5-6	Low permeability, limited potential, depletion from B Yates 15
Bridgeport	0-1	Almost no sand development
Runaway	2-3	Limited sand development, drained by B Yates 2
Beans Creek	0	No sand development
U Jasper Creek	0	No sand development
M Jasper Creek	5-6	Partial depletion from B Yates 3, 15?
L Jasper Creek	7-8	Partial depletion from B Yates 3, 15?
Vineyard	30-35	Substantial depletion from B Yates 7, 13, 15

The Trinity sequence looked as though it might encounter 5 to 6 ft of net pay, but this interval appeared to be low permeability. In addition, there was also the likelihood of some depletion from the B Yates 15 well to the east. There was almost no sand development expected in the Bridgeport, and only 2 to 3 ft of net pay projected in the Runaway. In addition, any pay in the Runaway was expected to be substantially drained by the B Yates 2 well to the northeast. There did not appear to be any sand development in the Beans Creek or the Upper Jasper Creek at the B Yates 18D location.

About 6 to 8 ft of net pay was expected in both the Middle and Lower Jasper Creek intervals. It appeared likely, however, that the Jasper Creek reservoirs at this location could be at least partially drained by Jasper Creek gas production from the B Yates 3 and 15 wells. Finally, some 30 to 35 ft of net pay was projected in the Vineyard. There was no doubt that a thick Vineyard interval would be found, but it was expected to be substantially depleted by gas production from the B Yates 7, 13, and 15 wells.

All in all, from an engineering and geological perspective, **the B Yates 18D location appeared to offer multiple completion possibilities**, but the degree of pressure depletion or reservoir quality to be expected in any particular sequence was somewhat uncertain. The location was, in fact, **in a favorable part of the project area** where at least four net pay intervals with a total of at least 1.5 net hydrocarbon feet were expected between the Lower Caddo and the Vineyard (see Figures B19 and B20 in Appendix B of Volume II). Ultimately, **however, the B Yates 18D location was chosen primarily from the 3-D seismic information.**

B Yates 18D—Seismic Interpretation Objectives

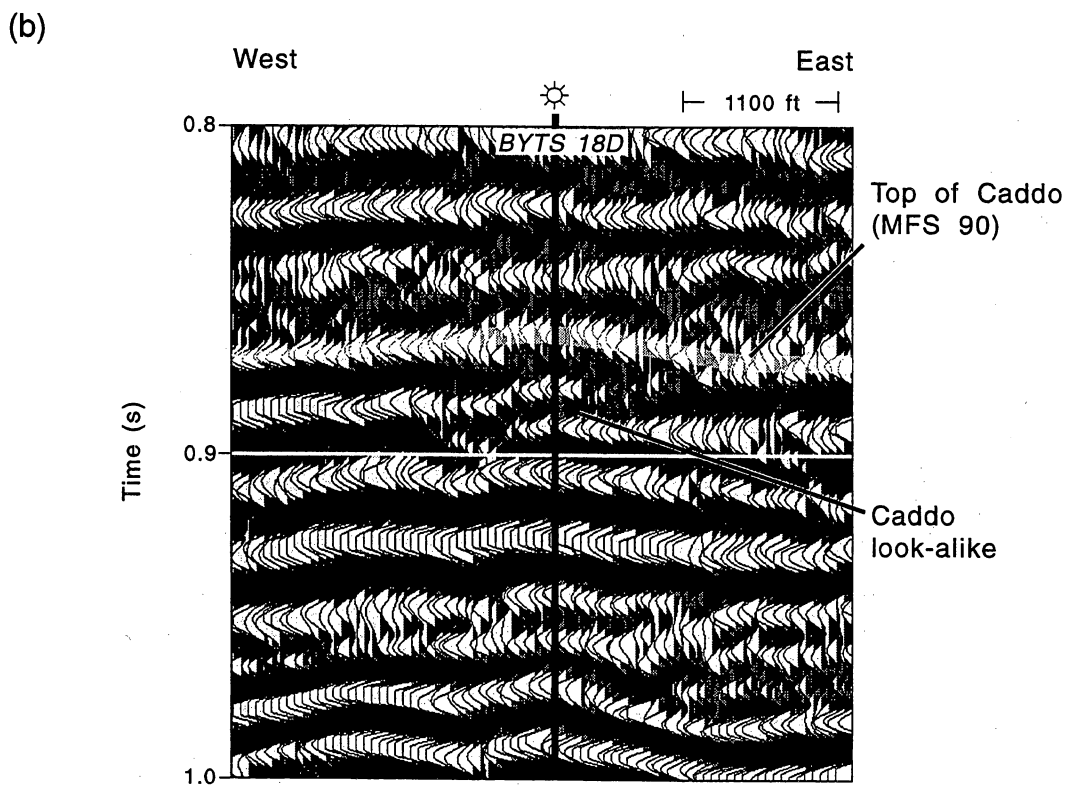
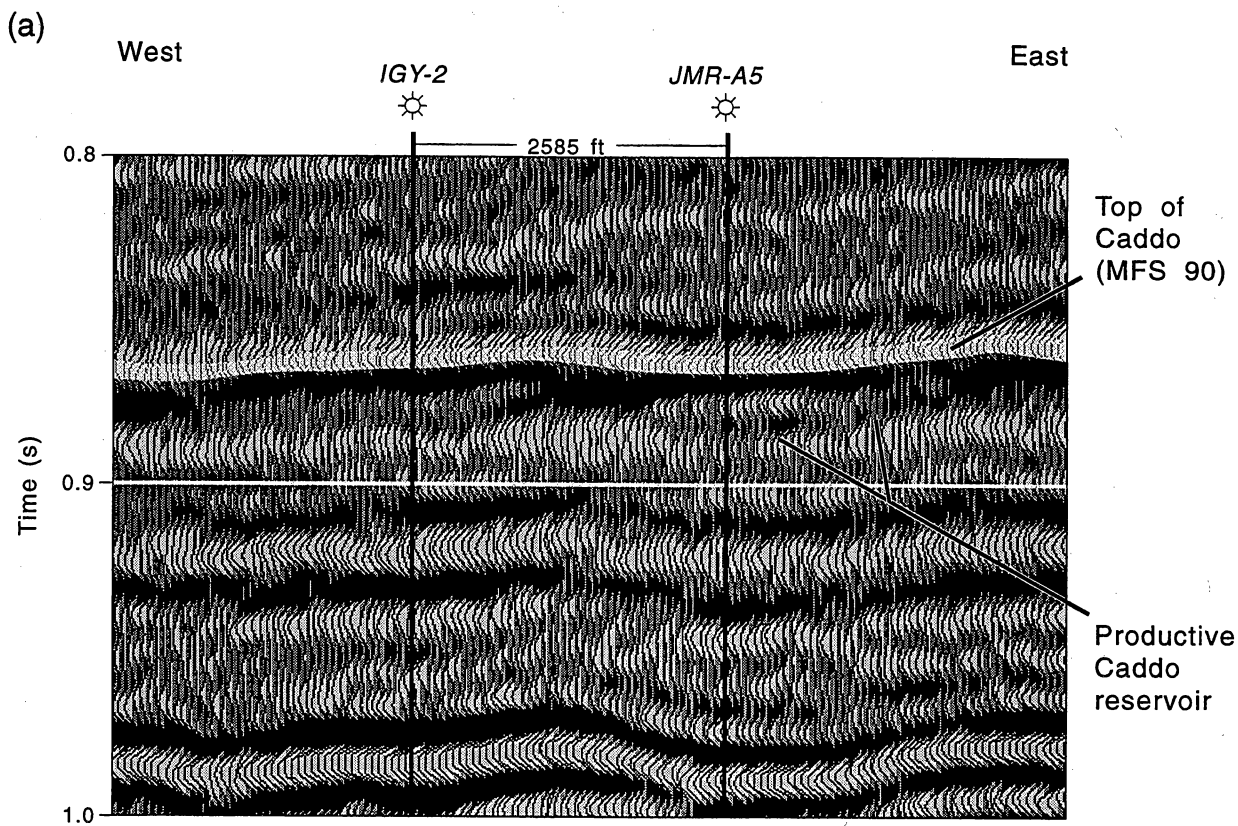
One objective that Threshold Development hoped to achieve with the B Yates 18D was to locate an uncontacted Caddo reservoir. Thus, a **dual-objective, seismic interpretation approach** was employed in the short time allowed to locate possible drill sites: the **primary objective being to find a Caddo seismic image that was a look-alike to the seismic image at a known productive Caddo reservoir, and the secondary objective being to ensure that attractive trapping geometries existed within several Bend Conglomerate sequences below any productive Caddo look-alike that could be found.**

The distinctive seismic response associated with the productive Caddo reservoir penetrated by the Mitchell J. M. Robinson A5 well was selected as the look-alike target that was kept in mind while reviewing the Caddo reflection response over the entire

26-mi² survey area. The reflection character at the Robinson A5 well is illustrated in Figure 6.3a. A Caddo seismic response much like the one occurring at the Robinson A5 well was found at crossline-inline coordinates 151, 111 and is presented in Figure 6.3b. This 3-D seismic coordinate point, which is where the B Yates 18D well was drilled, thus satisfied the primary objective for a drilling site—**that an attractive Caddo drilling target existed at the location.** The secondary drilling objective—that the site also had additional attractive Bend Conglomerate targets—was also satisfied as is documented in Figure 6.4. The seismic section shown here passes through the well coordinates and documents that a **vertical sequence of potential reservoir entrapments, consisting either of pinch-outs or small-throw faults, was stacked throughout the Bend interval at the B Yates 18D location.**

B Yates 18D—Caddo Facies

Even though the Caddo seismic response at the B Yates 18D well site resembled the seismic response at the productive Robinson A5 well, the Caddo facies found by the B Yates 18D well was not productive. Logs from the Robinson A5 and from the B Yates 18D wells are compared in Figure 6.5 and show that the Caddo response at the B Yates 18D location is caused by two thin limestone units, not by a productive sand as at the Robinson A5. (The B Yates 18D well log data are presented in more detail in Figures 6.6, 6.7, and 6.8.) The discrepancy between the depositional facies at these two Caddo seismic look-alikes illustrates a principle known by all experienced seismic interpreters—**seismic responses are not unique, and often two or more stratigraphic relationships can produce the same seismic response.** Thus, even though the search for look-alikes to the seismic response at a known productive reservoir is a sound and rather widely practiced procedure for identifying potential drill sites, **the technique does involve an element of risk,** as it did in this Caddo situation.



QAb263c

Figure 6.3. (a) East-west seismic profile showing the seismic response of a productive Caddo reservoir penetrated by the Robinson A5 well (JMR-A5). (b) East-west seismic profile showing the seismic response of a Caddo look-alike of the JMR-A5 response. The B Yates 18D well was drilled to test this look-alike feature.

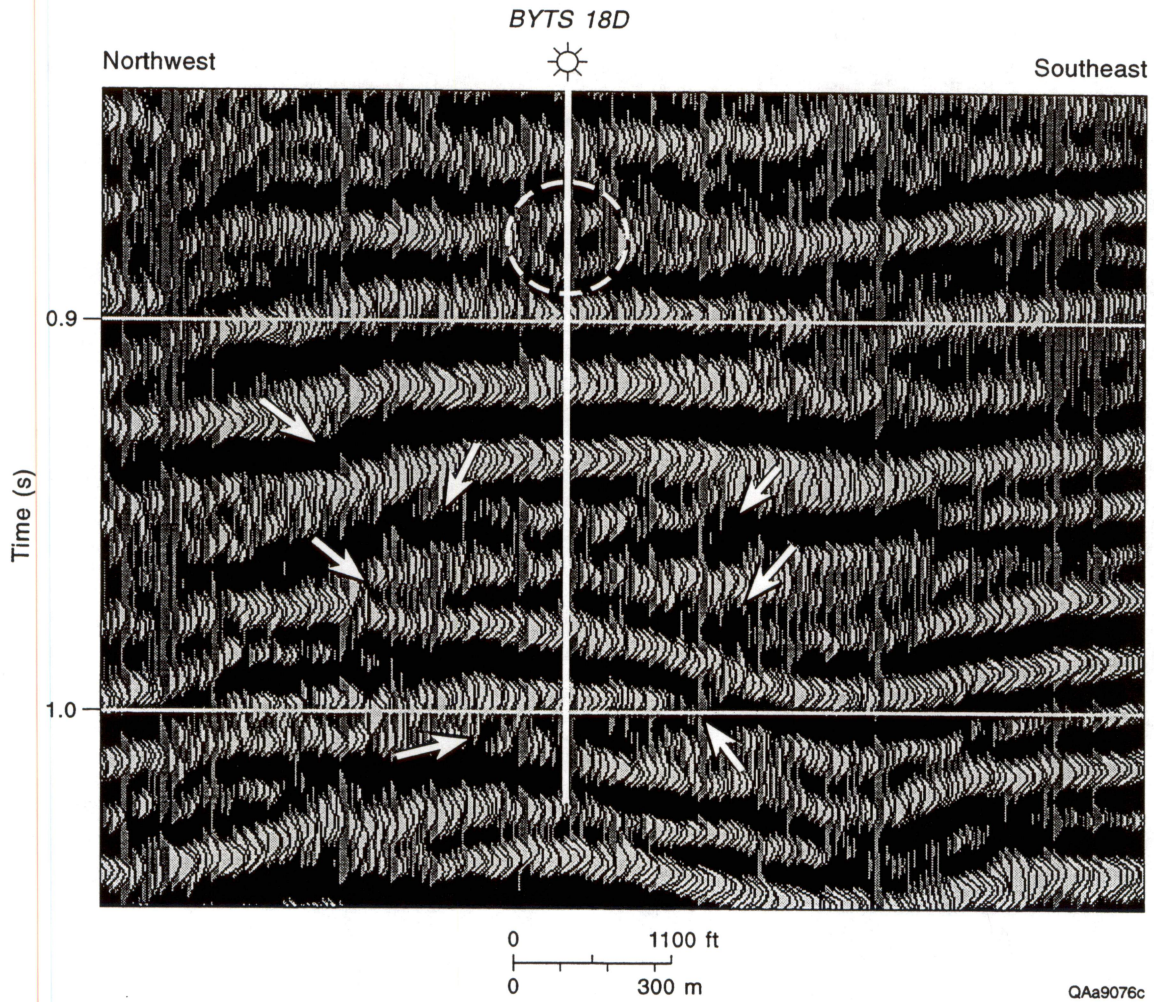


Figure 6.4. A northwest-southeast seismic profile passing through the B Yates 18D drill site. The circled feature just above 0.9 s is the Caddo look-alike of the Robinson A5. The arrows identify where numerous stratigraphic and fault entrapments occur within the Bend Conglomerate, providing a multiple-play opportunity at this drill site.

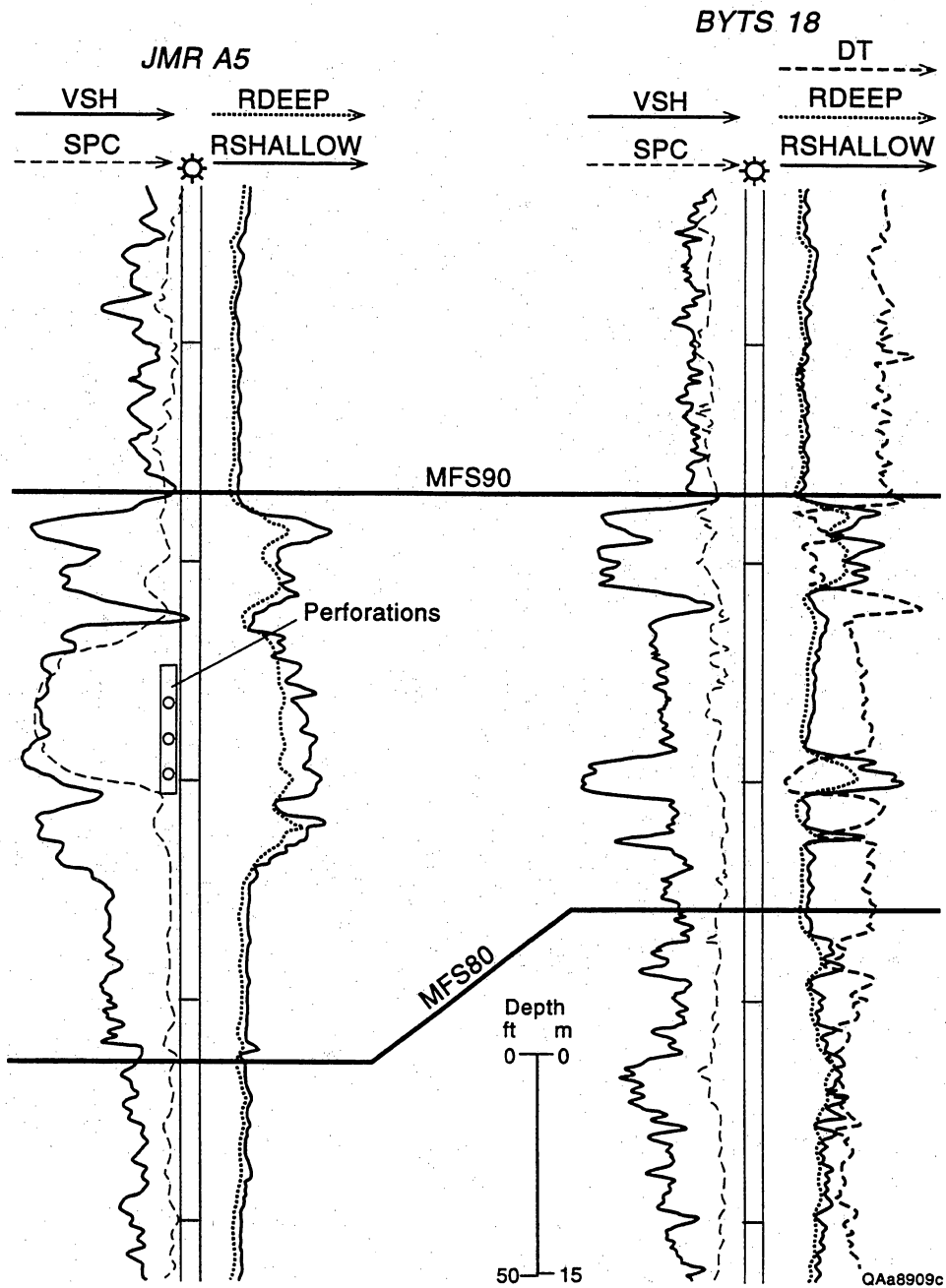
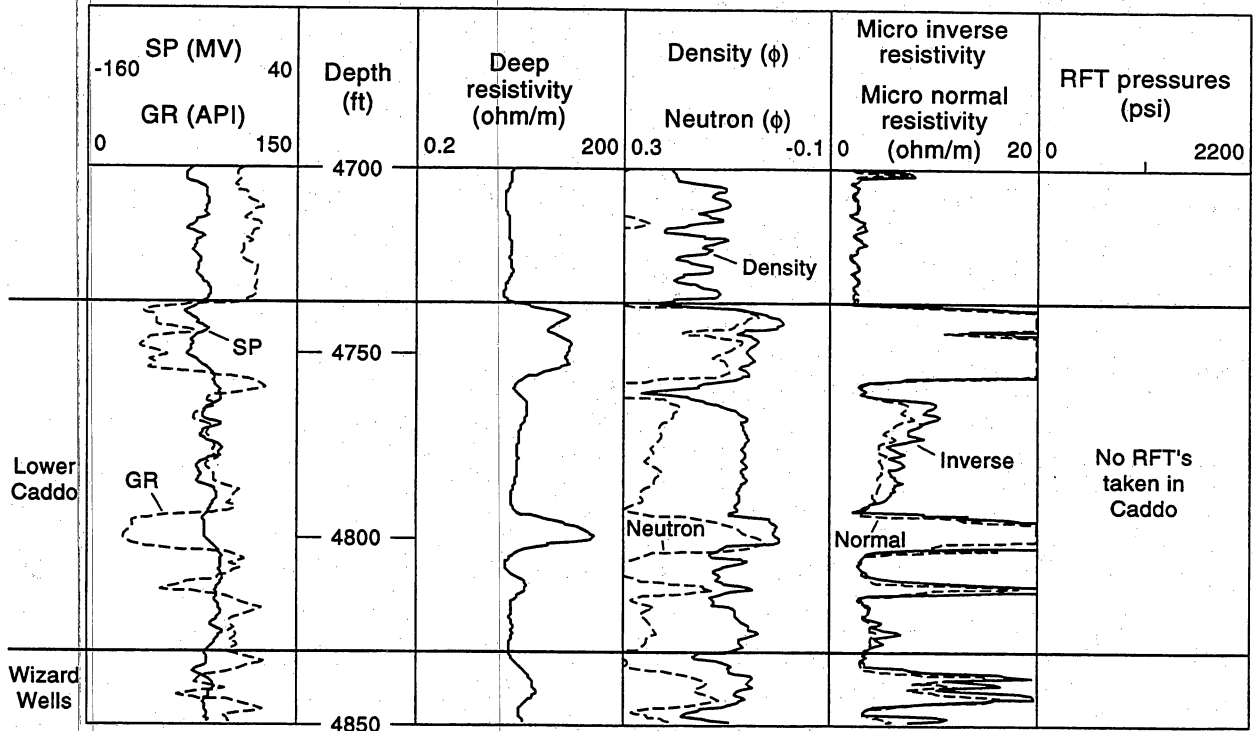


Figure 6.5. Comparison of log data from the productive Caddo interval at the Robinson A5 well with the log data from the Caddo interval at the B Yates 18D. The Caddo seismic response at the B Yates 18D is caused by two thin limestone units within the sequence, and no productive facies is present.



QAb735c

Figure 6.6. Open-hole logs run across the upper portion of the Bend intervals in the B Yates 18D well showing no Lower Caddo sand development.

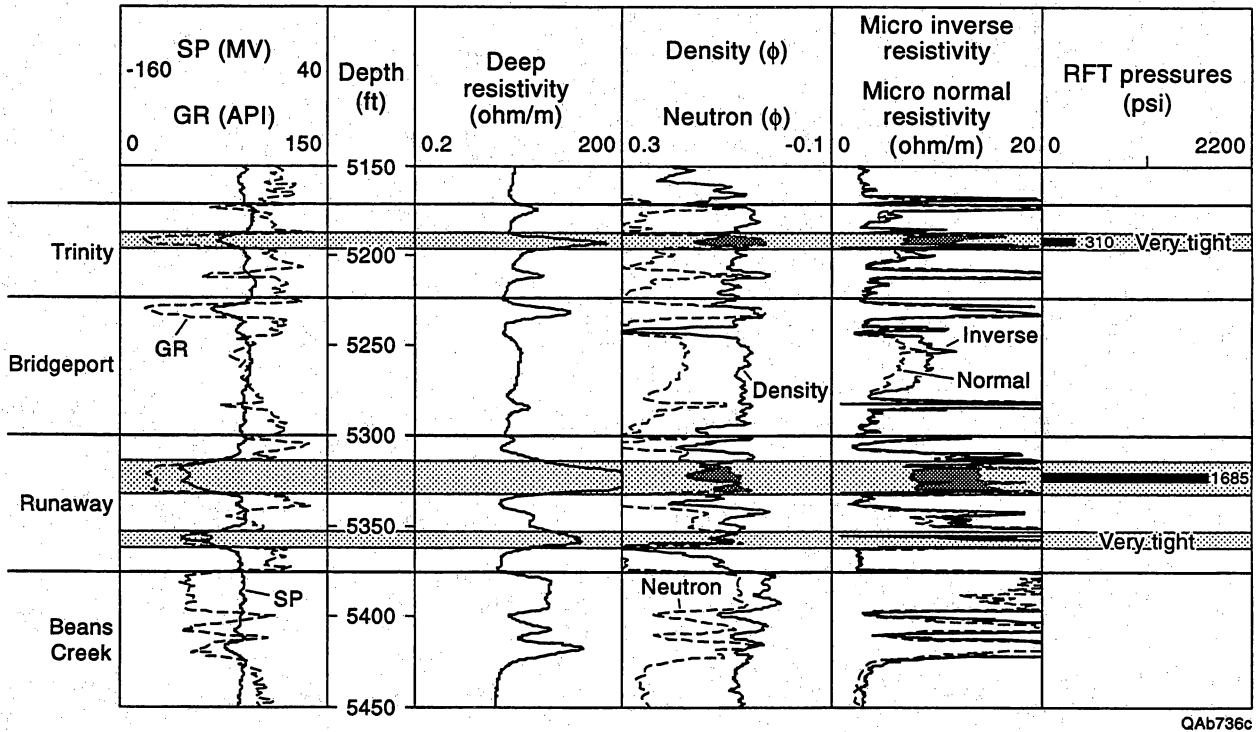
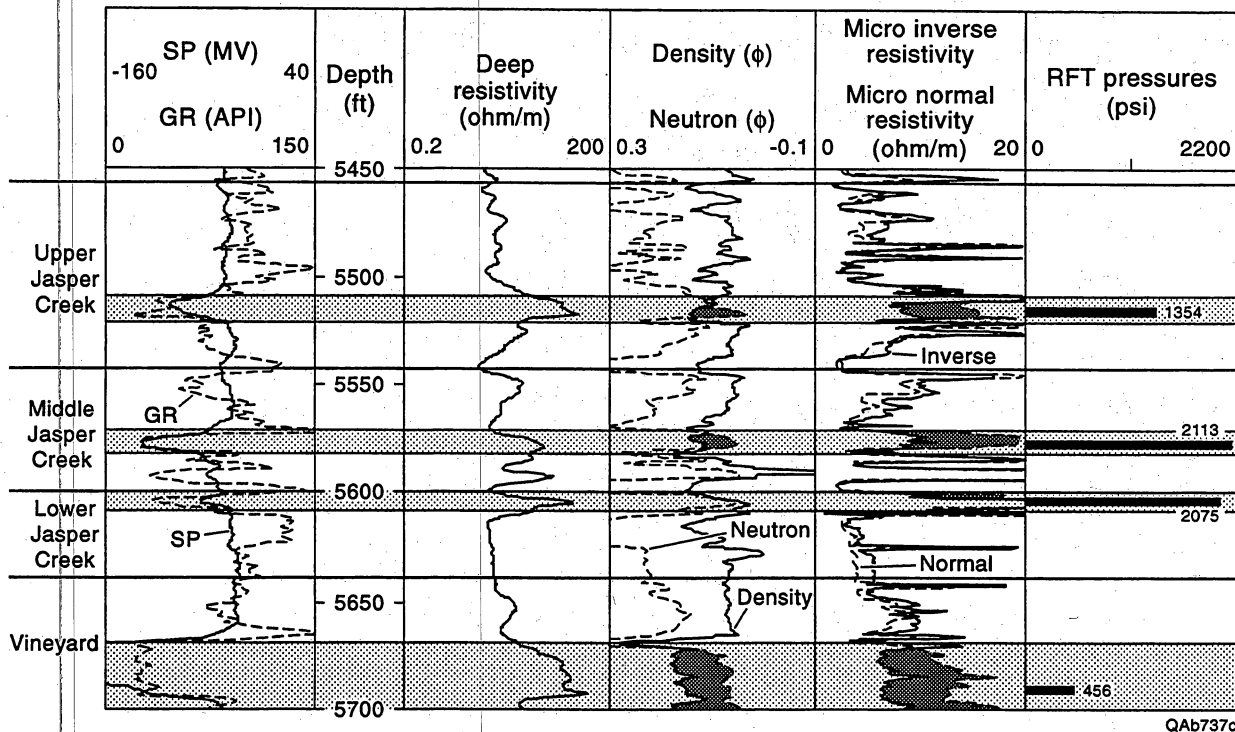


Figure 6.7. Open-hole logs run across the Trinity, Bridgeport, Runaway, and part of the Beans Creek sequences in the B Yates 18D well. The 20-ft sand encountered in the Upper Runaway appears to be an isolated reservoir at original pressure.



QA6737c

Figure 6.8. Open-hole logs run across the Jasper Creek and Vineyard sequences in the B Yates 18D well. Several of the Jasper Creek intervals appear to be isolated reservoirs. Good Vineyard zone encountered, as expected, with substantial pressure depletion.

B Yates 18—Well Operations

The B Yates 18D was drilled to a total depth of 5,750 ft through the Vineyard. As discussed earlier, the Lower Caddo sand was not developed as suggested by the initial seismic interpretation, but the Trinity, Jasper Creek, and Vineyard sequences were present much as expected. In addition, there was some sand development in the uppermost part of the Jasper Creek that had not been anticipated. The most encouraging feature encountered in the B Yates 18D was the development of a 20-ft sand in the upper part of the Runaway sequence. **This sand was not (and really could not have been) predicted from the available engineering or geologic data available prior to drilling this well.**

B Yates 18D—Log Interpretations

Figure 6.6 presents the upper section of the open-hole well logs recorded in the B Yates 18D. The logs shown in the figure include the SP, gamma-ray, deep-resistivity, neutron, density, microlog, and RFT tools. The section shown in Figure 6.6 includes the Caddo and the upper part of the Wizard Wells. As the logs indicate, there was no sand development in the Caddo and almost no porosity. The Caddo was not a productive interval, and, as expected, neither was the Wizard Wells sequence.

Figure 6.7 shows the open-hole logs recorded across the Trinity, Bridgeport, Runaway, and part of the Beans Creek sequences. As expected, the Trinity interval had 4 to 5 ft of net pay; notice the crossover in both the porosity logs and the microlog. Two attempts were made to measure pressures with an RFT in this interval. The behavior of the tests suggested that the zone is tight. One test did record a pressure of 310 psi, although pressure was still building when the test was concluded after about 15 minutes. This low measured pressure may suggest depletion from the Trinity reservoir via the

B Yates 15, but it more likely indicates a lower permeability interval in the Trinity and insufficient time for the pressure to build up completely.

In the Runaway sequence, the 2 to 3 ft of lower sand was what had been expected. RFT's run in this interval suggest that this sand is relatively tight. As mentioned previously, however, what was not anticipated was the 20 ft of sand encountered in the upper part of the Runaway. Qualitatively, according to the logs, this Upper Runaway sand has good gas effect on the porosity logs, and the microlog indicates that the reservoir is permeable. The RFT measured a pressure of 1,685 psi in this interval after about 20 minutes. **This is as high a pressure as any ever recorded in the project area in the Runaway sequence. This sand appeared to be an isolated Runaway reservoir at original reservoir pressure.**

Figure 6.8 shows the open-hole logs recorded across the Jasper Creek and Vineyard sequences. All three Jasper Creek intervals should be productive, but the Upper and Middle Jasper Creek appear to have the best reservoir quality. **The pressures measured with the RFT of 2,113 and 2,075 psi in the Middle and Lower Jasper Creek, respectively, are essentially original pressure, suggesting no drainage of gas at this location.** Because the pressure of 1,354 psi recorded in the Upper Jasper Creek was still building at the rate of several psi/min when the RFT was concluded, it should be considered only a lower-bound estimate of the current reservoir pressure. Even so, **this pressure would indicate only partial drainage from the Upper Jasper Creek at this location at best.** As mentioned previously, however, sand development in the Upper Jasper Creek was not anticipated in the B Yates 18D, because **this sequence is not encountered in nearby offsetting wells.** Thus, if the Upper Jasper Creek has been partially drained, it is not clear where the communication exists; geologically, **this sequence appears to be isolated at this location.**

Finally, Figure 6.8 shows that the Vineyard has 25 to 30 ft of net pay as expected and that the reservoir is substantially depleted at this location, as indicated by the 456 psi

pressure in the interval measured with the RFT. Although the pressure in the Vineyard is far below its original value, it should be remembered that this is the thickest, best connected, most productive gas-producing interval in the project area. Thus, depending on the reservoir pressure level in the Vineyard reservoir surrounding this well location and the effective drainage area, this zone may still contribute as much as 150 to 200 MMscf (or more) to the total gas recovery from this well. Note that the B Yates 13 well (Figure 6.2) recorded an initial pressure of 457 psi in the Vineyard in 1985 and has produced in excess of 350 MMscf from the Vineyard reservoir alone since then. **The Vineyard is neither compartmented nor poorly drained at this location, but it still may be an important completion interval in this well from the standpoint of ultimate gas recovery.**

In summary, **the B Yates 18D did not encounter an isolated Caddo compartment as anticipated, but it did find at least four intervals that encountered original or near original pressure in the Runaway and Jasper Creek sequences.** This result suggests that multiple, stacked, isolated reservoirs can still be found in the Bend Conglomerate as suggested by the seismic image in Figure 6.4. All in all, including the Vineyard interval, there may be **as many as 5 to 6 viable completion zones in this well.** The key to the successful long-term performance of this well, however, will be the size of the gas reserves associated with these compartments or poorly drained areas.

B Yates 18D—Engineering Analysis of Runaway Reservoir

Initially, Threshold elected to complete only the Upper Runaway sand from 5,317 to 5,331 ft. The zone was treated with 1,250 gal of acid and fractured with about 22,000 gal of nitrogen foam and 34,000 lb of sand. The well was produced for about 1 mo, and then shut in for a 2-week pressure buildup test.

The initial Runaway production from the B Yates 18D is shown in Figure 6.9. The well came on line producing about 1.4 MMscf/d, but both the flow rate and the flowing

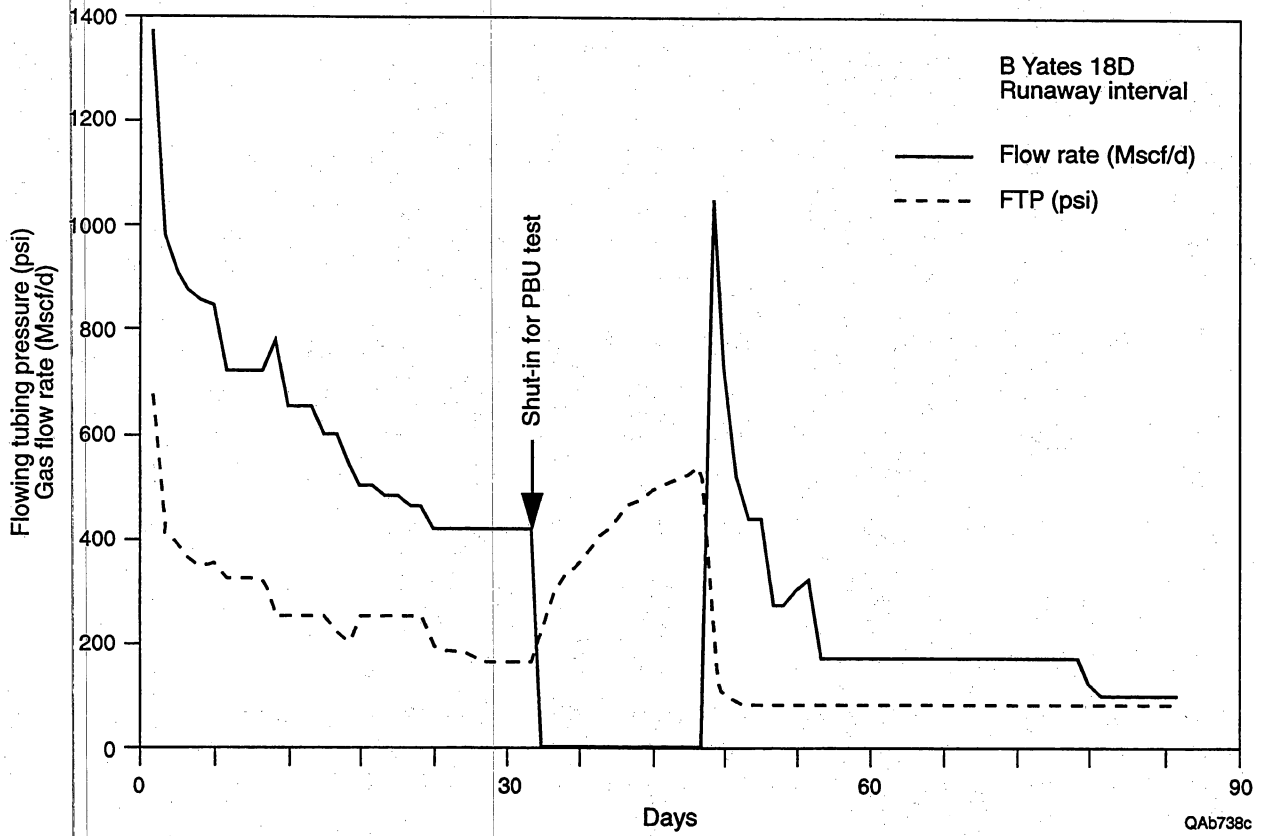


Figure 6.9. Flow rates and pressures for the Upper Runaway interval in the B Yates 18D well.

tubing pressure declined rapidly during the first month. The flow rate prior to shut-in for the well test was 420 Mscf/d. Cumulative gas production prior to the well test was about 20 MMscf.

Figures 6.10 and 6.11 present the well test results, which indicate that the **Upper Runaway interval is a very small reservoir**. As shown in the figures, the bottomhole pressure built up to only about 650 psia after 2 weeks of buildup and was beginning to level off. A quantitative analysis of the test data yields an average reservoir pressure of 720 psia. The initial reservoir pressure, as measured with the RFT, was at least 1,685 psia. Thus, **the reservoir pressure had apparently declined more than 1,000 psi after only about 20 MMscf of gas was produced. This suggest a reservoir size of about 8 acres.**

Figure 6.11 shows a log-log plot of the pressure change and pressure derivative for this well test. In this figure, adjusted pressure change versus adjusted equivalent time (Al-Huissnay and others, 1966; Agarwal, 1979, 1980; Lee, 1986) is plotted. The upper curve is the pressure data, and the lower curve is the derivative data. What these plots show are very early wellbore storage effects, followed by a period of bilinear flow, indicative of a finite conductivity hydraulic fracture. At an adjusted equivalent time of about 0.2 h, boundary effects are first observed in the test data. In this case, the boundaries appear to be the side(s) of a channel. Ultimately, near the end of the test, both the pressure and the pressure derivative begin to decrease, and the derivative data roll over and start to decline. This behavior suggests that we have likely encountered all reservoir boundaries during the test.

Figure 6.11 also shows the results of a history-match of the actual test data generated using a finite-difference reservoir simulator and the reservoir description shown in Figure 6.12. The reservoir description used to match the test data consists of a long, narrow channel that widens somewhat away from the well. The channel is only about 90 ft wide near the wellbore. **The total areal extent of the reservoir is just more than**

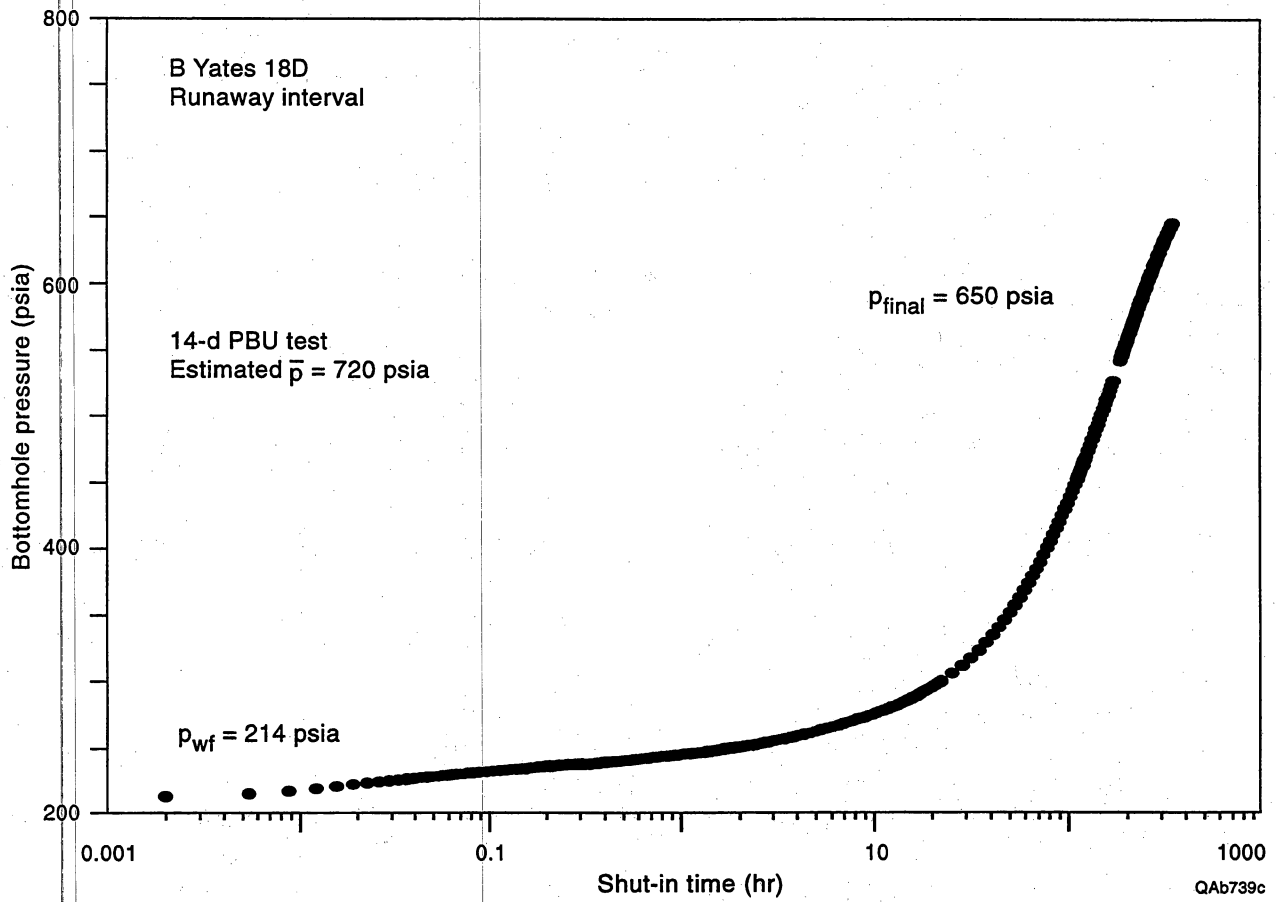


Figure 6.10. Pressure data recorded during the 2-week buildup test conducted in the Upper Runaway reservoir in the B Yates 18D well.

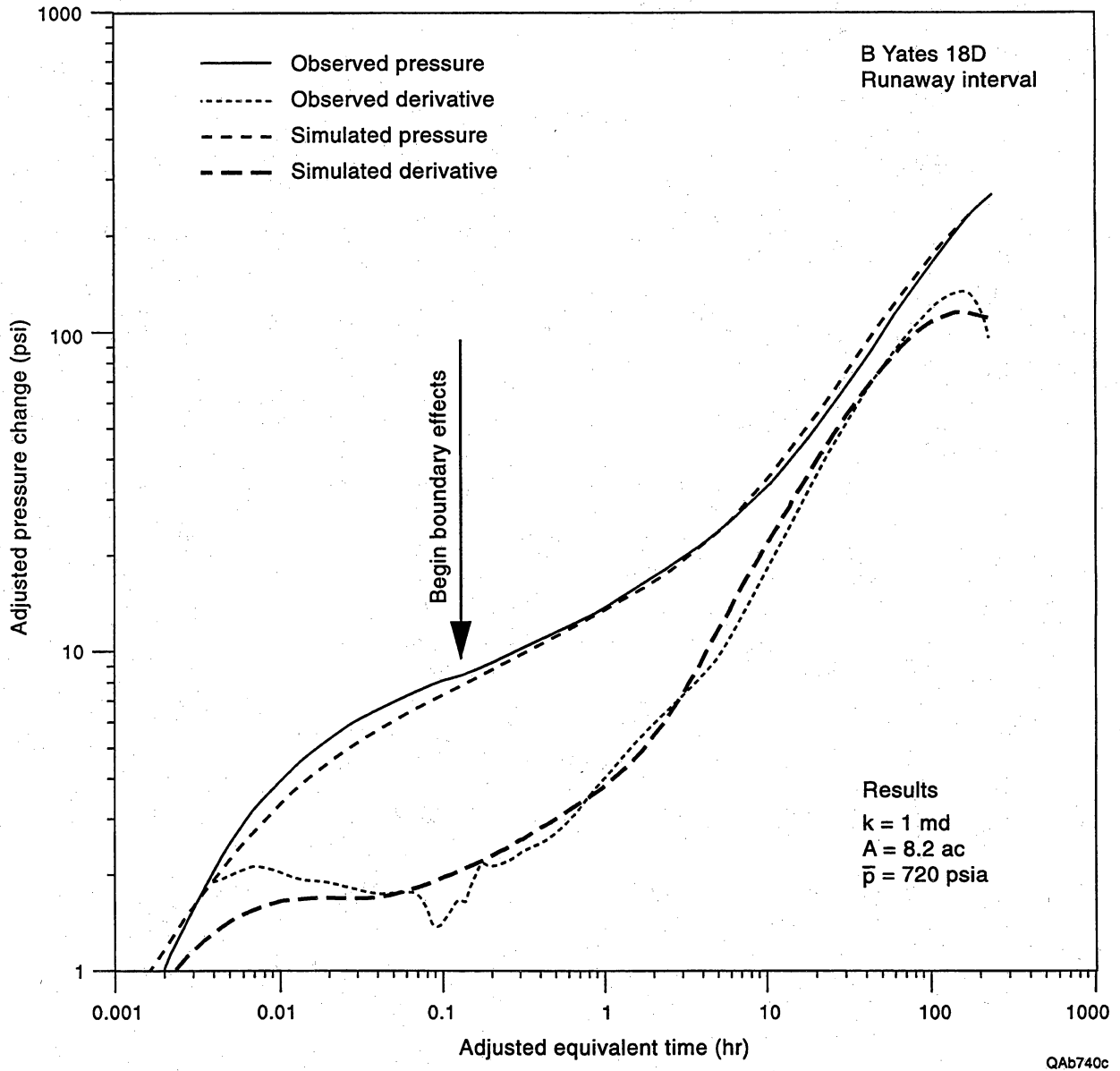


Figure 6.11. History match of B Yates 18D Upper Runaway well test. These data suggest a reservoir size of about 8 ac.

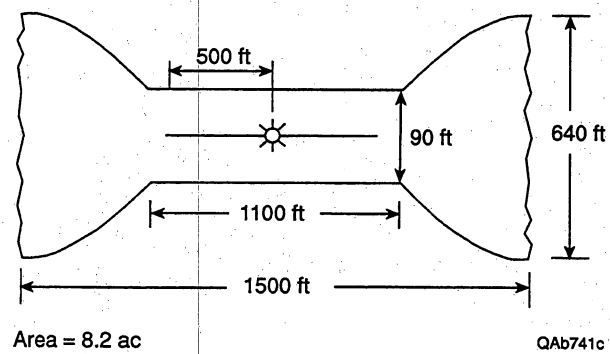


Figure 6.12. Schematic diagram of reservoir model used to history match B Yates 18D Upper Runaway well test data.

8 acres. Whereas this is a reasonable model for the test data, it is not unique, and other, similar reservoir descriptions may fit the data equally well. Even so, **a small reservoir size and a near-well boundary are features that must be included** in any reasonable interpretation of the test data.

Following the well test, the B Yates 18D was returned to production. As a result of the pressure buildup in the reservoir, the well came back on line making 1.05 MMscf/d. The flow rate declined quite rapidly, however, as shown in Figure 6.9, and within a matter of days, the well was producing at rates below those prior to the well test. Threshold produced the Upper Runaway reservoir for about another month following the well test, and in that time, the well recovered another 10 MMscf of gas. Finally, in mid-April, after producing only about 30 MMscf, Threshold abandoned the Upper Runaway, and recompleted the well in the three Jasper Creek intervals, commingling the production from all three zones.

B Yates 18D—Engineering Analysis of Jasper Creek Reservoir

Figure 6.13 shows the first few weeks of production from the Jasper Creek reservoirs; **these results look more encouraging.** The combined production from the Jasper Creek intervals was in excess of 1 MMscf/d initially, and these zones are currently flowing about 600 Mscf/d, with little decline in flowing tubing pressure. Cumulative production from these Jasper Creek reservoirs is approximately 40 MMscf after only 7 weeks on line. These early results suggest that the Jasper Creek reservoirs may have a larger areal extent than the Upper Runaway sand.

B Yates 18D—Seismic Analysis of Jasper Creek Reservoir

The Boonsville 3D seismic data indicate that a distinctive seismic facies is associated with the Middle–Lower Jasper Creek sequences at the B Yates 18D well.

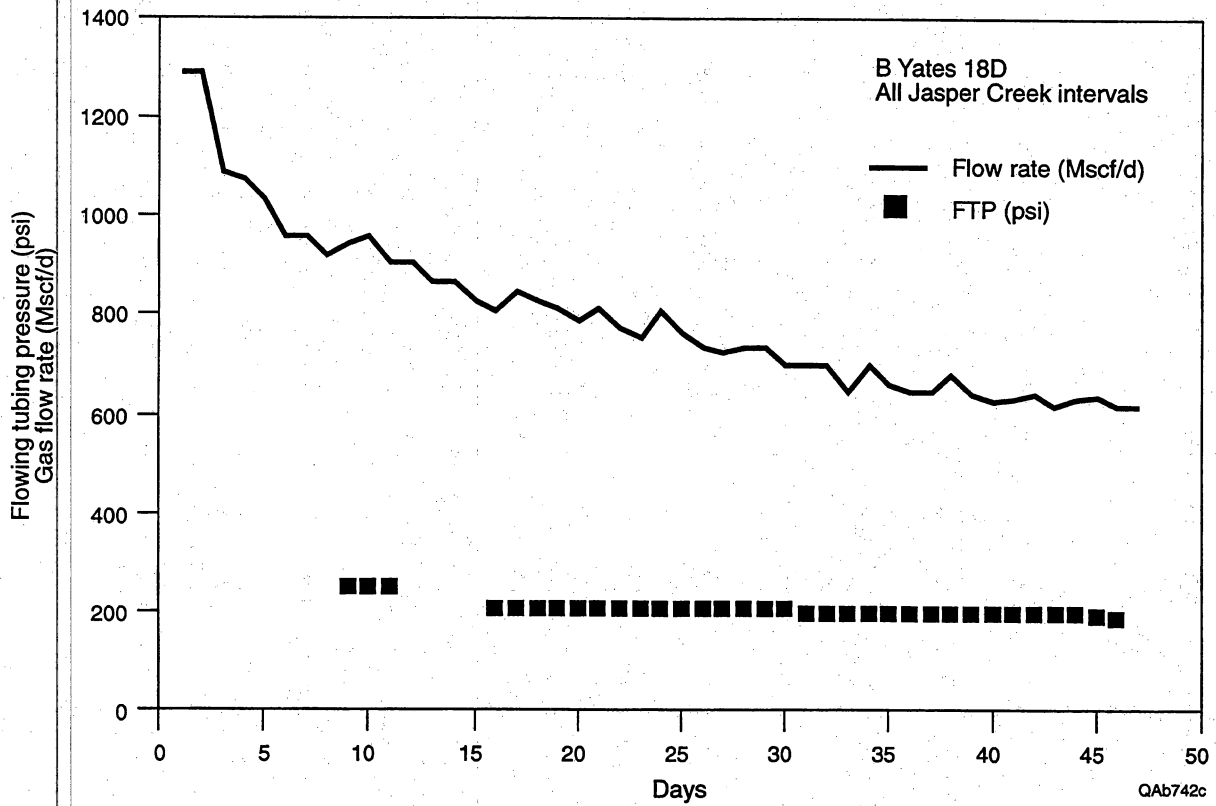


Figure 6.13. Initial production from the Jasper Creek reservoirs in the B Yates 18D well.

Tentatively we are assuming that this facies maps the productive limits of the Jasper Creek reservoir being produced at the 18D well. To illustrate the facies, a northeast-southeast seismic line (Line 1) traversing the B Yates 18D well is shown as Figure 6.14. The top of the Lower Jasper Creek sequence at this well, and at the B Yates 7 well to the northwest, is positioned on a low-amplitude reflection peak according to the B Yates 18D depth-to-time calibration function. This seismic section shows that the amplitude of this reflection event increases significantly as the Lower Jasper Creek boundary, the surface labeled MFS32 in the figure, is traced toward the southeast. It is **the low-amplitude portion of this reflection event, immediately adjacent to the B Yates 18D well, that results in the distinctive seismic facies that appears to indicate the producing reservoir facies.**

A map view of the Middle–Lower Jasper Creek reflection amplitude is presented in Figure 6.15. The position of Line 1 is labeled, as well as a second profile, Line 2, which will not be shown. This reflection amplitude map shows that small positive reflection amplitudes, that is, the amplitude range shown by that segment of the color bar between 0 and about +18,000, extend away from the 18D well as narrow trends toward the east, southeast, and northwest, and also seem to extend westward, past two interpreted faults, and reach the B Yates 7 well.

The conclusion that this low-amplitude reflection pattern is a distinct seismic facies is also supported by the instantaneous seismic frequencies, which are displayed in Figure 6.16. Narrow trends of anomalous frequency values, shown by the red bins, follow the same areal boundary pattern, as do the low-amplitude reflections, suggesting that the low-amplitude reflections are bounded by subtle stratigraphic and/or structural discontinuities. (See Appendix E of Volume II for illustrations of several relationships between stratigraphic and structural discontinuities and anomalous instantaneous frequencies.) To know whether these stratigraphic and structural changes form flow barriers without incorporating production history into the seismic interpretation is

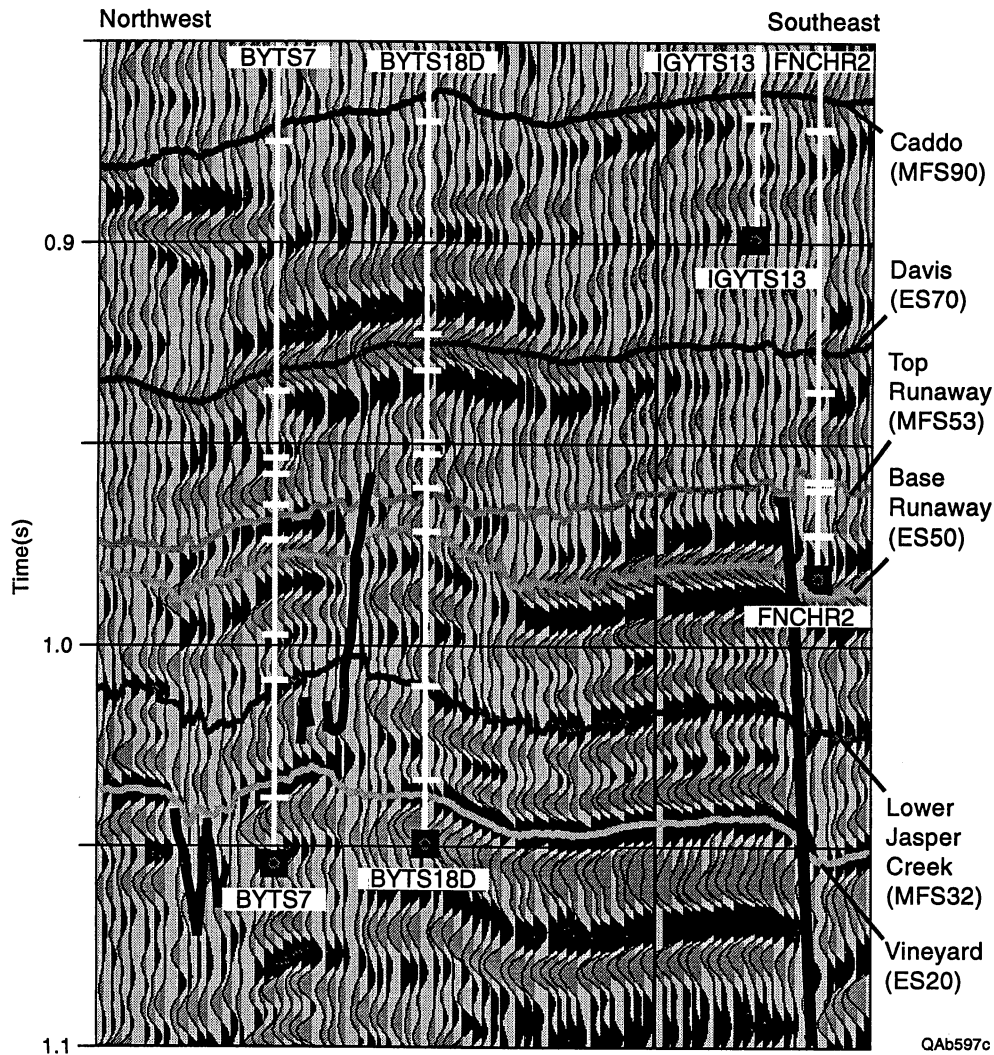


Figure 6.14. Seismic line traversing the BYTS 18D well and illustrating the distinctive, low-amplitude reflection facies associated with the Jasper Creek interval (MFS32) in the immediate vicinity and northwest of the 18D well. This profile is labeled Line 1 in Figure 6.15.

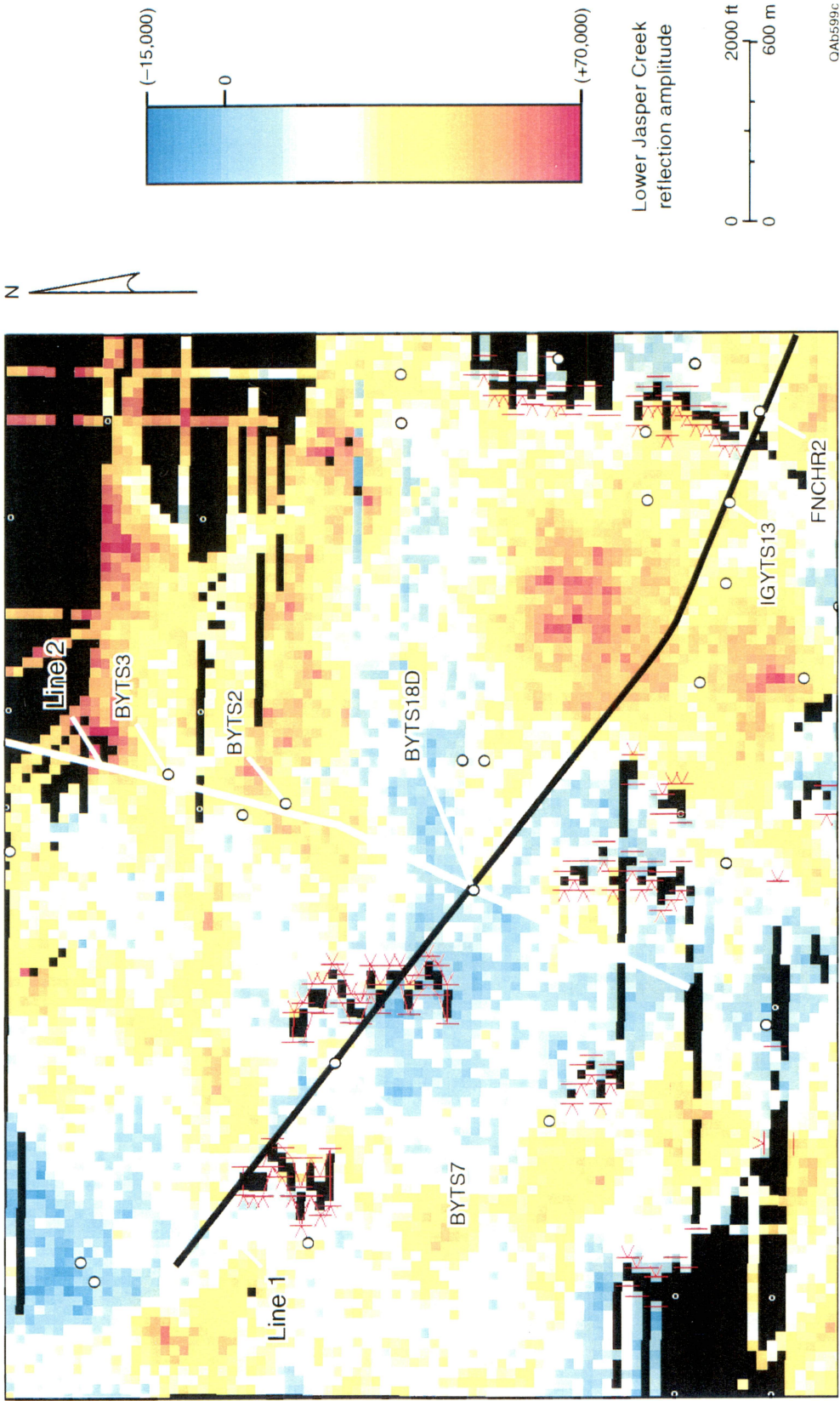


Figure 6.15. Map of seismic reflection across the MFS32 (Lower Jasper Creek) sequence boundary near the BYTS 18D well. The amplitude parameter that is displayed is the average amplitude in a 5-ms window centered on the MFS32 surface. Variations in the magnitude of this seismic amplitude attribute are assumed to indicate variations in rock facies in the Middle-Lower Jasper Creek interval. The areal pattern of low-amplitude (green) reflection facies is tentatively assumed to indicate the productive limits of the BYTS 18D Jasper Creek reservoir.

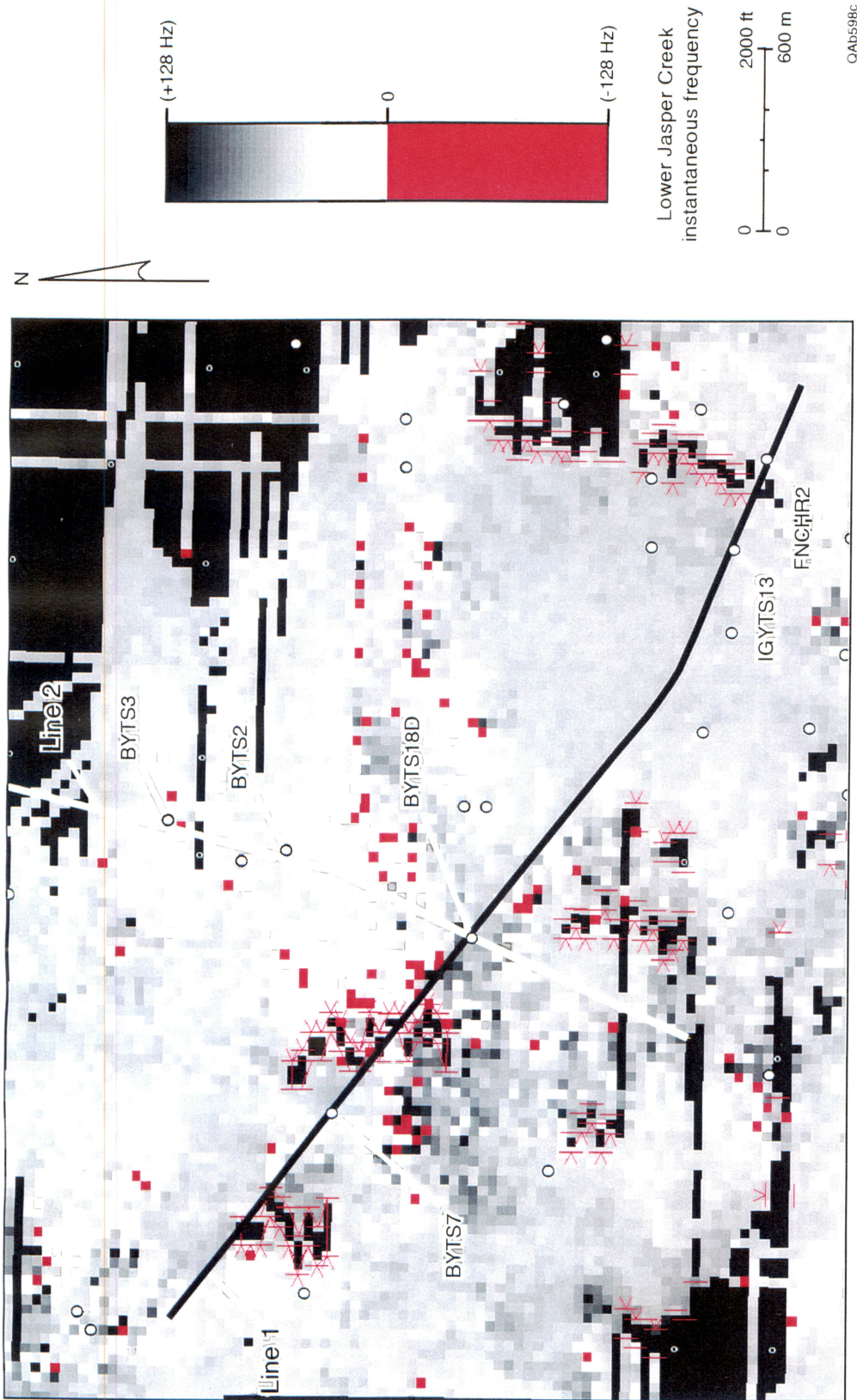


Figure 6.16. Map of instantaneous seismic frequency values across the MFS32 (Lower Jasper Creek) sequence boundary near the BYTS 18D well. Note that trends of anomalous negative frequencies (red stacking bins) follow the same areal pattern as does the low-amplitude reflection facies in the preceding figure. In Appendix E, anomalous negative values of instantaneous frequency are shown to coincide with distorted reflection waveforms, which in turn commonly indicate subtle stratigraphic and/or structural changes. Therefore, the instantaneous frequency behavior shown here supports the concept that the low-amplitude reflection facies in the preceding figure may be bounded by stratigraphic and/or structural disruptions, and thus be a distinct compartment.

impossible; however, a reasonable starting hypothesis regarding the size and the geometry of the producing Jasper Creek reservoir at the B Yates 18D well is that the areal distribution of the reservoir is portrayed by the low-amplitude reflection pattern shown in Figure 6.15.

B Yates 17D—Engineering Overview

Figure 6.17 shows the location of the B Yates 17D well in the west-central part of the project area. The B Yates 17D well was drilled about 1 mo after the B Yates 18D, and like the B Yates 18D, **the B Yates 17D was sited at a location (crossline, inline coordinates = 171, 53) where there appeared to be a vertical sequence of several stratigraphic and structural entrapments throughout the Bend Conglomerate interval (Fig. 6.18).** From a seismic standpoint, the primary targets were the Trinity and the Jasper Creek, where the 3-D seismic data suggested possible isolation from offsetting gas production.

Figure 6.19 presents an expanded view of the B Yates 17D location and the surrounding wells. Briefly reviewing the completion history of the wells offsetting the B Yates location, the B Yates 8 and 9 wells were drilled in 1957 and completed as oil wells in the Upper Caddo. Neither well penetrated the Bend intervals below the Caddo. The B Yates 8 well produced 70,000 STB of oil from the Upper Caddo through July 1979; the well is currently completed as a gas well in the Strawn sands up-hole. The B Yates 9 made 110,000 STB of oil from the Upper Caddo through December 1989; currently, this well is also producing from the Strawn sands up-hole.

The B Yates 10 was initially completed in the Vineyard, producing 3.43 Bscf from April 1958 through June 1980. From June 1980 through June 1993, this well was completed and commingled in the Davis, Trinity, and Beans Creek reservoirs, producing a total of 210 MMscf of gas and about 6,000 STB of oil–condensate from the three zones combined. In July 1993, this well was recompleted to the Strawn sands.

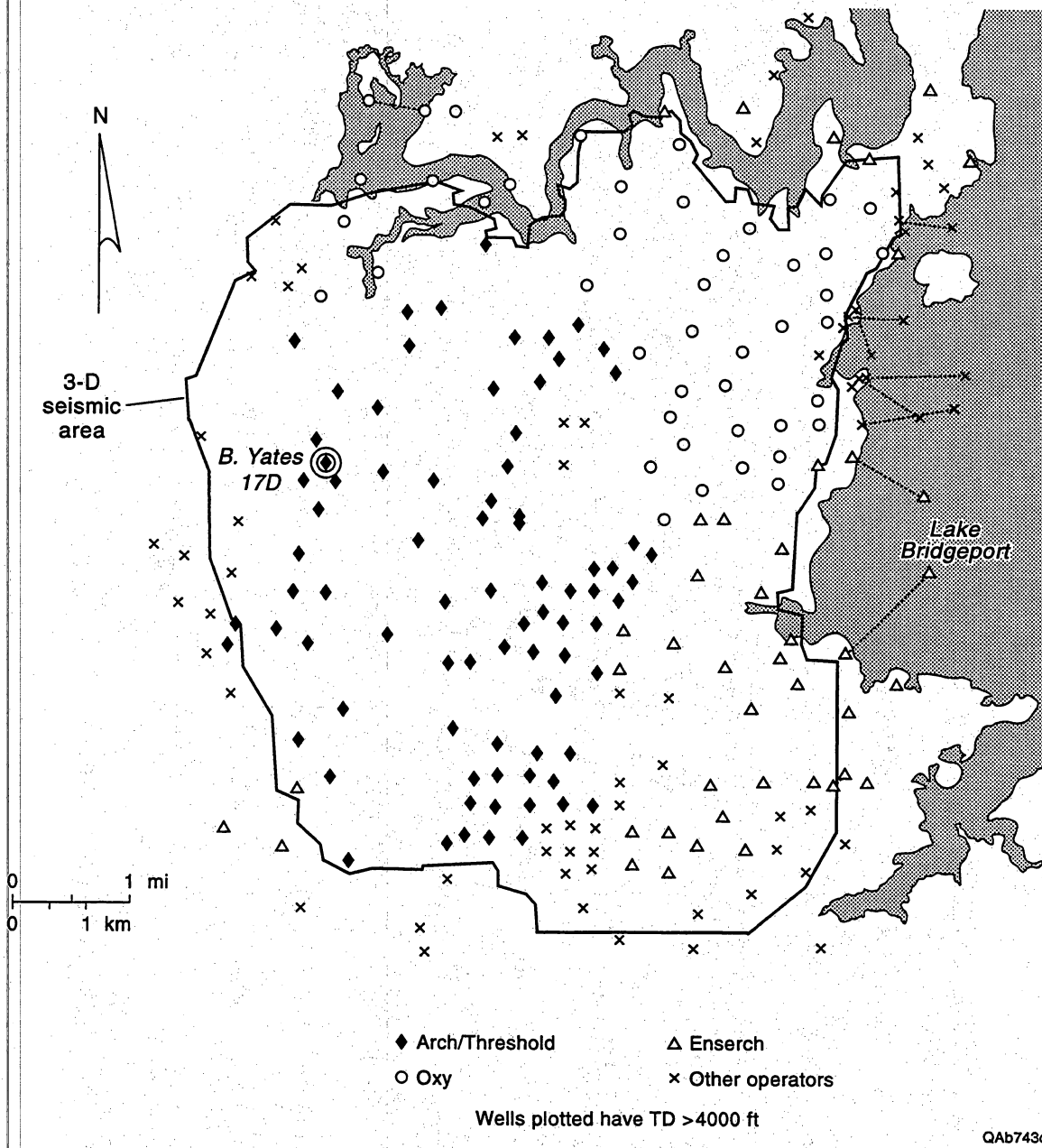


Figure 6.17. Location of the B Yates 17D well in the west-central part of the project area.

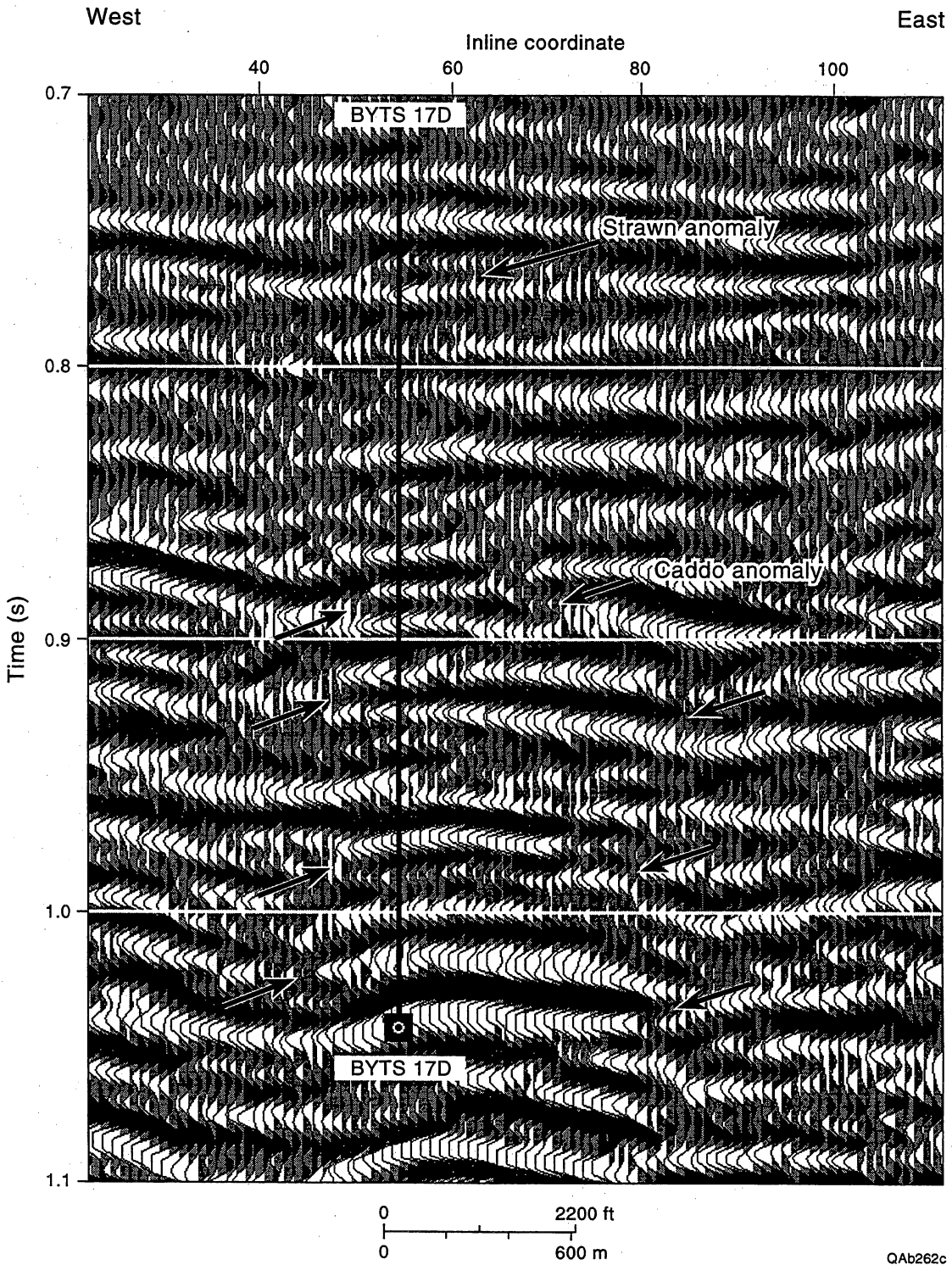
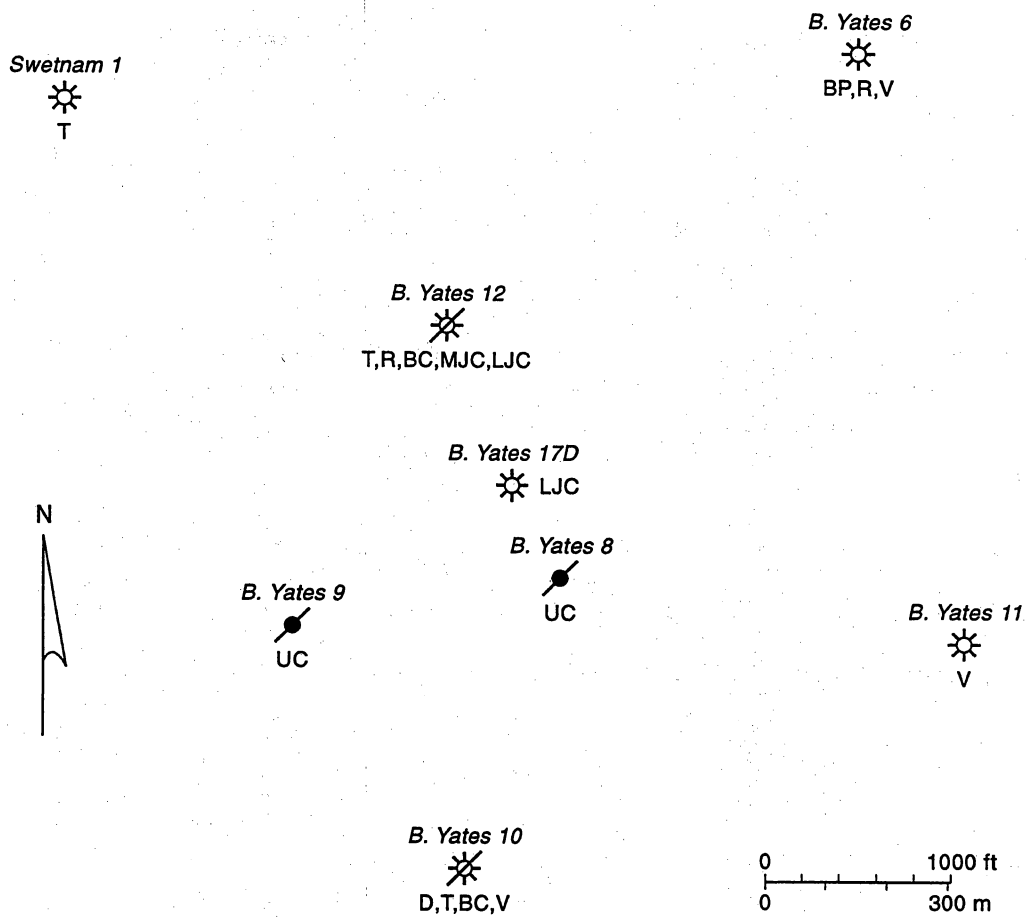


Figure 6.18. Seismic profile passing through the B Yates 17D well location showing the Caddo look-alike response to the Robinson A-5 well at about 0.88 s and several vertically stacked entrapment possibilities highlighted by arrows down to 1.03 s.



Note: Well symbols indicate Bend/Caddo completion status only.

- | | | | |
|----|-------------|-----|---------------------|
| UC | Upper Caddo | BC | Beans Creek |
| D | Davis | MJC | Middle Jasper Creek |
| T | Trinity | LJC | Lower Jasper Creek |
| BP | Bridgeport | V | Vineyard |
| R | Runaway | | |

QAb744c

Figure 6.19. Expanded view of wells offsetting the B Yates 17D location.

The B Yates 12 was drilled in September 1983 and initially completed in the Vineyard, Middle Jasper Creek, and Runaway zones. The Vineyard interval did not produce much gas after fracturing and was subsequently isolated below a bridge plug in May 1984. The Middle Jasper Creek and Runaway intervals were produced together, making a total of only about 90 MMscf. In February 1990, perforations were added in the Trinity, Beans Creek, and Lower Jasper Creek sequences. All five zones were commingled, and the well recovered another 45 MMscf through August 1992. The well has been shut in since then.

The B Yates 6 well was drilled in July 1957 and produced 1.44 Bscf from the Vineyard through December 1979. The Vineyard perforations were abandoned, and the well was recompleted in the Bridgeport and Runaway intervals. These zones are still producing commingled at 30 Mscf/d and have made about 440 MMscf to date.

The B Yates 11 well was drilled in July 1971 and completed in the Vineyard with an initial bottomhole pressure of 938 psi, indicating prior depletion in the Vineyard at this location. This well is still producing from the Vineyard at about 30 Mscf/d; it has recovered about 900 MMscf of gas to date. The Dallas Royalty Swetnam 1 was completed in the Trinity in April 1973. It was originally classified as an oil well and has been a marginal producer. The well is currently making about 10 Mscf/d.

B Yates 17D—Geological Perspective

From a review of the offsetting production history and the distribution of net pay and net hydrocarbons in the area, the B Yates 17D location appeared to offer multiple completion opportunities. As with the B Yates 18D well, the B Yates 17D location was also in a favorable part of the project area where at least four net pay intervals were expected between the Lower Caddo and the Vineyard (see Figures B19 and B20 in Appendix B of Volume II). Reservoir-quality sand development was anticipated in the Trinity, Bridgeport, Runaway, and Jasper Creek sequences prior to drilling, but the

degree of pressure depletion or reservoir quality in any particular sequence was not certain. Reservoir-quality sands were also anticipated in the Upper Caddo and Vineyard sequences, but both these intervals were expected to be substantially depleted by offsetting production. Note that this well was sited and drilled prior to development of the Caddo seismic attributes maps described in Section 3.

B Yates 17D—Well Operations

The B Yates 17D was drilled to a total depth of 5,650 ft through the Vineyard. From an analysis of the openhole logs run in the Bend interval, potential completion opportunities were identified in the Trinity, Runaway, and Middle Jasper Creek sequences. There was some sand development observed in the Lower Jasper Creek and Bridgeport sequences as well, although not enough for these zones to be considered viable completion targets. Most of these sands were thin (less than 10 ft), with fairly low porosity (5 to 7 percent). The prolific Upper Caddo reservoir present in the B Yates 8 and 9 wells was not found in the B Yates 17D; rather, the Upper Caddo is mostly limestone at this location. The Vineyard reservoir was present and substantially depleted (reservoir pressure of 500 psi) as expected.

RFT pressures were measured on only two intervals in this well, the Vineyard and the Lower Jasper Creek, because of problems with the tool itself. Lost circulation materials were added to the mud system in this well to combat a lost circulation problem encountered while drilling through the Vineyard. Due to this lost circulation material in the wellbore, the RFT tool plugged frequently and would not seat on occasion. The tool was removed twice from the wellbore to clean it and resume testing, but each time, it plugged again quickly after being run back in the hole.

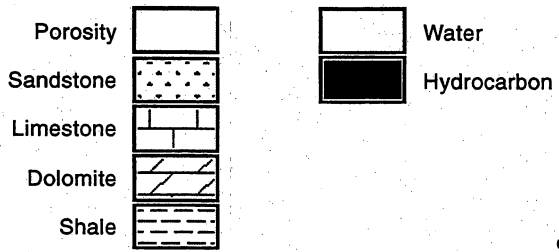
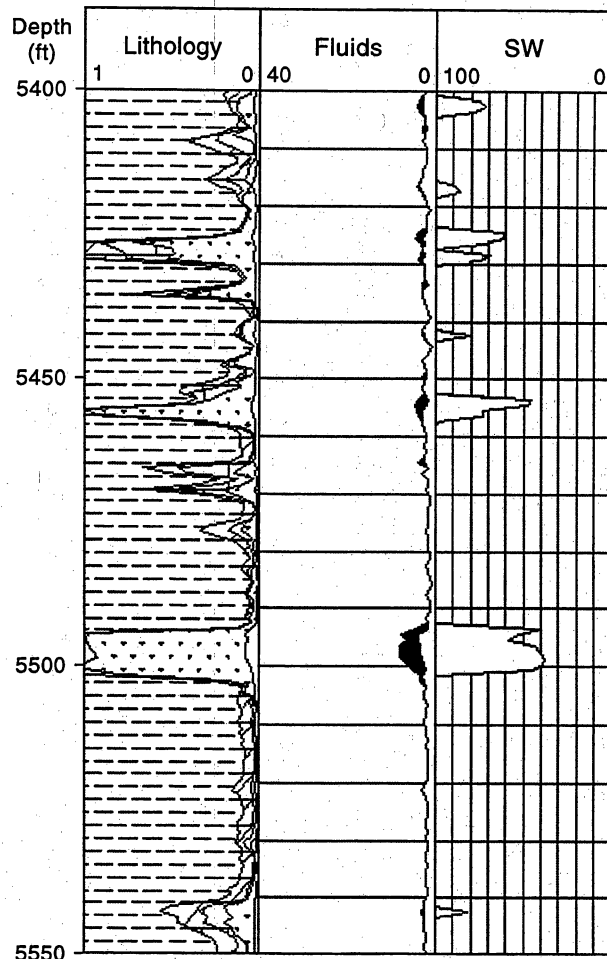
The only RFT value considered reliable from this well was the first test conducted in the Vineyard interval, which yielded a pressure of 500 psi. RFT pressures of 2,384 and 2,596 psi were measured in the Lower Jasper Creek interval, but these values do not

appear to reflect actual reservoir pressure. First, these pressures are much higher than the values of 1,900 to 2,100 psi generally associated with initial pressure in the Jasper Creek sequence in the project area (depending on depth). Further, considering that (1) the lower pressure of 2,384 psi was still increasing about 20 psi/min when the test was concluded and (2) the hydrostatic pressure of the mud column was about 2,630 psi at this depth (5,500 ft), it appears the tool was leaking and that these pressures reflect hydrostatic head and not the reservoir pressure in the Lower Jasper Creek. Unfortunately, **because of the problems with the RFT tool, it was not possible to conclude whether most of the potential Bend reservoirs are isolated compartments or are in communication with production from offset wells.**

Initially Threshold elected to complete only the Lower Jasper Creek sand from 5,496 to 5,502 ft in mid-January 1995. Figure 6.20 is an interpreted log across the Jasper Creek intervals in the well. The Lower Jasper Creek has 6 ft of net pay, with a porosity of 7.2 percent and a water saturation of 43.4 percent. This zone was hydraulically fractured with about 19,000 gal of fluid and 31,000 lb of 20/40 Ottawa sand. Following the treatment, the well was swabbed and cleaned up for several days; then it began flowing about 200 Mscf/d at 80 psi tubing pressure on a 20/64-inch choke. The well was put on production several days later making 250 Mscf/d against 60 psi flowing tubing pressure, producing into a compressor.

B Yates 17D—Engineering Analysis of Lower Jasper Creek Reservoir

Figure 6.21 shows the early production from the Lower Jasper Creek interval. In the first few months of production, the B Yates 17D well has averaged between 150 and 250 Mscf/d. The periodic declines in flow rate are due to liquid loading in the wellbore; the well makes 1 to 2 bbl of condensate periodically. When the liquids are swabbed from the wellbore, the flow rate jumps back up to about 250 Mscf/d. Threshold has recently installed a plunger lift in this well to keep the wellbore fluids lifted on a regular basis.



QAb745c

Figure 6.20. Interpreted log for the Jasper Creek sequences penetrated by the B Yates 17D well. The well is completed in the Lower Jasper Creek from 5,496 to 5,502 ft.

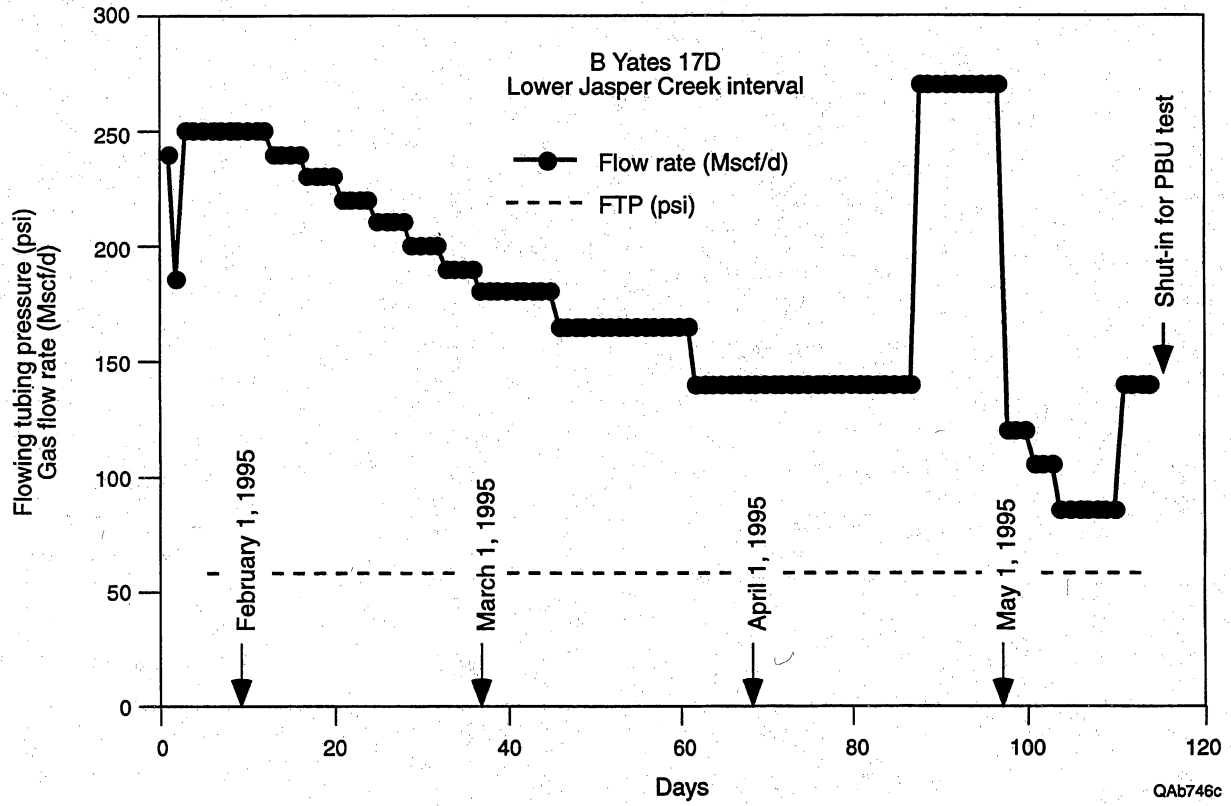


Figure 6.21. Initial production from the Lower Jasper Creek in the B Yates 17D well.

The B Yates 17D was shut in for a 2-week pressure buildup test in mid-May 1995. The final flow rate prior to shut-in was 140 Mscf/d at a flowing bottomhole pressure of 414.3 psi. The Lower Jasper Creek reservoir had produced about 20 MMscf of gas prior to the well test.

Figure 6.22 is a log-log plot of the pressure buildup test data, with adjusted pressure change plotted vs. equivalent adjusted time (Al-Huissany and others, 1966; Agarwal, 1979, 1980; Lee, 1986). The upper curve is the actual pressure change data, whereas the lower curve is the pressure derivative. The buildup test data were matched to a type curve developed by Cinco and others (Cinco and Samaniego, 1981) for analyzing wells with finite conductivity hydraulic fractures. This type curve is usually best when analyzing test data from hydraulically fractured wells with moderate permeability, as was the case for this Lower Jasper Creek reservoir.

The “hump” observed early in the test data (at an equivalent adjusted time of about 0.1 h) is most likely due to phase segregation (Fair, 1981); at this point, the pressure in the wellbore had built up sufficiently to force any liquid accumulated at the bottom of the hole back into the formation. Beyond this point, the test data match the type curve well, and the later-time data exhibit pseudoradial flow, suggesting that a straight line should develop on the semilog plot, whose slope can be used to calculate permeability. In addition, the type curve analysis shows no indications of reservoir boundaries being encountered during the test.

Figure 6.23 shows the semilog (Horner) plot of the test data (Horner, 1951). Using the slope of the straight line identified in the figure, a permeability of 3.6 md was calculated, using the net pay of 6 ft computed for the Lower Jasper Creek reservoir. This analysis also yielded an apparent skin factor (s') of -5.4 , indicating stimulation of the formation by the fracture treatment. Extrapolating this semilog straight line to infinite shut-in time yields a pressure (p^*) of 678 psi. This pressure should be a reasonable approximation of the current average reservoir pressure; the actual value for current

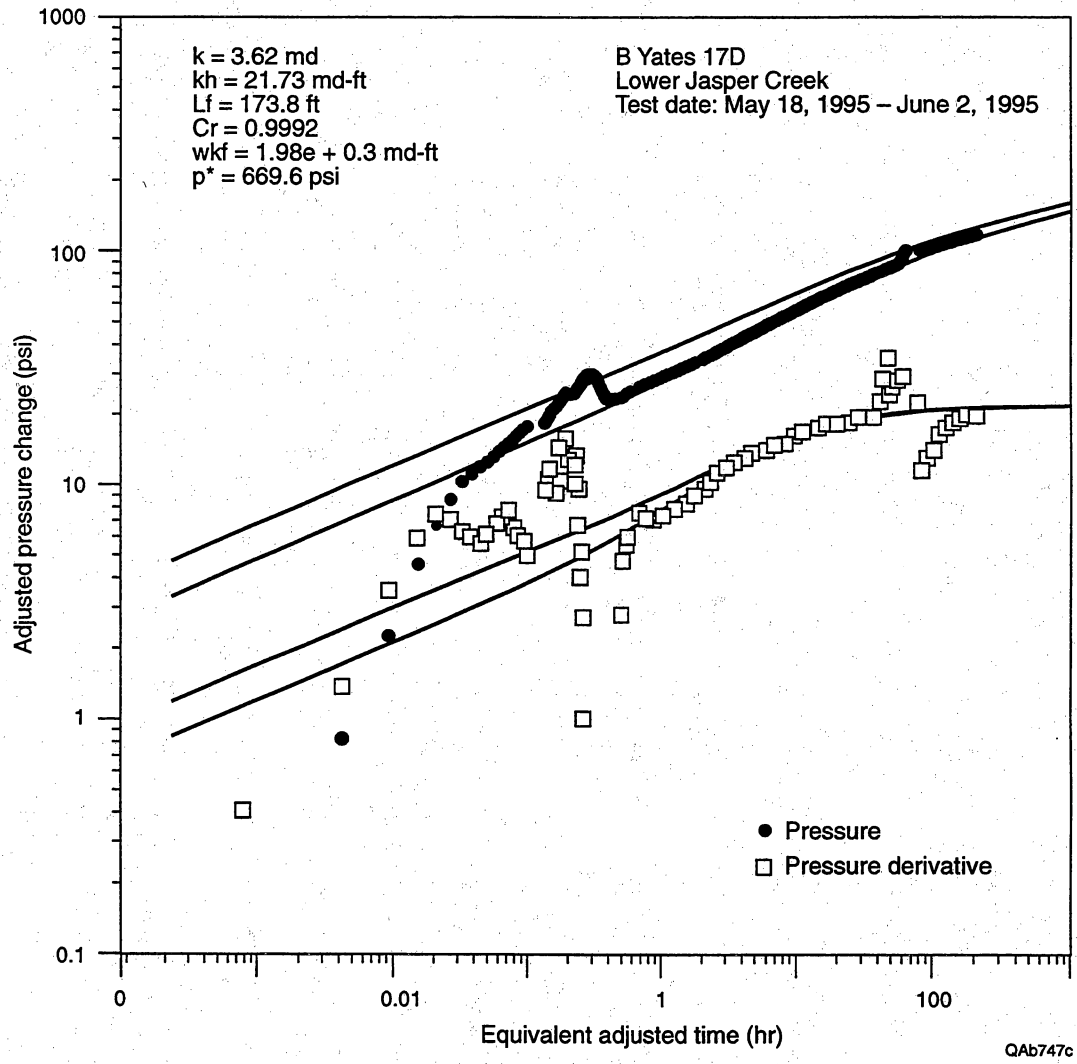


Figure 6.22. Log-log analysis of the pressure buildup test conducted in the Lower Jasper Creek reservoir in the B Yates 17D well.

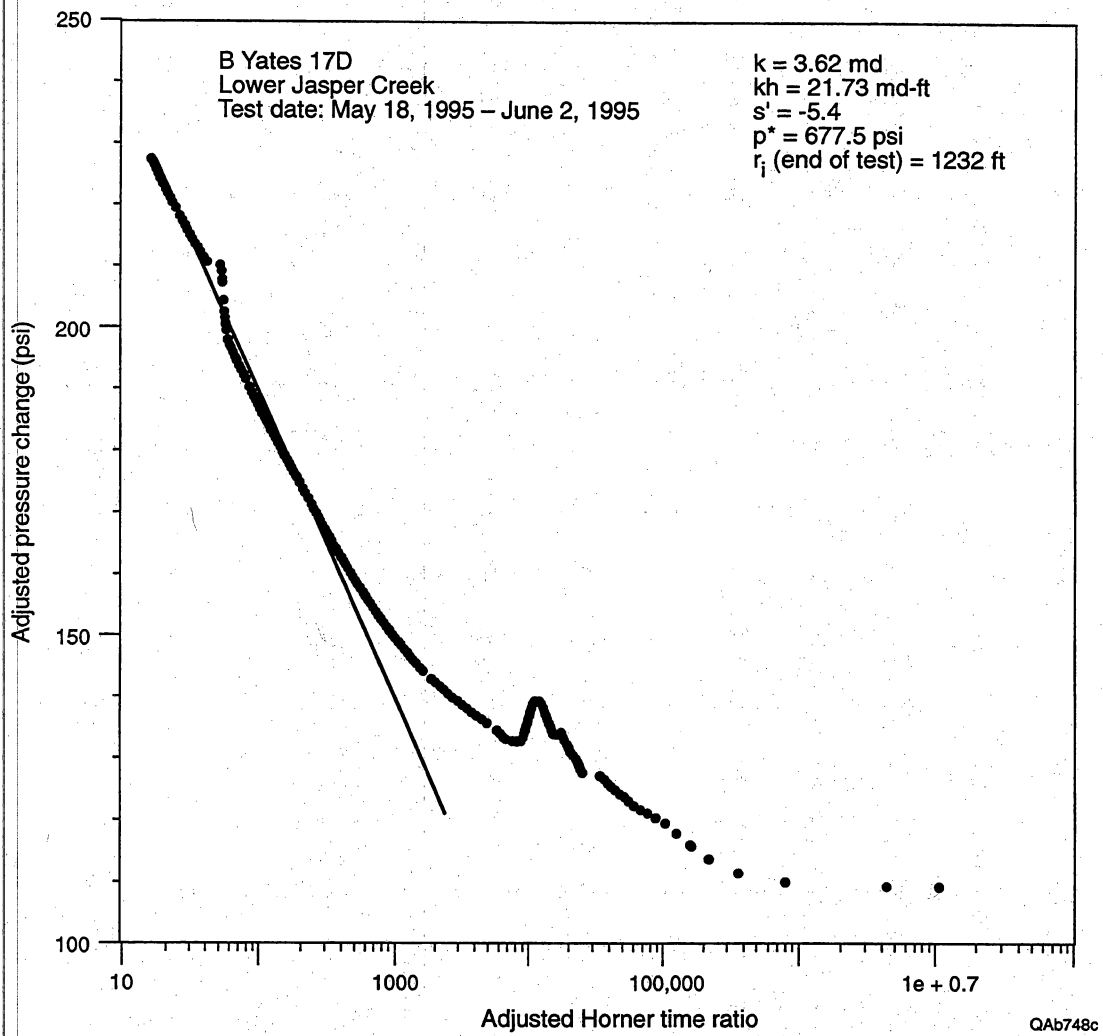


Figure 6.23. Semilog analysis of the pressure buildup test conducted in the Lower Jasper Creek reservoir in the B Yates 17D well.

average reservoir pressure depends on the actual reservoir size and geometry, but no attempt was made to assume any particular size or geometry and make that calculation.

The radius of investigation calculated at the end of this 2-week shut-in period was 1,232 ft. Because **no reservoir boundaries were observed during the test, this reservoir should have a minimum areal extent of about 109 acres**, assuming a circular drainage area. The actual drainage area is larger than this, but the exact value cannot be determined from the available data.

Returning to the log-log analysis in Figure 6.22, a fracture half-length of 174 ft was calculated using the permeability of 3.6 md. In addition, a fracture conductivity of about 2,000 md-ft was computed. Both values were considered reasonable, given the size of the fracture treatment and the fact that sand was used as the proppant.

Overall the interpretation of the pressure buildup test data appears to be quite consistent with the well performance and the way the well was stimulated. Further, given the well's initial performance (150 to 250 Mscf/d at 60 psi tubing pressure), the calculated permeability of 3.6 md, an estimated current reservoir pressure of about 700 psi, and the fact that this reservoir has a drainage area in excess of 100 acres, the pressure at the time of completion in the Lower Jasper Creek must have been on the order of 750 to 800 psi. This adds further support to the conclusion that the RFT pressures of 2,400 and 2,600 psi did not reflect reservoir pressure in the Lower Jasper Creek.

A pressure of 750 to 800 psi in the Lower Jasper Creek at the time of completion, however, **suggests that this interval was not isolated at this location**, but, instead, is in communication with offsetting production. The closest well completed in the Lower Jasper Creek is the B Yates 12, about 1,000 ft to the northwest (see Figure 6.19). As mentioned previously, however, the B Yates 12 has been completed in the Trinity, Runaway, Vineyard, and Middle and Lower Jasper Creek intervals, with a total gas production of only 135 MMscf for all zones combined. The Trinity and Lower Jasper

Creek perforations were added in 1990, and the well produced only about 45 MMscf after these zones were completed.

Because the contributions from the Lower Jasper Creek reservoir cannot be isolated, it is unclear whether there was sufficient production from this reservoir in the B Yates 12 to result in the degree of pressure depletion observed at the B Yates 17D location; however, due to the small volumes of gas produced from the Lower Jasper Creek, it appears unlikely that the drainage observed at the B Yates 17D location could all be associated with gas production from the B Yates 12. This suggests that the Lower Jasper Creek reservoir at this location may be in communication with the B Yates 7 well or the prolific B Yates 3 well (3.4 Bscf from the Middle and Lower Jasper Creek) to the east, even though these wells are approximately 4,000 and 7,000 ft away, respectively.

On the basis of the interpretation of the test data, the **ultimate gas recovery from this Lower Jasper Creek completion is projected to be only about 75 to 100 MMscf**, assuming the plunger lift equipment can successfully keep the liquids lifted from the borehole. Future completion attempts are expected in the Trinity, Runaway, and Vineyard sequences, and additional gas reserves from these zones will be needed if the B Yates 17D is to be an economical infill well.

B Yates 17D—Seismic Interpretation of Lower Jasper Creek Reservoir

North-south and east-west seismic profiles through the B Yates 17D well, with the interpreted position of the Lower Jasper Creek sequence boundary identified, are shown in Figures 6.24 and 6.25, respectively. These profiles show that small-throw faults occur in several directions about the well site. When the Lower Jasper Creek sequence interpretation is extended laterally away from the well location, a continuous sequence boundary is created, which allows areal distributions of seismic attributes to be calculated within an accurately defined Lower Jasper Creek seismic time window. **Two of the more**

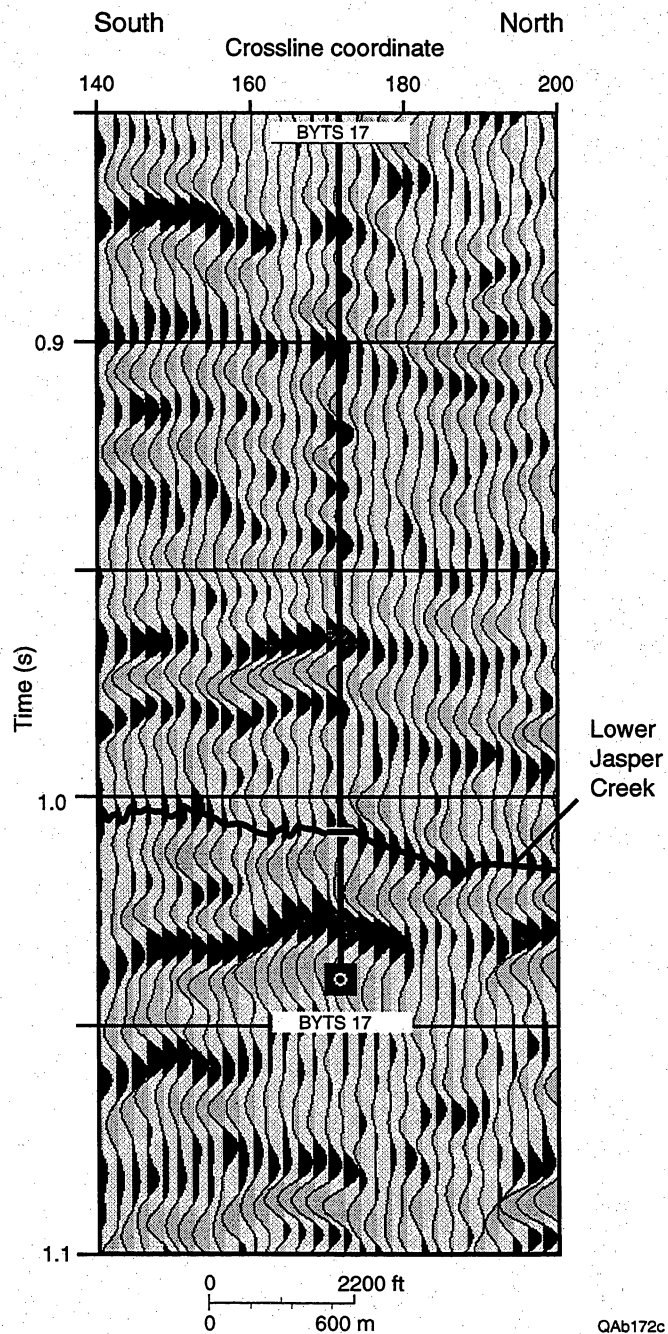


Figure 6.24. North-south profile through the B Yates 17D well location showing the position of the Lower Jasper Creek (heavy dash on the well profile) as determined by the depth-to-time calibration function used in the project area and the resulting interpretation of the Lower Jasper Creek sequence boundary.

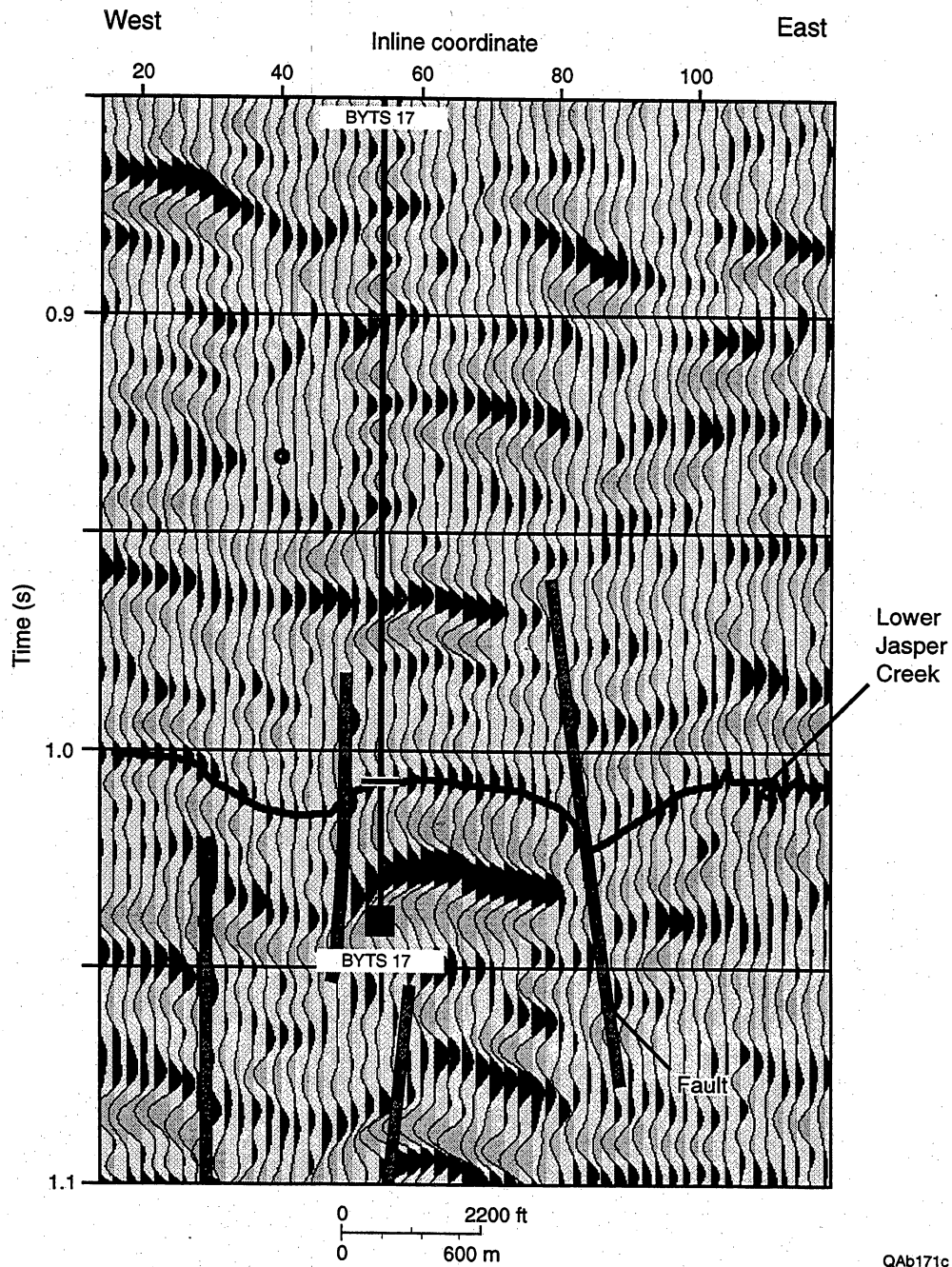


Figure 6.25. East-west profile through the B Yates 17D well location showing the position of the Lower Jasper Creek (heavy dash on the well profile) as determined by the depth-to-time calibration function used in the project area and the resulting interpretation of the Lower Jasper Creek sequence boundary. Several interpreted faults are also indicated.

diagnostic seismic attributes found at this site are instantaneous frequency and average reflection amplitude.

The instantaneous frequency behavior is plotted in Figure 6.26. This map shows that an almost continuous boundary of anomalous instantaneous frequencies encloses the B Yates 17D location. These anomalous frequency values start at a fault located between the B Yates 17D and B Yates 12 wells, extend north to the edge of the map, turn southeast and pass by the B Yates 6 well, then turn west along a fault system at the B Yates 11 well and pass just north of the B Yates 10 well. The B Yates 17D well appears to be sited just inside the southwest edge of the area encompassed by these anomalous frequencies. Referring to the examples in Appendix E of Volume II that illustrate how anomalous instantaneous frequency values pinpoint stratigraphic pinch-outs and/or faults, it is not unreasonable to assume that the closed, continuous boundary of anomalous frequencies described above possibly defines the areal size and shape of the Lower Jasper Creek reservoir found by the B Yates 17D well.

The reflection amplitude behavior associated with the Lower Jasper Creek sequence is displayed as Figure 6.27. This reflection strength attribute was derived by calculating the average positive reflection amplitude in a 16-ms window centered on the Lower Jasper Creek sequence boundary. The same fault systems occurring in the instantaneous frequency map (Fig. 6.23) are repeated in this average amplitude map. This display shows that the B Yates 17D well is located in the southwest corner of a dark (high amplitude) area that extends almost to the B Yates 12 and B Yates 11 wells. The areal extent of this amplitude anomaly is somewhat smaller than the area encompassed by the ring of anomalous instantaneous frequency values in Figure 6.26, and for the present, this amplitude map will be assumed to be the better estimate of size and shape of the Lower Jasper Creek reservoir compartment at the B Yates 17D well. **This high-amplitude reflection area covers approximately 100 acres.**

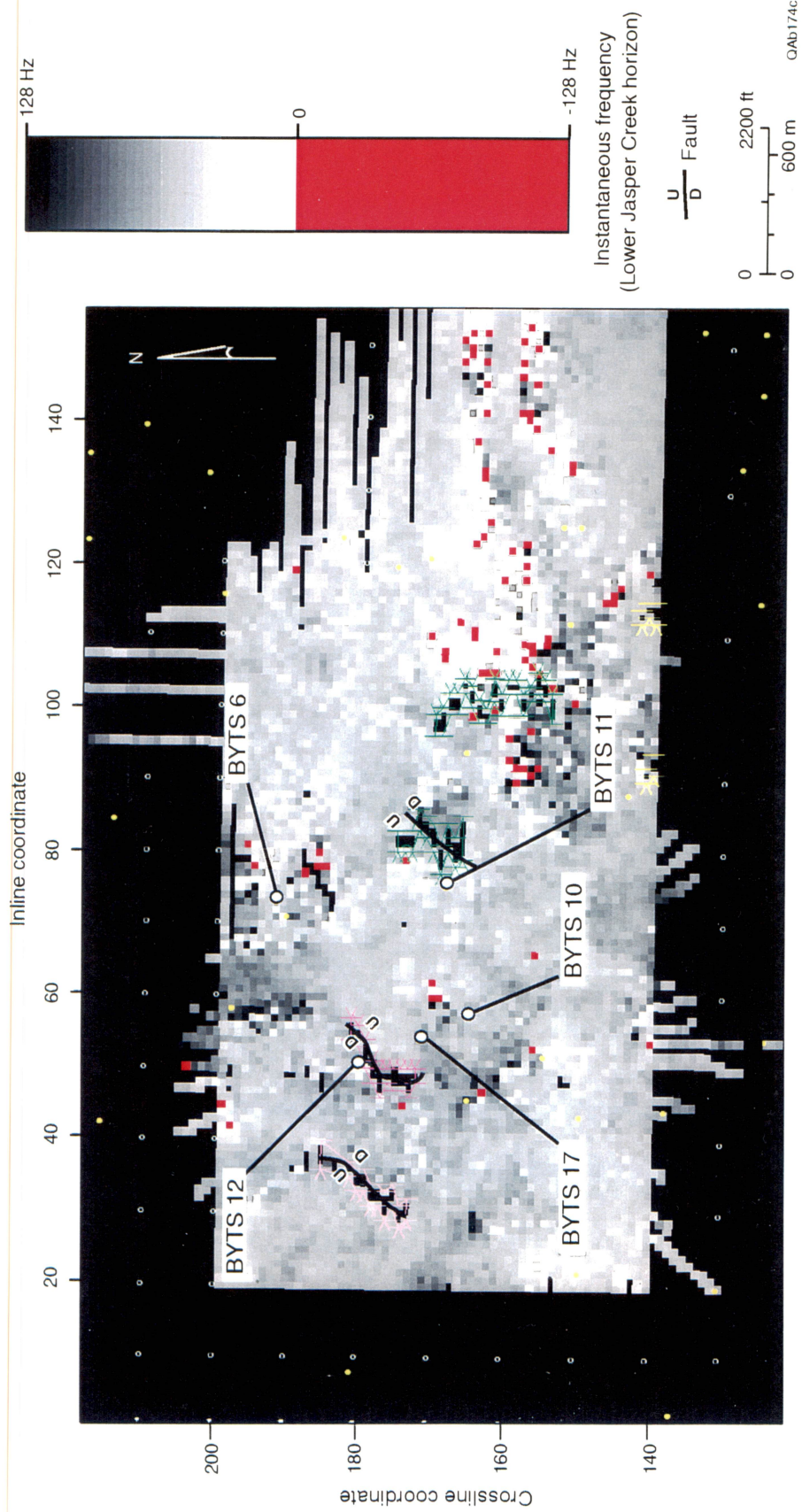


Figure 6.26. Instantaneous frequency behavior across the interpreted Lower Jasper Creek surface. The red and green bins show where the reflection waveform is distorted, which implies that a possible compartment boundary may occur at these coordinates.

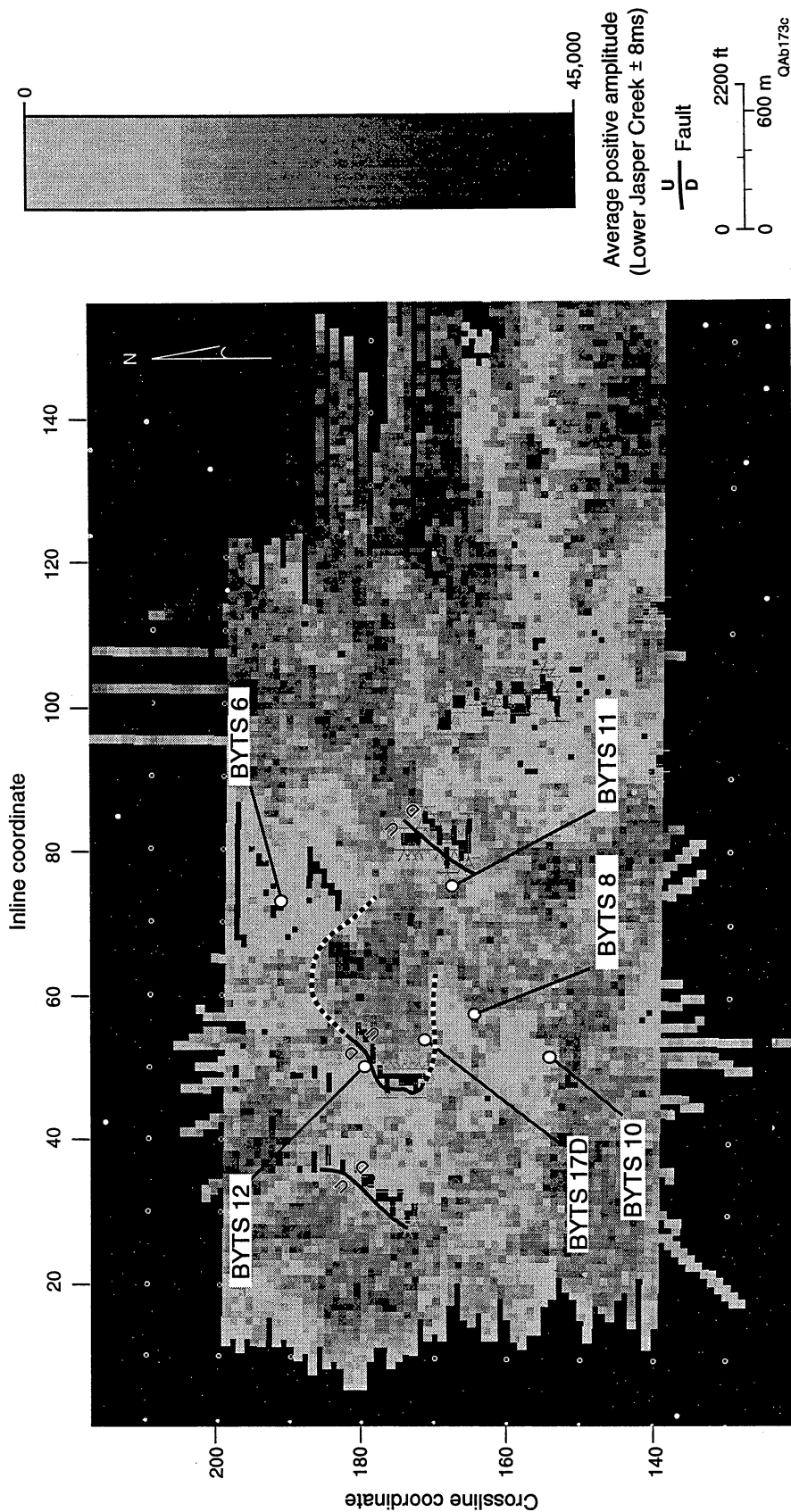


Figure 6.27. Reflection amplitude behavior across the interpreted Lower Jasper Creek surface. The parameter that is plotted is the average of the positive amplitudes occurring in a 16-ms window centered on the Lower Jasper Creek surface. The B Yates 17D well is positioned near the edge of an area where the reflection amplitudes have a moderate positive range, as indicated on the color bar. Assuming that this seismic amplitude facies maps a consistent stratigraphic facies, the compartment size (area inside the dashed boundary) is perhaps as large as 100 acres and may connect with a larger, equivalent seismic amplitude facies extending southward between the B Yates 8 and B Yates 11 wells, or with an equivalent facies to the east and north toward the B Yates 3 well.

Analysis of the early well performance and the pressure buildup data described previously indicates that the Lower Jasper Creek reservoir at the B Yates 17D location is in communication with offsetting production. As mentioned previously, a possible source of some of this communication is the Lower Jasper Creek production from the B Yates 12 well. The seismic interpretation shown in Figures 6.26 and 6.27, however, indicates a fault between the B Yates 12 and the B Yates 17D wells in the Lower Jasper Creek, although it is unclear the degree to which this fault may isolate the Lower Jasper Creek in the two wells. Further, as Figure 6.27 shows, the area of high amplitude associated with the B Yates 17D location may also connect with an area of equally high amplitude to the east and north of the B Yates 11 well, toward the B Yates 3 well, which is a prolific Jasper Creek completion. Although the B Yates 3 well is over 1 mi away, gas production from this well may be the primary source of the pressure depletion observed in the Lower Jasper Creek reservoir at the B Yates 17D location. The dimming in the amplitude response just north of the B Yates 11 well may indicate a thinning of the Jasper Creek reservoir, which is a classic seismic thin-bed response.

General Observation about Siting Infield Wells

Infield wells in Boonsville field should be sited where maximum opportunities exist for stacked, multiple completions. Ideally such sites should be selected by overlaying well-log-based facies maps developed for successively stacked genetic sequences and then prioritizing those sites when several reservoir facies trends overlap. The prioritization is done by referring to 3-D seismic interpretations of these same sequences and to engineering analyses of reservoir sizes and productivities in nearby wells. However, in the case of the B Yates 18D and 17D wells, the short time that was available for data analysis forced selection of both drill sites predominantly on the basis of 3-D seismic interpretation, although both wells were considered to be in areas favorable for multiple completion opportunities as determined from engineering analysis

(see Figures B19 and B20 in Appendix B of Volume II). **The dominant criterion that dictated the selection of these sites was the convincing seismic evidence that multiple stacked entrapments existed in many of the genetic sequences at each location (Figs. 6.4 and 6.18).**

Operators in the Fort Worth Basin and other Midcontinent basins should, therefore, acquire 3-D seismic data whenever practical and affordable and use these data in conjunction with reservoir facies distribution maps developed by sequence stratigraphic principles applied to well log control. **Neither the 3-D seismic data nor the well-log-based maps should be given greater emphasis in the interpretation;** both data bases have equal weight and value in providing information about wellsite locations.

The danger of using well-log-based information alone is that maps built from such data have to be interpolated across large interwell spaces, and the interwell coordinates where lateral changes of facies occur can only be approximated. Such maps are invaluable for establishing depositional trends but may fail to define interwell detail relating to reservoir compartmentalization.

The danger of relying strictly on 3-D seismic data, as was the (forced) situation for the B Yates 18D and 17D wells, is that even when the seismic data show that vertically stacked entrapments exist at a specific site, **the seismic data cannot define what type of rock facies is contained within the sequences.** Thus, the principal risk of the B Yates 18D and 17D wells was that no reservoir facies may exist in any of the seismically indicated entrapments. Fortunately, reservoir facies were present in some of the sequences, and the stratigraphic and structural boundaries associated with some of the entrapments caused the gas volumes in these zones not to be effectively contacted by surrounding producing wells.

7. REFERENCES

- Adler, F. J., Amsden, T. W., Anderson, E. G., Barnes, V. E., Bennett, J., Bennison, A. P., Brown, L. F., Jr., Caplan, W. M., Caylor, J. W., Clendening, J. A., Copeland, C. W., Craig, W. W., Culp, E. F., Deford, R. K., Denison, R. E., Downs, H. R., Ethington, R. L., Furnish, W. M., Jr., Gatewood, L. E., Gilbert, M. C., Glick, E. E., Groat, C. G., Hannum, C. E., Hansen, T. A., Harrison, W. E., Hart, G. F., Hills, J. M., McCord, D. L., McFarland, J. D., III, Milling, M. E., Morgan, W. A., Osborne, W. E., Pope, D. E., Rascoe, B., Jr., Repetski, J., Sprinkle, J., Stanton, R. J., Sutherland, P. K., Takken, S., Thomas, W. A., Wermund, E. G., Jr., Wilson, L. R., Wise, O. A., Jr., Yancey, T. E., and Young, K. P., 1986, Texas–Oklahoma tectonic region correlation chart, *in* Mankin, C. J., ed., Correlation of stratigraphic units in North America: American Association of Petroleum Geologists.
- Agarwal, R. G., 1979, Real gas pseudo-time—a new function for pressure buildup analysis of MHF gas wells: Society of Petroleum Engineers, Paper SPE 8279.
- _____ 1980, A new method to account for producing time effects when drawdown type curves are used to analyze pressure buildup and other test data: Society of Petroleum Engineers, Paper SPE 9289.
- Al-Hussainy, R., Ramey, H. J., and Crawford, P. B., 1966, The flow of real gas through porous media: *Journal of Petroleum Technology*, May, p. 623–636.
- Blanchard, K. S., Denman, O., and Knight, A. S., 1968, Natural gas in Atokan (Bend) section of northern Fort Worth Basin: Beebe, B. W., and Curtis, B. F., eds., *Natural*

gases of North America: American Association of Petroleum Geologists Memoir 9, v. 2, p. 1446–1454.

Carlson, M. P., Nodine-Zeller, D. E., Thompson, T. L., and White, B. J., 1986, Mid-Continent region correlation chart, *in* Adler, F. J., ed., Correlation of stratigraphic units in North America: American Association of Petroleum Geologists.

Chapin, C., Clemons, R. E., DeWitt, E., Harding, J. M., Hills, J. M., Hook, S. C., Knepp, R. A., Kottowski, F. E., LeMone, D. V., Maxwell, C., McBride, E. F., Mear, C. E., Moore, G., Nicholson, J., Peirce, H. W., Pray, L. C., Scarborough, R. B., Seager, W., Stewart, W. J., Thompson, S., III, Wilde, G. L., Wolberg, D., and Wright, W., 1983, Southwest/southwest Midcontinent correlation chart, *in* Hills, J. M., and Kottowski, F. E., eds., Correlation of stratigraphic units in North America: American Association of Petroleum Geologists.

Cinco, L. H., and Samaniego-V. F., 1981, Transient pressure analysis for fractured wells: *Journal of Petroleum Technology*, September, p. 1759–1766.

Fair, W. B., Jr., 1981, Pressure buildup analysis with wellbore phase redistribution: *Society of Petroleum Engineers Journal*, April, p. 259–270.

Flawn, P. T., Goldstein, A. G., Jr., King, P. B., and Weaver, C. E., 1961, The Ouachita System: University of Texas, Austin, Bureau of Economic Geology Publication No. 6120, 401 p.

Glover, G., 1982, A study of the Bend Conglomerate in S. E. Maryetta Area, Boonesville [sic] Field, Jack County, Texas: Dallas Geological Society.

Grayson, R. C., 1990, Canyon Creek: a significant exposure of a predominantly mudrock succession recording essentially continuous deposition from the Late Devonian

through the Middle Pennsylvanian, *in* Ritter, S. M., ed., Early to Middle Paleozoic conodont biostratigraphy of the Arbuckle Mountains, southern Oklahoma: Oklahoma Geological Survey, Guidebook for the South-Central Section of the Geological Society of America Field Trip No. 27, p. 85–105.

Horner, D. R., 1951, Pressure buildup in wells, *in* Proceedings, Third World Petroleum Congress: The Hague, Section II, p. 503–523.

Lahti, V. R., and Huber, W. F., 1982, The Atoka Group (Pennsylvanian) of the Boonsville Field area, north-central Texas, *in* Martin, C. A., ed., Petroleum geology of the Fort Worth Basin and Bend Arch area: Dallas Geological Society, p. 377–399.

Lee, W. J. 1986, Characterizing formations with pressure tests—textbook for videotape short course: Dallas, Society of Petroleum Engineers.

Manger, W. L., Miller, M. S., Mapes, R. H., 1992, Age and correlation of the Gene Autry Shale, Ardmore Basin, southern Oklahoma, *in* Sutherland, P. K., and Manger, W. L., eds., Recent advances in Middle Carboniferous biostratigraphy—a symposium: Oklahoma Geological Survey Circular 94, p. 101–109.

Masters, J. A., 1979, Deep basin gas trap, Western Canada: American Association of Petroleum Geologists Bulletin, v. 63, p. 152–181.

Meckel, L. D., Jr., Smith, D. G., Jr., Wells, L. A., 1992, Ouachita foredeep basins: Regional paleogeography and habitat of hydrocarbons, chapter 15, p. 427–444.

Railroad Commission of Texas, 1991, Field rules, section VI, Boonsville Field (Bend Conglomerate Gas), Order No. 9-36, 420.

Ravn, R. L., Swade, J. W., Howes, M. R., Gregory, J. L., Anderson, R. R., and Van Dorpe, P. E., 1984, Stratigraphy of the Cherokee group and revision of

Pennsylvanian stratigraphic nomenclature in Iowa: Iowa Geological Survey Technical Information Series, No. 12, 76 p.

Shaver, R. H., Clayton, L., Mudrey, M. G., Jr., Peters, R. M., Mikulic, D. G., Ells, G. D., Eschman, D. F., Fisher, J. H., Lilienthal, R., Collinson, C., Atherton, E., Baxter, J. W., Kolata, D. R., Jacobson, R. J., Lineback, J. A., Norby, R. D., Palmer, J. E., Sargent, M. L., Trask, C. B., Willman, H. B., Droste, J. B., Patton, J. B., Gray, H. H., Goldthwait, R. P., Rexroad, C. B., Noger, M. K., Dever, G. R., Jr., Smith, H. J., Williamson, A. D., Schwalb, H. K., Luther, E. T., and Copeland, C. W., 1984, Midwestern basin and arches region correlation chart, *in* Correlation of stratigraphic units in North America: American Association of Petroleum Geologists.

Sutherland, P. K., Archinal, B. E., and Grubbs, R. K., 1982, Morrowan and Atokan (Pennsylvanian) stratigraphy in the Arbuckle Mountains area, Oklahoma, *in* Sutherland, P. K., ed., Lower and Middle Pennsylvanian stratigraphy in south-central Oklahoma: Oklahoma Geological Survey, prepared for Geological Society of America Field Trip No. 2, p. 1-17.

Sutherland, P. K., and Grayson, R. C., Jr., 1992, Morrowan and Atokan (Pennsylvanian) biostratigraphy in the Ardmore Basin, Oklahoma, *in* Sutherland, P. K., and Manger, W. L., eds., Recent advances in Middle Carboniferous biostratigraphy—a symposium: Oklahoma Geological Survey Circular 94, p. 81-99.

Thompson, D. M., 1982, Atoka Group (Lower to Middle Pennsylvanian), northern Fort Worth Basin, Texas: terrigenous depositional systems, diagenesis, and reservoir distribution and quality: The University of Texas at Austin, Bureau of Economic Geology Report of Investigations No. 125, 62 p.

_____ 1988, Fort Worth Basin, *in* Sloss, L. L., ed., The geology of North America: Boulder, Geological Society of America, v. D-2, p. 346–352.

Turner, G. L., 1957, Paleozoic stratigraphy of the Fort Worth Basin, *in* Bell, W. C., ed., Abilene and Fort Worth Geological Societies 1957 Joint Field Trip Guidebook, p. 57–77.

Walper, J. L., 1977, Paleozoic tectonics of the southern margin of North America: Gulf Coast Association of Geological Societies Transactions, v. 27, p. 230–239.

Zachry, D. L., and Sutherland, P. K., 1984, Stratigraphy and depositional framework of the Atoka Formation (Pennsylvanian) Arkoma Basin of Arkansas and Oklahoma, *in* Sutherland, P. K., and Manger, W. L., eds., The Atokan Series (Pennsylvanian) and its boundaries—a symposium: Oklahoma Geological Survey Bulletin 136, p. 9–17.

8. GLOSSARY

All italicized words appearing in a definition are defined elsewhere in the glossary.

accommodation space — that volume below *base level* within a depositional basin that is available for the accumulation of sediments.

acoustic impedance — the product of *seismic velocity* and *rock density*.

aggradation — the vertical accumulation of sediment within a *depositional system* (cf. *progradation*, *regression*).

allocyclic — of or relating to changes in *cyclothem* deposition within a depositional basin that result from processes external to the basin (cf. *autocyclic*).

amplitude — the maximum numerical value expressed by a regularly and periodically varying quantity as measured from its equilibrium value (which, by definition, equals zero).

API units — one of two different measures of radioactivity on well logs as designated by the American Petroleum Institute. One unit is for the calibration of gamma-ray counters, the other for neutron detectors.

asthenosphere — the semimolten, plastic layer of the upper *mantle* immediately below the *lithosphere*, upon which the *tectonic plates* move.

Atoka Group — a *sequence of rocks* that overlies the *Marble Falls Formation* and underlies the *Strawn Group*. Within the *Fort Worth Basin*, it corresponds to the *Bend Conglomerate* (as designated by the Texas Railroad Commission) plus the *Caddo Limestone* and, as such, is nearly equivalent to the *Atokan Series*.

Atokan — the second *epoch* of the *Pennsylvanian Period*, extending from 308 to 310 million years ago; the *series* of stratigraphic *rock units* deposited during this time; of or relating to this *epoch* of time or its *series of rocks*.

autocyclic — of or relating to changes in *cyclothem* deposition within a depositional basin that result from processes within the basin itself (cf. *allocyclic*).

bandpass filter — a digital filter that is applied to *seismic data* to limit the frequency content of the data to a specific range. The range so designated is the pass band.

base level — the level below which a river cannot erode its channel. Base level is an equilibrium surface with erosion occurring above it and deposition occurring below it. In most situations, base level is equivalent to sea level.

- base level cycle** — a cycle of rise and fall in relative sea level resulting from periodic changes in *eustatic sea level*, sediment supply, *tectonic* subsidence, or *physiography* of the depositional substrate.
- basement** — the crystalline igneous and metamorphic rocks that underlie the younger sedimentary deposits of the *crust*; the *rock* units below those with which a study is concerned, usually implying *rock* units below the hydrocarbon-productive interval.
- bedding plane** — a planar or nearly planar surface of a stratified sedimentary unit that separates it from the next stratified unit; a plane of deposition.
- Bend Arch** — the *peripheral bulge* west of the *Fort Worth Basin* produced by incremental loading along the *Ouachita Thrust Belt*.
- Bend Conglomerate** — an informal grouping of *Atokan rocks* used by operators in the *Fort Worth Basin* and designated by the Texas Railroad Commission as extending from the top of the *Marble Falls Formation* to the base of the *Caddo Limestone*. In this report, we treat the Bend Conglomerate as equivalent to the formally designated *Atoka Group*, which extends from the top of the *Marble Falls Limestone* to the base of the *Strawn Group* (top of the *Caddo Limestone*).
- bin** — a small, discrete area, usually square or rectangular, inside a *3-D seismic* image that encompasses a single *seismic trace* of the final, processed 3-D data volume. The number of *bins* required to span the entire 3-D image space is the same as the number of data *traces* in the final processed 3-D data volume, one *trace* passing vertically through the center of each *bin*.
- biostratigraphy** — the correlation of *rock* units on the basis of their fossil content.
- bottom-hole pressure** — the fluid or gas pressure produced in a well bore at the depth of the *reservoir* formation, which, in many cases, is near the bottom of the well bore.
- bridge plug** — a volume of concrete or a mechanical device placed in a well bore at a specified depth to seal off the hole below it.
- Caddo Limestone** — a *carbonate* unit of *Atokan* age occurring within the *Fort Worth Basin*. The Texas Railroad Commission designated the top of the *Bend Conglomerate* as being the base of the *Caddo Limestone*, but the faunal and age relationships of the latter unit indicate that it should be included within the *Bend Conglomerate*, as is done in this report (cf. *Bend Conglomerate*).
- calcite** — a relatively soft *mineral* composed of calcium carbonate (CaCO_3) that may occur as a pore-filling cement in *reservoir* sandstones or may comprise a limestone.

- Cambrian** — the first *period* of the *Paleozoic Era*, extending from 530 to 510 million years ago; the *system* of stratigraphic rock units deposited during this time; of or relating to this *period* of time or its *system* of rocks.
- carbonate** — of or relating to a *mineral* containing the carbonate ion (CO_3^{-2}); of or relating to a *rock* consisting primarily of *minerals* containing the *carbonate* ion.
- carbonates** — *rocks* consisting primarily of *minerals* containing the carbonate ion (CO_3^{-2}), i.e., limestone.
- casing** — the metal pipe placed within a borehole and cemented into place to prevent fluids from flowing into or out of the borehole.
- cement** — *mineral* crystals precipitated within the pore spaces of a sediment that bind the individual *mineral* grains together, thereby creating a solid, coherent mass.
- Cenozoic** — the *era* of geologic time extending from 66 million years ago to the present and including the *Tertiary* and *Quaternary Periods*.
- centipoise** — a measure of viscosity defined as 1/100th of a *poise*.
- channel fill** — *fluvial* sediments filling a channel.
- checkshot** — a seismic measurement that establishes a rigorous relationship between stratigraphic depth and vertical *seismic* traveltime. The measurement is done by lowering a geophone by wireline to a specified depth in a well and then recording the *seismic* response generated by a surface energy source positioned near the wellhead.
- chert** — a hard, cryptocrystalline or microcrystalline silica *mineral* (SiO_2) exhibiting conchoidal fracture and commonly occurring as nodules in a *carbonate rock*.
- chronostratigraphic horizon** — widespread physical boundary, surface, or interval, the same age everywhere it occurs, therefore separating overlying younger strata from underlying older strata (cf. *time line*).
- clastic** — of or relating to *detrital* grains or a *rock* composed of them; the texture of such a *rock*.
- clastics** — *rock* composed of *detrital* grains.
- clean sand** — sandstone or sandy sediment that has been well sorted by natural processes so that it is almost entirely composed of *quartz* grains (>95%).
- clinoform** — the steeply dipping sediments deposited on the advancing frontal slope of a delta; of or relating to such sediments or the sloping delta front.

compartment — a space within a larger *reservoir* that, in terms of fluid flow, is totally or partially isolated from the rest of the *reservoir*.

condensed section — a thin, sedimentary succession or unit continuously deposited during times of very slow sedimentation. Condensed sections, often organic rich, correlate to much thicker sections elsewhere within the depositional basin.

convergent plate boundary — a boundary between two colliding *tectonic plates*, characterized by extensive geological activity and deformation.

craton — the geologically stable region of a continent that has not undergone significant *tectonic* deformation for several hundred million years. The craton includes both the *shield* and the surrounding *platform*.

Cretaceous — the third and last *period* of the *Mesozoic Era*, extending from 144 to 66 million years ago; the *system* of stratigraphic *rock* units deposited during this time; of or relating to this *period* of time or its *system* of *rocks*.

crossbedding — sedimentary layers more than 1 cm in thickness that are inclined relative to the main *bedding planes* because they were originally deposited on a sloping surface.

crossline — that direction in an onshore 3-D *seismic* survey that is perpendicular to the direction that the geophone cables are deployed (cf. *inline*).

crust — the outermost layer of the Earth, averaging in thickness from 30 to 45 km (18 to 27 mi) under the continents and 6 to 10 km (4 to 6 mi) under the oceans.

current-ripple mark — asymmetric ripple marks produced by unidirectional currents of air or water moving over a sandy surface.

cyclothem — very regular *facies* succession resulting from one cycle of periodic changes in relative sea level.

darcy — a standard measure of *permeability* defined as the passage of 1 cm³ of fluid of one *centipoise* viscosity flowing in 1 sec under a pressure differential of one atmosphere through a porous medium having a cross-sectional area of 1 cm² and a length of 1 cm.

deltaic — of or relating to river deltas or *depositional systems*.

depositional system — a depositional environment and its characteristic *facies*.

depth-to-time conversion function — a mathematical function used to convert *seismic* traveltimes to stratigraphic depths.

Desmoinesian — the third *epoch* of the *Pennsylvanian Period*, extending from 303 to 308 million years ago; the *series* of stratigraphic *rock* units deposited during this time; of or relating to this *epoch* of time or its *series* of *rocks*.

detrital — of or relating to the broken fragments derived by weathering and erosion of preexisting *rocks*.

Devonian — the fourth *period* of the *Paleozoic Era*, extending from 362 to 408 million years ago; the *system* of stratigraphic *rock* units deposited during this time; of or relating to this *period* of time or its *system* of *rocks*.

diachronous — being of different ages in different areas.

diagenesis — those changes that occur within a sediment or sedimentary *rock* between burial and *metamorphism*, exclusive of weathering and erosion. Diagenesis is defined as occurring at temperatures under 100° C., in contrast to metamorphosis, which occurs at temperatures over 100° C. (cf. *metamorphism*).

dip — the slope of a *rock* unit as measured perpendicular to *strike*, i.e., the angle a *rock* unit makes to the horizontal.

distributary — one of the small, diverging streams into which a larger river will split as it reaches its *base level*.

divergent plate boundary — a boundary between two *tectonic plates* that are separating.

dolomite — a *mineral* composed of calcium magnesium carbonate ($\text{CaMg}(\text{CO}_3)_2$) that may occur as a pore-filling cement in sandstones or may comprise a dolostone.

downcutting — the downward erosion within a stream channel (cf. *incisement*).

downdip — the direction in which a bed is *dipping*.

drainage area (of a well) — the region over which a given well is able to draw fluid or gas from the *reservoir rock*.

dyne — the force necessary to give 1 gm an acceleration of 1 cm/sec.

Ellenburger Group — a *sequence* of rocks, widespread across Texas, deposited during the *Ibexian Epoch* of the *Ordovician Period*. *Karstification* of the Ellenburger Limestone is responsible for much of the structural control on *facies* within Boonsville field.

epoch — a unit of geologic time into which *periods* are subdivided for more precise correlations.

era — a unit of geologic time consisting of one or more *periods*.

erosion surface (ES) — surface, boundary, or interval showing evidence of erosion associated with an abrupt decrease in water depth; e.g., coarse *channel-fill* sandstone overlying a sharp boundary with underlying marine shale. Because they indicate some interval of time not represented by strata, erosional surfaces are *unconformities*.

Euramerica — the *Paleozoic* continent consisting of what is now North America and Europe.

eustatic sea level — global sea level.

“Exxon” sequence — relatively conformable succession of genetically related strata bounded by *unconformities* or their correlative conformities.

facies — areally and stratigraphically restricted sedimentary unit that differs in appearance, *lithology*, or fossil content from adjacent sedimentary units, thereby allowing inferences to be made about its depositional environment; any group of *rocks* having a similar overall character.

facies dislocation — an interruption of a normal *Walther’s Law* succession of depositional *facies* (cf. *facies offset*).

facies offset — an interruption of a normal *Walther’s Law* succession of depositional *facies* (cf. *facies dislocation*).

fault block — a *crustal* unit, bounded by faults, that results from extensive *normal faulting* in a region such that the *crust* is broken into separate blocks with different orientations and elevations.

ferroan calcite — a variety of *calcite* having a significant amount of iron impurities.

field trace — a seismic response measured in the field by a single receiver group. Multiple field traces are typically processed to produce a final, summed *seismic trace* (cf. *seismic trace, fold*).

flexural moat — a deep, asymmetric *crustal* depression adjacent to an *overthrust belt* caused by incremental loading due to the emplacement of successive *thrust sheets* within the belt. The *flexural moat* shallows away from the belt, grading into a slightly upwarped *peripheral bulge* (cf. *foreland basin, peripheral bulge*).

flooding surface (FS) — a *chronostratigraphic horizon*, boundary, or interval showing evidence of an abrupt increase in water depth.

fluvial — of or relating to a river or its *depositional system*.

fold (stacking fold) — the number of discrete *seismic field traces* that reflect from the same subsurface area or *bin*. If N field *traces* reflect from a *bin*, these *traces* are processed and summed to create a single *trace* positioned at the center of that *bin*. This summed *trace* is said to have a stacking fold of N.

footwall — in describing a fault, the body of *rock* below an inclined fault plane.

foraminiferan — a protozoan belonging to the Class Sarcodina, Order Foraminifera, characterized by having a shell of one or more chambers composed of calcium *carbonate* or agglutinated particles.

foreland basin — a depositional basin created by subsidence immediately adjacent to an *overthrust belt* (cf. *flexural moat*).

formation — the fundamental *lithostratigraphic unit* and one whose thickness is sufficiently great to allow it to be adequately mapped. *Formations* are combined together into *groups* and subdivided into *members*.

Fort Worth Basin — a triangular-shaped depositional basin in North-Central Texas created during the Late *Paleozoic* by a *flexural moat* adjacent to the *Ouachita Thrust Belt*.

frequency — the number of cycles of a periodic motion in a unit of time, usually 1 sec.

fusulinid — an extinct, large foraminifer belonging to the Suborder Fusulinina characterized by a long, ellipsoidal shell with complex internal chambering.

gas gravity — the density or mass per unit volume of a gas.

genetic sequence — regressive, generally upward-coarsening succession of *facies* bounded by marine *flooding surfaces*. A *genetic sequence* records one complete cycle of changes in relative sea level (deep–shallow–deep).

Gondwanaland (Gondwana) — the *Paleozoic* continent consisting of modern South America, Africa, Antarctica, India, Australia, Arabia, and parts of southern Europe and the southeastern United States.

graben — the downthrown *crustal* block between two *normal faults*.

group — a *lithostratigraphic unit* consisting of one or more *formations*.

hanging wall — in describing a fault, the body of *rock* above an inclined fault plane.

high-fold bin — a *bin* containing a relatively large number of reflected *seismic field traces* (cf. *bin, fold*).

highstand — time during which *base level* elevation is at a maximum and therefore above the local *shelf edge*; of or relating to such a period.

highstand depositional systems tract (HST) — an upward-coarsening *facies* succession representing *progradational, offlapping facies* that filled *accomodation space* during a *base level* maximum and subsequent fall. The tract is usually capped by an *erosional surface*.

Hilbert transform — a mathematical calculation that extracts amplitude, frequency, and phase information from a *seismic trace*.

humus — macerated plant material derived from the land or present in a soil.

Ibexian — the first *epoch* of the *Ordovician Period*, extending from 476 to 505 million years ago; the *series* of stratigraphic *rock* units deposited during this time; of or relating to this *epoch* of time or its *series of rocks*.

impermeable — having no significant *permeability*.

index fossil — an easily recognized, widespread fossil having a short geologic range used to readily date the *rocks* within which it occurs.

incisement — the *downcutting* of a stream channel into the underlying *rock* so as to form a narrow, steep-walled valley.

infield reserve growth — increase of *reserves* within an oil or gas field that has typically been considered fully developed.

inline — the direction in which receiver cables are deployed when recording 3-D *seismic* data (cf. *crossline*).

inner core — that portion of the Earth's interior below the *outer core*. It extends from about 5,200 km in depth (3300 mi) to the center of the Earth and is about 1,200 km (725 mi) in radius. The inner core has a nickel-iron composition but is solid because of the incredible pressure.

instantaneous amplitude — the amplitude behavior of a *seismic trace* calculated at each time sample of the *trace* (cf. *Hilbert transform, seismic attribute*).

instantaneous frequency — a frequency property of a *seismic trace* calculated at each time sample of the *trace* (cf. *Hilbert transform, seismic attribute*).

instantaneous phase — the phase values of a *seismic trace* (limited, by definition, to the range of 0° to 360°) calculated at each time sample of the *trace* (cf. *Hilbert transform, seismic attribute*).

isopach — line on a map connecting points of equal true thickness of a *rock* or stratigraphic unit.

Jurassic — the second *period* of the *Mesozoic Era*, extending from 208 to 144 million years ago; the *system* of stratigraphic *rock* units deposited during this time; of or relating to this *period* of time or its *system* of *rocks*.

karst — a terrain, typically composed of limestone, dominated by erosion through dissolution. Areas that have *karst* topography are characterized by *sinkholes*, caverns, disappearing streams, etc.

karstification — the process by which an area acquires a *karst* terrain.

lamination — a very thin (<1 cm) layer within a sedimentary unit that is nevertheless recognizable because of its differing color, composition, and/or texture relative to the adjacent layers.

lithology — the physical characteristics of a *rock*, such as color, texture, and composition.

lithosphere — the uppermost, rigid part of the *mantle*, immediately beneath the *crust*. The *lithosphere* is about 100 to 150 km (60 to 90 mi) thick under the continents and 70 km (45 mi) thick under the oceans and constitutes the bulk of the *tectonic plates*.

lithostratigraphic unit — a stratified *rock* unit whose components are grouped together on the basis of shared or similar *lithology*, generally having recognizable contacts with adjacent rock units.

low-fold bin — a *bin* containing a relatively small number of reflected *seismic field traces* (cf. *bin, fold*).

lowstand — time during which *base level* elevation is at a minimum and therefore below the local *shelf edge*; of or relating to such a period.

lowstand depositional systems tract (LST) — terrestrial and transitional *facies* that filled *accommodation space* during a *lowstand*.

mantle — that portion of the Earth's interior between the *crust* and the *outer core*, extending from about 10 to 45 km (6 to 27 mi) in depth to 2,900 km (1,800 mi) in depth. The mantle is largely composed of semimolten *silicate minerals* under great pressure.

Marble Falls Formation (Limestone) — the predominantly limestone unit underlying the *Atoka Group* within the *Fort Worth Basin* and Llano area.

maximum flooding surface (MFS) — a *chronostratigraphic* interval associated with *facies* representing the deepest water depth encountered in a succession of strata; commonly represented by a thin, *condensed section* of black or dark-gray marine shales deposited in an oxygen-poor, sediment-starved environment.

member — a *lithostratigraphic unit* into which *formations* are subdivided for more precise correlations.

Mesozoic — the *era* of geologic time extending from 245 million years ago to 66 million years ago and including the *Triassic*, *Jurassic*, and *Cretaceous Periods*.

metamorphism — those changes that occur within a *rock* between *diagenesis* and melting. Metamorphism is defined as occurring at temperatures of over 100° C. (cf. *diagenesis*).

mineral — a naturally occurring, inorganic solid having an ordered internal atomic arrangement and a chemical composition that varies within known limits.

Mississippian — the fifth *period* of the *Paleozoic Era*, extending from 323 to 362 million years ago; the *system* of stratigraphic *rock* units deposited during this time; of or relating to this *period* of time or its *system* of *rocks*.

Missourian — the fourth *epoch* of the *Pennsylvanian Period*, extending from 295 to 303 million years ago; the *series* of stratigraphic *rock* units deposited during this time; of or relating to this *epoch* of time or its *series* of *rocks*.

Morrowan — the first *epoch* of the *Pennsylvanian Period*, extending from 310 to 323 million years ago; the *series* of stratigraphic *rock* units deposited during this time; of or relating to this *epoch* of time or its *series* of *rocks*.

net pay — the sum of the thicknesses of *reservoir rock* in a given locality.

normal fault — a fault in which the *footwall* has moved up relative to the *hanging wall*.

offlap — a *sequence* of sediments in which each overlying unit represents a more nearshore or terrestrial depositional environment and pinches out progressively closer to the center of the depositional basin. *Offlap* occurs as a result of *regression* produced by falling sea level or a rising landmass.

onlap — a *sequence* of sediments in which each overlying unit represents a more offshore depositional environment and pinches out progressively closer to the margins of the depositional basin. Onlap occurs as a result of *transgression* produced by rising sea level or a subsiding landmass.

Ordovician — the second *period* of the *Paleozoic Era*, extending from 439 to 505 million years ago; the *system* of stratigraphic *rock* units deposited during this time; of or relating to this *period* of time or its *system* of *rocks*.

Ouachita Thrust Belt — the linear trend of deformation and thrusting produced by the collision of *Gondwanaland* and *Euramerica* during the Late *Paleozoic*.

outer core — that portion of the Earth's interior between the *mantle* and the *inner core*, extending from about 2,900 km (1,800 mi) to 5,200 km (3,300 mi) in depth. The outer core has a nickel-iron composition and is molten because of the intense heat at this depth.

overthrust belt — a linear trend of deformation and thrust faulting produced along a *convergent plate boundary*.

paleomagnetism — the remnant magnetism left within a *rock* or *mineral* caused by its having crystallized with respect to the Earth's magnetic field; the study of paleomagnetism to determine the orientation and strength of the Earth's magnetic field during the geologic past.

Paleozoic — the *era* of geologic time extending from 530 million years ago to 245 million years ago and including the *Cambrian*, *Ordovician*, *Silurian*, *Devonian*, *Mississippian*, *Pennsylvanian*, and *Permian Periods*.

pay zone — the vertical interval in a stratigraphic section from which extraction of oil or gas is economically profitable.

Pennsylvanian — the sixth *period* of the *Paleozoic Era*, extending from 323 to 290 million years ago; the *system* of stratigraphic *rock* units deposited during this time; of or relating to this *period* of time or its *system* of *rocks*.

pentolite — an explosive used as a *seismic* energy source.

perforation — a deliberate puncture made in a well *casing* to allow fluids or gas to flow into the borehole from the *rock*.

period — the fundamental unit of geologic time originally recognized on the basis of its unique fossil assemblage. *Periods* are grouped together into *eras*, and subdivided into *epochs*.

peripheral bulge — a slightly upwarped area of *crust* distal to an *overthrust belt*. The subsidence produced by loading within the belt creates a *flexural moat*, which in turn induces a slight bulge around its distal margin (cf. *flexural moat*).

permeability — a measure of how well connected pore spaces are within a *rock*, i.e., how well fluids can be transmitted through the *rock*.

Permian — the seventh and last *period* of the *Paleozoic Era*, extending from 290 to 245 million years ago; the *system* of stratigraphic *rock* units deposited during this time; of or relating to this *period* of time or its *system* of *rocks*.

petrophysics — that branch of geology studying the physical properties of *rocks*.

phase — a point in a cycle of regular, periodic motion as measured with respect to the instant at which the motion started. The phase is expressed as a value from 0 to 360°, one cycle of the periodic motion beginning at 0° and returning to the starting point at 360°.

physiography — the surface features of the Earth or a descriptive study thereof.

platform — the geologically stable region of a continent covered by nearly horizontal, undeformed sedimentary units and underlain by crystalline *basement rocks*.

poise — a standard measure of viscosity defined as 1 *dyne/sec/cm²*.

porosity — that percentage of the total volume of a *rock* not occupied by *mineral* grains or intergranular cements.

potassium feldspar (K-spar) — a hard aluminosilicate *mineral* containing potassium (KAlSi_3O_8) and having two cleavage planes that intersect at approximately 90°.

Precambrian — the interval of time extending from the formation of the Earth until the formation of the base of the Cambrian (530 million years ago); of or relating to this interval of time or the *rocks* formed during it.

progradation — the seaward or basinward building, nearshore accumulation of sediment in a depositional setting (cf. *aggradation*, *regression*).

pyrite — a golden or bronze-colored metallic *mineral* composed of iron sulfide (FeS_2), which exhibits cubic crystal structure and a conchoidal fracture.

quartz — a common, hard, crystalline silica *mineral* (SiO_2) exhibiting conchoidal fracture and hexagonal symmetry.

Quaternary — the second *period* of the *Cenozoic Era*, extending from 2 million years ago to the present; the *system* of stratigraphic *rock* units deposited during this time; of or relating to this *period* of time or its *system* of *rocks*.

ravinement surface — a *flooding surface* in which the transgressive movement of the surf zone slightly erodes the underlying sediment.

reflection amplitude — the magnitude of the *seismic* waves that reflect from an interface between *rock* layers.

reflection peak — that part of a *seismic* wiggle trace that swings in the positive direction when plotted or displayed graphically.

reflection trough — that part of a *seismic* wiggle trace that swings in the negative direction when plotted or displayed graphically.

reflector — a boundary within the Earth between materials that have different elastic properties that therefore strongly reflects *seismic* waves and generates *seismic traces* for analysis.

regression — a situation in which relative sea level is falling, moving the shoreline seaward toward the center of the basin. As a result, nearshore and deeper water *facies* are overlain by progressively terrestrial and shallower water deposits.

reserves — identified resources of *mineral*-bearing or *reservoir rock* from which the *mineral* or fuel can be extracted profitably by means of existing technology and under current economic conditions.

reservoir — a *rock* unit with sufficient *porosity*, *permeability*, and *saturation* to yield oil or natural gas.

reverse fault — a fault in which the *footwall* has moved down relative to the *hanging wall*.

rock — an aggregate of one or more *minerals* and/or noncrystalline inorganic solids, or a mass consisting largely of solid organic material that has undergone burial and alteration in the form of *diagenesis* or *metamorphism*.

saturation — the percentage of pore space within a *rock* filled by fluid or gas.

secondary porosity — *porosity* resulting from fracturing or dissolution during *diagenesis*.

secondary recovery — artificially increasing the pressure within a *reservoir* or the mobility of *reservoir* fluids to enhance the retrieval of petroleum or natural gas; incremental recovery in the sense of additional recovery beyond that achieved in early phases of oil or gas field development.

seismic — of or relating to earthquakes or other vibrations within the Earth, including those produced artificially.

seismic attribute — any numerical parameter, such as amplitude, phase, or frequency, that can be extracted from a *seismic trace*.

seismic trace — a generic term used to refer to the data recorded by any receiver(s) detecting Earth movement.

seismic velocity — the speed with which *seismic* waves travel within the Earth.

sequence stratigraphy — conceptual framework for defining *reservoir* architecture. Its main premise is that *seismic* reflections represent *chronostratigraphic horizons* and that these surfaces bound genetically related, time-equivalent rock volumes. Familiar methods of *depositional systems* analysis and *facies* modeling are considered valid only within *rock* volumes (i.e., stratigraphic units) bounded by key *chronostratigraphic horizons*.

sequence — genetically related group of *rock* strata bounded by time-significant surfaces.

series — a *time-rock stratigraphic unit* consisting of those *rocks* deposited during a geologic *epoch*.

shelf — the continental shelf; i.e., that portion of the continental *crust* covered by the ocean. Although mostly limited to the continental margins today, this depositional environment was widespread in the past when large portions of the *craton* were flooded by shallow marine waters and became covered by extensive, nearly horizontal layers of sediments.

shield — the area of a continent in which the *Precambrian* crystalline *basement rocks* are widely exposed.

shoal — an uncemented buildup of coarse *clastic* sediment or shell debris over which the water depth is substantially less than in the area immediately around it.

shoreface — the narrow, inclined zone just seaward of the low-water line along the shore. The *shoreface*, always under water, grades into a lower-angle depositional surface farther offshore.

shut-in period — the time during which the well bore is closed to allow the *bottom-hole pressure* to build up to equilibrium with the fluid or gas pressure in the *reservoir*.

shut-in pressure — the *bottom-hole pressure* measured at the wellhead when the well bore is totally sealed.

silicate — of or relating to a *mineral* with the silicate tetrahedron (SiO_4) forming its basic structure; of or relating to a *rock* consisting primarily of *minerals* containing the silicate tetrahedron.

Silurian — the third *period* of the *Paleozoic Era*, extending from 408 to 439 million years ago; the *system* of stratigraphic *rock* units deposited during this time; of or relating to this *period* of time or its *system* of *rocks*.

sinkhole — a large, deep, roughly circular depression occurring in *karst* terrain formed by the collapse of a cavern roof or by relatively continuous dissolution of soluble rocks such as limestone.

stratal-dominated package — a sedimentary *sequence* deposited more or less continuously and therefore containing few *erosional surfaces* or *unconformities*. As a result, the *rock* units themselves represent much greater amounts of time than do the surfaces between them.

Strawn Group — a *sequence* of *rocks* that overlies the *Atoka Group* (*Bend Conglomerate*). Within the *Fort Worth Basin*, this sequence ranges in age from uppermost *Atokan* to lower *Missourian* and is therefore mostly equivalent to the *Desmoinesian Series*.

strike — the horizontal component of the trend or direction of a *rock* unit.

subaerial — exposed to the open air.

subaqueous — under water.

surface-dominated package — a sedimentary *sequence* containing numerous *erosional surfaces* and *unconformities*, the surfaces between the units representing much greater amounts of time than do the *rock* units themselves.

syntectonic — of or relating to the processes or events occurring during *tectonic* activity.

system — a *time-rock stratigraphic unit* consisting of those *rocks* deposited during a geologic *period*.

systems tract — linkage of contemporaneous *depositional systems*.

tectonic — of or relating to the large *crustal* plates that comprise the outer surface of the Earth or to the deformation resulting from their movement.

tectonic plate — the fundamental unit of the Earth's surface, idealized as a thin, rigid segment consisting of the *crust* and the underlying *lithosphere*. The Earth's surface is broken into about a dozen major and many minor *tectonic plates*, which move slowly upon the underlying *asthenosphere*.

terrigenous — derived or eroded from the land or continents.

Tertiary — the first *period* of the *Cenozoic Era*, extending from 66 to 2 million years ago; the *system* of stratigraphic *rock* units deposited during this time; of or relating to this *period* of time or its *system* of *rocks*.

3-D seismic survey — a data-recording technique in which the reflected *seismic* wavefield generated by a source at a specific coordinate point is recorded by a large number of receivers areally deployed about that source point. This technique differs significantly from 2-D *seismic* surveying, where receivers are deployed in a single straight line about the source point.

thrust fault — a low-angle ($<45^\circ$) *reverse fault*. Although the movement along the fault is technically vertical, the very low angle of most thrust faults causes the effective movement to be horizontal and typically results in displacements of tens to hundreds of miles.

thrust sheet — a body of *rock* displaced by a *thrust fault* whose surface is nearly horizontal.

tight — having a low *permeability*.

time line — a line drawn through a geologic cross section or correlation diagram that indicates contemporaneous units, separating overlying younger strata from underlying older strata. Ideally, a time line can be equated with an observable surface, boundary, or interval (cf. *chronostratigraphic horizon*).

time-rock stratigraphic unit — a rock unit deposited during a formally named interval of geologic time. The rocks within a time-rock stratigraphic unit are grouped together on the basis of their age, not their *lithology*.

transgression — a situation in which relative sea level is rising and slowly floods the land, moving the shoreline landward away from the center of the basin. As a result, shallow-water and terrestrial *facies* are overlain by progressively deeper water deposits.

transgressive systems tract (TST) — a sedimentary succession representing *onlapping transgressive facies* that filled *accommodation space* during a *base level* rise. The tract usually overlies a *ravinement surface*.

Triassic — the first *period* of the *Mesozoic Era*, extending from 245 to 208 million years ago; the *system* of stratigraphic *rock* units deposited during this time; of or relating to this *period* of time or its *system* of *rocks*.

unconformable — referring to strata or units that immediately overlie an *unconformity*.

unconformity — a contact between two *rock* units that represents some gap in geologic time between the formation of the underlying unit and the deposition of the

overlying sedimentary unit. The *unconformity* corresponds to a period of nondeposition or erosion, often as a result of continental uplift or a fall in sea level.

updip — in a direction opposite but parallel to that in which a bed is *dipping*.

Walther's Law — the stratigraphic principle that states that, in a conformable stratigraphic *sequence*, laterally adjacent *facies* will vertically overlie each other.

wavetest — a *seismic* measurement that determines the signal and noise characteristics of a *seismic* wavefield generated by a specific source and recorded by a specific receiver geometry. Source type and receiver geometry are varied to determine which source and receiver parameters produce wavefields that have desirable signal-to-noise properties.